

**NON-SELECTIVE, CALCIUM-PERMEABLE CHANNELS IN THE APICAL  
MEMBRANE OF RABBIT RENAL TUBULES AND IN THE BASOLATERAL  
MEMBRANE OF HUMAN RENAL TUBULES: AN EXPLORATORY  
PATCH CLAMP STUDY.**

by

**JAMES SAUNDERS, BSc(HONS)**

A Thesis Presented for the Degree of

**DOCTOR OF PHILOSOPHY**

in the Department of Physiology

**UNIVERSITY OF CAPE TOWN**

October, 1991

The University of Cape Town has been given  
the right to reproduce this thesis in whole  
or in part. Copyright is held by the author.

The copyright of this thesis vests in the author. No quotation from it or information derived from it is to be published without full acknowledgement of the source. The thesis is to be used for private study or non-commercial research purposes only.

Published by the University of Cape Town (UCT) in terms of the non-exclusive license granted to UCT by the author.

### ***Abstract***

The presence of calcium (Ca) channels has been investigated in the apical membrane of various segments of rabbit renal tubules and in the basolateral membrane of human tubules, using the patch clamp technique. The rabbit tubule segments comprised proximal straight tubules (PST), thick ascending limbs (TAL), distal convoluted tubules (DCT), and cortical collecting ducts (CCD). The human tubule segments could not be identified, but were probably of proximal origin. The luminal surfaces of the individual tubule segments were accessed by perfusing the tubule and inserting the patch pipette through the open end or, more frequently, by tearing open the tubule to allow direct access by a patch electrode. Either Ba (90 mM) or Ca (70 mM) was used in the pipettes. Where possible, channel activity was sought in voltage clamped (30 to -60 mV) excised patches. The data were digitized at 1 kHz, and filtered (200-500 Hz) by a six-pole Bessel filter.

Channel activity was detected in 37 PSTs, 15 TALs, 16 DCTs, 38 CCDs, and in 21 human tubule patches. Channel activity was essentially similar in both rabbit and human tubule segments, and could be qualitatively described by three temporal patterns of behaviour; thus "squares", "bursts", and "spikes" were distinguishing features of observed channel behaviour. When I-V relationships were determined for the collective (total rabbit) data sample for both "squares" and "bursts", the overall mean unit current amplitudes appeared to be independent of voltage above and below about 5 and -5 mV, respectively; it was therefore not feasible to measure the slope conductance of these data. The mean unit current amplitudes of "squares" was significantly higher than those of the "bursts". Overall the mean unit current amplitudes in the negative voltage clamp range were  $0.175 \text{ pA} \pm 0.019 \text{ pA}$  for "bursts" and  $0.315 \text{ pA} \pm 0.024 \text{ pA}$  for "squares"; in the positive voltage clamp range, the mean unit amplitudes were  $-0.172 \text{ pA} \pm 0.01 \text{ pA}$  for "bursts" and  $-0.324 \text{ pA} \pm 0.027 \text{ pA}$  for "squares". The unit current amplitude measured at both positive and negative voltages for the DCT patches was significantly greater than for the other tubule segments. The channels were voltage-sensitive, the fractional open time increasing with

displacement of the clamp voltage from the reversal potential (about zero mV). Detailed inspection revealed multiple subconductance states, the number of which varied with the absolute applied voltage. In most cases, the open- and closed-time histograms could be described by double exponentials, suggesting that the channel possessed two open and two closed states. In some cases, the channel was sensitive to the Ca channel blockers, nifedipene (0.1 mM), verapamil (0.1 mM), and D600 (0.1 mM); to the Ca channel agonist, Bay K-8644 (0.1 mM); to chlorothiazide, and to parathyroid hormone. A number of other channel varieties, including a probable low conductance K channel, and a high conductance non-selective channel, were also detected in this study. The properties of these channels, however, were not investigated further.

Overall, the data presented here are consistent with the presence of a voltage-sensitive, non-selective, Ba- and Ca-permeable cation channel in the apical membranes of rabbit PST, TAL, DCT, and CCD, as well as in the basolateral membrane of human (proximal) tubules. The presence of these channels in the apical membrane is in accord with descriptions of Ca reabsorption along the whole length of the nephron. However, their functional significance in the basolateral membrane is, at present, unclear.

## ***Acknowledgements***

I would like to thank the people who made this project possible:

**Professor Leon Isaacson;** for continued enthusiastic support and meticulous supervision of this project. He not only inspired me in the field of electrophysiological research, but also helped provide a way forward. His philosophical appraisal of life and accompanying humour created an environment conducive to thoughtful research.

**Professor Peter Belonje;** for a sustained interest in and continued support of this project, and for providing me with several valuable academic opportunities during the course of the work.

**Professor Felix Bronner;** for personal inspiration and ongoing support of this project. His visits to this laboratory were accompanied with some valuable discussion sessions.

**My mother, Diana Mackenzie;** for financial assistance when necessary, and for her sustained emotional support.

**Dr. Sue Nicolson;** for editorial comment, for her professional interest in the work and generous encouragement while working in this laboratory.

**Dr. Lauriston Kellaway;** for technical assistance, and professional advice when needed.

**Dr. Lindsay Weight;** for encouragement and general assistance.

**The Renal Unit of the Dept. Medicine, Groote Schuur Hospital, with particular co-operation of Drs. van Zyl-Smit, Swanepoel, Pascoe, Cassidy, and Zent;** for generous contribution of kidney biopsy samples during the final stages of the project.

**Dr. Maureen Duffield;** for sparing some renal tissue for experimentation at the end of each biopsy session.

**Professor Rodney Douglas;** for insightful criticism and interest in this work.

**Elsa Holtzhausen;** for encouragement and advice during the long and lonely hours of research.

**Basil Sedres;** for reliable provision of animals for the research.

**Riaat Terblanche;** for photographic assistance.

**The Medical Graphics team** - For help with photography and presentation.

**Dr. Cilliers;** for some very sound advice and for providing me with a place to stay during the final stages of the project.

**Harry Hall;** for professional construction of various components of the apparatus used in the project.

**Professor Bob Millar** and **Dr. James Davidson**; for generous donation of drugs for the project.

**Lara, Gerry, and Sarah**; for surrounding me with a healthy environment at a critical stage of this work.

**Professor William Els**; for editorial comment on the preliminary work.

**Dr. Dave Querido**; for general assistance during various aspects of this work.

**The Medical Research Council**; for the funding of this research with a grant to Professor L.C Isaacson.

**The CSIR**; For the award of a bursary to enable subsistence during this work.

### ***Glossary of abbreviations***

<b>F<sub>o</sub></b>	fractional open time
<b>P<sub>o</sub></b>	open probability
<b>mV</b>	millivolts
<b>mM</b>	millimolar
<b>M</b>	molar
<b>Ω</b>	ohms
<b>GΩ</b>	giga-ohms
<b>MΩ</b>	mega-ohms
<b>μ</b>	microns
<b>μM</b>	micromolar
<b>μl</b>	microliters
<b>g</b>	conductance
<b>PD</b>	potential difference
<b>(Cai)</b>	intracellular calcium
<b>n.s.</b>	not significant
<b>s.</b>	significant
<b>s.d.</b>	standard deviation
<b>pA</b>	pico-amperes
<b>pS</b>	pico-siemens
<b>V</b>	volts
<b>β</b>	beta
<b>α</b>	alpha
<b>d.f.</b>	degrees of freedom
<b>DHP</b>	dihydropyridine

## TABLE OF CONTENTS

Page no.

***Abstract***

***Acknowledgements***

***Glossary of abbreviations***

### **SECTION ONE: INTRODUCTION** 1

1.1. Ca channels: what are they?	1
1.2. A brief history of the patch clamp technique	3
1.3. The application of the patch clamp technique to renal physiology	5
1.4. The background and scope of this thesis	6
1.5. The aims of the present study	6

### **SECTION TWO: LITERATURE SURVEY** 8

2.1. Renal reabsorption of filtered calcium	10
2.1.1. Introduction	10
2.1.2. Calcium transport by the different nephron segments	11
2.1.2.1. The proximal tubule segments	11
2.1.2.2. Thin descending and ascending limbs of Henle's loop	13
2.1.2.3. The thick ascending limb of Henle's loop	14
2.1.2.4. The distal convoluted tubule	15
2.1.2.5. The cortical and medullary collecting duct	15
2.1.3. Apical membrane entry of calcium	16
2.1.4. Intracellular diffusion of calcium	17
2.1.5. Extrusion of calcium by the basolateral membrane	20
2.1.5.1. The Na-Ca exchange	20
2.1.5.2. Ca-ATPase	20
2.1.6. Sodium-calcium interdependence	21
2.1.7. Conclusion	24
2.2. Calcium channels: mediators of calcium entry	26
2.2.1. Introduction	26
2.2.2. Calcium channel types and distribution	28



2.2.3. Pharmacology of calcium channels	30
2.2.4. Regulation of calcium channels	33
2.2.5. Calcium channels in non-excitabile tissue	35
2.2.6. Concluding remarks	38
2.3. Ion channels in the kidney	39
2.3.1. The proximal convoluted tubule	39
2.3.1.1. Apical membrane	39
2.3.1.2. Basolateral membrane	39
2.3.2. Proximal straight tubule	41
2.3.2.1. Apical membrane	41
2.3.2.2. Basolateral membrane	41
2.3.3. Thick ascending limb	43
2.3.3.1. Apical membrane	43
2.3.3.2. Basolateral membrane	44
2.3.4. The distal convoluted tubule	46
2.3.4.1. Apical membrane	46
2.3.4.2. Basolateral membrane	47
2.3.5. Cortical collecting duct	48
2.3.5.1. Apical membrane	48
2.3.5.2. Basolateral membrane	49
2.3.6. Conclusion	50
2.4. Statistical analysis of patch clamp data	52
2.4.1. Introduction	52
2.4.2. Measurement of amplitudes	52
2.4.3. Measurement of durations	53
2.4.4. Bursts - a special case	56
2.4.5. Alternative methods: the study of fractals and unidimensional diffusion	57
2.4.5.1. Background	57
2.4.5.2. Fractal analysis in patch clamp	60
2.4.5.3. Diffusion models of ion channel gating	62
2.4.6. Conclusion	63
<b>SECTION THREE: METHODS</b>	<b>64</b>
3.1. Tissue preparation	65

3.1.1. Rabbit kidney	65
3.1.2. Human kidney	69
3.2. Application of the patch clamp technique	72
3.2.1. Patch pipette fabrication	72
3.2.2. Pipette filling and mechanical setup	73
3.2.3. Formation of a gigaseal	73
3.2.4. Patch configurations	73
3.3. Solutions and drugs	74
3.4. Data recording and storage	78
3.5. Data analysis	82
3.5.1. Event amplitude	82
3.5.2. Open- and closed-time histograms.	86
3.5.3. Fractional open time	87
3.6. Computer programs for data recording and analysis.	87
3.6.1. "Burst analysis"	89
3.6.2. Open- and closed-time interval measurement	90
3.6.3. Other options of the ANALYSE program	91
<b>SECTION FOUR: RESULTS</b>	<b>97</b>
4.1. The search for calcium channels in rabbit renal tubules	98
4.2. Further characterisation of the channel	125
4.3. The quest for similar channels in human tubule segments	137
4.4. Emergence of unexpected channel varieties in this study	150
<b>SECTION FIVE: DISCUSSION</b>	<b>158</b>
<b>5.1. DISCUSSION OF METHODS</b>	<b>159</b>
5.1.1. Tissue preparation	159
5.1.2. Application of the patch clamp	166
5.1.3. Solutions and drugs	167
5.1.4. Data recording and storage	169
5.1.5. Data analysis	173
5.1.5.1. Event amplitude	173
5.1.5.2. Open- and closed-time histograms	175

5.1.6. Computer programs for data recording and analysis	176
<b>5.2. DISCUSSION OF RESULTS</b>	<b>178</b>
5.2.1. The search for calcium channels in rabbit renal tubules	178
5.2.1.1. Are these real channel data?	179
5.2.1.2. Multiple identical channels, multiple channel types, or multiple conductance states?	181
5.2.1. 3. Individual channel data	184
5.2.2. The quest to further characterise the channel	186
5.2.2.1. Solution changes	187
5.2.2.2. Experiments with Ca channel agonists and antagonists, and parathyroid hormone: the expected and the unexpected.	188
5.2.3. The quest for similar channels in human tubule segments	192
5.2.4. Emergence of unexpected channel varieties in this study	193
<b>5.3. GENERAL DISCUSSION</b>	<b>196</b>
5.3.1. Some final comments on the methods	196
5.3.2. How do these data fit in with current evidence?	197
5.3.3. Is there an adequate model to describe the structure and gating kinetics of the channel?	204
5.3.4. What is the functional role of these channels in the kidney?	209
5.3.5. Where to from here?	211
<b>SECTION SIX: CONCLUSION</b>	<b>215</b>
<b>SECTION SEVEN: REFERENCES</b>	<b>218</b>
<b><i>Appendix</i></b>	

## **SECTION ONE**

### **INTRODUCTION**

## **SECTION ONE**

### **INTRODUCTION**

In mammals, the kidneys represent the dominant regulatory site of extracellular calcium (Ca) homeostasis. Renal clearance studies have established that 98% of the filtered load of Ca is reabsorbed by the kidney, and micropuncture studies have defined the nephron sites of Ca absorption and the relative contribution of each segment to total Ca transport (Friedman, 1988). While both transcellular and paracellular reabsorptive pathways have been posited, their relative contributions are unknown. In the case of transcellular absorption, extrusion of Ca across the basolateral membranes must be mediated by active transport processes to overcome the unfavourable electrochemical gradient. However the means by which Ca might cross the apical membrane to enter the tubular cells remains undefined; conceivably this influx could be by cation exchange, cotransport, a carrier mediated process, or via Ca channels.

#### **1.1. Ca channels: what are they?**

The mode of Ca entry into cells has been the subject of intense investigation in the last decade. The importance of Ca in body functions was first appreciated by Sidney Ringer in 1883, who found that frog hearts would not beat without it. Since this discovery, Ca has been recognised to play a major role in the contraction not only of heart muscle, but also of skeletal muscle and all forms of smooth muscle. The existence of Ca-selective channels has been postulated for nearly 40 years (Fatt and Katz, 1953). They are known to be complex proteins with a hydrophilic pore capable of transferring millions of permeant ions per second. In ion permeation through the Ca channel a role is played by Ca binding sites in the channel, at least two of which are occupied by Ca ions (or Ba ions if Ba is the charge carrier). Both voltage-sensitive and receptor-operated Ca channels have been discovered in many different tissue types (Miller

and Fox, 1990). Voltage-sensitive Ca channels have been the most widely investigated in recent years. Receptor-operated channels, on the other hand, are not as well understood. Most of the work on Ca channels has been done using excitable tissues, such as heart or skeletal muscle. There is also growing evidence for the existence of this channel in non-excitable cells, such as neutrophils or lymphocytes (Peterson, 1990). To date, however, there have been no direct studies revealing the presence of Ca-permeable channels in epithelial tissue.

Our present knowledge of the properties of Ca channels is largely attributable to the recently developed patch clamp technique. This technique has revolutionised electrophysiology, since for the first time, it has allowed the function of the molecular unit comprising the channel to be observed while the molecule is in its native environment in the cell.

## **1.2. A brief history of the patch clamp technique**

Up until about 15 years ago, the properties of ion channels in cell membranes could only be inferred indirectly by observation of transmembrane voltage changes in response to changes in ionic composition of the bathing solution, or, more recently, by noise analysis (Ruff, 1986). Both of these techniques, however, are only capable of providing information about the entire population of one or more species of ion channels in the cell membrane. An extraordinary breakthrough, however, came in 1976 in the laboratory of Erwin Neher and coworkers (1976). Up until then these workers had perfected the technique of isolating a patch of membrane using a glass micropipette, and studying the ion channels in that patch under voltage clamp conditions. Using this technique, they were able to detect acetylcholine (ACh)-activated channels in muscle cell membrane. However their approach was limited in that the resistance of the seal between the glass pipette and the cell membrane (10-50 mega-ohms) was very small relative to the channel resistance (10 giga-ohms). The current leak through such low resistance seals obscured that through the ion channels. In all likelihood the patch clamp technique evolved in an attempt to resolve this very problem, as these investigators discovered that by fire polishing the glass pipettes and applying gentle suction to the interior of the pipette when it made

contact with the surface of the cell, seals of very high resistance (1-100 giga-ohms) could be obtained (Neher and Sakman, 1976).

The high resistance seal (or gigaseal) reduces noise levels by an order of magnitude, enabling high resolution recordings to be made of single ion channel currents. The gigaseal also allows ion channel current recordings to be made under a much larger range of voltage clamp conditions. Another surprising bonus was the finding that the seal is mechanically stable. The electrically isolated membrane patch can be pulled off the cell (excised) in such a way that the inside of the plasma membrane faces the bath solution (inside-out) or alternatively so that the inside faces the solution in the micropipette (outside-out). By breaking the patch membrane in the cell-attached configuration, the solution in the pipette gains direct access to the cell interior and whole cell currents can be measured (Peterson and Peterson, 1986).

The patch clamp technique has been effective in determining specific properties of ion channels such as the relative ion selectivity, single channel conductance, and channel kinetics. These basic parameters constitute the channel's "signature" and allow the same channel to be recognised in different cells and tissues. The conductance and selectivity of the channel are perhaps its most basic characteristics, in that they reflect which ions are transported at what rate. These can both be determined from a plot of single-channel current ( $I$ ) vs. voltage ( $V$ ) across the patch.

The kinetics of the channel reveal how frequently the channel opens or closes. By measuring each time interval in which the channel is continuously open and continuously closed, the mean open time, mean closed time, the percentage of time that a channel is open or closed, and the rate of opening and closing can be estimated (Colquhoun & Hawkes 1983). Recently, alternative techniques such as fractal analysis have evolved and been applied to patch clamp data with some success (Liebovitch et al, 1986)

### 1.3. The application of the patch clamp technique to renal physiology

The first problem that arises in applying the patch clamp technique to any tissue is the formation of a giga-ohm seal. Certain epithelia, such as toad urinary bladder cells, have resisted all attempts to form these seals, presumably because of interference by mucus. Cultured cells have in many cases provided suitable preparations for the patch clamp. Since epithelial cells in culture grow with their apical membrane up, and basolateral membrane in contact with the substrate, it is the apical membranes that are accessible to the patch clamp electrode. It is generally believed, however, that some of the physiological properties of cultured cells may differ from those in their counterparts in the living animal. Thus, a major advance in this area was the finding that at least some epithelial cells can be studied directly without culturing and without prior cleaning with proteolytic enzymes. In renal tissue this was achieved either by opening up dissected kidney tubules so that their apical membranes could be accessed directly with the patch clamp pipette (Koeppen *et al*, 1984; Palmer and Frindt, 1986), or by using isolated perfused tubules in which one end of the tubule was left open and a clean tear in the tubule was made, exposing both the apical and the lateral membrane to the patch clamp pipette (Gogelein and Greger, 1984).

The first patch clamp study on renal tubules was that of Koeppen *et al* in 1984. A number of similar studies have followed revealing many different kinds of ion channels down the length of the nephron. Because the patch clamp technique can measure channel activity in small pieces of membrane, it has thrived on the heterogeneous nature of the nephron (Palmer, 1986). The technique, however, is not always a good approach to the understanding of the overall ion permeability properties of the membrane. The nature of the technique is to focus on small pieces of membrane that may have properties not representative of the membrane as a whole; thus the demonstration of a given channel type in a given membrane gives no clear indication of the number of such channels in the cell. The patch clamp technique is therefore best used in conjunction with more classical techniques, or perhaps with whole cell clamp to get a



complete picture of ion permeation across the cell membrane.

#### **1.4. The background and scope of this thesis**

Patch clamp on renal tubules was embarked upon shortly after the patch clamp technique was successfully set up for the first time in this department (Saunders, 1987). Initially, the isolated perfused technique (Gogelein and Greger, 1984) was used to gain access to the apical membrane by the patch electrode. Later, the ripped tubule technique (Koeppen et al, 1984; Palmer and Frindt, 1986) was used to achieve this end. The objective at this early stage was merely to confirm the feasibility of applying the patch clamp technique to renal epithelia, as already demonstrated by others (above).

Then in 1989, stimulated by Professor Felix Bronner, then visiting this department, I concentrated on looking for Ca-permeable channels in the apical membranes of segments of isolated renal tubules. During the course of the project, this main objective was extended as the research began to take the form of three separate, but closely related studies. These studies define the aims of this thesis and are presented in chronological sequence. Throughout all the phases of this project, considerable technical difficulties were encountered; the project was therefore essentially exploratory in nature.

#### **1.5. The aims of the present study**

The overall aim of the present study was to search for the existence of Ca-permeable channels in the apical membrane of rabbit kidney tubules using the patch clamp technique. Once the basic signature of this channel was determined using standard analytical techniques, this main aim was then extended to include two additional aims:

A) Further characterisation of the channel by determining its response to solutions of different ionic composition and various pharmacological

agents. The latter comprised Ca channel antagonists and an agonist, parathyroid hormone, and the diuretic, chlorothiazide.

B) A search for similar channels in the apical membrane of human kidney tubules obtained from renal biopsies (performed for routine clinical purposes by the Renal Unit of the Dept. Medicine, Groote Schuur Hospital). However, owing to the experimental difficulties involved - and a strange twist of fortune - this aim was later modified to a search for these channels in the basolateral membrane.

## **SECTION TWO**

### **LITERATURE SURVEY**

## **SECTION TWO**

### **LITERATURE SURVEY**

This section aims to set forth what is known about certain topics underlying the investigative procedures undertaken in this project. Section 2.1. is a detailed review of the role of the kidney in calcium homeostasis, and in particular explores possible mechanisms of calcium movement across the tubular epithelium. Section 2.2. reviews evidence concerning passive entry of calcium into cells via calcium channels. Since these channels had not yet been reported to exist in epithelial tissue, the emphasis in this review is on calcium channels in excitable tissue. Section 2.3. deals with the varieties of ion channels that have, to date, been discovered in renal epithelia, as elucidated by the patch clamp technique. Section 2.4. is a digression from biology and summarises the various statistical data analysis procedures that can be applied to patch clamp data, and the information that can be obtained from such procedures.

## **2.1. Renal reabsorption of filtered calcium**

### **2.1.1. Introduction**

In mammals, extracellular calcium homeostasis is maintained by the integrated activity of the gut, bone, and kidneys. Of these, the kidneys represent the dominant regulatory site. About 0.1% of total calcium is present in the extracellular space and about 1/3 of this is in the plasma. Approximately half of plasma calcium is bound to plasma proteins or complexed with organic anions, and half is in the form of free calcium ions. The ionised fraction is generally agreed to be the physiologically active component that is available for transport and cellular metabolism. Both forms are freely filterable through the glomerular basement membrane. Renal clearance studies have established that 98% of the filtered load of Ca is reabsorbed by the kidney, and micropuncture studies have defined the nephron sites of Ca absorption (see Fig. 2.1.1.) and the relative contribution of each segment to total Ca transport (Friedman, 1988). Renal Ca transport, like intestinal Ca transport, is described (Bronner et al, 1986) as the result of two processes: 1) a passive, paracellular process that predominates in most segments of the nephron, and which is energy independent; 2) a transcellular, energy dependent step.

The paracellular route is shared with other ions, e.g sodium or chloride and is presumably mediated by solvent drag, secondary to osmotically driven bulk flow of water. About 80% of the filtered Ca is reabsorbed by this passive process (Bronner and Stein, 1988). The transcellular route, on the other hand is defined by a three stage process: 1) Cell entry of Ca through the luminal membrane, 2) intracellular movement, and 3) extrusion of Ca by the basolateral membrane.

The aims of this review are threefold: Firstly to provide a summary of current knowledge on the handling of Ca by the different nephron segments; Secondly, to explore the mechanisms involved in transcellular Ca movement at the level of the single cell and lastly, to discuss the relationship that exists between Ca and sodium (Na) transport down the length of the nephron.

## RENAL CALCIUM ABSORPTION

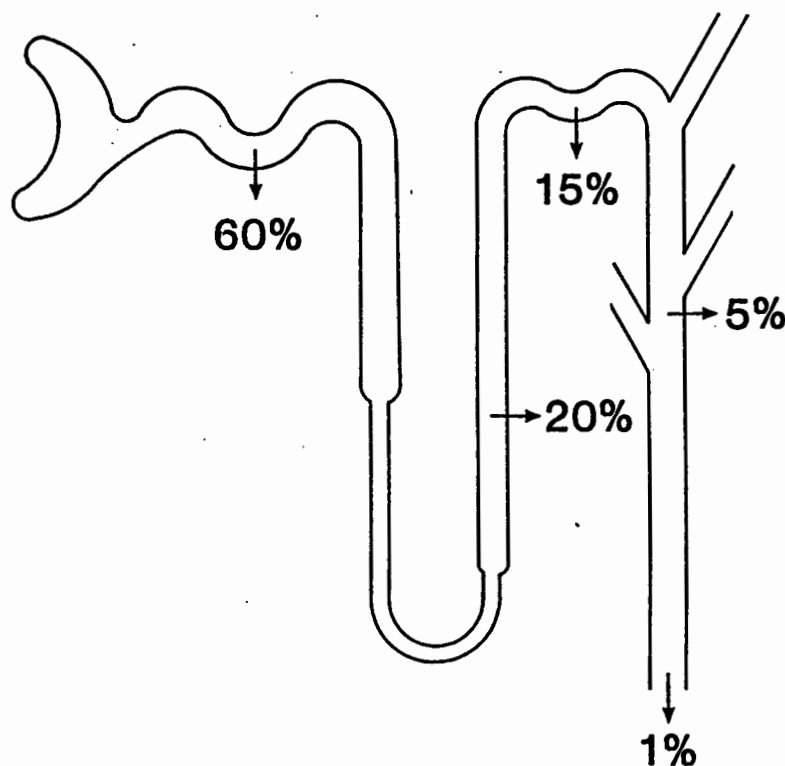


**Figure 2.1.1.** Schematic depicting the sites and percentages of Ca absorption down the length of the nephron.

### 2.1.2. Calcium transport by the different nephron segments

#### 2.1.2.1. The proximal tubule segments

About 60%-70% of filtered Ca is absorbed by the proximal tubule segments. These comprise the proximal convoluted tubule segments, S1 and S2, and the proximal straight tubule segments, S2 and S3.

Proximal convoluted tubule (S1 and S2):

Calcium movement in this segment is considered to be largely a passive process. The most convincing evidence to suggest this has come from micropuncture studies which have shown that Ca, water, and Na are

absorbed in parallel. This has been shown for two species of rat and the dog (Lassiter *et al*, 1963; Jamison *et al*, 1974; Edwards *et al*, 1974). This evidence is strengthened by studies done by Ng *et al* (1984) on rabbit superficial convoluted S2 segments. They found that when the transepithelial potential difference was altered by changing the composition of the perfusate, net Ca efflux was demonstrated with a lumen-positive PD and net Ca secretion with a lumen-negative PD, suggesting passive, voltage-dependent Ca transport in this segment. Despite convincing evidence for passive Ca transport in the PCT, there is also evidence for an active transport component. The active component of Ca transport in this segment has been partly evaluated by Ullrich *et al* (1976). These investigators evaluated the rate of active Ca reabsorption using the stop flow microperfusion technique with simultaneous capillary perfusion. Their results showed that active Ca transport, which contributed about 20% of total transport, declined towards zero if the ambient Na was replaced by choline or lithium. Parallel experiments in the golden hamster showed that active Ca transport vanished completely if active Na transport was blocked by ouabain. They concluded from their experiments that active Ca reabsorption from the proximal convoluted tubule depends on the active reabsorption of Na, presumably via a Na-Ca exchange. They proposed that the Ca transport out of the cell proceeds by a basolateral Na-Ca exchange, whereby the Na-K ATPase would deliver the primary driving force by pumping Na out of the cell, thereby creating an electrochemical gradient for Na ions. The Na ions running down this gradient into the cell would pull Ca out. An active transport component has also been shown for micropuncture studies in rats (Lassiter *et al*, 1963) and dogs undergoing an osmotic diuresis (Duarte and Watson, 1967). In summary, Ca movement across the proximal convoluted tubule is primarily passive and probably via a paracellular pathway. However, experiments have shown that there is also an active component in this segment. Rouse and Suki (1990) have suggested that this active component is probably confined to the S1 segment, a portion of the PCT which normally has lumen-negative PD and, hence, an unfavourable electrochemical gradient.

Proximal straight tubule segments (S2 and S3):

In the straight portion of the proximal tubule (S2), Bourdeau (1986) has provided evidence to suggest that Ca movement here is passive. The transport rate was voltage-dependent, which suggests paracellular diffusion. In the S3 segment, Rouse *et al* (1980), on the other hand, ascribed 75% of Ca absorption to active transport. Using the isolated perfused tubule technique, they measured unidirectional Ca flux in the pars recta and thin descending limb of Henle using  $^{45}\text{Ca}$  as the isotopic tracer. Their results showed that when the voltage was orientated negative in the lumen relative to the bath, a state which should have retarded efflux and enhanced backflow, Ca efflux was actually several times Ca backflux, resulting in a significant net efflux from this segment. This efflux could not be accounted for by water absorption, and so the demonstration that Ca could be transported against an electrical and a chemical gradient indicates the involvement of an active mechanism in its translocation.

In addition, these investigators performed experiments at room temperature instead of at  $37^{\circ}\text{C}$ , and showed no net Ca efflux under these conditions. They suggested from this observation that Ca efflux from this segment depends on cellular metabolism. Inhibition of the Na-K ATPase by ouabain did not seem to effect Ca transport in this segment, so suggesting the involvement of a Ca-ATPase in the efflux process, rather than a Na-Ca exchange mechanism.

The available evidence thus leads to the conclusion that Ca transport is largely passive in the S2 portion, and active in the S3 portion of the proximal tubule.

#### **2.1.2.2. Thin descending and ascending limbs of Henle's loop**

To date, only two studies have examined calcium transport in these segments. Both Rocha *et al* (1977) and Rouse *et al* (1980) have provided evidence to suggest that significant Ca transport does not take place in these segments.



### 2.1.2.3. The thick ascending limb of Henle's loop

The thick ascending limb of Henle's loop absorbs about 20% of the filtered load of Ca. Studies done by Bourdeau and Burg (1979) on this segment showed that Ca absorption here is largely voltage-dependent. Increasing the electropositivity of the lumen increased calcium absorption whereas when the lumen was electrically negative, Ca secretion was induced. They concluded from this that Ca absorption here is largely passive and presumably proceeds through paracellular pathways. In contrast to these findings are studies performed more recently by Friedman (1988), in which he examined the effects of parathyroid hormone (PTH) on calcium absorption in single, microperfused cortical thick ascending limbs, under conditions in which driving forces for passive calcium movement were eliminated. He found significant PTH-stimulated increases in active Ca absorption, and estimated that such active Ca absorption may represent some 40-60% of the total reabsorption in this segment. In agreement with these findings are studies done by Rocha *et al* (1977), in which they found that the flux ratio was greater than could be predicted from the PD using the Ussing equation. They also showed that the segments were able to decrease luminal calcium in the absence of water transport, and that ouabain reduced Ca efflux by only 10% while PD fell by 67%. These results suggested an active component of Ca transport in this segment. Thus overall, at least an appreciable fraction of the Ca reabsorbed in the TAL appears to be via an active transport mechanism.

Since increases in NaCl absorption in thick ascending limbs parallel increases in the transepithelial voltage (lumen positive), and, since Ca transport here appears to be partially voltage-dependent, a certain degree of obligatory coupling between sodium and calcium absorption is presumably present in this nephron segment. Primary stimulation of active Ca absorption in thick limbs, however, does not appear to alter the rate of NaCl transport. Sutton and Dirks (1975) hypothesized that the coupling is passive, absorption of both cations being driven by the common favourable electrical gradient. Because Ca is divalent, however, the electrical driving force should affect it more strongly than sodium, which is univalent. Therefore they speculated that passive Ca transport involves

the monovalent ion pair  $\text{CaCl}_2$

The thick ascending limb is a site of the hypercalcaemic action of PTH. PTH augments Ca absorption from this segment. The cellular processes responsible for, and the transepithelial routes followed by such hormone stimulated increments have not been defined. It has been suggested that PTH enhances the basolateral extrusion of Ca via the Na-Ca exchanger. It is also possible, however, that this hormone activates Ca channels in the luminal membrane via a second messenger system.

#### **2.1.2.4. The distal convoluted tubule**

The distal tubule absorbs 10-15% of the filtered Ca. Evidence provided by Costanzo and Windhager (1978) suggests that Ca movement in this segment occurs against its electrochemical gradient under both basal- and hormone- stimulated conditions; i.e., calcium reabsorption results entirely from active, transcellular movement. These investigators also showed that the capacity for Ca transport, during in situ perfusion, is indeed higher than that observed under free flow conditions, suggesting that Ca reabsorption in this segment is limited by the availability of transportable ions. Bronner *et al* (1988) have pointed out that the DCT has been shown to be the portion of the nephron that contains the highest concentration per mm length of Ca-ATPase, as well as the highest concentration of Ca binding protein (CaBP). This is consistent with the active transcellular transport of Ca in this segment.

In the same manner as in the thick ascending limbs, PTH specifically augments Ca absorption in the distal convoluted tubule. PTH also regulates the conversion of 25-OH-D3 to  $1,25(\text{OH})_2\text{D}_3$ , and thereby indirectly influences CaBP biosynthesis. Since there are a large number of receptors for  $1,25(\text{OH})_2\text{D}_3$  in the DCT, this might explain the PTH effects on Ca absorption in the DCT.

#### **2.1.2.5. The cortical and medullary collecting ducts**

About 5% of the filtered load of Ca is absorbed in these segments, which represent the final opportunity to adjust the composition of the urine. In

isolated, perfused cortical collecting tubule segments, three investigators have reported a low apparent permeability to Ca and an insignificant net flux which was voltage-sensitive (Bourdeau, 1986; Sharegai and Agus, 1982; Bourdeau and Hellstrom-Stein, 1982). In contrast to these findings are those by Imai (1981) who reported a substantial net Ca efflux which occurred against an electrochemical gradient and in the absence of water absorption. There is an apparent absence of active, hormone-stimulated Ca absorption in this segment, suggesting that adjustments may be completed in more proximal segments (Friedman, 1988).

Bengele *et al* (1980) have examined Ca transport in the medullary collecting tubule. Using an *in vivo* microcatheterisation technique, they estimated that 1.4% of the filtered load of Ca may be reabsorbed in this segment.

The apparent presence of Ca-ATPase and a Ca-binding protein in this segment (Taylor *et al*, 1982) has led to the suggestion that these proteins may be involved in the regulation of cytosolic Ca activity. Thus if there is indeed Ca transport in this segment, it is likely active.

The renal handling of calcium, as summarised here, is not immune to fluctuations *in vivo*, as the quantities reabsorbed and excreted are subject to influence from a number of factors. Some of these factors are: Hypercalcemia, dietary phosphate, volume status, acid-base status, hormones and diuretics. An in depth discussion of these factors is provided by Rouse and Suki (1990) and Bronner (1990).

### **2.1.3. Apical membrane entry of calcium**

Apical membrane entry mechanisms have not yet been characterised. Since entry at the luminal membrane is down an electrochemical gradient, it is unlikely to necessitate a pump and more probably utilises a channel.

The only (indirect) evidence for Ca channels has recently been supplied by Bindels *et al* (1990). These investigators examined the Ca influx mechanism in cultured opossum kidney cells, using Ca channel blockers. They discovered that D-600, diltiazem, and flunarizine all inhibited Ca uptake in a dose dependent manner, suggesting the existence of Ca-

permeable channels in this tissue. The possibility that calcium entry into the cell may be via a carrier should not be ruled out; however no direct evidence for this possibility has yet been reported (Bronner, 1991).

#### 2.1.4. Intracellular diffusion of calcium

In order for the Ca ions to move from the luminal membrane to the basolateral pole of the transporting cell, the divalent cation must move through a space that is crowded with organelles, whether fixed, e.g., the endoplasmic reticulum, the Golgi apparatus, or moveable, as in the case of lysosomes (Bronner, 1990). The concentration of ionized Ca inside cells ( $\pm 0.1 \mu\text{M}$ ) is at least 1000 times lower than in the extracellular environment. This value has been confirmed for epithelial cells using Ca-selective microelectrodes (Lee *et al*, 1980). The concentration of total Ca in cells (usually about .5 mM) may reach 8-9 mM (Bronner *et al*, 1990). A problem posed by the presence of transcellular Ca transport relates to the paradox of transferring large quantities of Ca through the cell while maintaining constant the low levels of free Ca within the cell. Friedman (1988) has proposed two possible mechanisms that would allow increased transcellular Ca absorption while protecting the low cytosolic Ca. 1) Coupling between apical Ca entry and basolateral Ca efflux may, as in the case of Na, be sufficiently tight that intracellular Ca activity remains constant. He suggested that organelles, such as mitochondria and endoplasmic reticulum, may offer short term buffering. It is well established that there is mitochondrial uptake of Ca which is enhanced as cytosolic Ca increases. 2) Alternatively, Ca entry and movement through the cell might involve an endocytic process or Ca binding protein, in which the cytoplasm is physically protected from the Ca moving through it.

There is increasing evidence to suggest the role of specific Ca binding proteins in the transport of Ca through the cell. These Ca-binding proteins are members of the calmodulin superfamily (Lawson, 1990), and therefore share some of the structural and functional properties of the calmodulins. A short discussion on calmodulin will thus help in understanding of calcium binding proteins (CaBP). Calmodulin, a heat- and acid-stable protein, was discovered as an activator of cyclic nucleotide phosphodiesterase and was identified as a CaBP (Klee, 1980). The term calmodulin is used to

denote that the protein is Ca modulated and that it also modulates the concentration of Ca. It is a multifunctional regulatory protein which activates a number of enzymes in a Ca-dependent manner. These include adenylate cyclase and phosphodiesterase (Cheung, 1980). It possesses 4 equivalent sites which specifically bind 4 moles of Ca with high affinity. This Ca binding induces significant conformational changes in calmodulin, and these Ca-induced changes produce sites on the surface of calmodulin through which it can interact with and activate the enzymes which it regulates (Vincenzi and Hinds, 1980). In contrast to other Ca-binding proteins such as troponin C, parvalbumins, intestinal CaBP, which are both tissue- and species- specific in structure and perform unique functions, calmodulin is a ubiquitous protein with multifunctional roles. Calmodulin appears to also be involved in the regulation of the Ca-pump, at least in the red blood cell, where it appears to significantly increase the  $V_{max}$  of the Ca-pump ATPase and Ca transport (Vincenzi and Hinds, 1980).

There are many specific Ca-binding proteins. Some examples of these are, parvalbumin, calbindin, and oncalmodulin (Heizmann, 1990). Those involved in Ca transport in the kidney and which will receive the most attention here, are the calbindins.

Two major forms of calbindins have been isolated and characterized, namely a high molecular weight form of MW 28,000 (calbindin-D28K), first isolated from chick intestinal epithelium, and a low molecular weight form (calbindin-D9K) first identified in rat intestinal mucosa (Bruns and Bruns, 1990). These proteins show distinct differences in their distributions, both among species and among tissues. In a recent study, Thomasset *et al* (1982) determined the distribution of rat CaBPs. They found high levels of the 28K protein in the cerebellum and kidney, whereas the smaller CaBP was concentrated in the duodenum, jejunum, and cecum. Many other organs contained small quantities of both CaBPs. Several studies have clearly demonstrated that renal CaBP (calbindin-28K) is confined mainly to the DCT (Bindels *et al*, 1990; Christakos *et al*, 1981; Pansini and Christakos, 1984; Taylor *et al*, 1982). This CaBP is regulated by  $1,25(\text{OH})_2\text{D}_3$ , and indeed the DCT has been shown to contain the highest concentration of receptors for  $1,25(\text{OH})_2\text{D}_3$  (Bronner and Stein, 1988; Pansini and Christakos, 1984). Interestingly, it has been found that the

25(OH)D-1 hydroxylase responsible for the synthesis of the  $1,25(\text{OH})_2\text{D}_3$  in the chicken is localised exclusively in the PCT, a finding which has been confirmed for the mammalian kidney. If the vitamin D-dependent CaBP is synthesized in the distal tubule as is reported here, then the  $1,25(\text{OH})_2\text{D}_3$  produced in the proximal tubule has to be secreted into the circulation and subsequently trapped by the target cell situated more distally (Christakos *et al*, 1981).

In the gastrointestinal tract, the efficiency of Ca absorption under various conditions correlates well with the intestinal mucosa content of CaBP (Bronner *et al*, 1986; Walters, 1990; Wasserman *et al*, 1990). Similar reasoning applies to the epithelial cell of the DCT and the cytosolic renal CaBP (Bronner, 1989). However, the exact mechanism whereby CaBP transports Ca is, at present, conjectural. Bronner (1990) suggested that since total transcellular flux, made up of entry, intracellular movement, and extrusion, cannot exceed any of its constituent rates, some mechanism must exist to amplify the intracellular diffusion rate of Ca so as to permit Ca flux to occur at the measured  $V_m$ . He proposed that the vitamin D-dependent renal CaBP, whose intracellular concentration is about 0.1 mM in the rat, can amplify the rate of intracellular Ca diffusion by the needed factor of some 70 times in both intestine and kidney. He suggested that the CaBP, in raising total Ca by three orders of magnitude, increases the transcellular flux of Ca and thus the free intracellular Ca ion concentration at the basolateral pole, allowing the Ca-Mg-ATPase to function near its maximum. This theory fits a recent suggestion by Walters (1990) that calbindin-D9K presents Ca to the pump.

A model for the process has recently been presented by Bronner and Stein (1988): the Ca gradient between the luminal border side and the basolateral end of the cell is the driving force for Ca through the cytosolic space. In the absence of CaBP, this gradient is determined by the concentration of free Ca. If a cell contains CaBP, free Ca and CaBP are in equilibrium, with the Ca partitioning between the bound and free states. As a result the very small cellular concentration of free Ca is greatly amplified and the transcellular total Ca gradient will approach the cytosolic concentration of CaBP. This amplified gradient provides the driving force for Ca extrusion. Finally, Ca ions that have been ferried to the basolateral membrane become dissociated from the CaBP, because the

Ca-binding affinity of the Ca-ATPase is greater than that of CaBP.

An alternative view for the intracellular diffusion of Ca has been supplied by Nemere (1990), who proposed the following model: uptake of Ca at the luminal membrane by endocytic vesicles, fusion of such vesicles with lysosomes, movement of Ca containing lysosomes along microtubules, and exocytosis of vesicular contents to complete the transport process.

### **2.1.5. Extrusion of calcium by the basolateral membrane**

Unlike apical Ca entry, basolateral membrane efflux is energy dependent because a steep electrochemical gradient opposes Ca exit. Two mechanisms capable of mediating basolateral membrane Ca efflux are Ca-ATPase and Na-Ca exchange.

#### **2.1.5.1. The Na-Ca exchange.**

The primary role of the exchange system is to mediate Ca efflux from the cells using the inwardly directed concentration gradient of Na ions (Reeves *et al*, 1990). This electrochemical gradient for Na is sustained by the primary active extrusion of Na from the cell by Na-K-ATPase. Evidence for a basolateral membrane Na-Ca exchange mechanism in the PCT has been provided by Ullrich *et al* (1976), and in the DCT, studies by Ramachandran & Brunette (1989) suggest that a Na-Ca exchanger may also be located in this segment. This mechanism has not yet been reported for the other segments. While there can be little doubt that a Na-Ca exchange mechanism operates at the basolateral membrane of proximal tubular cells, its role in terms of Ca extrusion as part of transcellular Ca transport is uncertain.

#### **2.1.5.2. Ca-ATPase.**

This is a primary active transport mechanism, because it is directly coupled to the hydrolysis of ATP. An in-depth description of the primary structure of the Ca-ATPase has been provided by Verma *et al* (1988). The translated sequence of the Ca-ATPase contains 1220 amino acids, with a calculated

molecular weight of 134683 daltons. It has a calmodulin-binding domain near the carboxyl terminus and two domains rich in serine and threonine, one of which matches the sequence found in protein kinase substrates that are cAMP dependent.

In the rabbit kidney, a magnesium-dependent Ca-ATPase has been identified in all segments of the nephron (Doucet and Katz, 1982). This enzyme was reported to be at the highest level in the DCT and CCD, intermediate in the PCT and TAL, and lowest in the PST and MCD, and appeared to account in theory for the active component of the unidirectional Ca flux found in the corresponding regions of the nephron with in vitro single tubule microperfusion techniques.

#### **2.1.6. Sodium-calcium interdependence**

Several features of renal Ca absorption bear similarities to the handling of Na by the kidney. Some of these features are: a) less than two percent of the filtered load is excreted, b) neither ion exhibits a tubular maximum, and c) changes in Ca excretion are closely paralleled by alterations in Na excretion (Friedman, 1988). These observations have been confirmed repeatedly in a number of species during various types of diuresis (H<sub>2</sub>O, NaCl, NaHCO<sub>3</sub>, mannitol, glucose, sucrose, furosemide) and during variations in Na intake. Thus it appears that Na and Ca ions are reabsorbed, and appear in the urine in roughly the same proportions as those in which they are present in the plasma.

In the proximal tubule, many investigators have shown that Na and Ca clearance as well as Na and Ca reabsorption correlate closely with each other (Beck and Goldberg, 1973; Duarte and Watson, 1967; Edwards *et al*, 1974; Vogel and Stoeckert, 1967; Walser, 1961). Furthermore, net Ca efflux from the proximal segment ceases when the Ca concentration in the tubular fluid falls to about 20% below that of the plasma ultrafiltrate. Again this is also true of Na (Walser, 1971). It is clear that water reabsorption must confer a high degree of interdependence between Na and Ca clearance proximally, however Frick *et al* (1965) have demonstrated not only that the net reabsorption of both ions was the same when related to their respective plasma concentrations, but also their influx from the interstitium into the perfused tubule lumen. They



inferred from this that the permeabilities of the tubular wall to these two ions were identical. Indeed Edwards *et al* (1973) have shown that in the proximal convoluted tubule, the transport rates of the two ions are identical even under experimental conditions in which thiazide diuretics were used. However between the end of the superficial proximal tubule and the bend of the loop of Henle, micropuncture studies have shown a dissociation of the transport of the two ions (Lassiter *et al*, 1963; Jamison *et al*, 1974). Rouse and Suki (1990) suggest that the dissociation of Ca and Na reabsorption in these studies could be explained by heterogeneity in the nephron populations sampled, (i.e., superficial PCT and juxtamedullary loops), or to Ca transport in excess of sodium transport in the proximal straight segments or thin descending limb.

Originally it was believed that the distal tubule reabsorbs Na and Ca proportionally in a similar manner to the proximal tubule. Subsequently, however, evidence has discredited this belief, as a number of situations exist where this parallelism is not observed. Ca and Na reabsorption are dissociated in situations in which distal nephron function is altered, particularly during administration of thiazide diuretics, which have a unique effect on renal excretion of Na and Ca (Costanzo and Weiner, 1974; Costanzo and Windhager, 1978; Edwards *et al*, 1973; Walser and Trounce, 1961). Over a decade ago, Costanzo *et al* (1974,1978) showed that chlorothiazide can dissociate Ca and Na transport in the distal convoluted tubule by increasing absolute Ca and decreasing absolute Na reabsorption. This pattern was first observed by Walser *et al* (1961), who postulated that the drugs, by decreasing Na transport, might, in turn, reduce the distal transepithelial potential difference. A decline in intraluminal electronegativity might decrease the passive backflux of Ca from blood to lumen and thereby increase net Ca absorption. The studies done by Costanzo *et al* (1974), however, are in disagreement with this hypothesis, as these investigators were unable to observe any influence of chlorothiazide on the distal transepithelial potential profile.

The mechanisms whereby thiazides exert their action are uncertain. Friedman (1988) has proposed a mechanism based on the observation that thiazide diuretics produce hyperpolarisation of intracellular voltage accompanying inhibition of Na transport. This hyperpolarisation would then increase the driving force for entry of Ca across apical membranes.

Thus the inhibition of NaCl absorption and resultant apical hyperpolarisation might augment transcellular Ca absorption. Another possible mechanism for the chronic effect of thiazides is that their effect may be mediated by PTH, however available evidence suggests that neither enhanced secretion of PTH, nor the presence of PTH, is required for the acute Ca retaining action of thiazides. An important question is whether Ca and Na are transported independently across the tubular epithelium in the distal nephron, with thiazides influencing only the Na transport, or whether there is at least some degree of linkage in the transport of these cations.

From the available evidence it appears likely that there is a common Na-Ca coupling mechanism down the length of the nephron. Evidence for such a mechanism in the nephron has been provided by Walser (1961). During sulphate diuresis, when approximately half of the urinary Ca is complexed by sulfate, he observed both that the resulting Na clearance was doubled and that the Ca clearance was multiplied approximately by a factor of five. This suggested that the tubular cells tend to maintain a constant ratio of Na to free Ca ions in the tubular fluid, rather than reabsorbing proportionate quantities of each. Walser proposed that during sulphate diuresis the concentration of sulphate in the tubular fluid rises along the nephron, leading to a fall in Ca ion concentration owing to complex formation. This could result in an increase in the proportion of Na to Ca bound in the membrane. Na reabsorption might then increase in relation to Ca reabsorption, tending to restore the original ratio of the effective concentration of the two ions in the tubular fluid. The net result would be that the fraction of filtered Na reabsorbed would exceed the fraction of filtered Ca reabsorbed, as is indeed the case. This hypothesis is in accord with evidence favouring competition between Na and Ca ions. If a constituent of the cell membrane binds both ions, a relative increase in the tubular fluid of either one could lead to an increase in absorption of that ion, tending to restore the original ratio.

Despite this impressive body of evidence pointing to some sort of coupling between Na and Ca transport throughout the nephron, the existence of a common pump mechanism that transports both cations has not been established. A number of situations in which Ca and Na clearance are poorly correlated have been found and have raised

doubts as to the existence of a common transport mechanism. One such system is adrenocortical hyper- or hypofunction; another is acidosis, and hypercalcaemia is another. Administration of thiazide diuretics, which act in the distal tubule to inhibit Na reabsorption, suggests that Na and Ca transport may be less inter-dependent in the distal convolution than in the ascending limb or proximal segment. Distally, neither Na reabsorption nor Ca reabsorption parallels water reabsorption. The distal transtubular negative potential should retard Ca reabsorption rather than facilitate it. A negative correlation between Na and Ca transport, such as evidently exists for Na and K transport in this region, might therefore be expected.

More recently Walser (1971) proposed a working hypothesis to encompass all considerations. Three sites with distinct types of inter-dependence are envisaged. In the proximal convolution, Ca reabsorption almost keeps up with Na reabsorption because of the effect of water removal in creating a favourable gradient. In the ascending limb, the Na-K ATPase indirectly promotes reabsorption of both cations, despite the fact that it is inhibited by Ca *in vitro*. Finally, a distal site exists at which aldosterone exerts its predominant effects. Here Na and Ca are negatively correlated, because the transtubular potential created by Na reabsorption retards the removal of Ca.

### **2.1.7. Conclusion**

The sites of Ca reabsorption down the nephron, and the percentages of absorption at these sites have been defined. The relative contributions of active and passive transport, however, remain controversial in some cases. In the proximal convoluted tubule, Ca reabsorption is largely a passive process coupled with the active transport of Na. Water reabsorption most probably plays a very important role in this passive movement of Ca. In the pars recta of this segment, a greater percentage of Ca reabsorption can be attributed to active transport, as the tubular epithelium is not as "leaky" here. In the thick ascending limb there are substantial components of voltage-dependent Ca movement, as well as PTH-stimulated increases in active Ca absorption. This is suggestive of both active and passive processes playing an important role in this segment. In the distal convoluted tubule, Ca movement occurs against its

electrochemical gradient, strongly suggesting that reabsorption of this cation results entirely from active, transcellular movement. Finally, in the cortical and medullary collecting ducts, which represent the final opportunity to adjust the Ca composition of the urine, there appears to be very little active Ca transport.

The mechanisms of transcellular Ca movement are not very well understood. Apical membrane entry of Ca is presumed to occur through Ca-permeable channels, although no direct evidence of these has yet been provided. Indeed one of the major questions remaining open for epithelial cells of any kind is a demonstration of the existence of Ca channels. The mechanism of intracellular diffusion of Ca is at present conjectural, although there is increasing evidence to suggest the role of specific Ca-binding proteins in the transportation of this cation through the cell. Basolateral extrusion of Ca is energy-dependent because of a steep electrochemical gradient. The Ca-ATPase and the Na-Ca exchange mechanism mediate basolateral Ca efflux.

The interdependence between Na and Ca reabsorption in the kidney is a well established phenomenon. The most interesting feature of this interdependence is the observation that changes in Ca excretion are closely paralleled by alterations in Na excretion, even during various types of diuresis or variations of Na intake. There is evidence to suggest that Ca reabsorption parallels Na reabsorption in all segments, with the possible exception of the proximal straight tubule and the distal tubule. In this latter segment, administration of thiazide diuretics inhibits only Na reabsorption suggesting that Ca and Na transport may be less interdependent here.

Although evidence does not favour a common pump mechanism for these two ions, it is difficult to envisage that the parallelism between Na and Ca clearance occurs without some finely tuned control mechanism in the nephron. It is therefore possible that a common channel exists in the apical membrane down the length of the nephron that is able to alter its selectivity to Na and Ca depending on the conditions it is exposed to. Such a mechanism could exert fine control over Na and Ca reabsorption to maintain the ratio of the concentration of these two ions that exists in the filtrate, even under a variety of manipulated conditions, as has been shown experimentally.

## 2.2. Calcium channels: mediators of calcium entry

### 2.2.1. Introduction

The role and function of cellular calcium most probably evolved in parallel with the needs of primeval cells to tap the available phosphate (Bronner, 1990). As cells learned to utilise the calcium ion for a variety of purposes - locomotion, contraction, export of cellular products, among many - the development of Ca entry and extrusion mechanisms became increasingly important. The study of Ca entry mechanisms, in particular, have been the subject of intense investigation in the last ten years. Ca entry is of central importance to both normal and abnormal activity in the heart (Mikami *et al*, 1989). It underlies rhythmic activity and slow conduction in nodal tissue; it helps support the action potential plateau, and regulates the supply of Ca for activation of contraction (Tsien *et al*, 1985). In skeletal muscle, the contraction is initiated by a transient depolarisation of the surface membrane which then propagates to the transverse tubule membrane and triggers a rapid release of Ca ions from its major intracellular storage site, the sarcoplasmic reticulum. In the brain, Ca entry participates in the generation of various forms of electrical activity, such as dendritic spikes, rhythmic firing and burst discharges (Yaari *et al*, 1987). Calcium also clearly plays a pivotal role as an intracellular messenger. When the  $(Ca_i)$  rises into the millimolar range, many important cellular events are initiated. Such events include muscle contraction, the release of neurotransmitters and of certain hormones, regulation of enzyme activities and the control of membrane ion permeabilities (Reuter, 1983). Transient increases in  $(Ca_i)$  which act as important intracellular signals can be initiated in two major ways: 1) by opening a Ca channel in the cell membrane or, 2) by causing Ca ions to be released from intracellular stores, probably contained within the endoplasmic reticulum (Miller, 1987). In most cases the release of internal Ca is the most important first event, the opening of the channel occurring later.

Some interesting forms of excitability in which Ca channels are found to play a role occur in the nodal regions of the heart, the cilia of Paramecium, or in the dendrites or growth cones of certain neurons (Tsien,

1983). Schramm and Towart (1985) have proposed at least four different types of Ca channels:

- 1) leak channels
- 2) voltage-sensitive channels
- 3) receptor-operated channels
- 4) stretch-sensitive channels

Ca influx through the leak channel is apparently a consequence of the large electrochemical gradient tending to drive Ca ions into the cell. Mechanical effects on vascular smooth muscle are said to promote Ca influx through a stretch-sensitive channel, which can be distinguished from the others in a variety of ways. The voltage-sensitive channel is well studied and its existence is undisputed. It is so named because it is controlled by voltage-dependent gating, that is, its opening and closing kinetics are the result of changes in membrane potential. Present evidence suggests that a "voltage sensor" in the membrane, e.g., a protein group with dipole properties, which may be an integral part of the ion channel, reacts to the electric field. Any change in membrane potential will cause a reorientation of the charged sensor within the field and, therefore, a change in the ion flow through the channel (Reuter, 1983). It is widely distributed in different tissues in the human body as well as throughout the animal kingdom. Finally, the receptor-operated channel is a Ca influx pathway which has been proposed to account for the fact that many neurotransmitter ligands activate Ca influx in the absence of changes in membrane potential. They are also thought to be activated by a variety of smooth muscle constrictor substances including  $\alpha$ -adrenergic agonists, Ach, histamine and a number of peptides (Goto et al, 1989). In addition, they are often not as selective for Ca as the voltage-sensitive Ca channels.

There is a large electrochemical driving force for the inward movement of Ca across the cell membrane, because in unstimulated cells the equilibrium potential,  $V_{Ca}$ , according to the Nernst equation, is greater than 120 mV. However the measured reversal potential, where net current flow through Ca channels is zero, is much more negative. In cardiac cells and chromaffin cells, K and Cs ions can move through Ca

channels in the outward direction, and in so doing, cause a shift of the membrane voltage by 50 - 70 mV negative. It has been shown that Na ions can move through Ca channels both in cardiac muscle and molluscan cells, particularly with low extracellular Ca (Reuter and Scholz, 1977; Garnier *et al*, 1969; Kostyuk *et al*, 1977).

Voltage-sensitive Ca channels have been widely investigated in recent years, and a large number of publications concerning their properties have been forthcoming. Receptor-operated channels, on the other hand are not as well understood and, as will be shown below, apparently bear little relevance to the work presented here. This review therefore summarises much of the recent literature on voltage-sensitive Ca channels, both in excitable tissue and in non-excitable tissue types.

### **2.2.2. Calcium channel types and distribution**

Voltage-sensitive Ca channels have been identified in a number of cell types. Traditionally they have been associated with excitable cells, such as muscle, neurons and endocrine cells. However they have also been shown to exist in a number of non-excitable cell types. One theme that runs through recent work is the heterogeneity of voltage-sensitive Ca channels, and it is clear that more than one type exists. It is thus important to know how many types exist and how their properties differ. In particular, studies on neuronal cells (Nowycky *et al*, 1985) and cardiac cells (Nilius, *et al* 1985) have provided sound evidence for the existence of three types of voltage-sensitive Ca channels:

- 1) "T"-type (transient) voltage-sensitive Ca channel: this channel contributes a relatively tiny current and has the smallest conductance value (about 5-10 pS in 100 mM Ba). T- channels do not as yet have a well developed pharmacology. They are widely distributed and are also termed "low-threshold" or "fast" Ca channels by some authors (Miller and Fox, 1990).

- 2) "L"-type (long-lasting) voltage-sensitive channel: this is the best characterised type of Ca channel. The L-type channel contributes long-lasting currents at strong depolarisations. It has the largest conductance

(about 20 - 25 pS in 100 mM Ba) and is probably the most widely distributed. L-currents display less voltage-dependent inactivation than T currents, and are therefore termed "long-lasting". Ca currents carried through T- and L-type channels can be readily distinguished by their different voltage responses. However the major reason that the L-type channels have been the most thoroughly investigated is that an extensive pharmacology exists for these channels (Miller and Fox, 1990). Compounds such as the dihydropyridines, which block or enhance L-currents, play a key role in the isolation and characterisation of L-channels. Divalent cations, such as Cd and Ni are also good L-channel blockers. It has been suggested that, due to their chemical similarity to Ca, they displace Ca from its binding sites on the outer membrane surface near the Ca channels whose occupation with Ca is necessary for Ca to pass through. It is also possible that these inorganic blockers actually become trapped within the channel structure and thereby block the channel (Grissmer and Cahalan, 1989).

3) "N"-type (neuronal) voltage-sensitive Ca channels: in addition to T and L-type Ca channels, Nowycky *et al* (1985) reported a third type of channel (N), which has a conductance intermediate between T and L (approximately 13 pS in 100 mM Ba). N-type channels are potently blocked by Cd, but appear to be resistant to the dihydropyridines. The N-channels are not as widely distributed as the other two varieties, and appear to be present only in neurons.

The question that is frequently asked is whether there are only three types of voltage-sensitive Ca channels, or whether more exist. Even though voltage-sensitive Ca channels fall comfortably into the three channel categories described, clear differences are also apparent within each class. Miller and Fox (1990) have proposed that three classes exist which actually represent closely related families of channels rather than a single invariant molecular type.

The distribution of voltage-sensitive Ca channels varies from one tissue type to another. Different kinds of cells possess different complements of channels, sometimes in radically different numbers. For example, chick dorsal root ganglion cells were found by Nowycky *et al* (1985) to possess



all three types of channels, whereas certain types of cardiac muscle, e.g., rabbit atrial cells possess L- but no T- channels (Bean, 1989). A further aspect of organization to be considered is the distribution of the different varieties of channels within cells. This concept of microorganisation is feasible when one considers that a cell, e.g., a neuron, may have a very complex structure, with different parts of the cell simultaneously engaged in different activities. Yoshino *et al* (1988) suggested that each channel type contributes to different physiological functions, such as a source of Ca ions during excitation-contraction coupling, the generation of pacemaker activity and the release of neurotransmitters from nerve terminals.

An exciting development in the characterisation of voltage-sensitive Ca channels was made by Tsien *et al* (1985) using the patch clamp technique. They proposed three modes of channel gating. Mode 1 is characterised by brief openings occurring in rapid bursts. The probability of openness in this mode is relatively low. Mode 0 refers to a condition where the channel is unavailable for opening. Voltage-dependent inactivation increases the time a channel spends in this mode. Mode 2 is distinguished by relatively long-lasting channel openings and typically brief closings. The probability of these channel openings is typically high. These investigators found that exposure of cardiac cells to dihydropyridines (DHP) did not alter the amplitude of unitary Ca channel events, but produced a striking change in the pattern of channel opening. They proposed that binding of drugs does not plug the pore, but instead favours one or more modes of gating. Pure agonist effects arise when mode 2 is specifically favoured, and pure antagonist effects result when mode 0 is preferentially stabilised; these extremes encompass a wide range of intermediate possibilities for partial agonist or antagonist effects.

### **2.2.3. Pharmacology of calcium channels**

A large number of compounds have been shown to modulate voltage-sensitive Ca channels, and in particular, many of the major drug classes appear to be relatively specific for L-channels. These drugs not only have therapeutic importance (mainly in the cardiovascular field), but are also

important in the identification and purification of the L-type channels.

Fleckenstein (1988) was the first to observe that the effects of certain phenylalkalines such as phenylamine and verapamil on cardiac muscle mimicked the effects of Ca withdrawal from the bathing medium. It then became clear that these drugs actually worked by blocking voltage-sensitive Ca channels. Blockade of Ca channels has also been described for drugs such as the flunarizine series. Many other drugs also block Ca channels; for example, drugs such as diltiazem and nifedipene have been considered to be relatively specific Ca channel antagonists.

A most exciting and important development in the pharmacology of Ca channels occurred when Schramm *et al* (1983) described the dihydropyridine Bay K-8644, which was shown to activate rather than inhibit L-channels. In the case of some dihydropyridines, different optical isomers can produce opposing effects. Also different drugs inhibit L-type channels in different ways. For example verapamil-like drugs block voltage-dependent Ca channels better when the channel is opening and closing at high frequencies. Thus verapamil may only have access to its site of action through the opening of a hydrophilic pathway such as the open channel pore. In contrast, most of the dihydropyridines show frequency-independent block and their action can be powerfully modulated by changes in membrane potential. In cardiac muscle, for example, changes in membrane potential can alter the potency of dihydropyridine antagonists over three orders of magnitude. Dihydropyridines are thus considerably more potent at depolarised membrane potentials (Kass and Arena, 1989). In electrophysiological studies in heart and smooth muscle it has been shown that agonist and antagonist DHPs alter the voltage-dependence of the Ca channel current (Hess *et al*, 1984). They appear to shift the voltage dependence of the steady state inactivation of the Ca current to more hyperpolarised voltages. The important effects of membrane potential on the actions of dihydropyridines may also blur the distinction between dihydropyridine agonists and antagonists. In general, however, agonist activity is favoured by hyperpolarised potentials, and antagonist effects by depolarised potentials. Many examples illustrate the fact that the effects of dihydropyridines are not only dramatic, but also very complex (Miller and Fox, 1990). A particular drug may act as an agonist, antagonist, or

produce no effect, depending on the prevailing conditions. Thus occasional reports of dihydropyridine blockers acting as agonists or dihydropyridine agonists acting as antagonists are not all that surprising. For example, the effects of Bay K-8644 are voltage-dependent. Whereas it usually increases Ca current, it behaves like a Ca antagonist under partly depolarized conditions (Schramm and Towart, 1985).

At the level of the single channel, effects of dihydropyridines on the gating properties of channels are apparent. Dihydropyridine agonists produce channel activity that exhibits extremely long openings, while dihydropyridine antagonists produce no channel openings whatsoever. The major classes of organic L-channel blockers, e.g., dihydropyridines, phenylalkylamines, and benzothiazepines, all bind to separate and specific sites on the L-channel. Affinity labelling studies have shown that all three binding sites are associated with the same subunit of the L-channel. A number of models have been used to explain the action of DHPs on Ca channels. Sanguinetti *et al* (1986) suggested that the effect of agonist DHPs may result from slowing the backward transition rate from the opening to the resting channel state. An explanation proposed by Kass and Arena (1989) is that the DHP receptor is located within the Ca channel, and that DHP molecules reach the receptor via hydrophilic or hydrophobic pathways. They suggested that the DHP receptor for these channels is buried in the lipid bilayer adjacent to the external end of the channel.

Naturally occurring toxins have also played an important role in our understanding of the properties of certain channel types. The toxin known as  $\omega$ -conotoxin, derived from the venom of a marine snail was the first to be used successfully in the blockade of voltage-sensitive Ca channels (Olivera *et al*, 1985). The toxin appears to have little effect on T-channels, but clearly blocks at least some types of L- and N-channels. In addition, the site of action of  $\omega$ -conotoxin on neuronal L-channels is clearly distinct from that of the dihydropyridines or other known organic Ca channel blockers (Miller and Fox, 1990).

#### 2.2.4. Regulation of calcium channels

The influx of Ca into cells via voltage-sensitive Ca channels, as previously discussed, is a major mechanism for regulating many cell functions. Thus it is not surprising that these channels are themselves regulatable. Regulation of these channels can change the moment to moment influx of Ca into the cell. The activity of voltage-sensitive Ca channels can be increased or decreased by a variety of neurotransmitters which operate through a variety of second messengers and G-protein-link pathways.

In patch clamp experiments it was found that  $\beta$ -adrenergic agonists increased the open probability of L-channels in cardiac myocytes (Walsh *et al*, 1989). That the probability of L-channel opening is increased when  $\beta$ -agonists are added outside the patch pipette is evidence that a diffusible second messenger is involved in the modulation of channel function (Trautwein and Pelzer, 1988; Tsien *et al*, 1988). Indeed it is widely believed that cAMP is responsible for virtually all aspects of the stimulation of L-channel activity in the heart, thus mimicking the effects of  $\beta$ -adrenergic agonists. For more information on Ca channel modulators and second messengers, as well as the molecular structure of voltage sensitive Ca channels, the reader is referred to an excellent review by Miller and Fox (1990). Hormonal regulation of Ca entry in electrically non-excitable cells is of great importance in cell signaling. Here the reader is referred to a review by Peterson (1990) in which he discusses Ca entry in cells that do not exhibit action potentials. Table 2.1 shows examples of multiple types of voltage-sensitive Ca channels in excitable tissue types from different vertebrate species.

**Table 2.1.** Examples of multiple types of voltage-sensitive Ca channels in excitable cells of vertebrate tissue.

<u>PREPARATION</u>	<u>Ca CHANNEL TYPES</u>	<u>AUTHORS</u>
Chick dorsal root ganglion	T, N, L	Nowycky <i>et al</i> , 1985

Mouse d.r.g	HTI, LTI, HTN	Fox <i>et al</i> , 1987
Adrenal glomerulosa	T, L	Kostyuk <i>et al</i> , 1987
Intestinal smooth muscle	FI, SI	Cohen <i>et al</i> , 1988
		Yoshino <i>et al</i> , 1988
Rat vas deferens smooth muscle	3 types (unnamed)	Nakazawa <i>et al</i> , 1988
Rat portal vein smooth muscle	Fast, Slow	Loirand <i>et al</i> , 1989
Snail neurons	1 type	Gutnick <i>et al</i> , 1989
Mammalian hippocampal cells	LVA, HVA	Yaari <i>et al</i> , 1987
Pancreatic $\alpha$ 2 cells of guinea pig	FD, SD	Rorsman, 1988
Cardiac ventricular cells of guinea pig	T, L	Nilius <i>et al</i> , 1985
Clonal pituitary cells	FD, SD	Armstrong <i>et al</i> , 1985
Airway smooth muscle	1 type	Worley <i>et al</i> , 1990
Neuroblastoma cells	T, L	Pang <i>et al</i> , 1990
Rat cerebellar Purkinje fibres	T, L	Regan, 1989
Intestinal smooth muscle	T, L	Yabu <i>et al</i> , 1989

Frog sympathetic nerve cells	N, L	Lipscombe and Tsien, 1987
Dog atrial cells	Fast, slow	Bean, 1985
Rabbit ear artery	T, L	Benham <i>et al</i> , 1987
Rat hippocampal pyramidal CA3	T, N, L	Madison <i>et al</i> , 1987
Frog skeletal muscle	Fast, Slow	Cota and Stefani, 1985
Mouse myoblasts	Fast, Slow	Beam <i>et al</i> , 1986
Chick d.r.g	LVA, HVA	Carbone and Lux, 1984
Rat hippocampal granule	T, N, L	Gray and Johnstone, 1986

---

where: FD and SD = fast and slow deactivating

FI and SI = fast and slow inactivating

LVA and HVA = low voltage and high voltage activating

HTI and LTI = high threshold and low threshold inactivating

HTN = high threshold non-inactivating

## 2.2.5. Calcium channels in non-excitabile tissue

Voltage-sensitive Ca channels are found in most cells capable of generating action potentials. However outside the neuromuscular system there are very many cell types that evidently do not function in this way. In many epithelial cells, hormones or neurotransmitters evoking Ca entry do not elicit action potentials, and in many cases hyperpolarising rather than depolarizing responses are seen. Although the processes regulating Ca inflow are widely understood, little is known of the molecular mechanism underlying Ca entry.

Two possible routes of Ca uptake have been proposed by Peterson (1990): 1) through non-selective channels, and 2) through Ca-selective voltage-insensitive channels. Peterson and Maruyama (1983) proposed that non-selective Ca-activated cation channels may have some limited permeability for divalent cations. In 1986, von Tscharner *et al* demonstrated Ca flux through Ca-activated non-selective cation channels and suggested that this pathway was functionally important in receptor-activated Ca influx in neutrophils. The ion channels activated by inositol 1,4,5-triphosphate in T-lymphocyte plasma membrane are permeable to Ba, and therefore probably also to Ca, but their selectivity has not yet been tested. More recent investigations by Penner *et al* (1988) in mast cells also suggest that these channels are largely non-selective. At the moment the possible physiological role of non-selective cation channels in receptor-regulated Ca entry is very doubtful. Non-selective cation channels are not attractive candidates for this role since a small Ca influx would inevitably be accompanied by a large Na influx. The excess Na would have to be pumped out at great energy expenditure for the cell. One possibility, however, is that non-selective channels might operate in conjunction with Na-Ca exchange. The stoichiometry for the Na-Ca exchange is normally 3:1, and the large Na efflux that would be needed for Ca entry through such an exchanger might therefore fit in well with the large Na influx mediated by non-selective cation channels (Peterson, 1990).

Recently, Zschauer *et al* (1988) demonstrated single Ba-selective channels obtained by incorporating membrane vesicles from thrombin-stimulated platelets into planar bilayers. It was suggested that these channels were the long sought after receptor-operated channels. This study was important for demonstrating the existence of a Ca-selective voltage-insensitive channel in non-excitabile tissue. Evidence for a Ca-permeable channel in the membrane of T-lymphocytes has been provided by Gardner *et al* (1989). In their studies, the channel apparently accounted for the enhanced transmembrane Ca flux following stimulation of T-lymphocytes by the mitogen phytohemagglutinin.

In the kidney, Bacskai and Friedman (1990) have recently provided some evidence for the possible existence of Ca channels in renal

epithelial cells. These investigators examined Ca influx in single cultured cells from distal renal tubules sensitive to PTH, by measuring intracellular Ca. Their observations suggest that the PTH- stimulated rise in Ca results from Ca entry through DHP- sensitive channels and is consistent with the view that PTH leads to the recruitment of new, or activation of existent, plasma membrane Ca channels. This Ca entry was activated by Bay K-8644, and inhibited by nifedipene. Table 2.2. summarises some examples of Ca-permeable channels found in non-excitabile tissue.

**TABLE 2.2.** Examples of Ca-permeable channels in non-excitabile tissue types

PREPARATION	CA CHANNEL TYPES	AUTHORS
Human T-lymphocytes	1 Ca-specific channel	Kuno and Gardner, 1987
Human neutrophils	2 non-selective channels (18, 5 pS)	von Tscharner <i>et al</i> , 1986
Thrombin-stimulated human platelets	1 Ca-selective voltage-insensitive channel	Zschauer <i>et al</i> , 1988
Human carcinoma	2 Ca-selective channels (3, 13 pS)	Mozhayeva, 1990
Basophil leucocytes	1 receptor-operated channel	Tedeschi <i>et al</i> , 1990
Pancreatic B-cells	L-type channel	Findlay <i>et al</i> , 1989 Ashcroft <i>et al</i> , 1989



### 2.2.6. Concluding remarks

Calcium entry into cells is of great importance and underlies such important events as muscle contraction, cell signalling, and electrical activity in the heart and nervous system. In excitable tissue types, there appear to be both voltage-sensitive Ca channels and receptor-operated Ca channels. The more widely studied of these two species are the voltage-sensitive Ca channels. These are divided into three classes, the L-type, T-type, and N-type channels. These are distinguished both by their electrophysiological properties, and their response to various pharmacological agents. Three classes of drugs, the dihydropyridines, phenylalkylamines, and benzothiazepines are of particular importance, especially in the characterisation of L-type channels. A toxin,  $\omega$ -conotoxin, and various inorganic ions (Ni, Cd, Mn) have also been useful in characterising these channels.

In non-excitable tissue, only two kinds of Ca-permeable channels have been characterised: Ca-permeable non-selective channels, and Ca-selective voltage-insensitive channels.

In excitable tissue, Ca entry plays an important role in many electrical events. It is thus probably important that since Ca ions are outnumbered by other ions, high selectivity is needed if the channel is to allow Ca influx rather than a general cation influx. This may also be the reason that there are three specific types of voltage-sensitive Ca channels. In non-excitable tissue, the need for selectivity is probably not as great, as the purpose of Ca channels here would simply be to increase  $[Ca]_i$  above a certain threshold level required for hormone release. It is therefore conceivable that a non-selective channel is the mediator of Ca influx in these tissue types.

## 2.3. Ion channels in the kidney

In renal epithelia, ion channels, which work in conjunction with pumps, exchangers, and cotransporters, are key components of systems that transport ions, organic solutes and water between urine and blood. These ion channels have been shown to be regulated by a number of factors, including transmembrane potential, pressure differences, and interaction with small ions, especially Ca and H (Palmer and Sackin, 1988).

The aims of this chapter are to provide an overview of ion channels in renal tubule segments as elucidated by the patch clamp technique, and to discuss the possible function and regulation of some of these channels.

### 2.3.1. The proximal convoluted tubule

#### 2.3.1.1. Apical membrane

Two studies on cultured renal cells of rat and rabbit have provided evidence for the existence of channels in the apical cell membrane. A non-selective cation channel ( $g=13$  pS) was reported in rabbit proximal convoluted tubule by Merot *et al* (1988). Channel activity was not voltage-dependent but required a high calcium concentration (1 mM Ca) on the cytoplasmic face. The channel was Cl-impermeant and was thought to probably be involved in cell volume regulation or Na reabsorption.

In tissue culture of rat proximal tubular cells, Marom *et al* (1989) discovered two kinds of channels: the first was a 15 pS K channel which was Ca-activated, and the second was a 50 pS cation channel (PNa/PK = 1-5:1). This latter channel was neither voltage- nor Ca-dependent. These workers suggested that the two channels contribute significantly to a K conductance and a Na conductance respectively in this membrane.

#### 2.3.1.2. Basolateral membrane

In the basolateral membrane of rabbit proximal convoluted tubule, Parent *et al* (1988) discovered a K channel. The methods these investigators

employed was simply to soak the tubule in a bathing solution containing collagenase (400 U/ml). This procedure was found to be well-suited for removing the connective tissue surrounding the basolateral membrane, and they reported a good seal success rate (55%). The channel had a conductance of 54 pS in 200 mM KCl, was inwardly rectifying, and exhibited subconductance states. It was suggested that since the transmembrane potential is one of the most common channel gating mechanisms involved in control of K-ion permeability, this K-conductance may be voltage regulated. This K channel is probably functional in ensuring a cell negative potential that enhances the rate of sodium entry at the apical side.

In Necturus proximal convoluted tubule, in which the basal adventitia was pared away to expose the basolateral membrane, two K channels were found in studies performed by Sackin and Palmer (1987). These two channel types were identified on the basis of their kinetics: a short open-time K channel with a mean open time of <1 ms, and a long open-time K channel with a mean open time of >20 ms. Because the short open time channel was consistently observed both in cell-excised and cell-attached patches, it was studied in more detail than the long open time channel. Thus, with K-Ringer in the pipette, the conductance of the short open time channel was 47 pS in the cell-attached configuration and the K:Na selectivity ratio was 12:1. The channel was found to be voltage-dependent: the open probability increased with hyperpolarisation. The most striking property of the short-open time channel was that application of a negative pressure to the patch pipette increased the open probability ( $P_o$ ) of this K channel. In a more recent study, Sackin (1987) has shown that the short-open channel in cell-attached patches can be activated by decreasing the osmolarity of the bathing solution, causing the cell to swell. This finding is consistent with the short open time K channel having a role in cell volume regulation. Thus during cell swelling, the basolateral membrane stretches. The resulting increase in open probability of the K channel could restore cell volume by loss of K, followed by osmotic exit of water.

Thus far, neither Na or Cl channels have been detected in cell-attached patches of this tissue. (Cl channels have been found in brush-border vesicles, but never in apical or basolateral membranes.)

### 2.3.2. Proximal straight tubule

#### 2.3.2.1. Apical membrane

On the apical membrane of isolated perfused tubules, Gogelein and Greger (1986) have demonstrated the existence of a Na channel. In the cell-attached mode this channel had a conductance of 12 pS, was voltage-independent, and amiloride-sensitive. They suggested that this channel could play a role in Na reabsorption. These investigators also measured the intracellular potential, and demonstrated a value of -65 mV for cells in this segment.

In the Necturus proximal tubule, Kawahara *et al* (1987) demonstrated a K channel in the apical membrane. This membrane was exposed by ripping the tubule open with a fine needle. The channel had a conductance of 60 pS (with 100 mM KCl in the pipette), and a K:Na selectivity ratio of 32:1. It was found to be Ca-insensitive. This channel is thought to contribute substantially to apical K conductance in this segment.

In opossum kidney cell culture, two populations of stretch-activated channels have been demonstrated (Kolb, 1990). It was not specified in which membrane these channels were found, but since most cells in culture orientate themselves with their apical membrane upwards, these were probably apical channels. The channels had conductances of 25 and 42 pS, and were cation-selective. In addition these investigators reported three K channels in this membrane, with conductances of 12, 80, and 120 pS. These channels are probably involved in K efflux in this segment.

#### 2.3.2.2. Basolateral membrane

Gogelein and Greger (1986) have demonstrated the existence of a non-selective channel using the isolated perfused technique, and patching on the lateral surface. The channel did not discriminate between Na and K ions, and the permeability for cations was twice that for anions. The channel was voltage-dependent and had a conductance of 28 pS with

KCl Ringer in the pipette. An interesting observation of these studies was that in cell-attached patches, channel activity was nearly absent at a holding potential of 0 mV, i.e., the channel was inactive under physiological conditions. This may indicate that the channel is mostly inactive under physiological conditions and only becomes active when the cell becomes substantially depolarised. Although the significance of this non-selective channel in proximal tubular function is still unclear, it is possible that it is involved in the contraluminal exit mechanism of various anions, as well as a role in cell volume regulation processes. A year later, Gogelein and Greger demonstrated, using the same techniques, a K channel in this segment. The channel had a slope conductance of 50 pS at an infinitely positive clamp potential, and the I-V plot showed inward rectification. The channel was permeable to K in both directions, independent of Ca ions, and inhibited by Ba. These channels are thought to be responsible for the basolateral K conductance. A similar K channel was found in Necturus proximal tubules, in which the basal cell membranes were exposed by carefully paring away the basement membrane with fine forceps (Kawahara *et al*, 1987). The conductance of this channel was 49.8 pS in the cell-attached mode. The PK:PNa ratio was 10:1 and the fractional open time increased with hyperpolarisation. They suggested that this voltage-dependent K conductance mediates K recycling in accordance with basolateral pump activity to maintain the constancy of cell K content in the presence of fluctuations of pump activity and membrane potentials. A schematic of a proximal tubular cell depicting the ion channel pathways is shown in Figure 2.3.1. below.

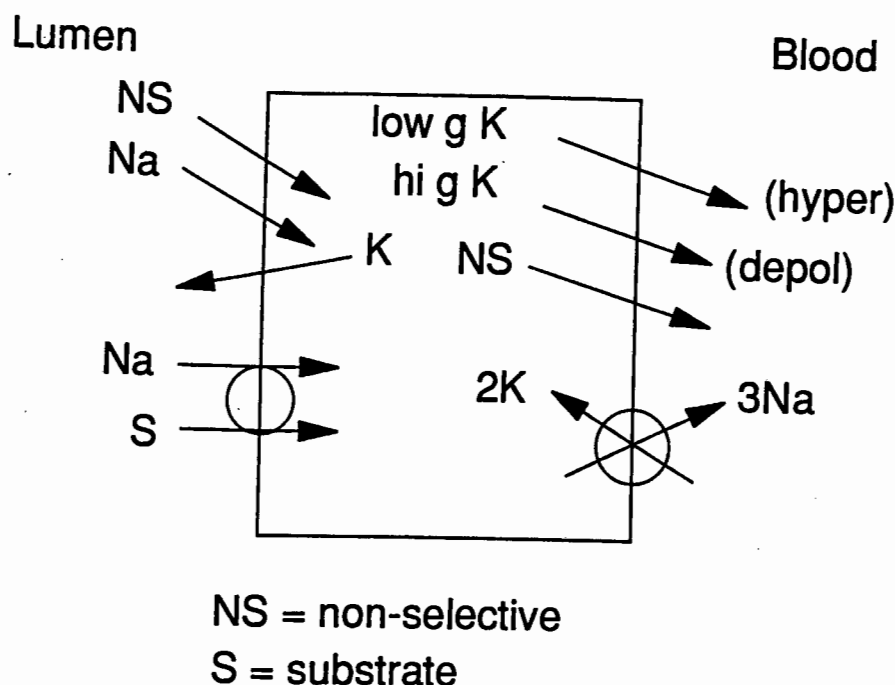


**Figure 2.3.1.** Schematic of a proximal tubular cell, depicting the ion conductive pathways through the membrane walls.

### 2.3.3. Thick ascending limb

#### 2.3.3.1. Apical membrane

A very thorough study on this segment was undertaken recently by Bleich *et al* (1990) using the isolated perfused tubule technique, patching on the luminal membrane. Out of 455 patch trials, only 65 elicited K channel activity in this segment. In the cell-attached configuration with KCl in the pipette, the conductance was 60 pS; and with NaCl in the pipette the conductance was 34 pS. The channel had one open and two closed time constants, and the open time probability was increased by depolarisation. It was Ba-sensitive, and a number of channel blockers were effective in reducing the open probability of the channel (verapamil, diltiazem, quinidine). The open probability was also down-regulated by decreasing

pH, as well as increasing ( $\text{Ca}_i$ ). The channel appears to be responsible for the K recycling in the TAL, i.e., the Na-2Cl-K carrier is the major site of entry of Na, K, and Cl into the cell. Most of the K that is reabsorbed by the cotransport system is recirculated out of the cell into the lumen via a conductive pathway.

In cell culture studies, in which patch clamp and microelectrode studies were used in parallel, Guggino *et al* (1987) reported a very large conductance K channel (121 pS). The channel was Ca-sensitive, inhibited by Ba, and was activated by depolarisation of the cell membrane. Again, it is likely that this channel plays a role in generating the K conductance. In a further study to characterise the channels, these investigators found that Ba and charybdotoxin are slow blockers, while TEA and quinine are fast blockers of this channel. An interesting observation was that the Ba blocking rate was many times greater when Ba was applied on the inside than on the outside, i.e., the energy barrier for Ba is much higher when it enters from the outside.

No Cl channel has yet been reported for this membrane.

#### 2.3.3.2. Basolateral membrane

In the thick ascending limb of mouse kidney, Paulais and Teulon (1989) have reported a non-selective cation channel with a conductance of 25-30 pS. These investigators soaked the segments in collagenase before patching directly onto the basal membrane of the cells. In excised patches the open state probability of the channel was reversibly reduced by adenine nucleotides. A definitive physiological function has not been assigned to this channel; it could, however, play a role in the modulation of NaCl reabsorptive flux through the epithelium.

Recently, Greger *et al* (1990) reported a Cl conductance in this segment, using the isolated perfused tubule technique. In cell-attached patches the mean conductance was 42 pS for positive clamp voltages, and 31 pS for negative clamp voltages. The channel was outwardly rectifying and its open probability increased with depolarisation. This channel probably plays a role in Cl diffusion from the cell interior to the ECF (Paulais and Teulon, 1989). In addition these investigators also demonstrated non-selective channels in both (apical and basolateral)

membranes and in a few excised patches, these channels coexisted with either a K channel or a Cl channel. The properties of these channels were not explored; however, they apparently occurred only upon excision of the patch, which renders it likely that they are gated by unphysiologically high  $\text{Ca}$  activities on the cytosolic side.

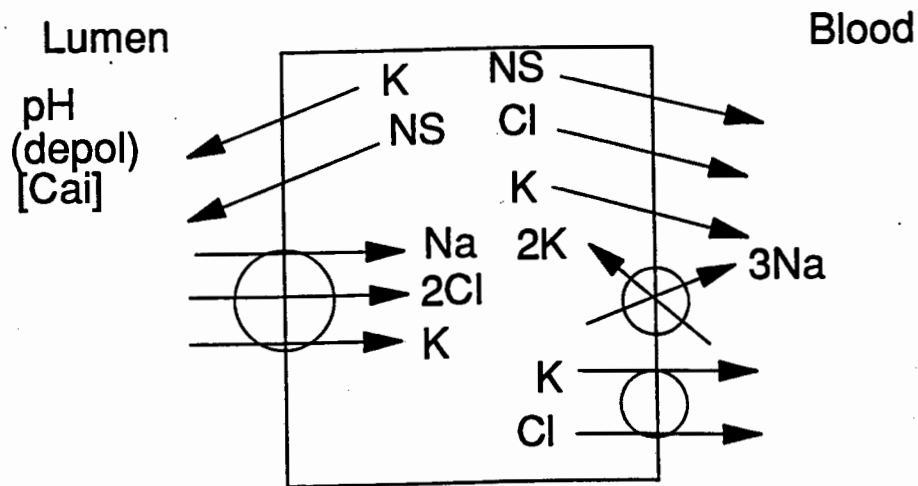


**Figure 2.3.2.** Schematic of a cell from the thick ascending limb, depicting the conductive pathways for ion transport across the membrane walls.



### 2.3.4. The distal convoluted tubule

#### 2.3.4.1. Apical membrane

In Amphiuma diluting segment, two K channels have been reported (Hunter *et al*, 1986). The first had a conductance of 120 pS, was inhibited by Ba and low pH values, and was Ca-activated. The open probability of this channel increased with depolarisation. The second K channel was found only in cell-attached patches. The channel had a conductance of 30 pS, and exhibited inward rectification such that K flowed into but not out of the cell. This channel was shown to have four parallel equally conductive subunits and one main gate (Hunter and Giebisch, 1987 - see thesis discussion).

Recently, Marunaka and Eaton (1990) reported Cl channels in the apical membrane of a distal nephron A6 cell line. They found a 3 pS and a 8 pS channel in this membrane. The 3 pS channel was found on 80% of all patches). The channel was voltage-dependent, the open time probability increasing with depolarisation. It was also Ca-activated, exhibited outward rectification, and was cAMP-dependent. The 8 pS channel was far less common, had one open state and two closed states, and was neither voltage-, cAMP-, nor Ca-dependent. It is a widespread belief that conductive transtubular Cl movement is through the paracellular path. It is however possible that the 3 pS Cl channel is the site for regulation of apical Cl entry through changes in the level of cAMP. It may also play a role in facilitating Na transport by providing a hyperpolarising conductance to maintain a significant driving force for Na entry. A role for the 8 pS channel is less clear as this channel was rarely recorded and presumably had a low density on the apical membrane. It is however possible that both channels play a role in controlling the apical membrane anion conductance of A6 cells under conditions of varying Na transport rate.

In another MDCK cell culture (Mardin-Darby canine kidney), Lang *et al* (1990) have provided evidence for three K channels: 1) a non-rectifying K channel with a conductance of 221 pS, 2) an inward rectifying K channel with a conductance of between 34 and 59 pS, and 3) an outwardly

rectifying K channel with a conductance of 20 pS and 98 pS for inward and outward directed currents respectively. All three varieties were activated by increasing concentrations of  $(Ca_i)$ . In addition these investigators reported a high- conductance Cl channel ( $g=460$  pS), which was stimulated by cAMP. They suggested that cell swelling might lead to the activation of the K and Cl channels.

#### 2.3.4.2. Basolateral membrane

Recently, Taniguchi *et al* (1989), using the isolated perfused tubule technique, reported the existence of two K channels in the basolateral membrane of the DCT of rabbit. The channels had conductance values of 48 and 60 pS, and were both blocked by the presence of 0.1 mM BaCl<sub>2</sub> on the cytoplasmic side. Neither channel was voltage dependent. Since local recycling at the basolateral membrane is largely dependent on a K conductance, these K channels probably constitute conductive pathways for K in this membrane.

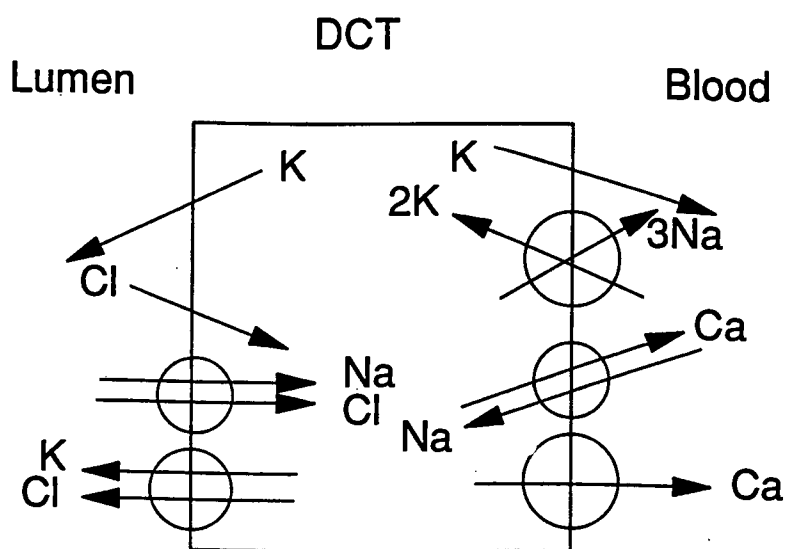


**Figure 2.3.3.** Schematic of a cell from the distal convoluted tubule, depicting the conductive pathways for ion transport across the membranes.

### 2.3.5. Cortical collecting duct

The cortical collecting duct consists of roughly two thirds principal cells, where Na reabsorption and K secretion take place, and roughly one third intercalated cells where H and HCO<sub>3</sub> secretion take place (with Cl absorption).

#### 2.3.5.1. Apical membrane

Using the "ripped tubule" technique, Palmer and Frindt (1986) found an amiloride sensitive Na channel with a low conductance in 140 mM NaCl Ringer (5 pS). It was presumed that this channel mediates Na reabsorption *in vivo*. In a further investigation into the properties of the channel, Palmer and Frindt (1988) found that these channels had a mild preference for Li over Na, and were activated by hyperpolarisation, which is unlike Na channels in excitable tissue. Another important finding was that single channel current saturated as a function of (Na) or (Li). These investigators also reported the existence in this segment of a non-selective channel with an intermediate conductance (23 pS). The properties of this channel, however, have not yet been elucidated.

Using the "ripped tubule" technique, Hunter *et al* (1986) have established the existence of a K channel in rabbit cortical collecting duct. The channel had a conductance of 40 pS; the open probability increased with membrane depolarisation. In addition, the channel had two open and two closed states, was Ba-sensitive and Ca-activated. These workers suggested that this channel is the probable route for transcellular K secretion by the cortical collecting tubule. They also speculated that it might play a role in situations where aldosterone causes an increase in Na conductance. In such an event, an increase in (Na<sub>i</sub>) brings about an increase in (Ca<sub>i</sub>) by the basolateral Na-Ca exchanger which increases the apical K conductance. Also, since an increase in (Na<sub>i</sub>) depolarises the cell, this would also contribute to increasing the K conductance.

Using a similar technique, Frindt and Palmer (1989) have reported a low conductance K channel in the apical membrane of rat cortical

collecting duct. The channel had a conductance of 9 pS, and a K:Na permeability ratio of 10:1. The open probability of the channel was voltage-independent, but decreased on addition of Ba. The channel was Ca-insensitive. It is believed that in spite of its low conductance, this channel contributes substantially to the K conductance in this membrane, since the open probability is relatively high under physiological conditions.

In cultured cortical collecting duct intercalated cells, Light *et al* (1990) have found a Cl channel with a very large conductance (303 pS). This channel was rarely active in cell-attached patches (2% of patches); however channels were activated after patch excision (18% of patches). The Cl:Na permeability ratio for this channel was approximately 10:1. The open time probability was not altered by pH changes or alterations in  $[Ca]_i$ . The channel showed rapid flickering and occasional subconductance states. While the principal cells in the tubule segment are thought to be involved in Na reabsorption and K secretion, the intercalated cells are thought to transport H, Cl, and  $HCO_3$ . The Cl channel may thus be involved in cell volume regulation or in Cl and  $HCO_3$  secretion.

In principal cells of rabbit cortical collecting duct, grown in tissue culture, Gross *et al* (1988) have provided indirect evidence for an apical membrane Na conductance, an apical membrane K conductance, and a small apical Cl conductance. These investigators did not, however, use the patch clamp technique and were unable to say whether the cells they used had the properties of fully matured principal cells. The only direct evidence for the existence of a Cl channel in the apical membrane of principal cells has come from Christine *et al* (1987), who observed a Cl channel in principal cell monolayer cultures. The channel had a conductance of 120 pS and was observed in both on-cell and cell-excised configurations. Contrary to popular belief, therefore, there may be some Cl absorption across principal cells.

#### 2.3.5.2. Basolateral membrane

Very little work has been done to uncover the existence of ion channels in this membrane. Gross *et al* (1988) have provided evidence for a large basolateral Cl conductance in rabbit, as well as a K conductance. The K

conductance is probably involved in K secretion into the tubule, while the presence of a Cl conductance suggests that at least a small portion of Cl flux may proceed through the cells. The major portion, however, is likely to pass through the tight junctions between the cells.

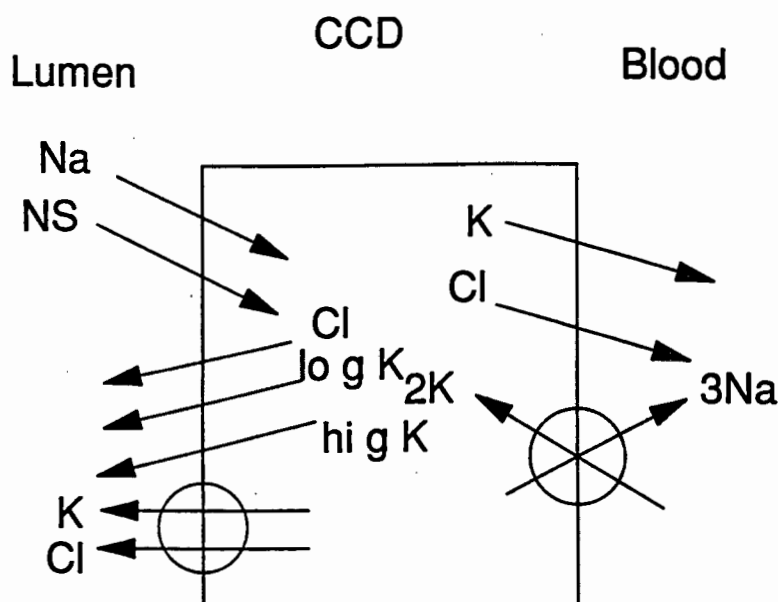


**Figure 2.3.4.** Schematic of a principal cell from the cortical collecting duct, depicting the conductive pathways for ion transport across the membranes.

### 2.3.6. Conclusion

Since epithelial cells do not undergo the large, rapid shifts in membrane potential that are characteristic of nerve and muscle, it is not surprising that some of the channels reported were voltage-insensitive. An unusual finding, however, was that some of the channels activated on hyperpolarisation of the cell. This is opposite to what happens in excitable tissue.

Thus far, Na channels, K channels, and non-selective channels have been fairly well characterised down the length of the nephron. Cl channels thus far have not been reported in the proximal nephron. In the

thick ascending limb, their existence has been established on the basolateral membrane, while in the cortical collecting duct, their existence has been derived from transepithelial flux studies and patch clamp studies on cultured cells only. The functional significance of these channels has in many cases been investigated using such procedures as cell stretching, changing Ca concentrations, pH changes, and addition of various blockers and drugs. However, further studies are needed to characterise the exact role played by some of these channels *in vivo*. No direct evidence has yet been provided for the existence of Ca channels anywhere along the length of the nephron.

## **2.4. Statistical analysis of patch clamp data**

### **2.4.1. Introduction**

Once an adequate seal has been formed and channel activity observed and recorded, the next challenge is to identify the channel. The detail or depth in which this channel is analysed will depend on the quality and quantity of the collected data. Thus the aims of analysis are to a) observe the results at leisure, and to determine the qualitative features, b) to perform a quantitative analysis of measurable variables, in which quantities are compared with theoretical distributions, and c) to infer a biological mechanism from the result (Colquhoun, 1987). Essentially this involves the procedures of measuring the amplitude of channel currents, and durations of closed and open periods. Because these measurements can be time consuming, automatic methods of analysis have been developed, in which distributions are produced by a computer program.

The analysis techniques used to measure these variables have become a standard procedure, and will be only briefly summarised here. A detailed description of the theory and practice of these techniques is provided elsewhere (Colquhoun, 1987; Colquhoun and Sigworth, 1983). The recent development of alternative analysis techniques, such as fractal analysis, have been the focus of some attention and controversy in the last few years, and will be discussed in greater detail.

### **2.4.2. Measurement of amplitudes**

Channels isolated by the patch clamp technique are integral membrane proteins which allow the diffusion of ions across cell membranes. From an idealistic viewpoint, conformational changes in these channels will be resolved electrically as pulses of current with a fixed amplitude, which are typically "rectangular" or "square" in shape. Amplitudes of channel openings can be measured only for openings that are clearly long enough to reach full amplitude. The amplitude may be estimated by averaging points at the shut levels, and points at the open level. The distribution of the digitized current values can be plotted as a histogram.

Amplitude histograms generated at different clamp voltages and under varying ionic conditions can be used to obtain estimates of single channel conductance, channel selectivity, the open time probability of the channel and its possible modulation by agonists and antagonists. In some experiments, single channel currents of more than one amplitude are seen, i.e., either two or more channels or multiple subconductance states are present. Thus the amplitude histogram can be used as a check for multiple channel populations or multiple subconductance levels.

The shape of the current-voltage (I-V) plot yields information on the type of conduction processes of the channel. A linear plot is obtained if the channel is acting as an ohmic conductor while rectification is indicated by a curvilinear plot. The slope of the I-V plot gives the conductance, which may depend on the voltage and ionic conditions. For example, when symmetrical solutions are used to bathe the membrane patch the I-V curve passes through the origin. Imposition of an ionic gradient across the patch should displace the plot to either the left or the right depending on the direction of the imposed ion gradient and the channel selectivity. The point at which the plot intersects the voltage axis is the reversal potential. For a channel that is perfectly selective for one ion species, the reversal potential will equal the Nernst potential for that ion. A deviation from the ideal Nernst potential reflects the channel's selectivity to other ions. Depending on the non-selectiveness of the channel, the value of the reversal potential might then be best described by the Goldman equation.

### **2.4.3. Measurement of durations**

A temporal recording of the current flowing through a single channel can be thought of as depicting a series of rectangular current pulses of relatively fixed amplitude, the individual pulses reflecting time-independent transitions of the channel protein between any number of different conformational states. The time a channel resides in any given conformational state is an exponentially distributed random variable.

In the measurement of open- and closed-time durations, there are two problems to be solved; firstly transitions from one current level to another must be detected, then the duration of time between one level



and the next must be measured. The two methods in use are 1) the threshold crossing method, and 2) the time course fitting method. The most common of these is the threshold crossing method. Usually a threshold is set halfway between the fully open and fully shut current levels, and every time the observed current crosses the 50% threshold, a transition is deemed to have occurred (Colquhoun, 1987). In order to keep the position of the threshold correct, it is necessary to keep track of any drift there may be in the baseline. The time at which a transition occurred can be estimated by taking the data point on either side of the crossing of the threshold, and interpolating between them to estimate the time at which the threshold is crossed. The problem in identifying channel activity in an experimental record is that very short channel openings may be indistinguishable from random noise fluctuations about the baseline, i.e., an inappropriate sampling interval and/or a filter cut-off frequency of the recording apparatus will produce a recorded response that does not reach full amplitude; similarly short closed-times are indistinguishable from fluctuations away from the open-channel current level. The duration of intervals will thus be underestimated. Technically the challenge is to be able to resolve as many of the actual transitions as possible, including the briefest openings and closings, and to perform the analysis as accurately as possible. The filters cut-off frequency, and the form of the filters frequency response characteristic can be varied to optimise the probability of detection. In addition, the threshold needs to be high enough to avoid counting an excessive number of noise peaks as channel events, but low enough to catch as many true events as possible. The 50% threshold method is thus not always optimal.

There are only two discretely observable types of temporal distribution, the distribution of open times and the distribution of shut times. Analysis of event durations is based upon their random distribution. The first thing to define is what is meant by random. In the present context, what is meant is that the probability that an open channel will shut during a short time interval is constant regardless of what has gone before. In other words what happens in the future depends only on the present state of the system, and not on its past history. Statisticians call processes with this characteristic "lack of memory" homogenous Markov processes.

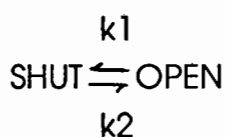
This concept can be compared to a series of tosses of a coin. The

probability of getting heads at each toss is the same regardless of what has happened before. The relevant analogy to tossing a coin is the random thermal movements of the channel protein molecule. It is the randomness of thermal motions that underlies the randomness of the open- and closed-lifetimes. The bonds of the protein molecule will be vibrating, bending and stretching, and much of this motion will be rapid. One can imagine that each time the open channel molecule stretches there is a chance that all its atoms will get into a position where the molecule has a chance to surmount the energy barrier and flip into the shut conformation (Colquhoun, 1987).

For construction of open-time histograms, the time taken for the opening and subsequent closing of a channel is first recorded and then placed in an appropriate bin, the width of which is a prespecified time interval. The number of events that occupy a specific bin is then plotted against the time interval represented by the bin. The process is similar for the construction of a closed-time histogram but the event measured is the time between closing and subsequent opening of a channel. These times can then be used for a kinetic analysis of the channel activity. In order to find the mean lifetime with an accuracy of 10%, Colquhoun and Sigworth (1983) have stipulated that it is necessary to measure at least 100 or so individual lifetimes. It will rarely be satisfactory to measure fewer than 200 openings, and for a complete distribution, 1000 to 2000 openings may need to be measured to obtain reasonable precision.

The open- and closed-time distributions can be described by the sum of one or more exponentials. Thus the histograms are fitted with an exponential distribution, the fitted distribution usually being tested to determine the goodness of fit. The parameter values are chosen to maximise the goodness of fit. One such method for the goodness of fit is the minimum chi-squared method. Here the data for the fitting are the frequencies of the observations in each bin. The chi-squared statistic is a measure of the deviation of this observed value from the fitted frequency. This method can be regarded as a weighted least squares approach. The fitted exponential distribution can be used to formulate a model to account for the observed number of conformational states. In practice it is usually observed that more than one exponential curve is required to fit the distribution. This is exactly the result expected if a) the system exists in

several discrete states, and b) the transitions between these states occurs at a constant rate. The number of exponentials indicates the number of open or closed states. Deriving kinetic parameters from multistate channels requires the investigator to choose a kinetic model. The simplest possible example is a channel that can exist in only two states, open and shut. The states will be numbered one and two respectively, so that the rate constant for transition from shut to open is denoted  $k_1$ , and that for the transition from open to shut,  $k_2$ . The mechanism is conventionally written as:



This is simple for two reasons. Firstly it is simple because there are only two states, and secondly it is simple because these states are distinguishable on the record. In reality, however, kinetic models are far more complex than this. Kinetic models are complicated by a number of factors. For an accurate analysis of channel kinetics, long recordings containing many openings and closings are required.

In general any model for channel behaviour must predict not only the time course of channel opening but also the statistics of opening and closing (Aldrich and Yellen, 1983). Determination of kinetic parameters in obviously multichannel patches is, if not impossible, extremely difficult and requires not only picking what one hopes is an adequate model but assuming that the channels are identical and functionally independent.

#### **2.4.4. Bursts: a special case:**

A "burst" of openings can be defined as any series of openings separated by closures that are less than a specified duration. Thus a "burst" is several openings occurring in quick succession. "Bursts" of openings can themselves be grouped into clusters with long gaps between clusters.

In cases in which the openings are observed to occur in "bursts", there is often reason to think that all the openings in one "burst" may originate from the same channel, so the closures between "bursts" may be easier to

interpret. "Bursts" vary in duration because of changes in the number of openings in each "burst" (Pallota, 1991). In this study, as will be shown later (see methods), the definition of a "burst" has been extended to cover the case where a single channel, while remaining open, shows frequent jumps from one subconductance state to another.

Colquhoun (1987) has suggested that if the record can clearly be divided into "bursts" of openings, then other distributions can be investigated; for example the distribution of the "burst" length, the distribution of the number of openings per "burst", the distribution of the total open time per "burst", and the amplitudes of "burst" events.

#### **2.4.5. Alternative methods: the study of fractals and unidimensional diffusion**

##### **2.4.5.1. Background**

Recently, the study of fractals (short for "fractional exponentials") and closely related chaotic dynamics have been widely applied to many different fields. Chaos and fractals are subjects associated with the discipline of non-linear dynamics: the study of systems that respond disproportionately to stimuli. Under some circumstances, deterministic non-linear systems, (those that have only a few simple elements), behave erratically, a state called chaos. Chaotic behaviour occurs in low-dimensional dynamical systems. Low dimensional means that the system can be described by a small number of independent variables. A dynamical system is one whose variables are a function of time. The system variables have well defined values at any point which can be computed uniquely from the preceding values. Thus the system is deterministic. If the initial conditions are known, then we can compute the entire future behaviour of the system. However since the initial conditions, can in practice be specified with only finite accuracy, the long term behaviour of the system is unpredictable. Thus these systems are deterministic but unpredictable in the long term (Liebovitch and Toth, 1991). Deterministic chaos is not the same as chaos in the dictionary sense of complete disorganisation of randomness. Non-linear chaos refers to a

constrained kind of randomness.

A working definition of chaos has been provided by Campbell (1987): namely the random, "unpredictable motion in time of deterministic dynamical systems having no external stochastic forces, so that randomness derives from sensitive dependence on initial conditions". In the field of engineering, McRobie and Thompson (1990) elaborated on the concept of chaos: if a periodic force is applied to a linear system, the system will rock, or oscillate erratically for a while - these are the transients - before settling down to a steady vibration with the same frequency as the applied force. This final motion does not depend on the situation's initial conditions, its velocity and position when the force was first applied. If non-linearities are included in the system, then more than one steady state is produced and the one at which the system settles will depend upon its initial conditions. Occasionally, however, when the transients decay, the system may not settle into any regular oscillation, but may continue to vibrate erratically, never quite repeating any earlier manouvre, and yet never escaping from the well. Chaotic processes are reviewed in a non-technical way by Gleick (1987).

The study of chaos is now a major enterprise, with convincing experimental evidence for its relevance to such fields as electronics, optics, and hydrodynamics (Schaffer, 1987). A recurrent theme is that apparently random fluctuations sometimes turn out to be entirely deterministic. Schaffer (1987) ascribed four attributes to chaos:

- 1) Determinism: there are no random inputs.
- 2) Complex dynamics: chaotic systems exhibit sustained motion. They do not settle to equilibria or simple dynamics.
- 3) Sensitive dependence on initial conditions: small differences in initial conditions are amplified, and since one can never specify a system's state with infinite precision, long term forecasting becomes impossible.
- 4) Road to chaos: typically one is interested not in single dynamical systems, but in whole families of equations which differ, the one from the other, in the value of a parameter. Often a succession of dynamical states is observed as one varies the parameters. The transitions are called bifurcations.

Fractal structures are often the remnants of chaotic non-linear dynamics. Wherever a chaotic process has shaped an environment,

fractals are likely to be left behind. For example in nature an earthquake, a dynamic process, might shape a coastline, which can be described in terms of fractals. A fractal, as first conceived by Benoit B. Mandelbrot (quoted in Goldberger *et al*, 1990), consists of geometric fragments of varying size and orientation but similar shape. It is remarkable that the details of a fractal at a certain scale are similar (though not necessarily identical) to those of the structures seen at larger or smaller scales. For example, if one saw two photos of dendrites of a neuron at different magnifications, one would have difficulty deciding which photo corresponded to which magnification. All fractals have this internal, look-alike property called self-similarity.

A tool for analysing the dynamics of a complex non-linear system is a "phase space" representation. This technique tracks the values of independent variables that change with time. For many complex systems, the independent variables cannot be readily measured or identified. For such systems, phase space representations can be plotted using the method of delay maps. The mathematics of this concept has been discussed by Takens (1981): for the simplest delay map, each point corresponds to the value of some variable at a given time,  $x(t)$ , plotted against the value of the same variable after a time delay,  $x(t + T)$ . A more complex delay map plots the same variable after a number of time delays, the number of delays corresponding to the number of dimensions of the plot. Thus a series of points at successive times underlies a curve or trajectory that describe the system's evolution. To identify the system's dynamics, one determines the trajectories for many different initial conditions. Then one searches for an attractor - a region in space that attracts trajectories. The simplest kind of attractor is the "fixed point" which describes a system that always evolves to a fixed point. The next most complex is the "limit cycle" which describes a system such as an ideal frictionless pendulum which evolves to a periodic state. Other attractors are simply called "strange", and describes a system that is neither static nor periodic. The system described by a strange attractor is chaotic. The attractor is "strange" in that its structure is often fractal: if one looks at finer and finer resolution, one sees more and more detail to the attractor.

The universality of "chaotic dynamics" in mathematical and physical systems has prompted renewed interest in the application of non-linear

analysis to biological processes. Attention has also been focussed on the physiological and medical implications of these subjects. Some examples of the applications of chaos and fractals are to be found in respiratory physiology (Demongeot *et al*, 1987), cardiac medicine (Goldberger and West, 1987), and renal physiology (Jensen *et al*, 1987). In the human body, fractal-like structures abound in networks of blood vessels, nerves, ducts, and the lungs to mention a few (Goldberger *et al*, 1990). Fractal structures in the human body arise from the slow dynamics of embryonic development and evolution. In the last few years, there has also been an explosive growth in the study of objects and processes that have been found to have fractal properties. A few examples include: the perimeters of clouds; the surface areas of proteins; Brownian motion, and the intensity of earthquakes (Lovejoy, 1982; Lewis and Rees, 1985; Lavenda, 1981; Kagan and Knopoff, 1981 - quoted in Liebovitch and Sullivan, 1987).

#### **2.4.5.2. Fractal analysis in patch clamp**

Up until recently, the modelling of ion channel gating has been rooted in the concepts of classical kinetics. In accord with these concepts, channels are proposed to exist in a finite number of discrete states, with transitions between states governed by first order rate constants. The additional assumption that the rate constant is independent both of time and of the preceding history of the channel defines the model as a Markov chain model. Recently, Liebovitch *et al* (1987) applied Mandelbrot's (1983) fractal concepts to the gating of ion channels. In contrast to Markovian assumptions, it is assumed in Liebovitch's fractal model that the channel can exist in an infinite number of energy states, perhaps due to subtle differences in protein conformation (Liebovitch, 1989). Moreover changes in protein conformation occur over many time scales from picosecond rotations around bonds to unfolding modes that last for minutes. Consequently, transitions from one conductance state to another would be governed by a continuum of rate constants, rather than a few discrete states. The simplest fractal model of ion channel gating postulates that there is one non-conducting (closed) and one conducting (open) state, and that the rates for transition between these states vary as a function of time (Liebovitch *et al*, 1987); thus the channel

behaves as if it has a memory. This model is "fractal" in that the statistics that describe the gating kinetics are self-similar when viewed at different time scales. Liebovitch and Sullivan (1987) proposed that if the closed and open states are each represented as a continuum of many conformational states, the kinetic rate constant for leaving the closed or open state is then a mixture of rate constants for leaving this collection of states.

In the classical kinetic model, the minimum number of open and closed states is found by counting the numbers of exponential components in the observed open and closed time distributions. Pallota (1991) has added to the argument that these kinetic states probably correspond to many different conformational states; he suggested that unless the conformational states directly affect channel opening and closing, the kinetics approach cannot detect them. This concept lends itself to the application of fractal analysis. Unlike the sums of exponentials predicted by conventional kinetic models, this mechanism predicts that open- or closed-lifetime distributions ought to be described by an empirical equation. The fractal scheme of channel gating has been described by the simple scheme,



The forward and reverse rate constants of the simple model are a function of time and follow the form  $k(t) = At \exp(1-D)$ , where  $A$  is the "kinetic setpoint" and  $D$  is the fractal dimension. Armed with interval distributions containing many thousands of events, this prediction can easily be tested by determining the goodness of fit to either sums of exponentials or to the fractal equation.

Liebovitch *et al* (1987) have shown that a log-log plot of open- and closed-time distributions is a sensitive method to analyse ion channel kinetics. If there are multiple plateaus on this plot, then the channel has multiple, discrete states that can be well represented by a Markov process. However if the kinetics of the channel are fractal, then this plot will be a straight line. Recently, it has also been shown that phase space plots can also be used to differentiate between deterministic and random channel kinetics (Liebovitch and Toth, 1991). Several data sets have been



well described by the fractal model. For example, Liebovitch and Sullivan (1987) have shown that the open and closed times and voltage dependence of a potassium channel from cultured mouse hippocampal neurons are well described by the fractal model. In contrast, Korn and Horn (1988) have shown using maximum likelihood methods that two different sets of data (a 90 pS Ca-activated K channel and a non-selective channel from rabbit corneal endothelium) could both be best described by Markov models, but conceded that the data were probably too few to discriminate accurately between the two models.

#### **2.4.5.3. Diffusion models of ion channel gating:**

Recently, an altogether different view of ion channel kinetics has been proposed by Millhauser *et al* (1988a). This was based on a correlation that these workers found between the amplitudes and the rate constants in certain cases (Millhauser *et al*, 1988b). The model that these workers devised, uses Markov processes with fixed rate constants, as in the conventional view, but invokes a large number of conformational transitions with equal rate constants. In their view an ion channel protein randomly samples a large number of different (but simply related) configurations during the gating period. The transitions are rapid compared to the patch clamp time scale, so the dynamic process appears to be diffusive. The model requires many states but few parameters, and predicts event-time histograms that are close to power-law distributions. These workers suggested that if their diffusional model could be applied to the data, then the logarithmic display of open- and closed-time intervals would show a linear regime followed by a precipitous drop.

These workers have also shown that such a model naturally gives rise to commonly observed characteristics such as "bursts". To illustrate how such a model might give rise to "bursting" behaviour, they used the illustration of a particle undergoing an unbiased Brownian random walk in one dimension. At one position along the line is an unpassable barrier that, when encountered, causes a channel opening. When the particle is near the barrier, the probability of encounter is high so that when one

event occurs, it is very likely that several more will follow. When the particle is far from the barrier, the probability of encounter is low and a long quiescent period will follow. It was suggested that the one-dimensional diffusion process corresponds to a type of twisting motion that opens and closes these channels. In support of the unidimensional ion diffusion theory is the view expressed by Condat and Jackle (1989) that the chain structure of the protein molecule comprising the ion channel favours one-dimensional motion along a main chain. In addition, Liboff and McLeod (1988) have suggested that ions moving through channels follow prescribed helical paths.

#### **2.4.6. Conclusion**

At present there is controversy as to whether ion channel proteins occupy a few discrete independent states, as assumed by the Markov model (Colquhoun, 1983), or an infinite number of states linked by scaling as assumed by the fractal models (Liebovitch, 1987).

It is not, however, as simple as "Markov vs Fractal". There are really two separate issues: a) are there a small number or a large number of channel states, and b) are the kinetic rates between these states independent or connected by a simple relationship? All four combinations are possible. An exponential model with a few discrete states may have independent rates, or it may have a set of kinetic rates with a fractal scaling. A continuum model may not have a simple relationship connecting the states, or it may have a fractal scaling connecting the states. Conceptually, the conformational properties and molecular dynamics of the protein molecule comprising an ion channel lend credibility to the more complex fractal and unidimensional models of ion channel gating. To enhance this credibility, however, there is a definite need to apply these alternative analysis procedures successfully to a wider spectrum of patch clamp data.

## **SECTION THREE**

### **METHODS**

## SECTION THREE

### METHODS

#### 3.1. Tissue preparation

Apparatus:

Dissecting dish with Peltier cooling device

Fine forceps (Dumont no. 5)

Insulin syringes (1 cc with 28 G bore needles, B-D)

Transferring pipette (fabricated from a pasteur pipette; Lasec)

Carbon steel surgical blades (Swann Morton, no's. 11 and 22)

Dissecting microscope (Zeiss)

##### 3.1.1. Rabbit kidney

Rabbits (either sex, preferably young) were sacrificed by stunning and exsanguination. The left kidney was then removed, and two thin midsagatal sections were cut for dissection. These were immediately placed into Ringer solution (p.74). The dissection was then carried out using fine forceps and syringe needles in cold Ringer (6-8°C, kept cool by means of a peltier cooling device). The sections were teased apart using fine forceps until individual tubule segments were isolated (Burg *et al*, 1966). The segments were then cut using the sharp syringe needle.

Tubules were then transferred using a transferring pipette to the patch clamp chamber, where they were bathed in Ringer at room temperature (20 - 24°C). Here they were identified under high magnification (up to 300 times) using an inverted microscope. The segments comprised proximal straight tubules (PST), cortical thick ascending limbs (TAL), distal convoluted tubules (DCT), and cortical collecting ducts (CCD). The luminal surface of the individual tubule segments was then accessed by

one of two methods:

a) Tubule segments were cannulated and perfused from one end as described by Burg et al (1966) (see Figure 3.1.). The other end was open and freely accessible to a patch pipette which was then inserted through the open end into the lumen and brought into contact with the membrane. This technique closely follows the strategy of Gogelein and Greger (1984).

b) More frequently the tubule was torn open using broken patch electrodes to expose the lumen. This is a modification of the "ripped tubule" technique described by Frindt and Palmer (1989), and Hunter et al, (1986). Two patch electrodes were broken about 100  $\mu$ M from the tip. One electrode was used to pin the tubule down; the other was placed alongside the first halfway across the tubule diameter and moved laterally. This action usually resulted in the tubule simply breaking apart; however, the procedure was repeated down the length of each tubule until a portion of tubule segment was torn longitudinally, exposing the luminal membrane (Fig. 3.2.). The individual cells of the luminal membrane were usually clearly visible, and could be accessed by a patch electrode.

A

67

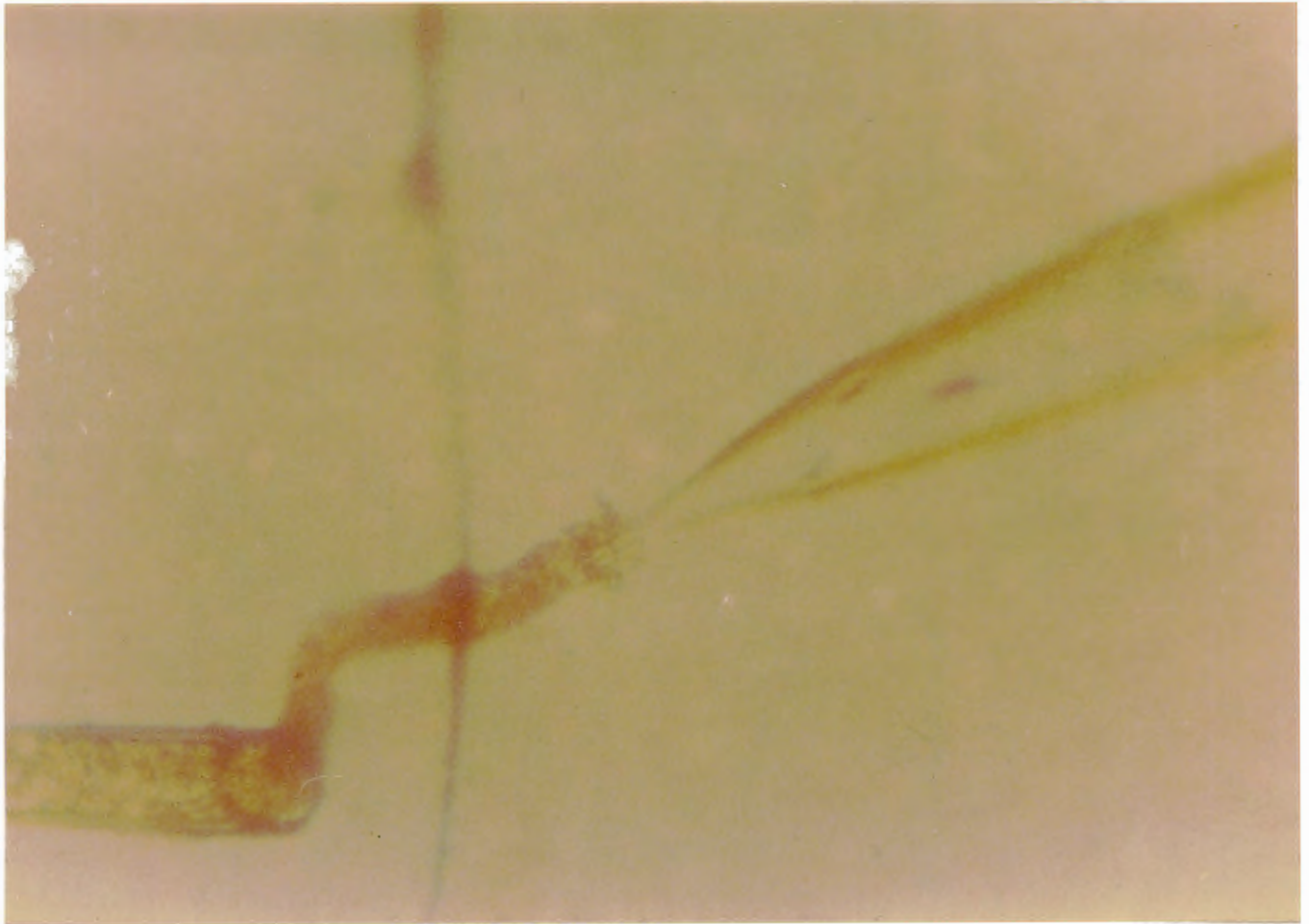
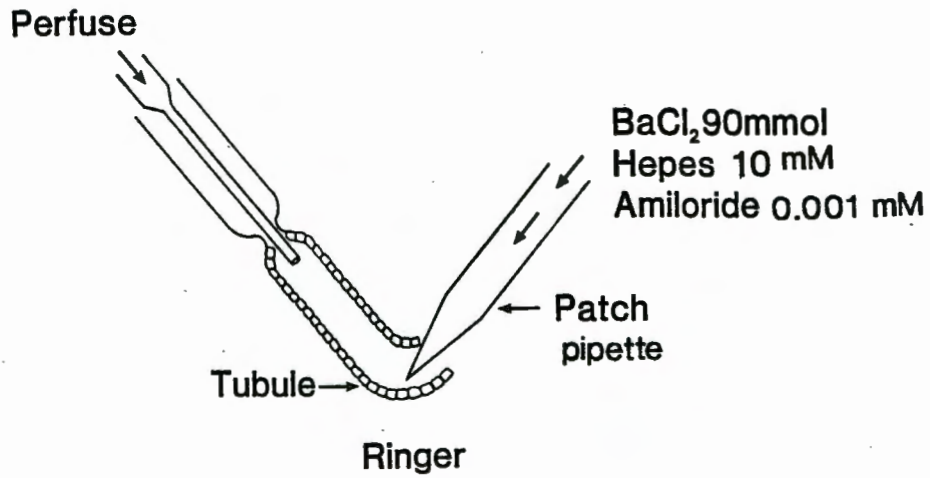
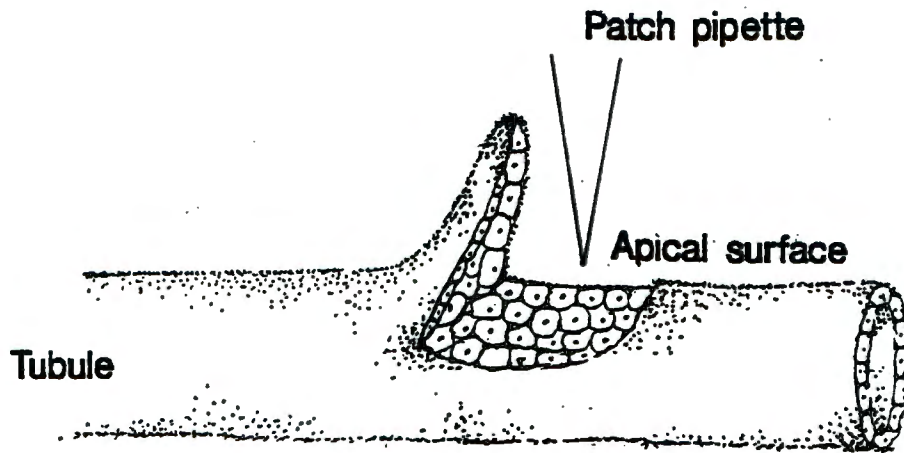


**Figure 3.1. A**, schematic of the isolated perfused tubule preparation used. The tubule was cannulated using an external holding pipette, and perfused with an inner perfusing pipette. A patch electrode could then be inserted into the open, free distal end of the tubule. **B**, photograph of the same preparation (magnification = 60 times). The vertical line in the photograph is a piece of concave glass that was placed at the bottom of the bath to raise the tubule orifice towards the patch pipette.

A

68



B

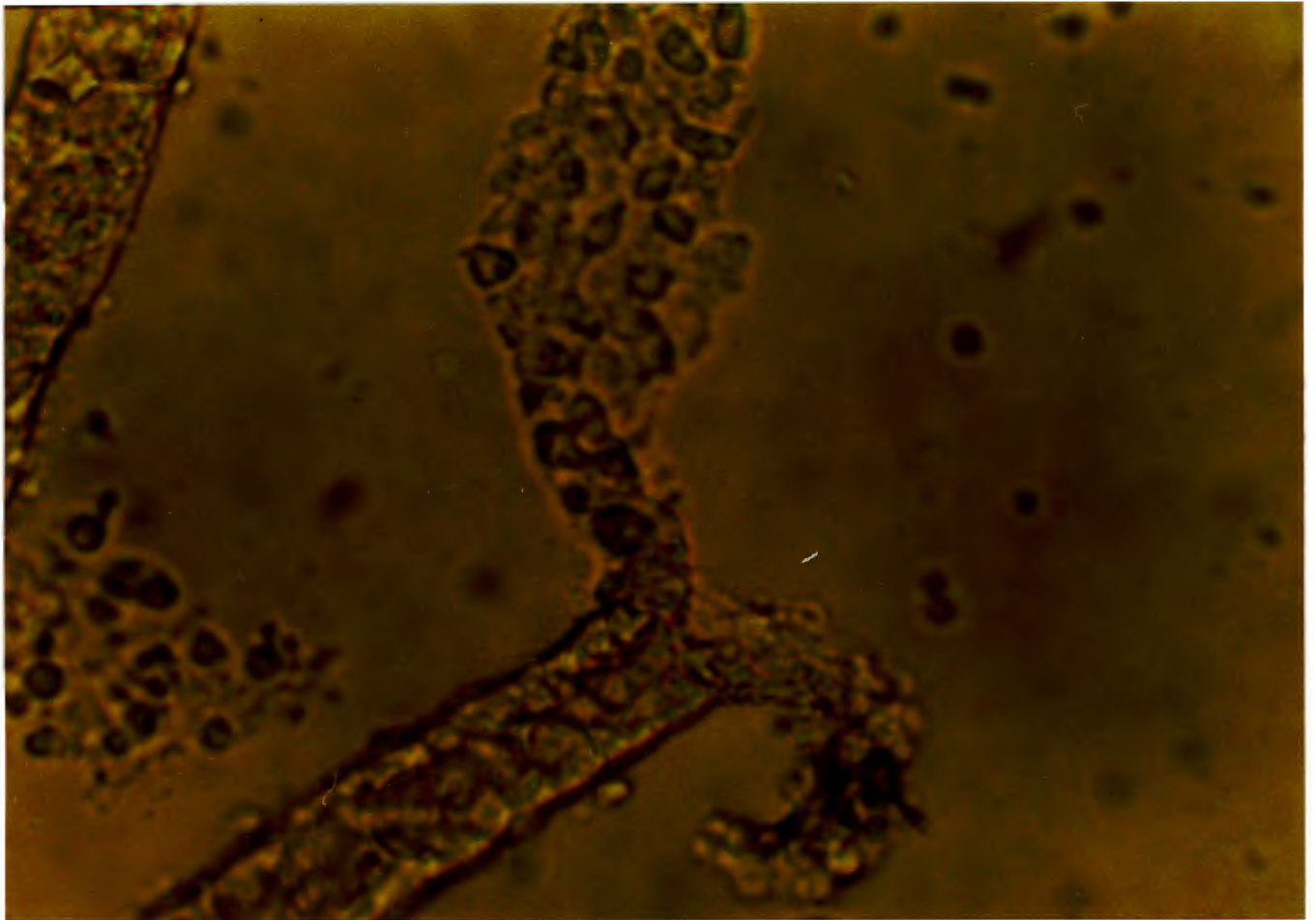


**Figure 3.2.** **A**, Schematic of the "ripped tubule" technique. The tubule was simply torn open using broken patch electrodes to expose the luminal membrane (adapted from Hunter *et al*, 1986). **B**, photograph of a CCD torn open in this manner (magnification = 300 times).

### **3.1.2. Human kidney**

Human kidney segments were obtained from renal biopsies performed on patients at Groote Schuur hospital for routine clinical purposes. Only those fragments of tissue deemed redundant by an on-site pathologist were employed in this study. Biopsy specimens were transported from the hospital in cooled Ringer (p.74). These were dissected and transferred in a manner similar to that described for rabbit.

The majority of tubule segments obtained from the biopsy specimens were considerably shorter than dissected rabbit tubules and were often found after dissection to have no basement membrane (see Fig. 3.3.). In these cases, therefore, exposure of the apical membrane was not attempted, and the patch clamp pipette was applied directly to the basolateral membrane.

Whole kidneys were also obtained from two surgical patients; these were transported from the operating theatre to the laboratory in saline (and packed in ice), where they were sectioned and dissected in a manner similar to that described for rabbit kidney.



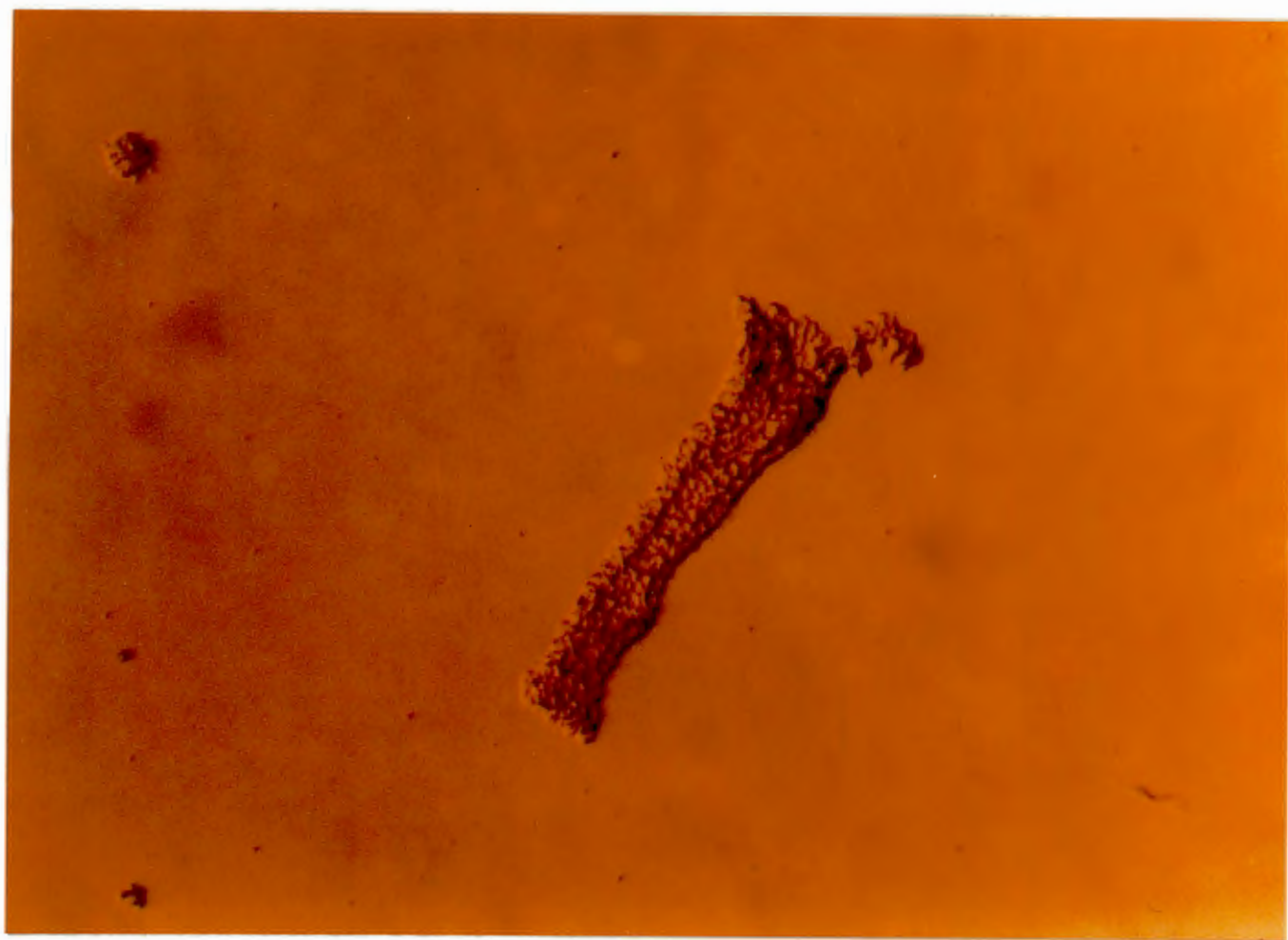


**Figure 3.3. A,** photograph of a human tubule segment (magnification = 60 times). The tubule does not have a basement membrane; the individual cells are thus clearly visible.

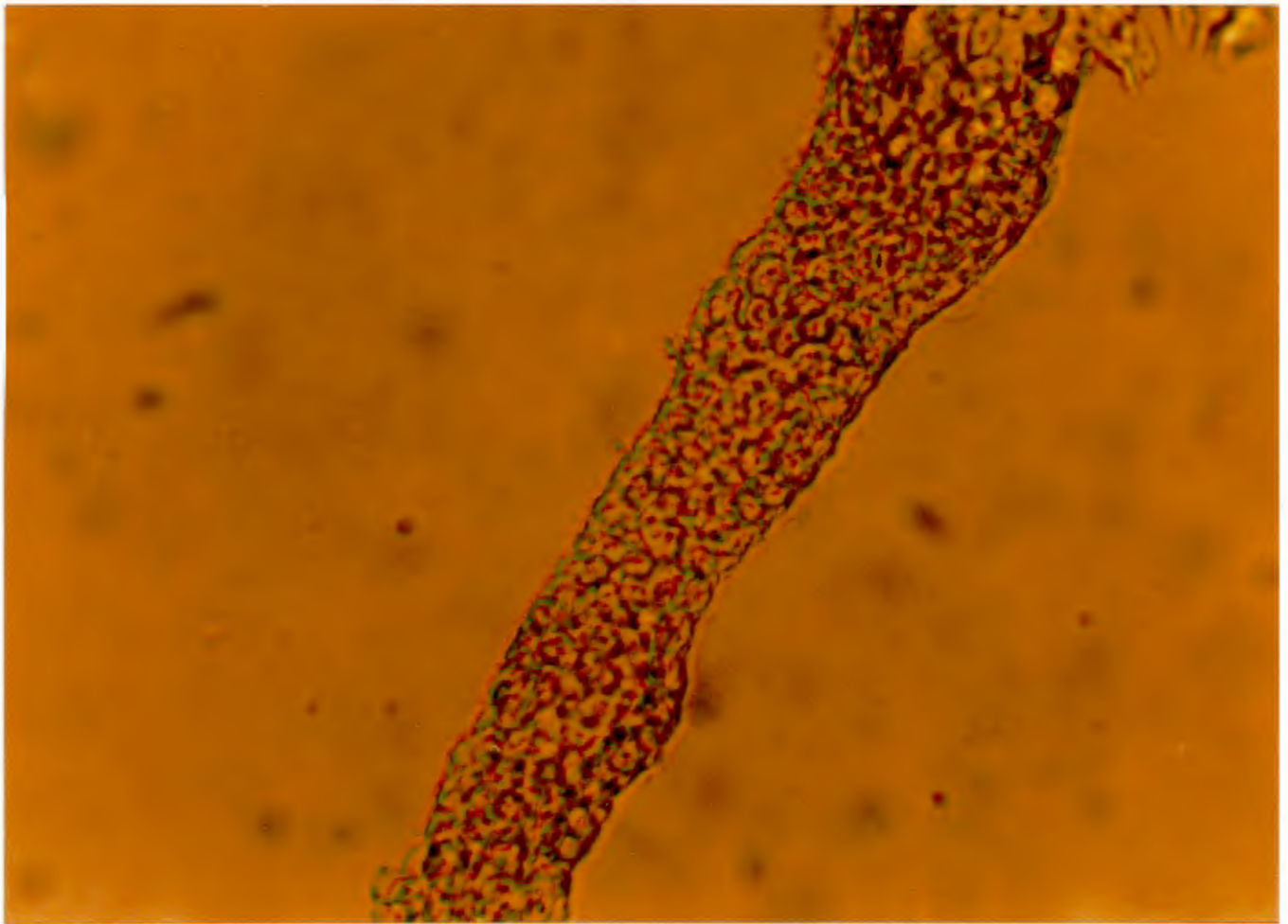


**Figure 3.3. B,** photograph of the same human tubule segment (as the one in Figure 3.3. A) at a higher magnification (150 times). See Figure 5.2. for comparison of tubules with and without basement membranes.

### 3.2. Application of the patch clamp technique

#### Apparatus:

Patch clamp chamber

Agar bridges (NaCl Ringer)

Pipette and bath electrode (Ag.AgCl wire)

Patch clamp amplifier (Axopatch 1B, Axon instruments)

Haematocrit capillary glass tubes (soda-lime, Modulohm I/S)

Electrode puller (David Kopf instruments)

Patch electrodes (pulled from haematocrit soda-lime capillary glass tubes, Modulohm I/S)

Inverted microscope (Olympus)

Electrode holder and suction tube (after Hamill et al, 1981)

Millipore filters (0.22  $\mu$  pore, Millex-GV)

Micromanipulator (Leitz)

The essence of the patch clamp technique resides in the formation of an electrical "gigaseal" (so called because the seal resistance is in the gigaohm range) between the tip of the glass micropipette and the cell surface. In order to achieve this, particular care has to be taken in the fabrication of the patch pipettes. Once a gigaseal has formed, several different patch configurations can be used to record channel activity.

#### 3.2.1. Patch pipette fabrication

The instrumentation, techniques and geometries involved in constructing a patch clamp electrode have been described in extensive detail by Hamill et al (1981), Corey and Stevens (1983) and Sakman and Neher (1983).

Essentially capillary glass tubes were pulled in two stages using a vertical microelectrode puller. This produced a rapidly tapering pipette which had a lower series resistance than more gently tapering pipettes. The pipettes were then fire-polished by bringing the tips within a few microns of a heated filament.

Initially, the resistances of completed patch pipettes were measured using the "bubble number" technique (Corey and Stevens, 1983), and typically had a resistance of about 2-10 M $\Omega$ . The tip diameters of these electrodes were between 0.5 and 2  $\mu$ . This measurement was confirmed for a few typical patch electrodes using scanning electron microscopy.

### **3.2.2. Pipette filling and mechanical setup**

All solutions were filtered through a membrane filter immediately before use. The patch pipettes were then mounted on the suction pipette holder, which was connected to the headstage amplifier. A Ag<sub>2</sub>AgCl<sub>2</sub> wire formed the electrode within the pipette. This entire assembly was attached to a Leitz micromanipulator, used to control both coarse and fine movements of the electrode.

### **3.2.3. Formation of a gigaseal**

The formation of a gigaseal has been well described by Hamill *et al* (1981). Essentially a gigaseal was formed by gently lowering the electrode tip onto the cell surface, and applying a very gentle suction (of the order of 10-20 cm H<sub>2</sub>O) through the patch pipette. Gigaseal formation occurred when the glass-membrane resistance increased by as much as three orders of magnitude. This was monitored audio-visually after applying an oscillating voltage pulse to the patch at the electrode tip.

On the apical membrane of dissected rabbit tubules, the formation of a gigaseal was sometimes a sudden event, and other times a gradual process. This variability necessitated the maintenance of a prolonged suction (up to 5 minutes) for each trial. Seals used for recording had resistances of 5-20 G $\Omega$ .

### **3.2.4. Patch configurations**

Owing to the unexpected physical strength of tight seal patches, they can be widely manipulated without major deterioration of the glass-

membrane seal, to produce one of three patch configurations. Formation of each configuration starts in the cell-attached mode. From this position the combination of either rupturing the membrane patch with suction and/or withdrawal of the pipette will produce either the cell-excised "inside-out" mode, the whole cell mode, or the "outside-out" mode. A detailed review of patch configuration formation is presented by Hamill *et al* (1981) and Peterson *et al* (1986).

In this study only the inside-out, and cell-attached configurations were used.

### **3.3. Solutions and drugs; changes and additions**

Solutions: The bath Ringer contained (in mM): NaCl 143, KCl 4.7, CaCl<sub>2</sub> 1.3, MgCl<sub>2</sub> 1, glucose 5, HEPES 10, and Na acetate 3; the pH was brought to 7.4 by addition of NaOH. The patch pipette contained (in mM): BaCl<sub>2</sub> 90 or CaCl<sub>2</sub> 70, HEPES 10, and amiloride .001; the pH was adjusted to 7.4 by addition of Ba(OH)<sub>2</sub>. Collagenase (0.2 g/l; Sigma) was sometimes added to the bath solution in attempt to clean the cell surfaces and thus facilitate tight seal formation. In some experiments, in which we attempted to assess the channel's chloride permeability, the Ringer was diluted with an equal volume of isosmotic mannitol (Gogelein and Greger, 1986). In this thesis, this solution is often referred to as "half Ringers solution" or simply "NaCl/2". The chloride-free solutions, Na acetate and Na thiocyanate (140 mM) were sometimes also used in the bath to assess the channel's chloride permeability. Drugs used in the experiments were the Ca channel blockers, verapamil (Holpro), nifedipene (Rolab), D600 (Minden), and the Ca channel agonist Bay K-8644 (Bayer). These were added to the bath solution to give final concentrations of 0.1 mM, except verapamil (0.005 mM). Parathyroid hormone (Sigma-bovine parathyroid acetone powder; concentration approximately .00001 mM) was also added in some cases to preparations of TAL and DCT segments, as was the diuretic hydrochlorothiazide (0.1 mM; Lennon). Stock solutions of the drugs and of PTH were made up in ethanol (100%), and these were then diluted in Ringer to make the final concentration. In all drug and hormone experiments, the patch pipette contained CaCl<sub>2</sub> (70 mM), and the bath

solution contained Ringer. In a few early experiments, a KCl Ringer solution was used in the bath or the pipette. This was identical to the bath Ringer except for the KCl concentration (143 mM) and the NaCl concentration (4.7 mM) which were simply reversed.

Initially the patch chamber was divided into three compartments enabling exposure of the membrane patches to solutions of different ionic composition. Each of these compartments was electrically connected to the bath electrode, a Ag.AgCl wire immersed in Ringer, via a Ringer agar bridge. Another Ag.AgCl wire formed the electrode within the patch pipette. The interelectrode potential was zeroed before attempting patch formation. In early experiments, transfer of the patch pipette from the bath to an alternate solution was achieved by simply lifting the patch pipette tip through the air - water interface and placing it into the new solution. Later, this was facilitated by using a plastic sleeve to prevent the tip from being exposed to the air during transfer. This was a modification of a technique devised by Quartararo and Barry (1987):

Prior to each experiment, a small length of polythene tubing was fitted loosely over the patch electrode. This was about half the length of the electrode and was positioned centrally on the electrode. After formation of an inside-out patch, this "sleeve" was pushed down using fine forceps to cover the pipette tip. Capillary action resulted in an immersion of the entire bottom half of the pipette in bathing solution. The pipette was then withdrawn from the bath solution and transferred to a bath solution of different ionic composition without exposure of the pipette tip to the air. When in new solution the plastic sleeve was simply retracted to allow exposure of the patch to the new bathing solution. In later experiments, the movement of the plastic sleeve was controlled by a system comprising of two air-filled syringes joined by a piece of tubing. The plunger of one of these syringes was attached to the sleeve by a thin strip of perspex, and was secured in place on the headstage amplifier. The second syringe was secured to the baseplate. Manipulation of this latter syringe resulted in the fine control of the movement of the plastic sleeve.

The most successful technique used to study channel activity in

excised patches, in solutions of different ionic composition or in solutions containing drugs, was a slightly modified version of the "hanging drop" technique (see Fig. 3.4), described by Vassilev (1990). In essence, this technique utilised only one bath solution. The procedure was as follows:

A small drop of the alternate bath solution or of the solution containing a drug was suspended from a Ringer agar bridge held a mm or two above the air-H<sub>2</sub>O interface. The Ringer agar bridge was held in place by a small block of perspex attached to the bath platform, and was electrically connected to the common bath electrode. In most experiments in which this assembly was used, the tissue sample under investigation was placed as close as possible to the hanging drop. This necessitated minimal lateral or forward movement when positioning the patch electrode, and hence minimal disturbance of the excised patch.

The pipette was then manipulated such that the pipette shank was positioned directly beneath the hanging drop. From this position the electrode was quickly lifted above the surface of the bathing solution and the patch immediately introduced into the drop.

In experiments performed with PTH, the hormone was administered directly to the bath in cell-attached preparations. A 50  $\mu$ l aliquot of a  $10^{-5}$ M stock solution was added to the bath (approximately 500  $\mu$ l) using a pipette. Assuming effective diffusion of the aliquot throughout the solution, the final concentration of PTH in these experiments was approximately  $10^{-6}$ M.



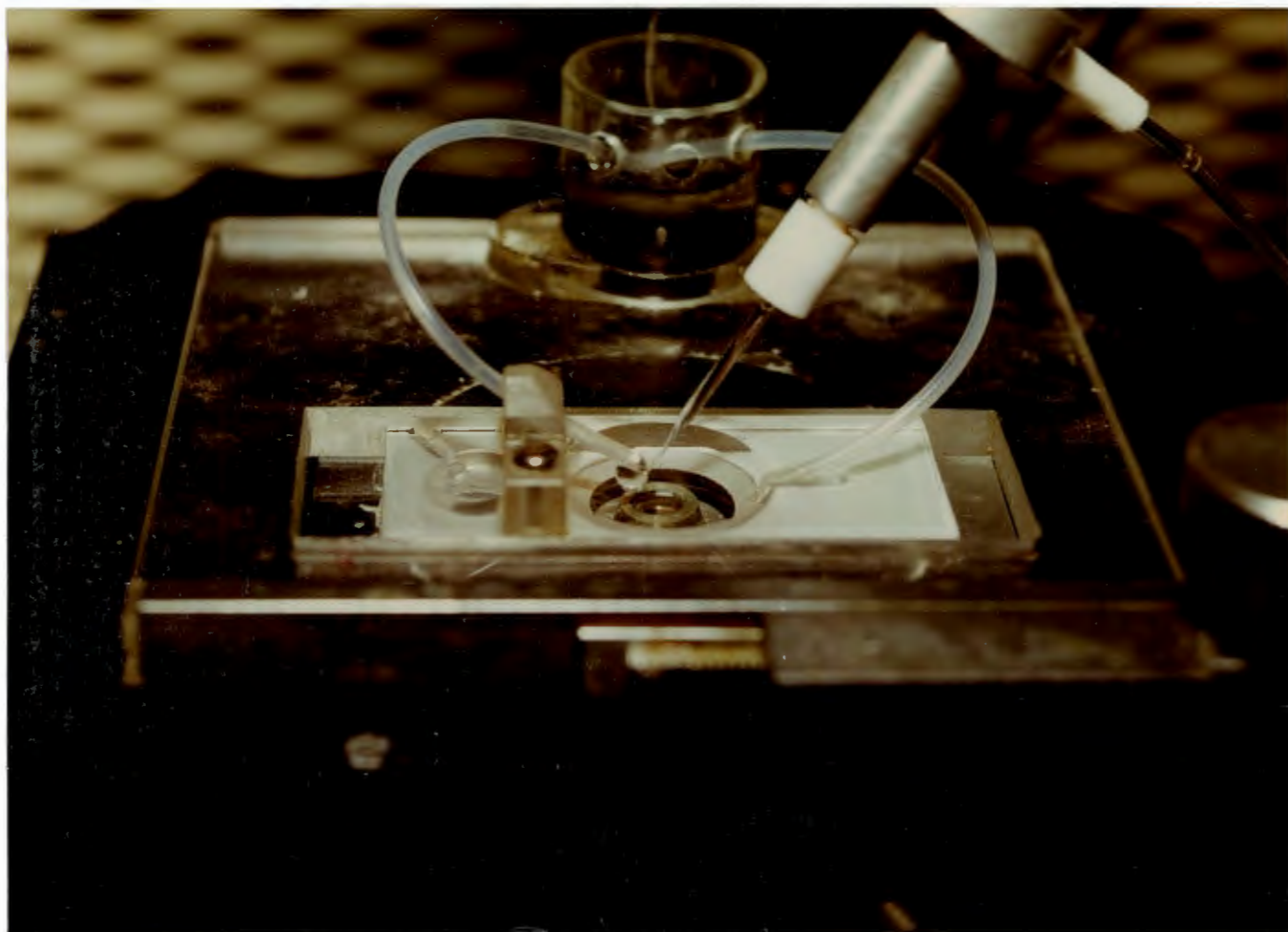


**Figure 3.4.** Photograph of the hanging drop technique. The membrane patch is exposed to the alternate solution in the drop. The reference electrode is immersed in Ringer solution (cf p.74) in the cylindrical chamber at the rear. It is connected to both the bath and the hanging drop by two Ringer agar bridges (the polythene tubing to the left and right).



### 3.4. Data recording and storage

#### Apparatus:

Oscilloscope (Tektronix, T922)

Transient recorder (Datalab, DL901)

A/D converter (built in this laboratory)

Axopatch 1-B amplifier (Axon instruments)

Archimedes 440 computer (Acorn Computers Ltd; Cambridge, England)

Computer discs (Boeder 3.5", 2DD; 800 Kbytes capacity)

Computer recording and analysis programs (written in this laboratory)

Digital-audio tape deck (Sony, DCT-75ES)

Following attainment of a "tight" seal, channel currents from cell-attached and inside-out patches were detected by an Axopatch 1B patch clamp amplifier, filtered with a 6-pole Bessel filter at cut-off frequencies ( $-3$  dB) of 200 Hz or 500 Hz, and sampled at 1 or 2 KHz by the analogue to digital (A/D) converter. This 8-bit A/D converter was constructed in this department and included a preamplifier with adjustable offset and gain controls. The gain was set such that the maximal resolution of the recording apparatus was 0.05 pA. The offset control permitted the vertical position of the trace on both the oscilloscope and computer screens to be adjusted simultaneously. The digitised signals were monitored on the oscilloscope and recorded on an Archimedes' 440 computer using a data acquisition program developed in this laboratory; they were later stored on disc. Recordings were of up to 10 min duration. When possible, consecutive recordings (each usually of 1-3 minutes duration) were obtained with the patch voltage clamped at 30 mV to -60 mV, usually in 10 mV steps, the actual range for any one patch being determined by the "tightness" of the seal. Fig. 3.5 shows the components used in recording and storing data in a flow chart and photograph respectively. Throughout this study, the term "bins" is used in two different contexts: a) for the histograms (defined later), and b) for the computer screen where a "bin" is 256 data points. This represents 256 msec, and at maximal resolution on the monitor, fills the whole screen from left to right; the maximal (shortest) recording on the screen is thus 256 msec ( $\pm$  a quarter of a second). The

computer programs for data recording and analysis also allow four bins or eight bins at a time to fill the screen, thus displaying one second and two second recordings respectively.

During the final stages of the project, a digital-audio tape deck (Sony, DCT-75ES) was purchased and used to record much longer periods of channel activity (recording capacity of 3 hours). Selected stored data could then be transferred to computer memory and saved to disc.

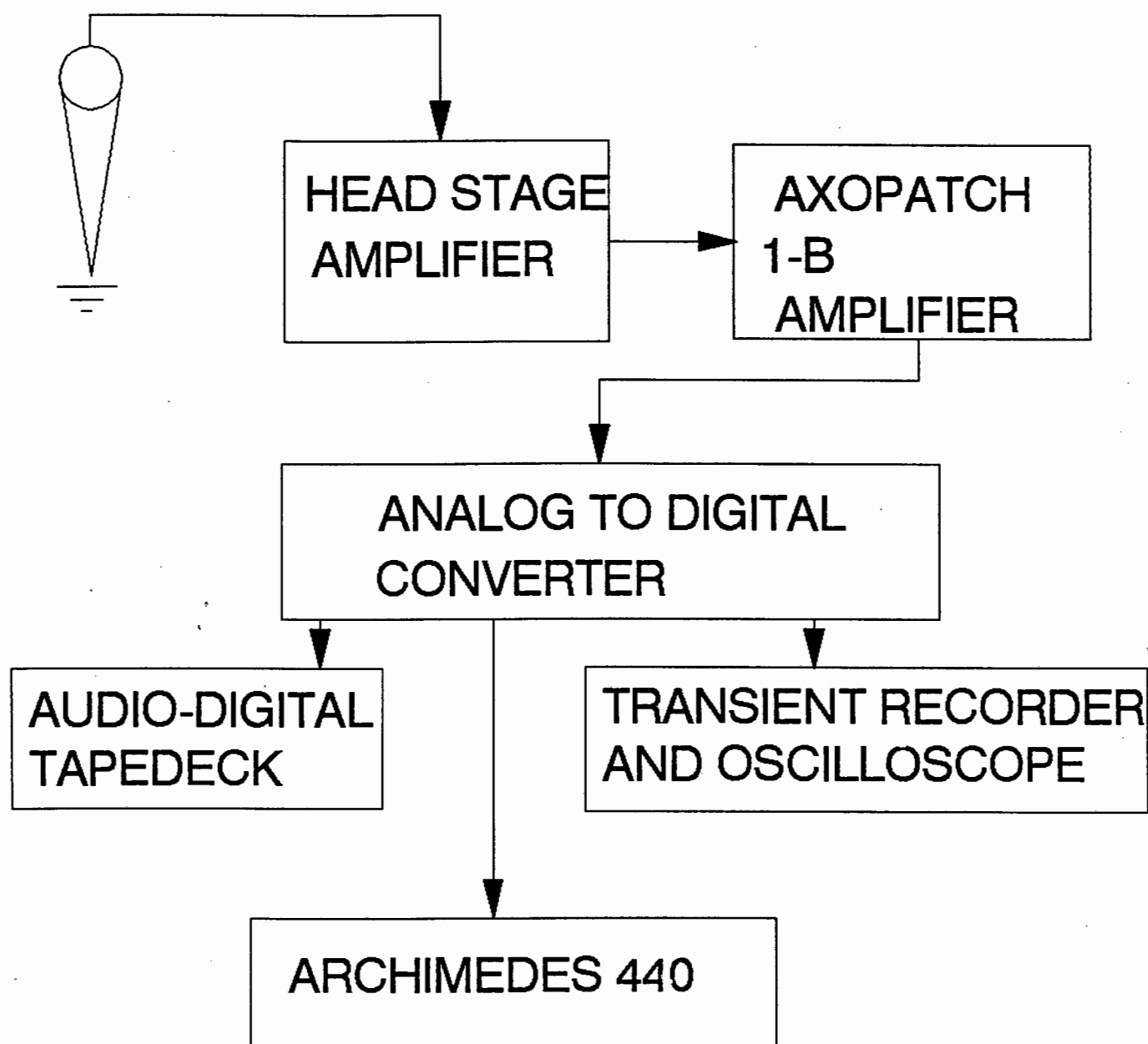


**Figure 3.5. A,** flow chart schematic of the recording apparatus used in the study.

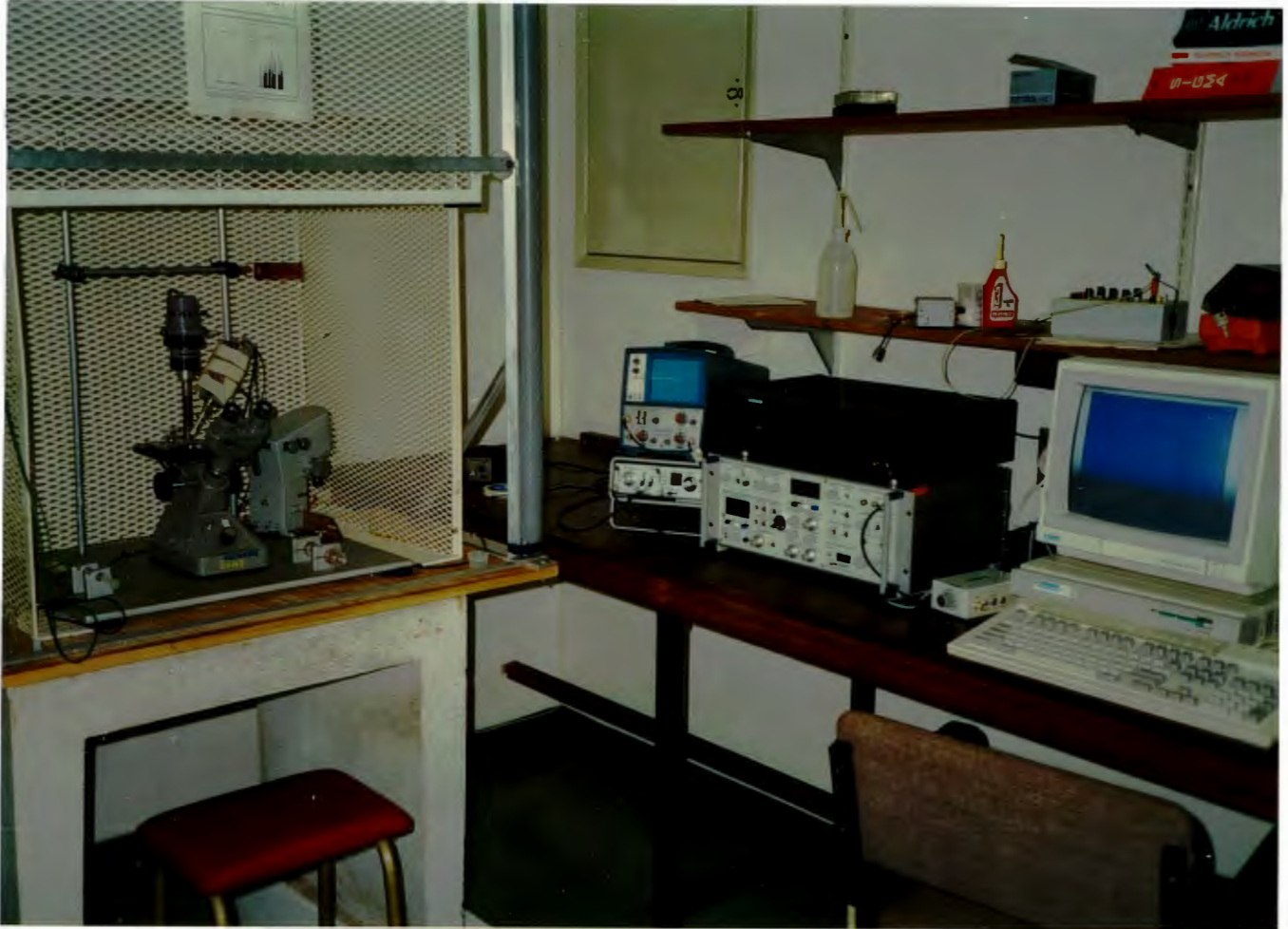


**Figure 3.5. B**, photograph of the components depicted in the schematic in A. The oscilloscope and transient recorder are on the far left of the bench; the digital-audio tape deck is above the Axopatch 1-B; to the right of this, the small box between the latter and the computer is the A/D converter (the offset control in front of the A/D converter is for centering the trace on both the oscilloscope and computer screens simultaneously); the microscope, patch chamber, headstage amplifier, and micromanipulator are situated in the Faraday cage on the left of the photograph (the syringe, held in place by masking tape onto the headstage is a relic of the method used before the hanging-drop technique).

### **3.5. Data analysis**

After recording and storing the channel data, the next task was to identify the channel. Some basic information concerning channel identity was obtained by measuring amplitude of channel currents, durations of shut periods, and durations of open periods.

Automated analysis of the stored digitised signals was accomplished using a program written in this laboratory. This analysis closely follows the strategy of Colquhoun and Sigworth (1983); in all instances, the results of the automated analysis were later checked by direct inspection on the computer screen. What follows is a detailed description of channel event analysis and how this was achieved using the software developed in this laboratory.

#### **3.5.1. Event amplitude**

Measurements of channel amplitude were used to obtain estimates of single channel conductance and channel selectivity.

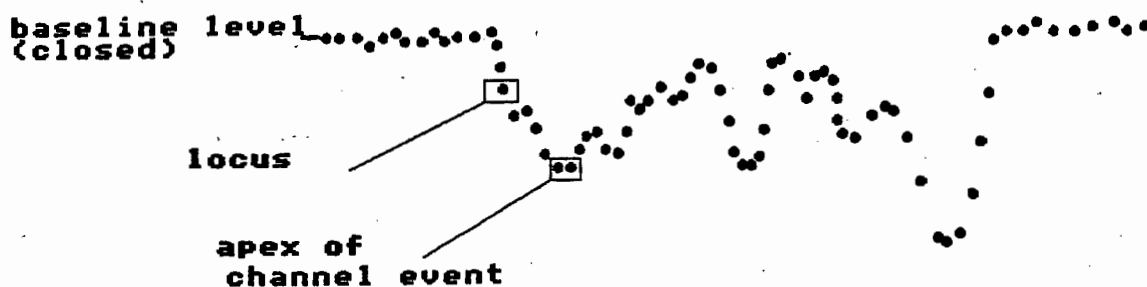
Typically, the channel activity recorded could be categorised into three modes of activity (see schematic in Figure 3.6)

a) "Bursts" - these are classically defined as a series of openings occurring in quick succession. But in this study, the definition of a "burst" has been extended to cover the case where a single channel, while remaining open, shows frequent jumps from one subconductance state to another.

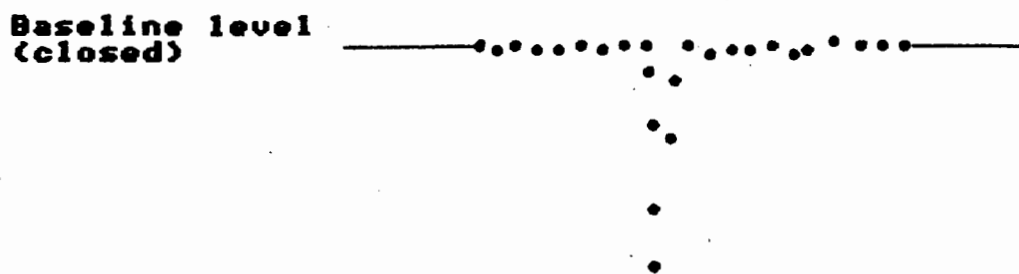
b) "Squares" - defined as events with a sharp transition into the open or closed state and a relatively constant amplitude.

c) "Spikes" - defined as single very short duration events.

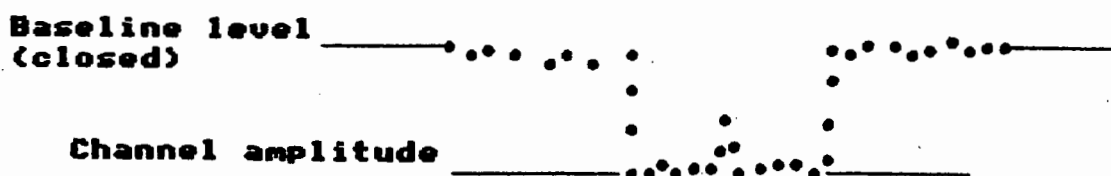
A

**BURST**

B

**SPIKE**

C

**SQUARE**

**Figure 3.6. A,B, and C,** digital schematics of a "burst" event, a "spike" event, and a "square" event. Each point (•) represents a single data point as sampled by the A/D converter, and is defined by the analysis program as a "locus". **A,** the varying amplitude levels of successive peaks during the burst were regarded as subconductance levels; those peaks in a "burst" comprising of only one data point almost certainly did not represent the true amplitude (see discussion on sampling rate). Note the absence of a closure in a burst (cf p.57, 82). **B,** since "spike" events all probably had only one data point at the peak, these peaks most likely did not represent the true amplitudes. **C,** the "square" event shown has a partial closure; such a "closure" would most probably have a value less than the chosen threshold, and would therefore be ignored during automatic analysis.

Two separate channel amplitude measuring procedures were used for "squares" and "bursts":

**SQUARES:** Since "squares" nearly always occurred together with "bursts" and "spikes", their amplitudes and durations could not be measured independently by the automatic analysis program. The amplitudes and durations of the "squares" were thus measured by eye using a cursor available in the program. The methods used were in essence the same as those used by Palmer and Frindt (1989).

For each voltage record, two "screen" bins at a time ( $\pm 512$  ms segments) were scanned and searched for "squares". The criterion used for "square" measurement was that it should have a "flat top" or relatively constant open time, of at least 4 ms duration.

The procedure for measurement of "squares" was to place the cursor at the beginning of the event halfway through the baseline noise, and then at the open state, halfway through the noise. The value in picoamps (pA) of each cursor position was displayed on the screen and the difference between the two values gave the event amplitude. Where possible the amplitudes of 20 of the smallest "square" events were measured on each recording. The mean unit current amplitude was then calculated. The term, "small squares analysis" was used in this laboratory to describe this procedure.

**BURSTS:** "Bursts" were analysed using an automated "burst analysis" feature of the software (see section 3.6.). For the purposes of this analysis, "bursts" are defined as on p.57; thus the main purpose of this analysis was only to distinguish between different levels of peak amplitude during the "burst". Where possible this analysis was performed on at least three separate "bursts" at each voltage clamp step. For each of these "bursts" only two bins ( $\pm 512$  msec) were selected for analysis, so minimising the effects of possible base-line drift.

The program measured the amplitude of each "burst" event relative to an arbitrarily set baseline. The start or end of an event was defined when the

difference in amplitude between successive data points changed sign, and exceeded 0.05 pA in amplitude.

The peak amplitudes so obtained were then automatically tabulated and an amplitude histogram generated. In most cases the amplitude histograms revealed a number of more-or-less clearly defined peaks corresponding to favoured degrees of opening (subconductance states) of the channel (see for example Fig. 4.1.4. B, p.112). The data between peaks are presumed to reflect the presence of noise, and/or of innaccurate data sampling (i.e., the rate of change in current amplitude was faster than the sampling rate - 1 kHz - employed here). The chi-squared test was used to test the significance of the observed frequency distribution of the peak amplitudes, against the theoretical frequency distribution expected for a purely random signal.

At each level of voltage clamp, the mean of the differences in amplitude between successive peaks was then calculated. This value was defined as the mean unit current amplitude for "bursts" between favoured degrees of opening (subconductance states) of the channel, at that voltage. The average of three separate such "mean current amplitudes" (as determined by the above methods) was computed at each level of voltage clamp.

In both "burst" and "square" analyses, mean current amplitudes were determined for all segments at all levels of voltage clamp; these were used to construct current-voltage (I-V) plots, so that the slopes of the individual I-V plots, (as calculated by linear regression), and the reversal potential (zero current potential) might then be determined giving estimates of channel conductance and specific ionic selectivity. Amplitude data were also pooled to enable construction of "collective" I-V plots of the entire data sample. The unpaired t-test statistic was used in all comparisons of unit amplitude data.

In addition, for each patch, two other types of amplitude histogram were generated: 1) a "jump" histogram was computed for the amplitude differences between successive peaks in the "bursts". This histogram thus



depicts the relative frequency of the differences in amplitude between successive peaks. As the results will show, this is an exponential fall, i.e., large jumps in amplitude, between successive peaks are less frequent than small jumps; as the relationship is exponential, this is consistent with the magnitude of successive jumps being randomly determined. 2) an amplitude histogram was generated for an entire voltage clamp record in which the amplitude of all three modes of activity was measured. In the latter instance, the analysis procedure used was the same as that used to evaluate open and closed-time intervals (see next section). A value for total mean current could also be generated by this procedure. This mean current amplitude value was used to construct current-voltage plots (see results).

### **3.5.2. Open- and closed-time histograms**

Open and closed durations of channel events were measured using the automated analysis program. All events ("squares", "bursts", and "spikes") were detected by setting an arbitrary threshold just outside the noise level of the baseline, to capture all events (small and big "squares", "bursts", and "spikes").

After each voltage clamp record was analysed in this way, the analysis was validated visually using the cursor; occasional errors in the automatic analysis were corrected on-screen.

For construction of open- and closed-time histograms the time taken for the opening (closing) and subsequent closing (opening) was first recorded and then placed in an appropriate bin, the width of which was a prespecified time interval. For the "burst" analyses, the bin width was 0.05 pA, the maximal resolution of the recording apparatus. Thus the "burst" histograms in fact depicted the distribution of all the digitised data points. The number of events that occupied a specific bin was then plotted against the time interval represented by the bin. Technically the challenge was to be able to resolve as many of the actual channel transitions as possible, including the briefest openings and closings. Because the data was sampled at 0.5 or 1 ms intervals and low pass filtered at 500 Hz, the

possibility existed that very fast openings were not detected. The probability of missing such real but fast openings is discussed later.

The histograms were then fitted for exponentials (cf p.122), the fitted distribution being tested to determine the goodness of fit. This fitted exponential distribution was used to determine opening and closing rate constants.

### **3.5.3. Fractional open time**

The fractional open time was calculated as the total time spent in the open state, divided by the total time of the recording at any particular voltage. This value was calculated by the program and displayed with the open- and closed-time histograms.

## **3.6. Computer programs for data recording and analysis**

The software used in this laboratory was developed by Professor L.C. Isaacson. This software was programmed in accordance with standard analysis procedures developed by Colquhoun and Sigworth (1983). Some unique aspects of this software are described in greater detail below.

a) PATCH: A data recording program.

For sampling continuous records the program "Patch" was used. The options available in this program are:

- Cal (calibrate)
- Run (record)
- Speed (sampling interval selection)
- Y-gain
- Plot
- Monitor
- Squeeze
- Disc (save or load)

## Quit

The formation of a tight seal could be monitored on the screen using the "monitor" option. The option "Run" stored the incoming data in RAM memory. "Speed" enabled sampling the data at 0.25, 0.5, or 1 msec intervals. The "Cal" option (selected only on initially switching on the computer) calibrated these sampling intervals. The program recorded (stored in RAM) a maximum of 620 Kbytes of data, so permitting recording of 2400 "bins", each of 256 bytes. At sampling intervals of 0.25, 0.5, or 1 msec, this corresponded to 2.5, 5, or 10 minutes continuous recording, respectively. The "y-gain" option enabled full-screen display of 5, 10, or 20 pA on the computer monitor. The "plot" command enabled printout of any screen to a dot-matrix printer. The "squeeze" command enabled the full-screen display of 256 msec, 512 msec, 1024 msec, or 2048 msec of data. The "disc" option enabled either saving the data stored in RAM to disc, or transferring data already on disc, into RAM.

## b) ANALYSE: A data analysis program.

The goal of this program is to construct a list of channel transition times and amplitudes from records sampled by "patch", and then to generate amplitude, open- and closed- time histograms from this list. Operation of the program is largely automatic. A flow chart for the program is shown in Figure 3.8.A and B, illustrating the options and their functions. The option used to analyse the data is "autoanalyse". Selection of "autoanalyse" prompts the operator to enter a number of parameters suitable to the type of analysis being performed.

These parameters are:

Clamp voltage (mV)

Baseline amplitude (pA)

Baseline noise - peak to peak (pA)

Lower bound (default 0.01 pA, or -.01 pA for downward events)

Upper bound (default 8 pA)

Square channels or peaks (S/P)

Burst/flickering or spikes (B/S)

Threshold (default 0.05 pA)

The type of analysis being performed will determine which parameter options are chosen. Also, when choosing parameters, it should be taken into consideration that the program must be able to identify events even though they have variable shapes, are distorted by limited bandwidth, and contaminated by noise. What follows is a detailed description on how the program performs "burst analysis", open- and closed-interval measurement, estimation of fractional open time, and digital filtering of the data record.

### **3.6.1. "Burst analysis"**

The "burst analysis" procedure is used to measure the amplitude of each event in a "burst" occupying two bins ( $\pm 512$  ms). The option "peaks", followed by "bursts" should be selected in the parameters list. The baseline amplitude setting is arbitrary as "burst analysis" is essentially concerned with measuring the differences between individual current amplitudes (cf p.82). The threshold default value of .05 should also be selected, so that every data point will be displayed on the amplitude histogram. The program measures "burst" activity in the following way (refer to Figure 3.6.):

The program follows the data points (loci) in an orderly sequence. Beginning from the second data point in the "burst", each subsequent data point (locus) is subtracted from the preceding locus. An amplitude peak is detected when the difference between two subsequent loci changes sign, and exceeds 0.05 pA. Subsequent peaks are detected similarly.

The absolute amplitude of each peak is measured by subtracting its value from the baseline amplitude value. The interval between peaks is also measured. A "burst" amplitude histogram can then be generated from these data, revealing possible favoured conductance levels of the channel.

For automated "square" channel analysis (not used in our study, as the majority of recordings contained "bursts", and "spikes", as well as "squares") the amplitude is measured by averaging data point amplitudes at the shut levels, and data point amplitudes at the open level. The difference between these two means gives the channel amplitude.

### **3.6.2. Open- and closed-time interval measurement**

To measure open- and closed-time intervals, the option "peaks", followed by "spikes" was chosen. In these analyses, an arbitrary threshold of roughly twice the peak-to-peak noise level on the baseline was chosen to include as many events as possible from all three modes of channel activity. The principles used by the program to detect events follow standard procedures outlined by Sigworth (1983).

Since the baseline typically shows a slow drift with time, the program automatically compensates by identifying event-free segments of the record and correcting the mean baseline estimate continuously.

When the analysis is complete, it is validated using a cursor validation procedure. The cursor marks the amplitude and duration of each channel event chosen by the automated analysis. The entire trace is scanned in this way and appropriate changes made, on screen, to individual channel events.

The output from these programs is a list of numbers representing the time of each transition in the current record and the amplitude of the transition. The program then generates the open- and closed-time interval histograms and the amplitude histogram. Bin widths can be altered at will. The program also generates the fractional open time for the trace, and a chi-squared estimate for the amplitude histograms (see discussion). A display of the listed values can be printed or saved to disc for the curve-fitting procedure. An additional procedure that was later incorporated into the program enabled the generation of a "phase space" plot of event amplitudes. This was used to look for possible deterministic chaotic properties of the channel kinetics.

### 3.6.3. Other options of the ANALYSE program

Other options of the ANALYSE program included: "Filter", "Rodent", "Expand", "Squeeze", "Notes", and "Bin". The "Filter" option (after Savitzky and Golay, 1964) invoked a 9 point least-squares smoothing digital filter, to enhance the signal-to-noise ratio of the data recording. As this procedure necessarily distorted the data, to some extent, it was not used often. The filter was used to good effect in an example of a cell-attached recording from a DCT patch in the presence of PTH (Fig. 3.7.); automated "burst analysis" of a two second segment revealed burst histograms with discrete peaks of favoured current activity that were far more easily distinguished after filtering of the raw data trace, than before (the number of events corresponding to the peak amplitudes in both histograms differed significantly ( $p < 0.001$ ) from the mean number of events per bin). This form of filtering, therefore, appears to be useful in minimising the background noise of recordings.

The "Rodent", "Expand", and "Squeeze" commands enabled various graphic options on the monitor screen and/or dot-matrix printer. The "Notes" command enabled short comments on the data to be recorded to disc. The "Bin" command enabled the operator to select any one of the 2400 256-byte bins of data for inspection on the monitor.

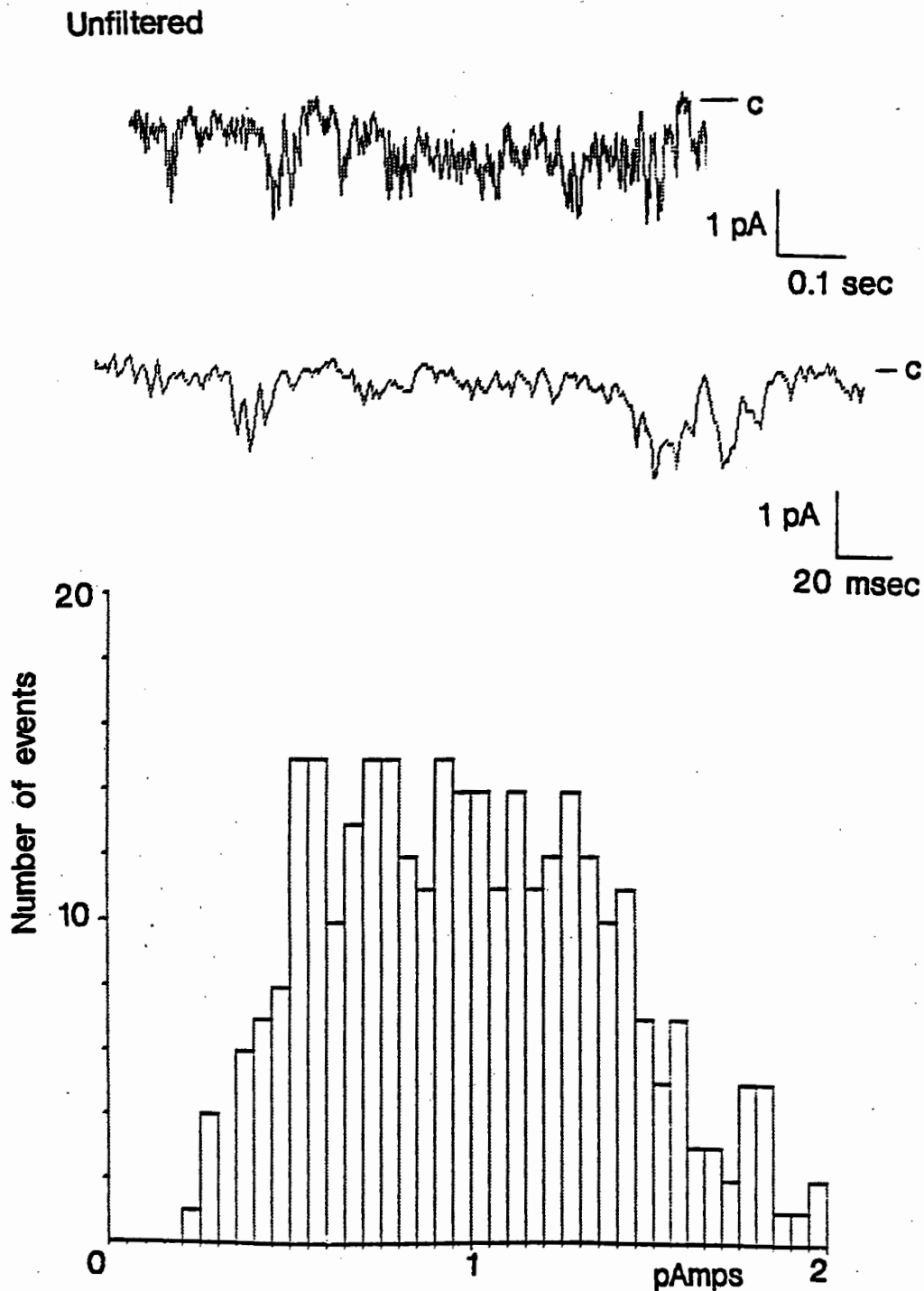


**Figure 3.7. A,** a two second trace depicting unfiltered bursting activity (top) in a cell-attached patch from a DCT in the presence of PTH. The first 256 ms of this trace are presented directly below, using an expanded time base. The amplitude histogram, presented below, reveals peaks of favoured current amplitude which are only just visible against the background noise.

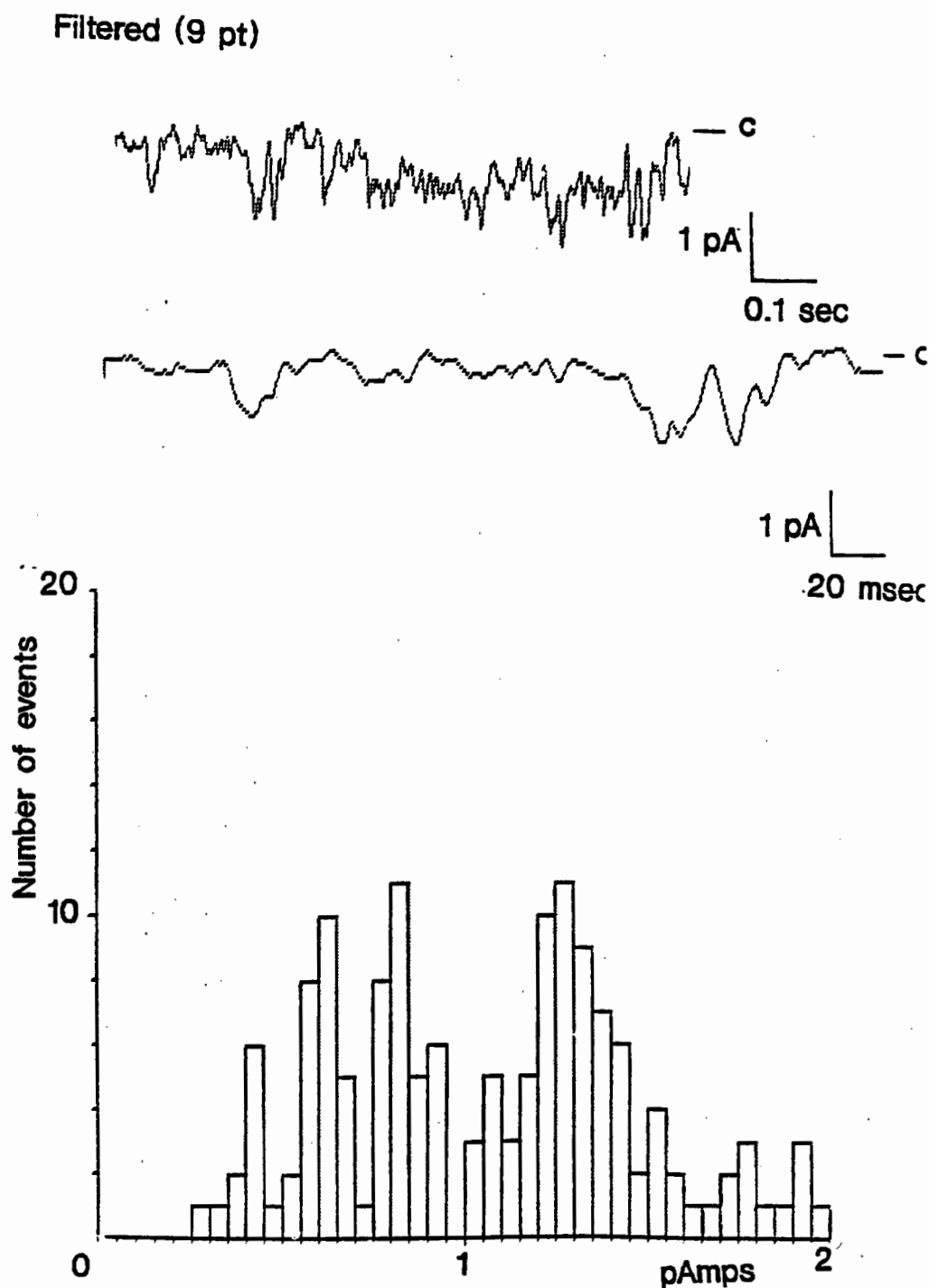


**Figure 3.7. B**, the same two second trace as in A above, after filtering. The first 256 ms of the trace are presented directly below, showing the smoothing effect of the filter. The amplitude histogram for the filtered trace is shown at the bottom, and demonstrates discrete peaks of favoured current amplitude which are clearly visible against a fairly low background noise.



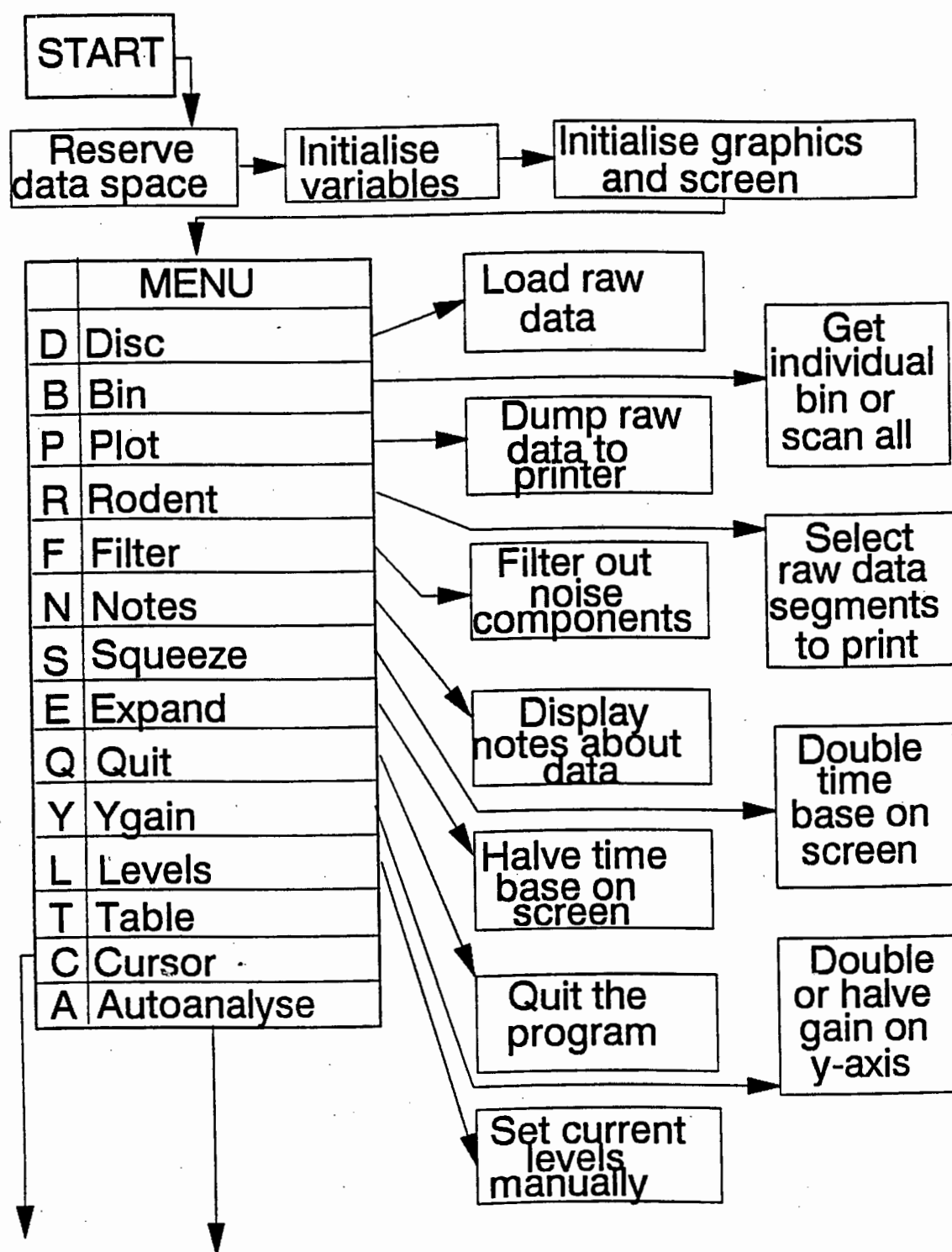


**Figure 3.8. A,** flow chart summarising the main options and procedures in the 'ANALYSE' program.

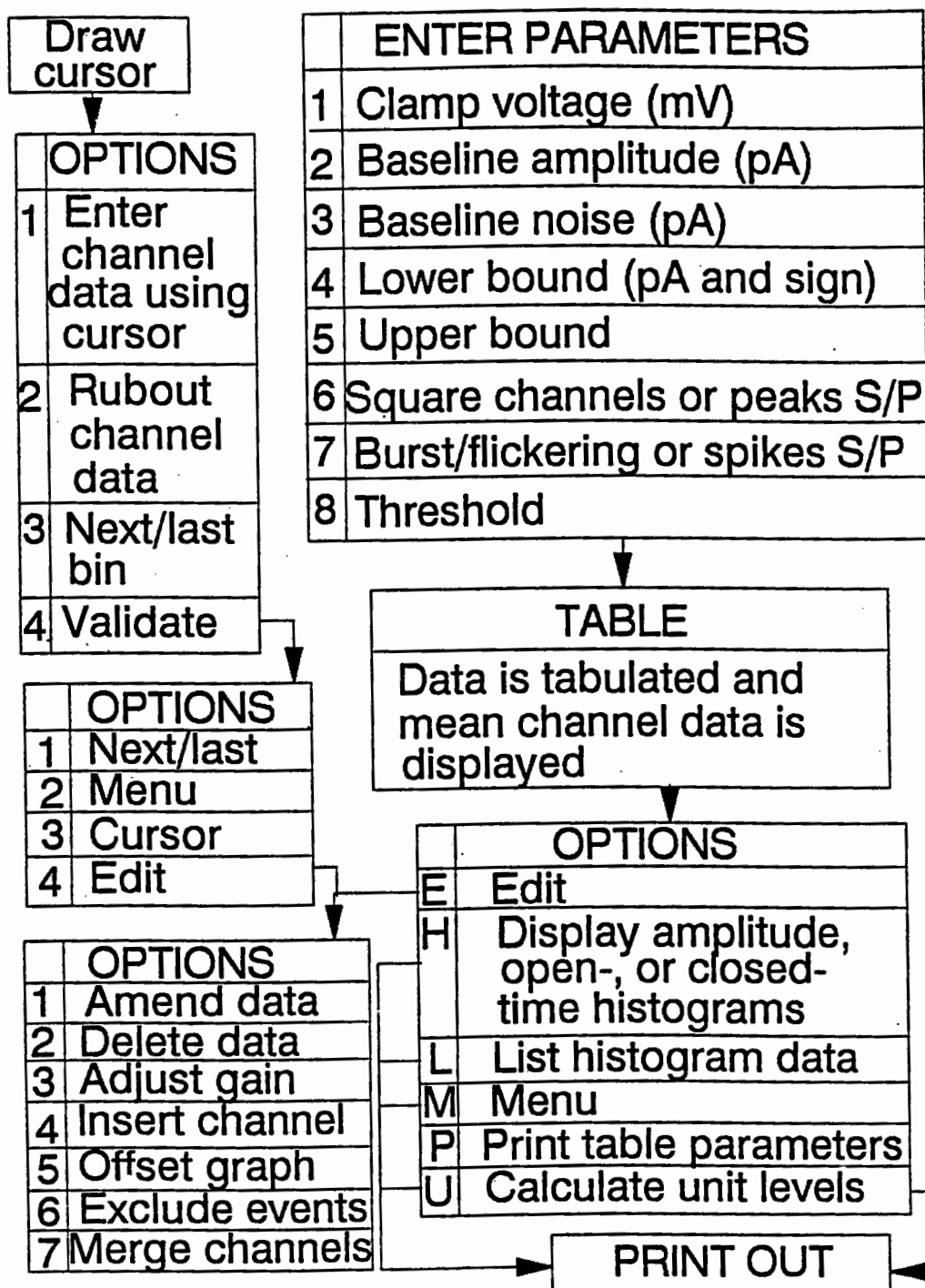


**Figure 3.8. B,** flow chart summarising the cursor routine and the autoanalyse routine in the 'ANALYSE' program. The autoanalyse routine starts with the prompt to enter the parameters.

c) CURVEFIT: An exponential curve-fitting program, based on that of Schreiner et al (1985)

This program produces a least squares fit of all the data in the open- and closed-time interval histograms. The user supplies the program with the listed histogram data, a suggested function (single or multiple exponentials) with adjustable parameters, and a set of initial values for these parameters. The program then adjusts the parameters until it minimises the sum of the squares of the difference between Y values calculated from the function and Y values in the data. The program calculates and displays the best value for these parameters that is consistent with the data, and will generate a statistical report of how good the fit is. More importantly, the program has built-in sophisticated plotting routines that allow the user to visually compare his data to the fitted function. This program was later modified to include a log-log plot of the open- and closed-time histograms. This was included to test whether fractal or unidimensional diffusion models were feasible in describing the gating kinetics of the channel data.

## **SECTION FOUR**

### **RESULTS**

## SECTION FOUR

### RESULTS

In this section, only such data are presented as provide a "signature" of the channel under investigation. In all the following, the polarity of the clamp potential given, is that of the pipette interior relative to the bath. Currents corresponding to movement of cations from the pipette into the bath are presented as downward deflections in the figures.

#### **4.1. The search for calcium channels in rabbit renal tubules**

Table 4.1.1. shows the experimental numbers involved in the project. Patches with tight seals (5 - 20 G $\Omega$ ) were obtained from fewer than 10% of the kidneys dissected. Of these only about .6% lasted long enough to allow prolonged recordings of channel activity. Channel activity was observed in about 80% of these recordings, except those obtained from CCDs. In recordings from these segments, the incidence of channel activity appeared to be somewhat less (about 60%), however tight seals, once formed, lasted longer on average in the CCDs than in other segments. The isolated perfused tubule technique was used in about a third of all experiments before it was replaced by the "ripped tubule technique". The short average lifespan of a tight seal in these experiments did not allow the effects of drug additions and solution changes to be investigated as fully as had been hoped. Twenty-six drug or hormone additions and 15 solution changes were achieved. Overall, stable recordings were obtained from 106 patches. These consisted of 37 PSTs, 15 TALs, 16 DCTs, and 38 CCDs; the seal lasted long enough for recordings to be obtained at multiple levels of voltage clamp in 11 PSTs, 5 TALs, 8 DCTs, and 19 CCDs.

Channel activity was essentially similar in all tubule segments studied. Three temporal patterns of channel activity were observed to occur

together in most patches.

Fig. 4.1.1.A shows channel events with a typically "square" nature, i.e. sharp transitions between open and closed states and relatively constant current amplitudes. The closed and open levels are denoted by the dashed lines. Such events with open-time durations of greater than 4 ms occurred in most recordings and were used in the "small square analysis" (see methods). Square current events of longer duration (>50 ms) occurred in relatively few patch recordings. Fig. 4.1.1. A also shows current transitions to other levels (shown within the circles); these probably correspond to subconductance states of the same channel. The square current events were usually not interspersed with flickering or bursting. Episodes of "bursting" occurred in most patches (Fig. 4.1.1.B); these were of variable amplitude and duration. Frequently, channel activity also manifested as current "spikes" of short duration (1-10 ms) as shown in Fig. 4.1.1.C. "Squares", "bursts", and "spikes" usually occurred together even within fairly short time segments of the same recording.

In this study, it was decided that the most reliable estimate of current amplitude for individual voltage clamp values was measurement of the smallest "squares" at each voltage. Fig. 4.1.2 shows a current-voltage plot for the entire data sample ( $n=106$ ), as determined by "small squares analysis". An estimate of the mean slope conductance could not be determined from this plot, as the small "square" current amplitudes appeared to be independent of voltage above 5 mV and below -5 mV. The reversal potential is close to zero mV. The shape of the plot is interesting as it reveals complete saturation of small square channel conductance above and below the reversal potential. Collective current-voltage relationships were determined for each tubule segment, and the shapes were similar to that of Fig. 4.1.2 (see appendix). For example Fig. 4.1.3. A shows an example of a recording from an inside-out patch of a DCT clamped at varying voltages. The collective DCT current-voltage relationship, as determined for "small squares analysis" (Fig. 4.1.3.B) shows again that for this segment the unitary current amplitude appeared to be independent of voltage above and below the reversal potential.

As standard procedure, "burst analysis" was applied to three or four "burst" segments from each recording of each level of voltage clamp (see methods). An example of such a segment is shown in Fig. 4.1.4.A, which is

a two second trace recorded from a TAL at 20 mV. The portion of the segment that was used for the analysis is shown in the box, enlarged directly below. The computer generated amplitude histogram is shown beneath the enlarged trace (Fig. 4.1.4.B). The histogram revealed three discrete peaks of favoured current amplitude an equal distance apart from each other. Measurement of the differences in amplitude between peaks formed the basis of "burst analysis", and provided the smallest estimate of unitary current amplitude. "Burst analysis" of most segments yielded discrete peaks of favoured current amplitude as shown in Fig. 4.1.4.B. Part of the "burst analysis" procedure was to generate a "jump histogram" of the same data (Fig. 4.1.4.C). This histogram, which plots the absolute differences in peak current between successive peaks, (cf p.85) rather than the absolute amplitude of the peaks, revealed that large differences (jumps) in successive peak amplitudes occurred rarely; the distribution appears to be exponential. A phase space plot of the amplitudes of all data points of the same data segment (Fig. 4.1.4.D) revealed no detectable pattern, and was not explored further.

Fig. 4.1.5.A shows a collective current-voltage plot for the entire data sample ( $n=106$ ) as determined by "burst analysis". The shape of this plot is similar to the small "squares" I-V plot in that the mean unitary current amplitudes appeared to be independent of voltage above and below the reversal potential. It is interesting that the shape of the plot is similar to the one in Fig. 4.1.2, which was determined using small "square" measurement. The mean current amplitudes for the "bursts" and "squares" are shown in Table 4.1.2. These were all in the range of tenths of a pico-ampere; for each tubule segment, the mean unit current amplitudes at both negative and positive voltages for "bursts" was significantly different to, and approximately half the amplitude of the mean unit amplitudes of the "squares". The mean unit amplitudes for the DCT were significantly higher ( $p<0.05$ ) than those for the other segments, for both "bursts" and "squares". A third and final variation in current-voltage relationships was explored using total mean current amplitude for each voltage clamp value, and represented the mean current for "squares", "bursts" and "spikes" (see methods). The current-voltage plot in Fig. 4.1.5.B represents mean current amplitude as a function of voltage and was determined for 5 PSTs, 1 TAL, and 1 CCD. This data sample represented patches exposed

to a wide range of voltage values. For both plots in Fig. 4.1.5, the slope conductance was not determined, and the reversal potential was again in the vicinity of zero mV.

Channel behaviour usually exhibited multiple levels of amplitude; successive channel events were frequently at multiples of a unit current amplitude. This was evident in many of the "burst" amplitude histograms (as in Fig. 4.1.4.B), and was also sometimes observed in recordings of "squares". Fig. 4.1.6.A shows two separate traces recorded from a PST patch. The two traces occurred within a few seconds of each other, at the same clamp voltage. The dashed lines (Fig. 4.1.6.B) show that the second event rose abruptly to a level approximately four times that of the unit amplitude of the first, before falling equally abruptly to zero. The minor inconsistencies are presumably attributable to background noise, to intrinsic variability in single channel conductance, or to inadequate sampling of very fast events.

Fig. 4.1.7.A depicts one-second segments of 1-2 minute recordings of channel events in a single CCD patch, clamped at a number of voltages between 20 mV and -30 mV. The traces demonstrate "squares", "bursts" and "spikes" occurring in the same patch. Qualitatively, the mean open-time and the frequency of channel events were observed to increase as the clamp voltage departed from the reversal potential (-10 mV). The current-voltage relationship for the recordings, as determined by "burst analysis", is shown in Fig. 4.1.7.B. The slope conductance, as calculated by linear regression, was 9 pS. Fig. 4.1.7.C depicts the current-voltage relationship for the same data, as determined by "small squares analysis"; here the slope conductance, as calculated by linear regression, was 17 pS. The channels were voltage-sensitive, the fractional open time increasing with displacement of the clamp voltage from the reversal potential (Fig. 4.1.7.D). The comparative mean slope conductances for "bursts" and "squares" (presented in Table 4.1.3) did not differ significantly for the different tubule segments. An exception to this, however, was the DCT, which had a mean conductance value about twice that of the other tubule segments. Interestingly this was true both of "bursts" and of "squares". Reversal potentials were usually close to zero mV, suggesting a non-selective channel.

Fig. 4.1.7.E depicts the open- and closed-time histograms for the



same CCD patch in A, clamped at 10 mV; these could both be fitted by double exponentials. The mean open time was 3.2 ms, and the mean closed time was 32.2 ms. The mean open time at 20 mV voltage clamp was 5.25 ms; at 0 mV, it was 2.5 ms; at -20 mV, it was 2.6 ms; and at -30 mV it was 4 ms. The mean open time thus increased with displacement of the clamp voltage from the reversal potential. The rate constants for the open-time histogram were 5.5 and .369; the rate constants for the closed-time histogram were .167 and .022.

The log-log plots for open- and closed-time histograms (Fig. 4.1.7.F), determined at 10 mV voltage clamp, yielded high correlations ( $r=0.965$  for the open-time histogram, and  $r=0.959$  for the closed-time histogram). Log-log plots of the open- and closed-time histograms were determined for 20 patch recordings including all tubule segments. The correlations were all high ( $r>.9$ ) in all cases; however in most cases, the double exponential curve-fitting procedure on the normal plots yielded the lowest standard error of the estimate for the fit (see table in appendix). The predominance of double exponentials suggests that the channel possesses two open and two closed states.

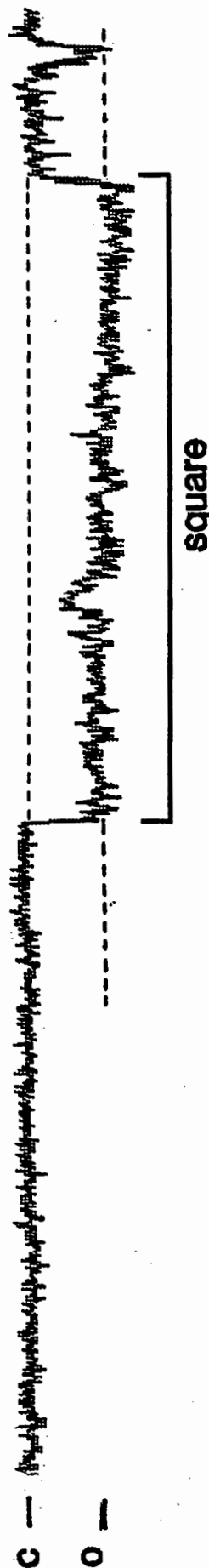
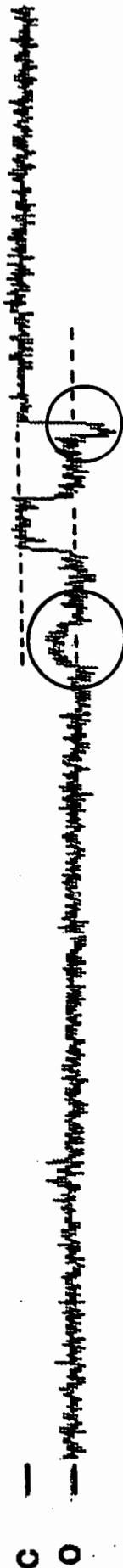
The amplitude histogram for the same CCD patch clamped at 10 mV is shown in Fig. 4.1.7.G. The histogram includes all three types of channel activity ( $n=1074$  events), and takes the form of an exponential decay curve. This suggests multiple subconductance states of the same channel. A phase space plot of all channel openings of the same section of recording, is shown in Fig. 4.1.7.H. The plot revealed no strange attractor.

**TABLE 4.1.1. Experimental numbers**

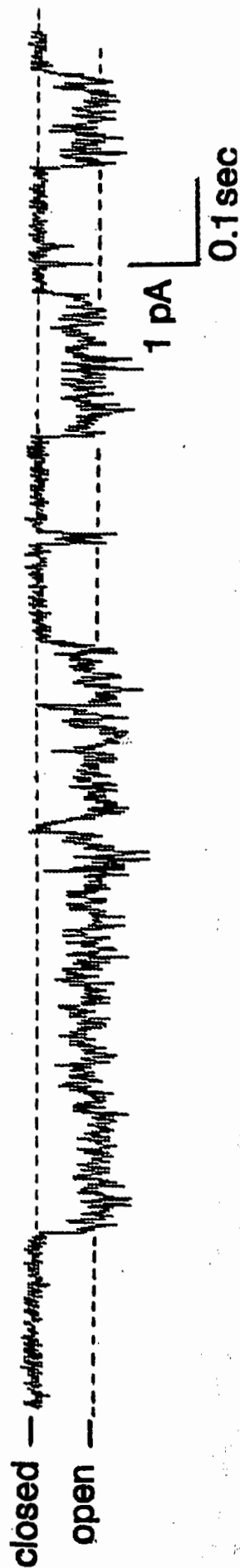
Species	Experimental procedure	Number (rate)
Rabbit	Kidneys dissected	195
	Isolated perfused tubule technique	63
	Ripped tubule technique	132
	Patch pipette trials (in sample of 34 experiments)	1007
	Tight seals (in same sample)	91 (9%)
	Patch recording (in same sample)	6 (.6%)
	Drug (hormone) additions : Bay K-8644	8
	Nifedipene	8
	D-600	1
	Verapamil	1
	Chlorothiazide	2
	Parathyroid hormone	6
	Solution changes : Na-Cl/2	10
Human	Na Acetate	4
	Na thiocyanate	1
	Human Biopsies dissected	15
	Patch recordings	21
	Tight seal success	about 20%
	Drug additions : Bay K-8644	1
	Nifedipene	2

**Figure 4.1.1.** Recordings from the apical membrane of tubule segments showing the three temporal patterns of channel activity observed. **A.1 and 2**, recordings from cortical collecting duct and thick ascending limb patches respectively, both clamped at 10 mV. The channel events shown have sharp transitions into the open and closed states, with relatively constant current amplitudes (lasting for longer than 5 ms), and were categorised as "square" channels. The segments depicted within the circles are probably different subconductance levels of the same channel. **B**, "Burst" activity, depicted for a thick ascending limb patch clamped at 10 mV, occurred in most patches, and was frequently interspersed with current "squares" and "spikes". They were usually irregular in amplitude. **C**, channel activity also manifested as current "spikes" of short duration (1-10 ms) and variable amplitude, as shown in this recording from a cortical collecting duct patch clamped at 20 mV. The three temporal patterns occurred together in most patch recordings yielding channel activity.

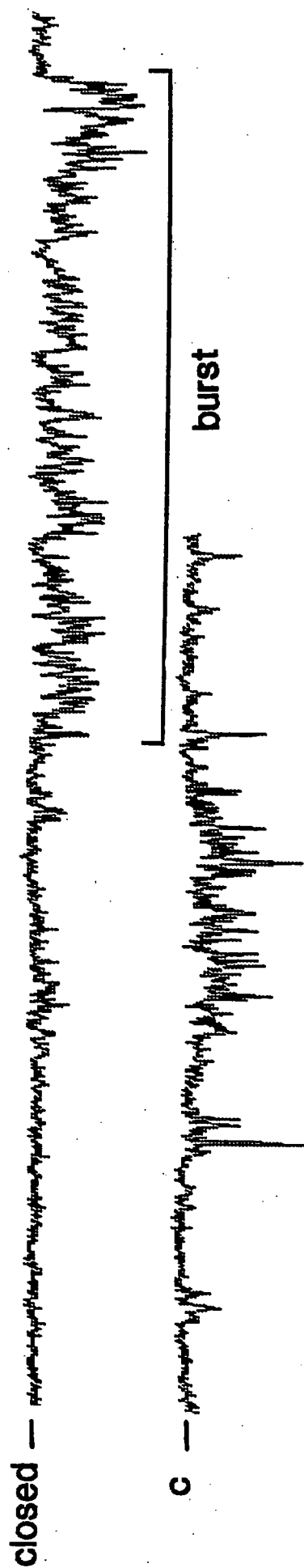
A 1



2



B



C

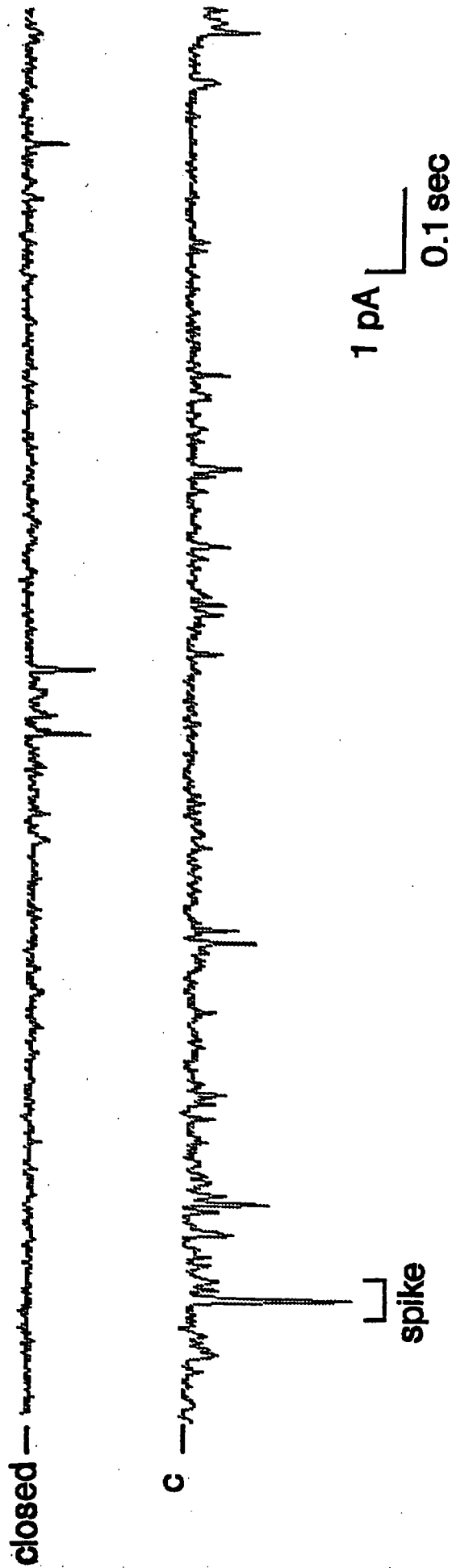


**Figure 4.1.2.** A current voltage plot derived from the entire data sample from all tubule segments ( $n=106$ ). The points represent the means and the error bars for the standard deviations of the smallest "squares" measured at each voltage. Absent error bars denote standard deviations too small to be depicted graphically. The slope conductance could not be measured for this plot, as collectively, the channel current amplitudes were independent of voltage above and below the reversal potential. The reversal potential was close to zero mV.

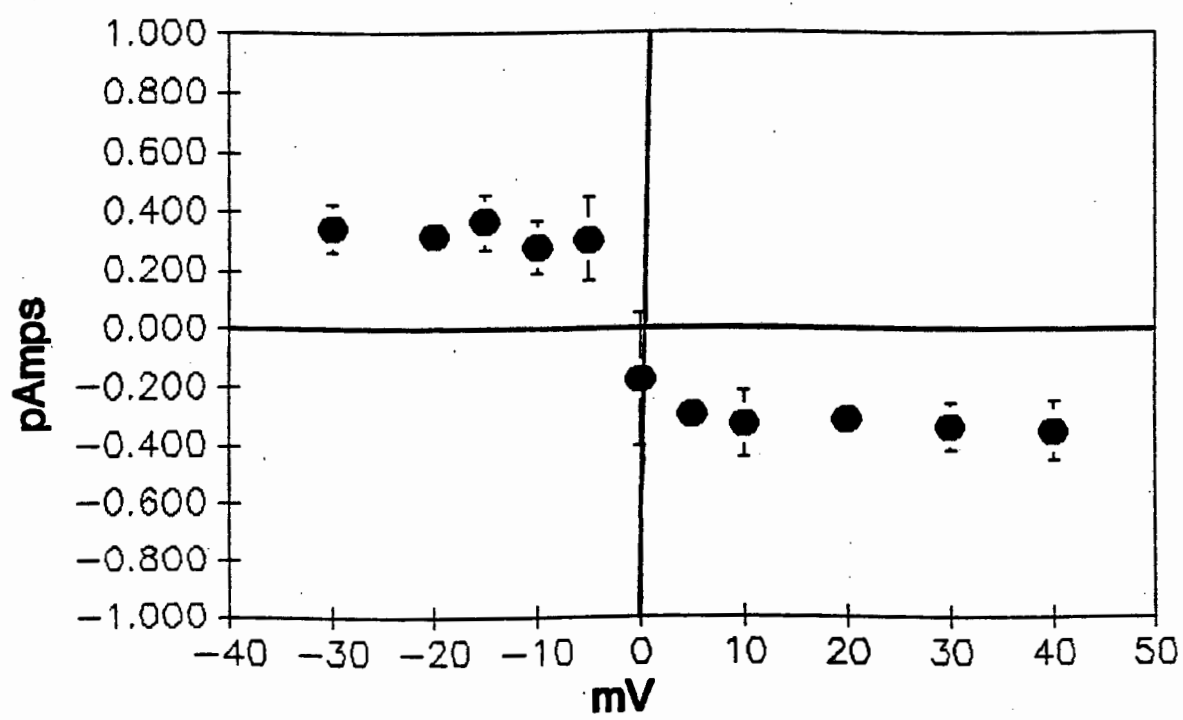
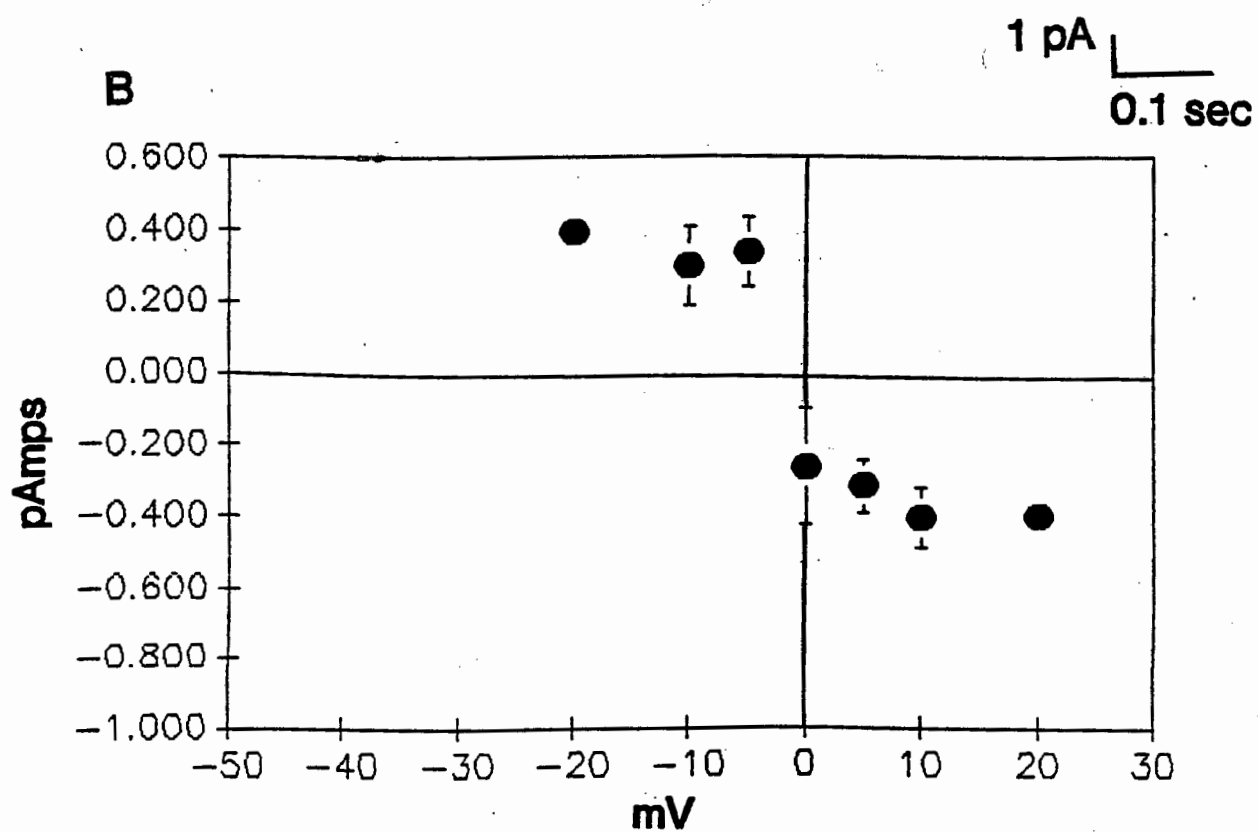
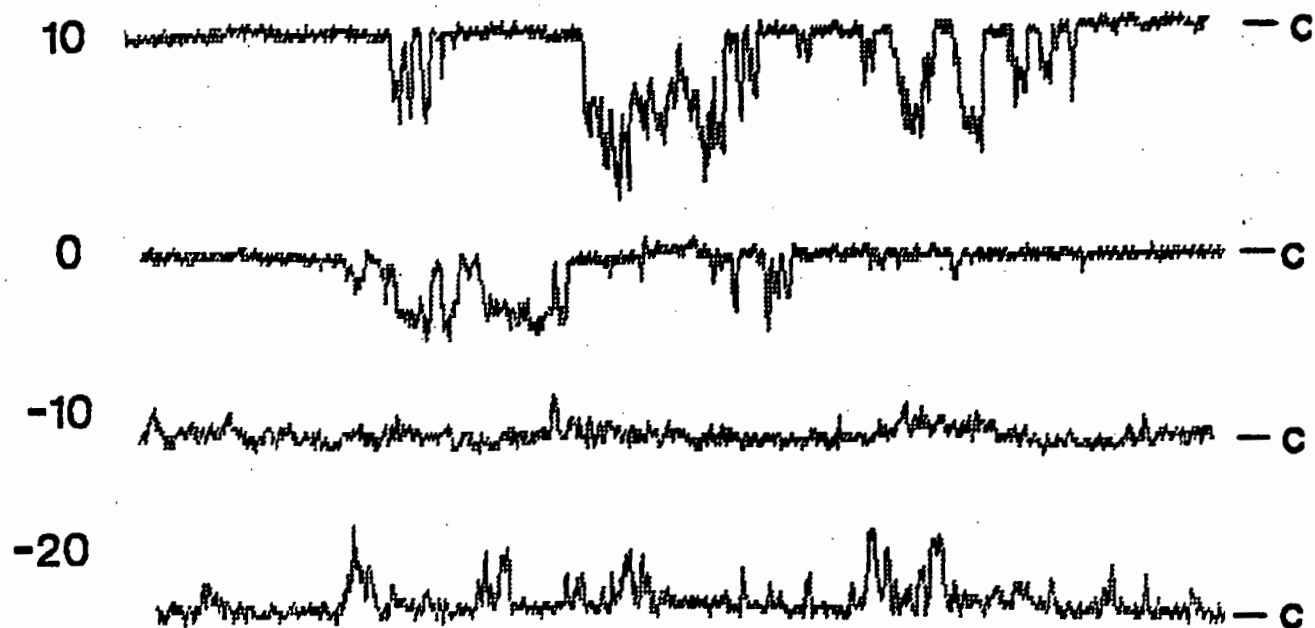


**Figure 4.1.3.** **A**, recordings from an inside-out patch of the apical membrane of a DCT, clamped at varying voltages. **B**, a current-voltage plot of collective "small squares" from the DCT data sample ( $n=8$ ). The channel current amplitudes appear to be voltage-independent, and the slope conductance of this plot could not be measured. Absent error bars denote standard deviations too small to be depicted graphically.

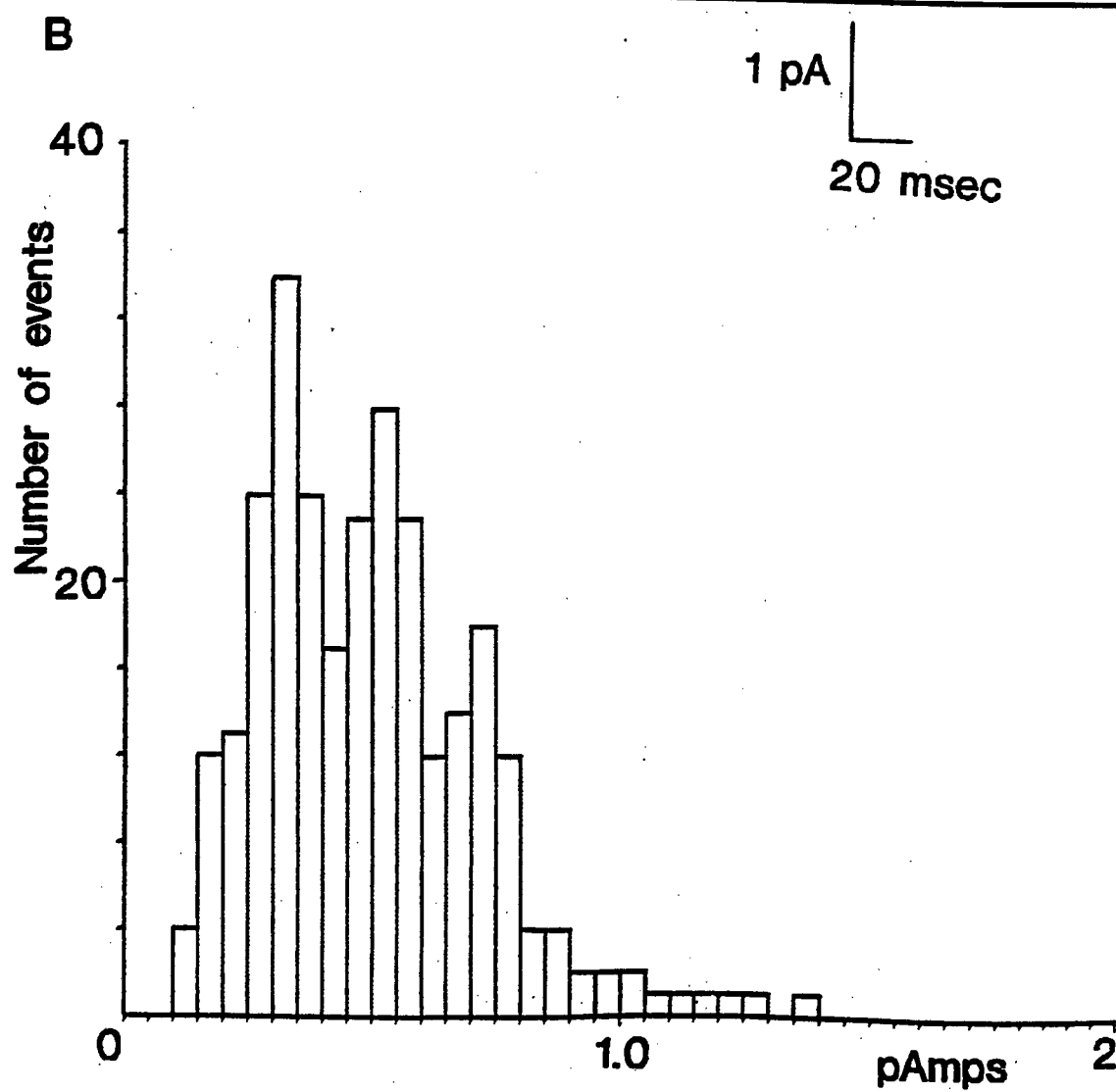
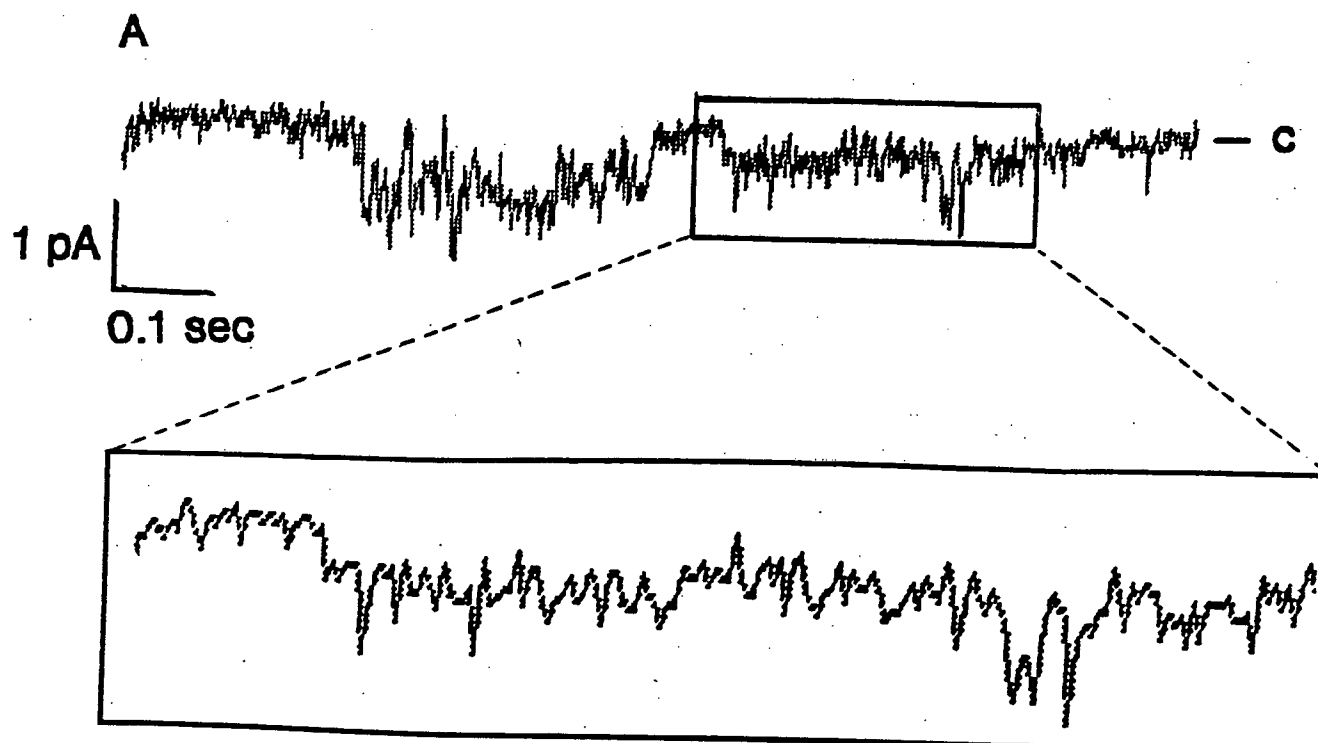


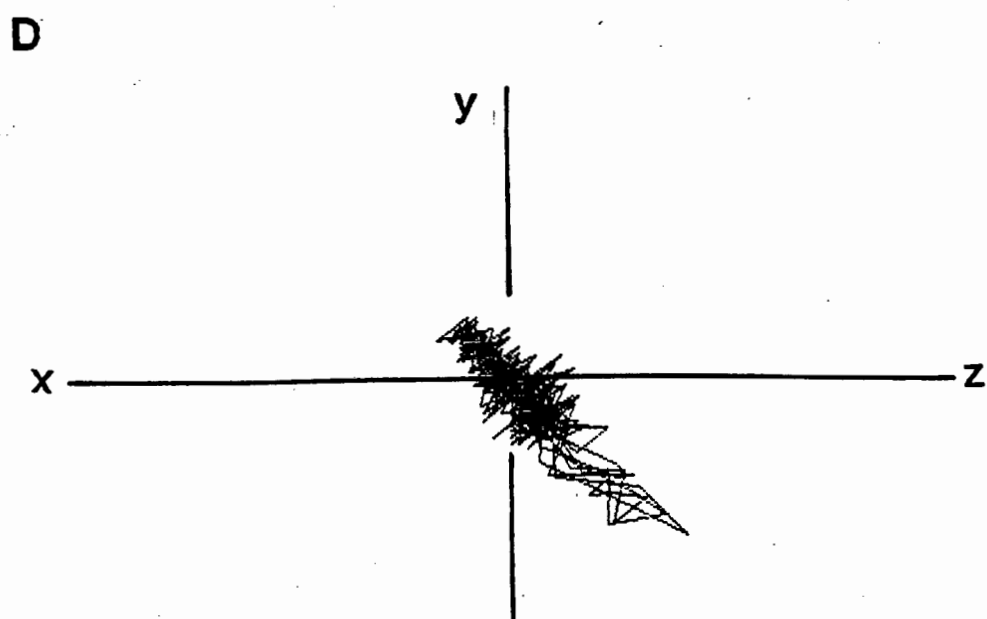
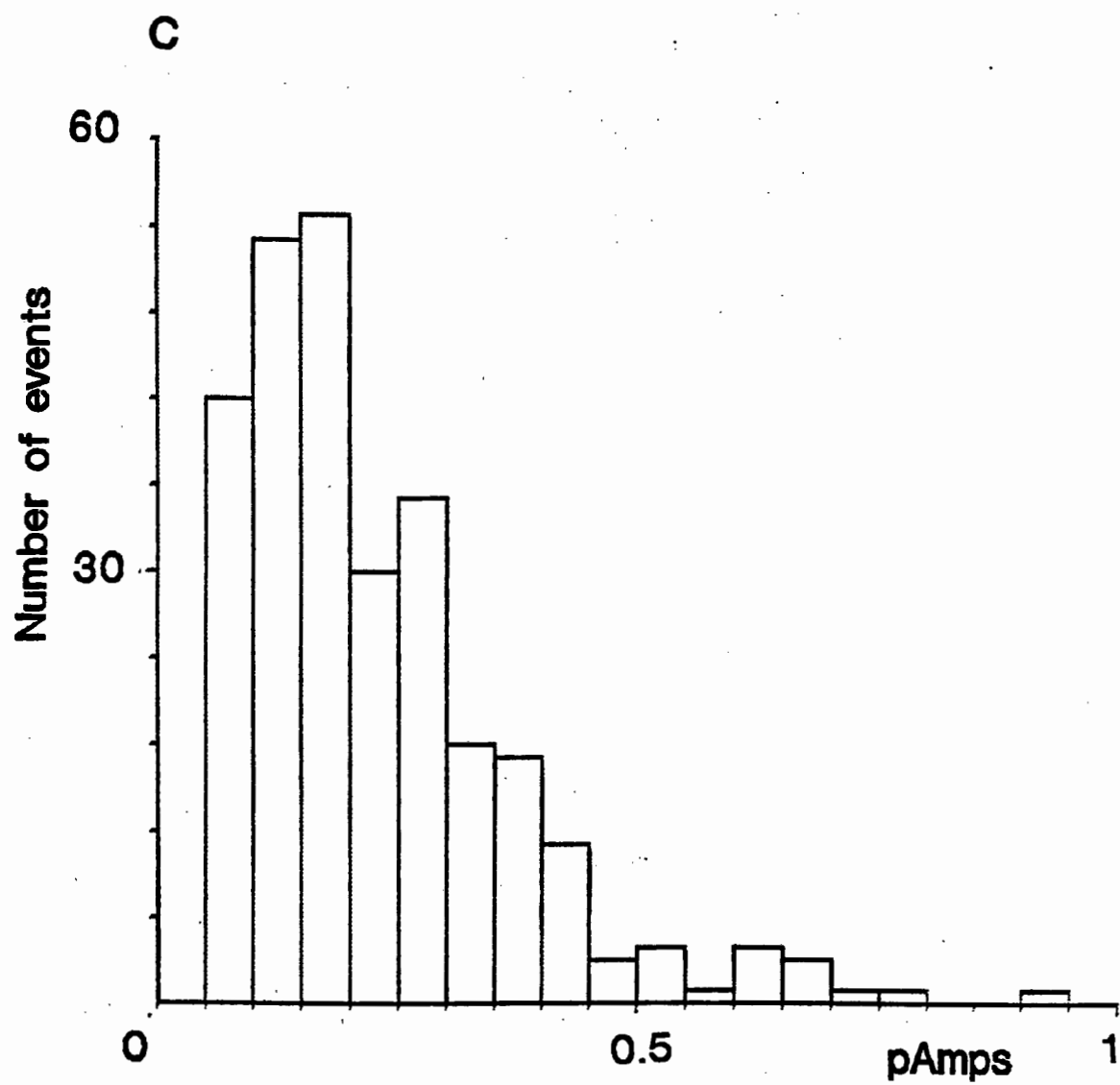
A

Vp (mV)

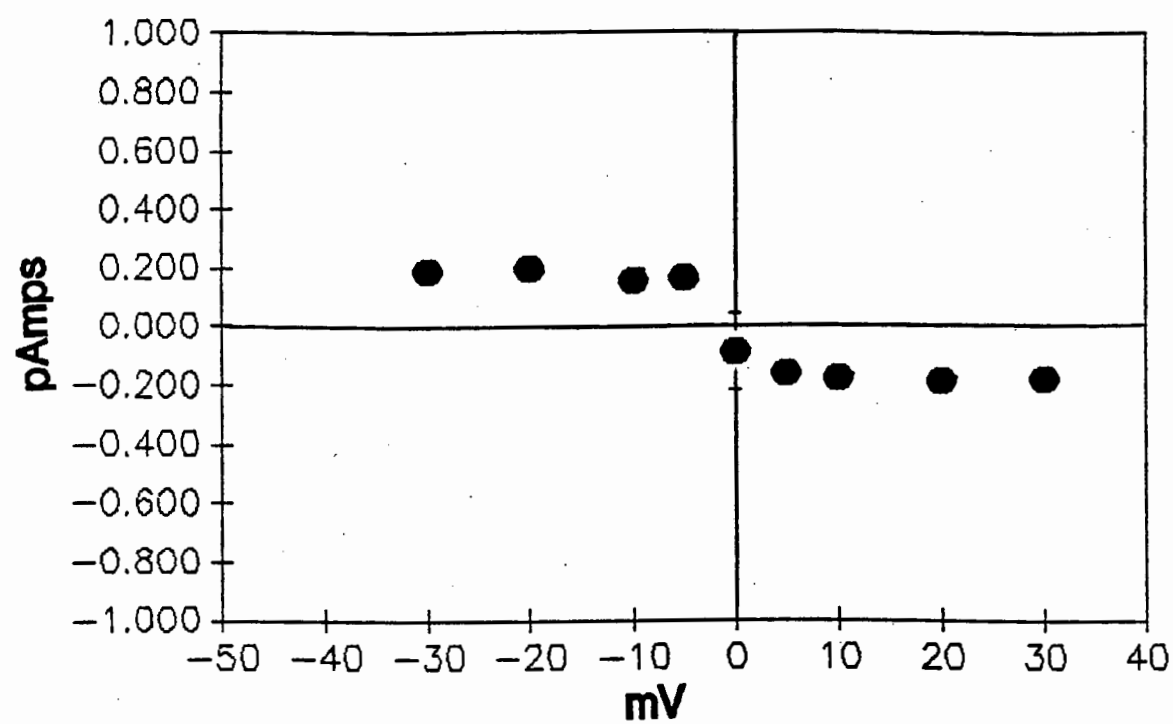
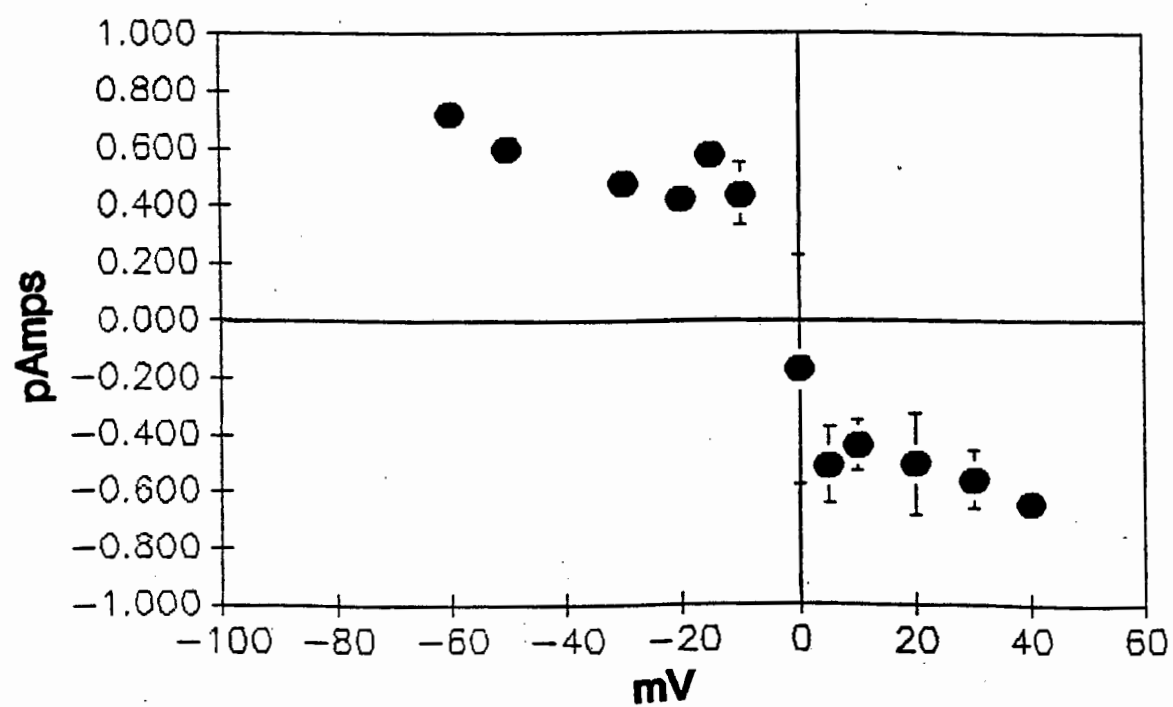


**Figure 4.1.4.** **A**, a two second trace depicting "bursting" activity in a TAL patch clamped at 20 mV (top). An expanded view of a portion of this "burst" is presented directly beneath the trace. **B**, amplitude histogram of the trace in **A** directly above, demonstrating discrete peaks of favoured current amplitude. Measurement of the differences in amplitude between peaks formed the basis of "burst analysis". The chi-squared value for this histogram was 250.4. The number of events in the bins corresponding to the histogram peaks therefore differs significantly ( $p < 0.001$ ) from the mean number of events per bin (10.6). **C**, "jump" histogram depicting relative frequency of amplitude of "jumps" from one peak to the next, in the "burst". **D**, a phase space plot of all data points for the burst in **A**. The X-axis represents the amplitude of any given data point on the trace (with a value of say  $x$ ); the Y-axis represents the amplitude of the preceding data point ( $x-1$ ), and the Z-axis represents the amplitude of the data point preceding that on the y-axis ( $x-2$ ).





**Figure 4.1.5. A,** collective current-voltage relationship for the entire data sample using "burst analysis" to determine current amplitude (see methods). **B,** current-voltage relationship for the total mean current amplitude as derived collectively from a sample of 5 PSTs, 1 TAL, and 1 CCD. In both A and B, the slope conductance was not determined; in both A and B, absent error bars denote standard deviations too small to be depicted graphically. The reversal potential was in the vicinity of zero mV.

**A****B**

**Figure 4.1.6.** **A**, single channel events in a PST patch held at zero mV clamp potential. The two traces are from the same recording and occurred within a few seconds of each other. **B**, the same events are depicted using an enlarged time scale. The amplitude of the second event (as depicted by the dotted lines) is four times the unit current level of the first event.

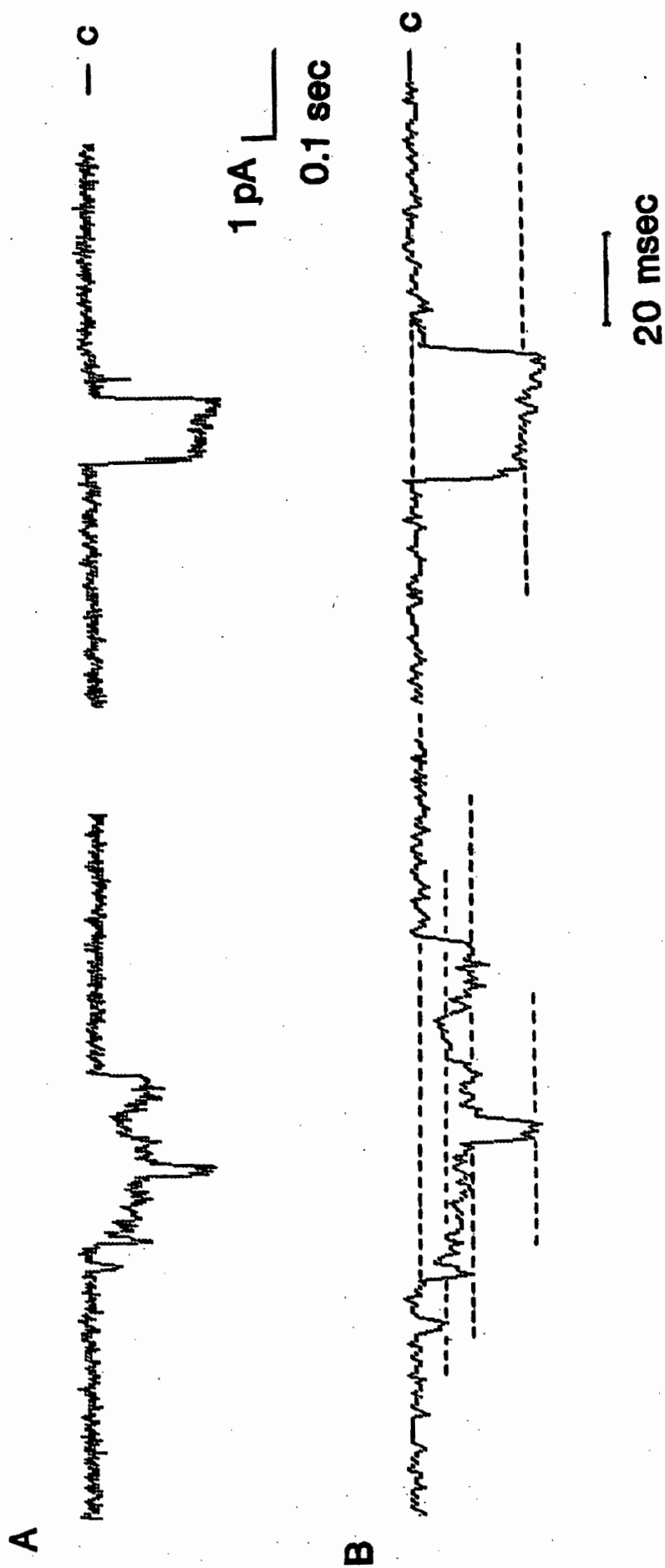




**Figure 4.1.7.** **A**, Recordings from an inside-out patch of apical membrane of a CCD, clamped at varying voltages. The mean amplitude, frequency of channel events and the fractional open time increased as the clamp voltage departed from the reversal potential. The channel current also reversed direction at either side of the reversal potential. **B**, current-voltage relationship for the CCD patch in **A**, as measured by "burst analysis" (see methods). The slope conductance as calculated by regression analysis, was 9 pS and the reversal potential was -10 mV. **C**, current-voltage relationship for the CCD patch in **A**, as measured by "small squares analysis". The slope conductance as calculated by linear regression, was 17 pS. **D**, plot of fractional open time as a function of the clamp potential for the same recording. **E**, Open- and closed-time histograms from the same CCD patch held at a clamp voltage of 10 mV. Both the open- and closed-time distribution could be fitted with two exponentials. **F**, log-log plots of the open- and closed-time histograms for the CCD patch held at a clamp voltage of 10 mV. **G**, Amplitude histogram for the same CCD patch held at a clamp voltage of 10 mV ( $n=1074$  events). Most of the events were of small amplitude; the number of events fell exponentially at larger amplitudes. The threshold for detection of channel events was set at 0.2 pA. **H**, a phase space plot of channel open-times for the same CCD patch recording at 10 mV. The X-axis represents the open time of any given channel event; the Y-axis represents the open time of the preceding channel event, and the Z-axis represents the open time of the twice preceding channel event.

A

 $V_p$  (mV)

20

— c

10

— c

0

— c

-10

— c

-20

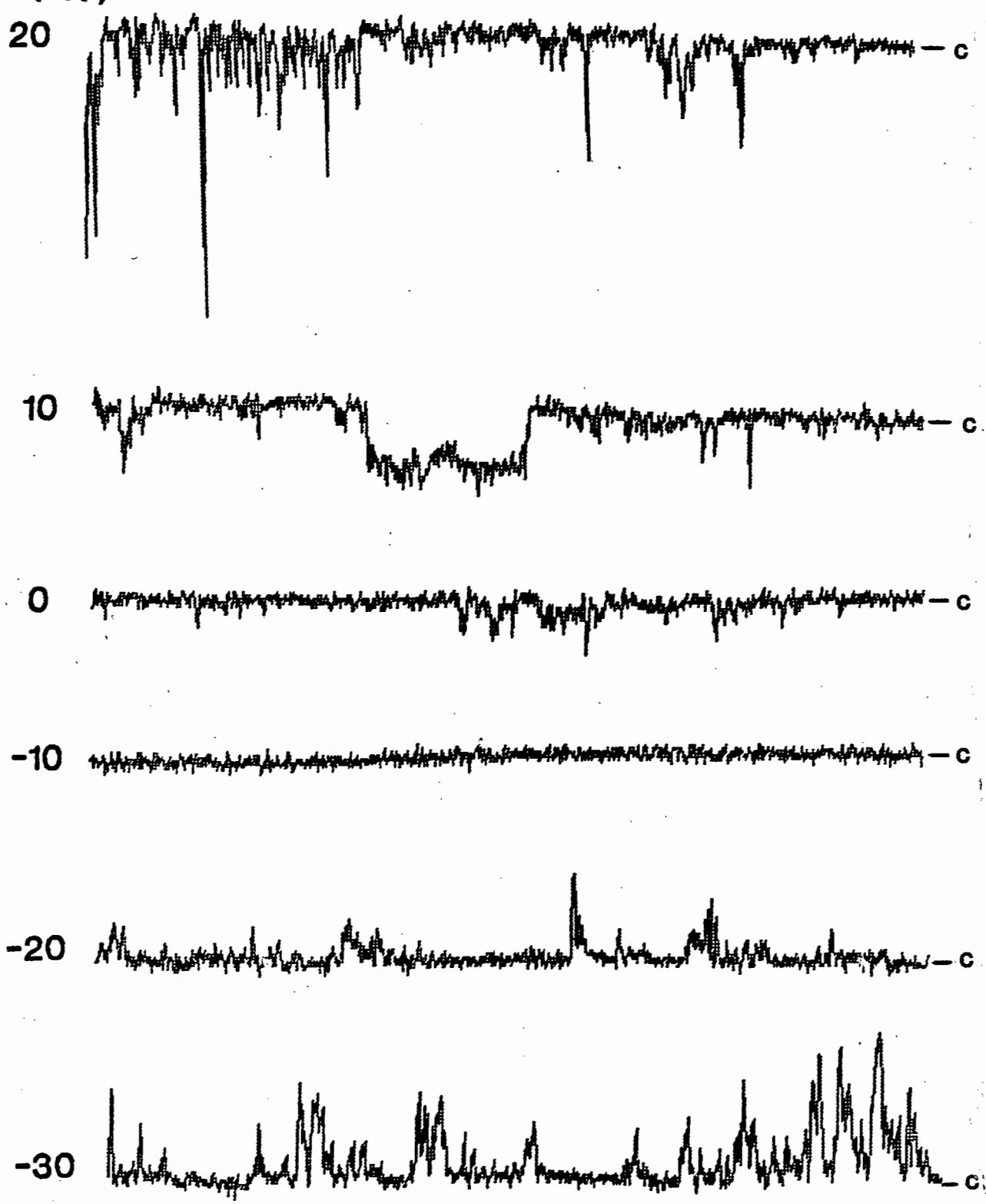
— c

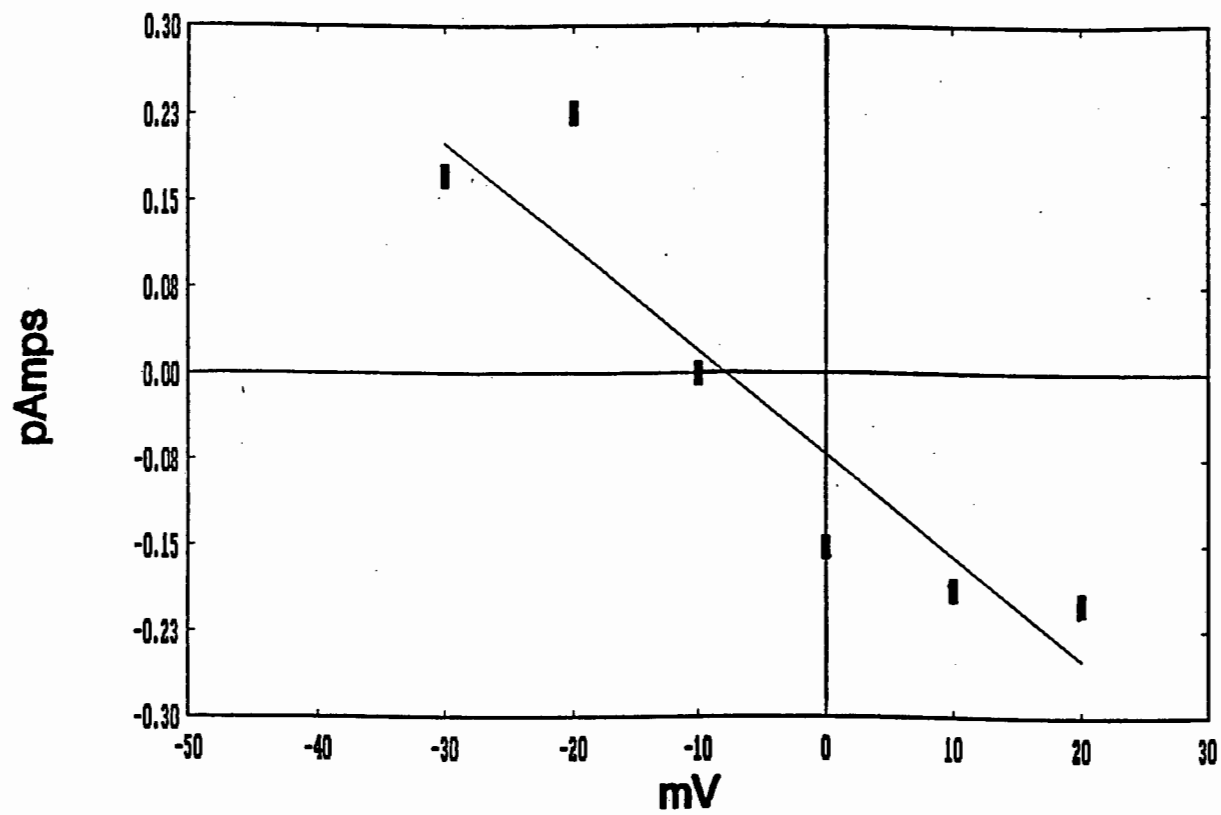
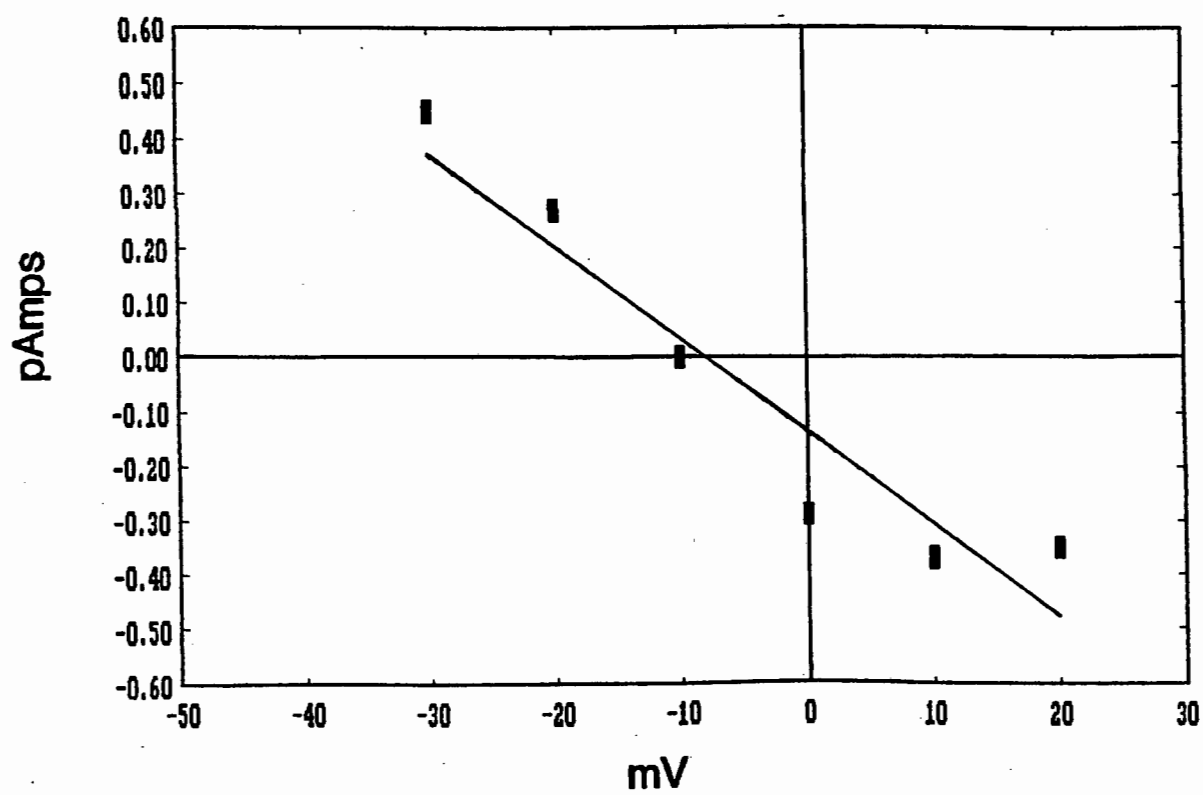
-30

— c

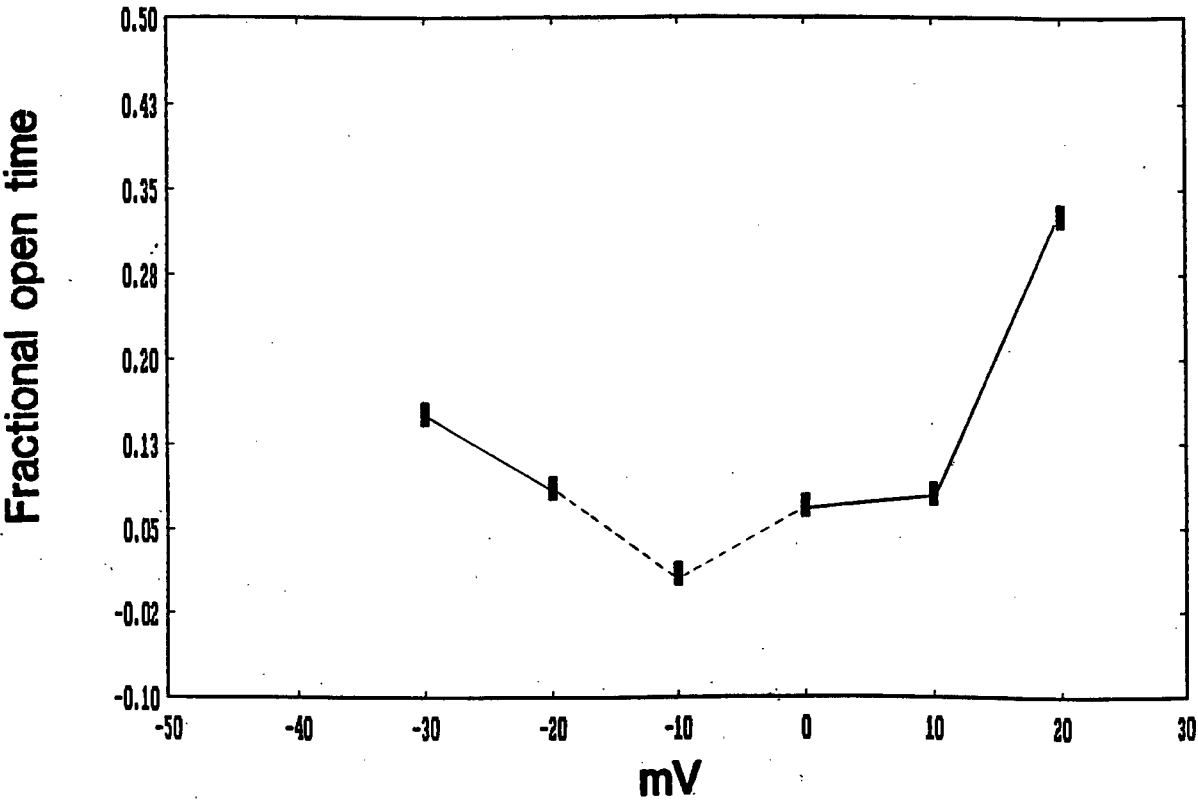
1 pA

0.1 sec

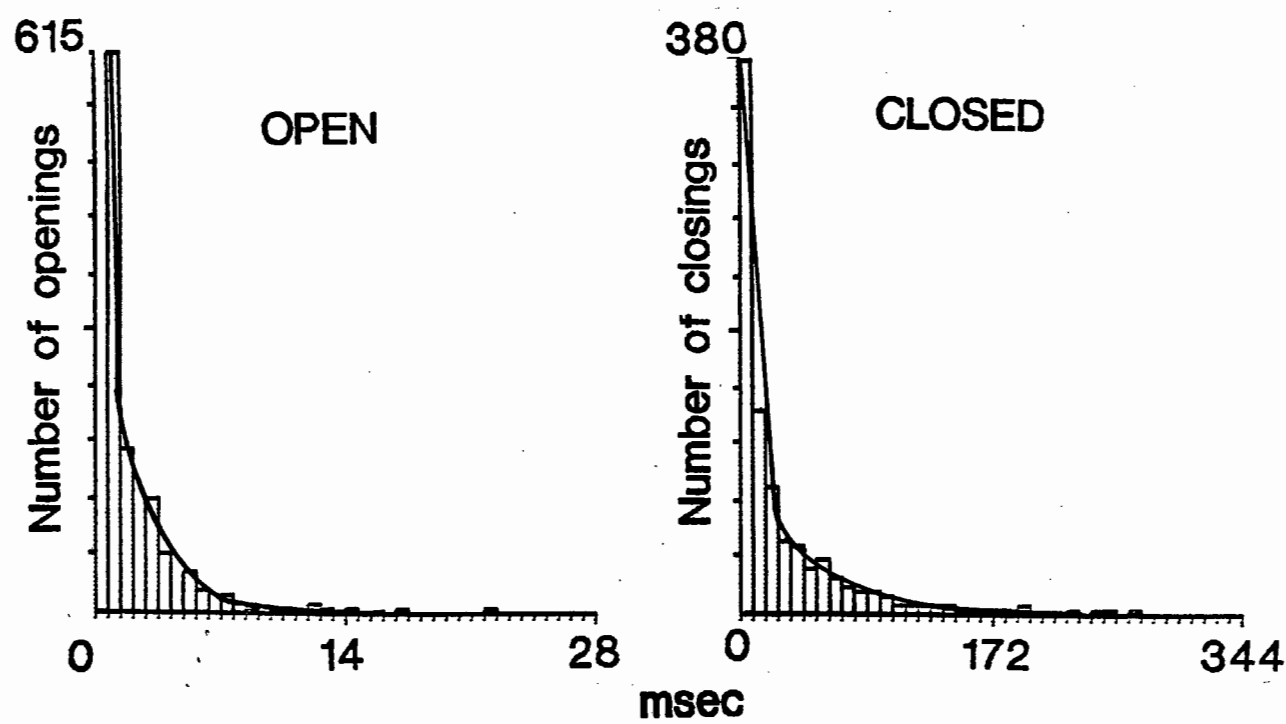


**B****C**

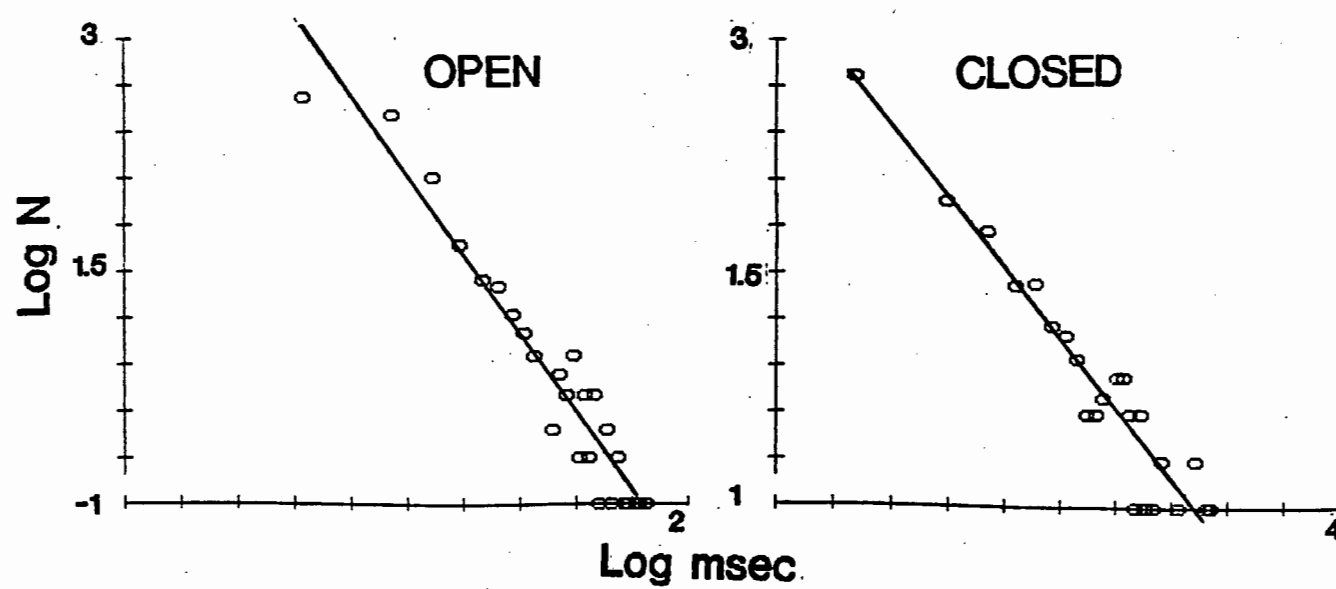
D

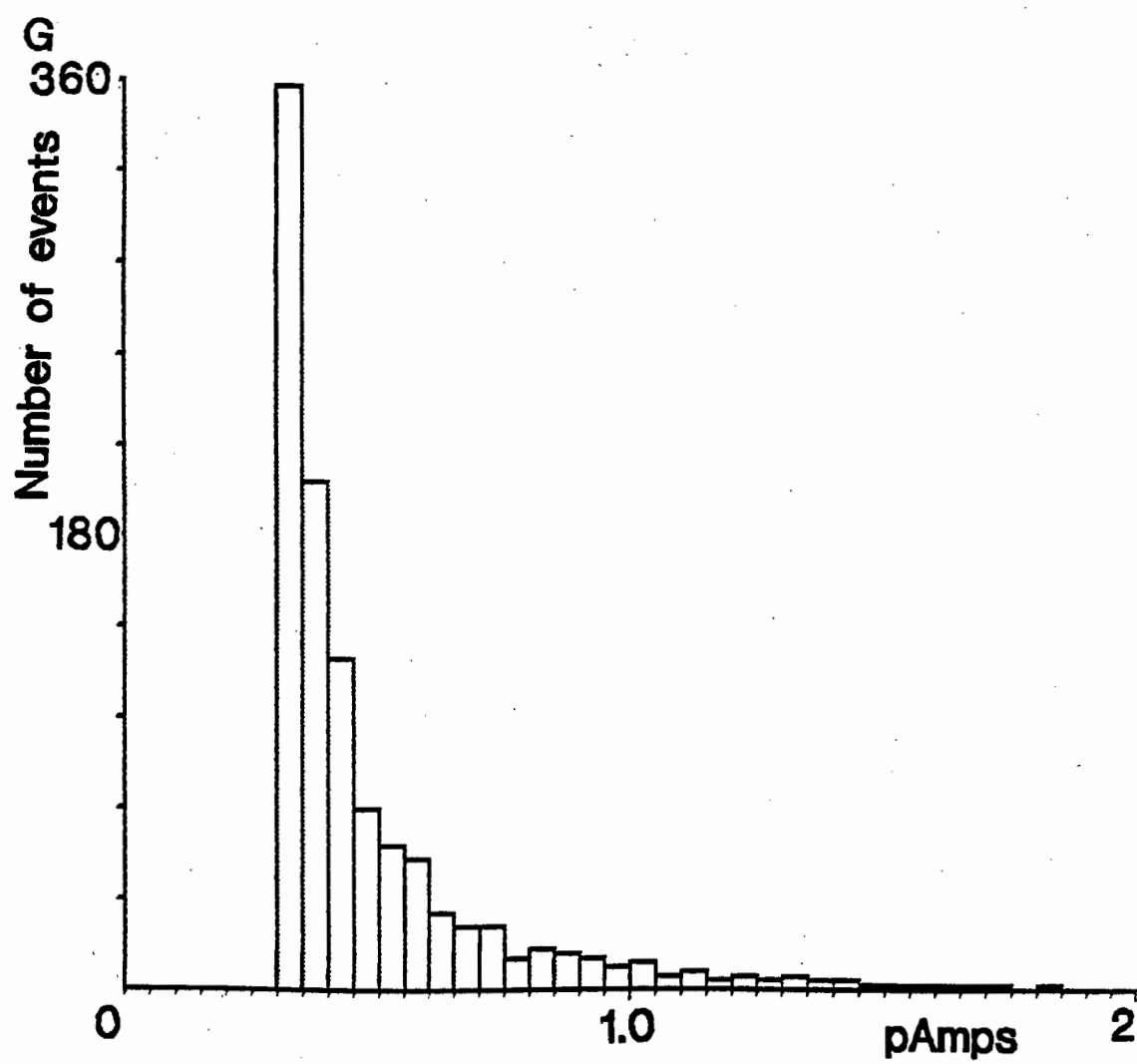


E



F





H

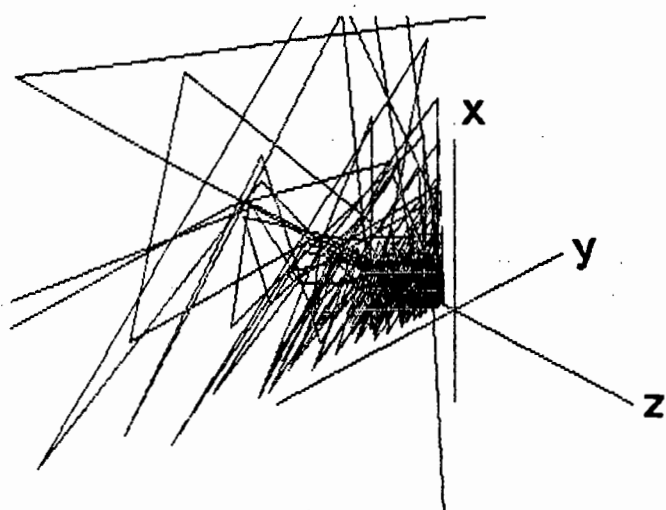


**TABLE 4.1.2.** Comparison of mean unit current amplitudes as determined for "burst analysis" and "square analysis" for all tubule segments studied, using the unpaired t-test.

Tubule	Voltage range	Mean unit amplitude (pA $\pm$ s.d.)		df.	p
		Bursts	Squares		
PST	-ve	.147 $\pm$ .025	.319 $\pm$ .037	22	s.
	+ve	-.169 $\pm$ .013	-.275 $\pm$ .086	33	s.
TAL	-ve	.188 $\pm$ .005	.255 $\pm$ .007	4	s.
	+ve	-.183 $\pm$ .007	-.327 $\pm$ .06	21	s.
DCT	-ve	.192 $\pm$ .017	.344 $\pm$ .046	18	s.
	+ve	-.18 $\pm$ .002	-.359 $\pm$ .064	20	s.
CCD	-ve	.176 $\pm$ .053	.306 $\pm$ .039	54	s.
	+ve	-.156 $\pm$ .035	-.296 $\pm$ .055	52	s.
Total	-ve	.175 $\pm$ .019	.315 $\pm$ .024	108	s.
	+ve	-.172 $\pm$ .01	-.324 $\pm$ .027	136	s.

**TABLE 4.1.3.** Comparison of channel conductances as determined for "burst analysis" and "square analysis" for all tubule segments studied, using the unpaired t-test.

Tubule segment	No. patch recordings	No. voltage clamp recordings	Mean conductance (pS $\pm$ s.d.)		p	Mean reversal PD (mV $\pm$ s.d.)
			Bursts	Squares		Squares
PST	37	11	14.8 $\pm$ 7	27.6 $\pm$ 24.4	n.s.	-2.6 $\pm$ 7.4
TAL	15	5	14 $\pm$ 13.1	23.25 $\pm$ 23.5	n.s.	-.63 $\pm$ 3.5
DCT	16	8	23.5 $\pm$ 11.3	51.3 $\pm$ 22	s	-1.45 $\pm$ 2.12
CCD	38	19	14.2 $\pm$ 4	26.25 $\pm$ 9.3	s	1.02 $\pm$ 2.9
Total	106	43	16.2 $\pm$ 8.9	31.1 $\pm$ 20	s	-.73 $\pm$ 4.5

## 4.2. Further characterisation of the channel

Studies involving exposing the patch to solutions of different ionic composition, and solutions containing drugs (calcium channel agonists and antagonists) and parathyroid hormone were undertaken to further characterise the channel.

To assess the channel's possible Cl permeability, CCD patches (n=11), PST patches (n=3), and a DCT patch were transferred to bath solutions of isosmotic diluted Ringer ("half NaCl Ringer") (n=10), Na acetate (n=4), or Na thiocyanate (n=1), so halving the bath (Na) and (Cl) concentration, or reducing the Cl concentration to zero. The results of this investigation are presented in Table 4.2.1. For the CCDs, the reversal potential shifted towards a substantially more negative voltage in two cases; towards a more positive value in eight cases, and in one case the reversal potential did not shift significantly at all. The PST reversal potentials in the alternate solution could not be determined due to excessive noise and drift in the recordings. In the case of the DCT patch, a solution change into Na thiocyanate resulted in a reversal potential shift towards a negative voltage. Fig. 4.2.1. shows recordings from a CCD patch clamped at a number of different voltages before and after solution change into "half NaCl Ringers". In this example, the reversal potential shift is towards a more negative voltage.

The response of the channel to the Ca channel blockers, verapamil (n=1), D600 (n=1), and nifedipene (n=8), and of the agonist, Bay K-8644 (n=9), was also investigated. The response of the channel to PTH was investigated for DCTs and TALs, and in two cases the effects of the diuretic, chlorothiazide, were also investigated. Table 4.2.2 summarises the fractional open-time ( $F_o$ ) response of the channels to the different drugs and PTH. Some patches were exposed to a number of voltages in the presence of drugs; each voltage is considered separately; thus after addition of the agonist Bay K-8644, two cases showed increased channel activity, two showed decreased activity, and nine showed no change at all. The antagonist nifedipene induced two increased responses, one decreased response, and had no effect in five cases. D600 induced one increased response; verapamil induced two increased responses, one



decreased response, and had no effect on one voltage clamp recording; chlorothiazide induced one slightly decreased response, and had no effect in three cases; PTH induced ten increased responses, and had no effect in three cases. Some of the changes in fractional open-time responses before and after the addition of drugs were substantial; others were slight.

Fig. 4.2.2.A depicts the effects of nifedipene and subsequent Bay K-8644 on a PST patch held at -20 mV. Channel activity first totally abolished by 0.1 mM nifedipene was near maximal after exposure to the agonist Bay K-8644. The channel activity was predominantly of the "burst" variety. The open- and closed-time histograms for the control and for recordings after the addition of Bay K-8644 are shown in Fig. 4.2.2.B. All histograms could be described by two exponentials. For the control recordings, the rate constants were 2.40 and .736 for the open-time histogram and .219 and .026 for the closed-time histogram. The mean open time was 1.3 ms and the mean closed time was 20.6 ms. For the recordings after the addition of Bay K-8644, the rate constants were .425 and .056 for the open-time histogram and .611 and .018 for the closed-time histogram. The mean open time was 15.1 ms and the mean closed time was 6.5 ms.

PTH exerted an effect in a number of cases; the best example is shown in Fig. 4.2.3 which depicts a cell-attached recording from a DCT exposed to a number of different clamp voltages before and after addition of PTH (100  $\mu$ M) to the bath. Before the addition of PTH there was no channel activity on the membrane patch. After addition of PTH, the patch remained quiescent for a further 5-10 minutes. It then became active at all voltages tested and remained active until the end of the experiment, some 15 minutes after hormone addition.

**TABLE 4.2.1. Reversal potential shift after solution changes**

Tubule segment	No.	Solution change	Reversal PD BEFORE(mV)	Reversal PD AFTER (mV)	Reversal PD SHIFT (mV)
CCD	1	NaCl/2	2.8	-5.4	-8.2
	2	NaCl/2	-3.3	1.0	4.3
	3	NaCl/2	3.2	about -30.0	about -27.0
	4	NaCl/2	0.1	5.9	5.8
	5	NaCl/2	0.1	22.6	22.5
	6	NaCl/2	-0.3	57.6	57.9
	7	NaCl/2	-6.3	about -6.0	-
	8	NaCl/2	-10.0	31.6	41.6
	9	NaCl/2	1.6	22.0	20.4
	10	Na Acetate	-6.3	-1.5	4.79
	11	Na Acetate	0.1	22.4	22.3
PST	1	NaCl/2	0.8	cannot	
	2	Na Acetate	0	calculate	
	3	Na Acetate			
DCT	1	Na thiocyanate	-2.8	-43.8	-41.0
where NaCl/2 ="half Ringers solution"					

**Figure 4.2.1.** Channel activity in a CCD patch clamped at various voltages, before (A) and after (B) exposure to "half NaCl Ringer" (see text). The reversal potential (not determined) appears to have become more negative.

B Bath: 1/2 NaCl

Vp (mV)

+20



+10



0



-10



1 pA  
0.1 s

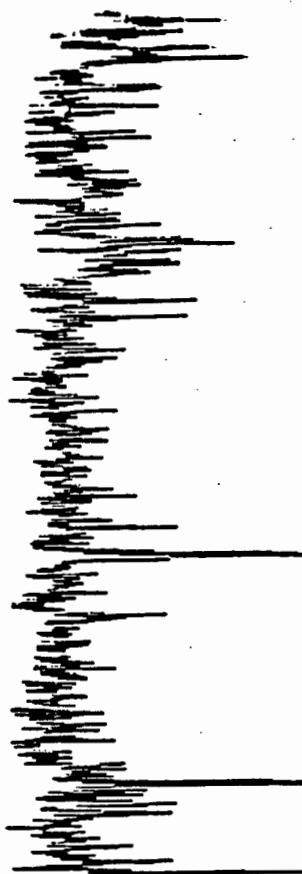


**TABLE 4.2.2. Channel response to drugs (calcium channel agonists and antagonists) and parathyroid hormone.**

Tubule segment	No.	Drug or hormone	(mV)	Fo BEFORE	Fo AFTER	Channel response Increase - I Decrease - D No change - N
CCD	1	Bay K-8644	-10	0.043	0.031	D
	2	Bay K-8644	-5	0.107	0.203	I
	3	Bay K-8644	-20	0.000	0.000	N
			-10	0.000	0.000	N
			0	0.000	0.000	N
	4	Bay K-8644	-10	0.000	0.000	N
	5	Bay K-8644	-5	0.000	0.000	N
			0	0.000	0.000	N
	6	Bay K-8644	-10	0.101	0.104	N
			0	0.000	0.000	N
	7	Bay K-8644	0	0.020	0.000	D
	8	Nifedipene	-20	0.011	0.027	I
	9	Nifedipene	-20	0.000	0.000	N
	10	Nifedipene	-10	0.996	0.996	N
	11	Nifedipene	-15	0.048	0.045	N
	12	Nifedipene	-10	0.000	0.000	N
	13	Nifedipene	-5	0.000	0.000	N
	14	Nifedipene	-10	0.101	0.140	I
PST	15	D-600	-10	0.043	0.071	I
	16	Verapamil	-20	0.381	0.189	D
			-10	0.04	0.052	I
			0	0.000	0.000	N
			10	0.147	0.213	I
	17	Chlorothiazide	10	0.322	0.000	D
PST	1	Bay K-8644	-20	0.022	0.924	I
		Nifedipene	-20	0.022	0.000	D

TABLE 4.2.2. (continued)

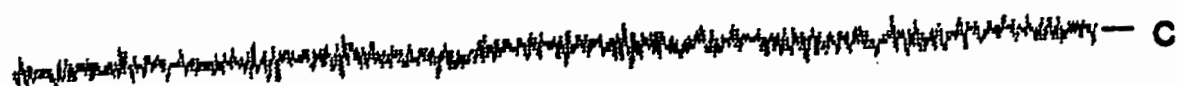
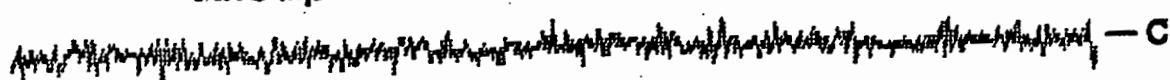
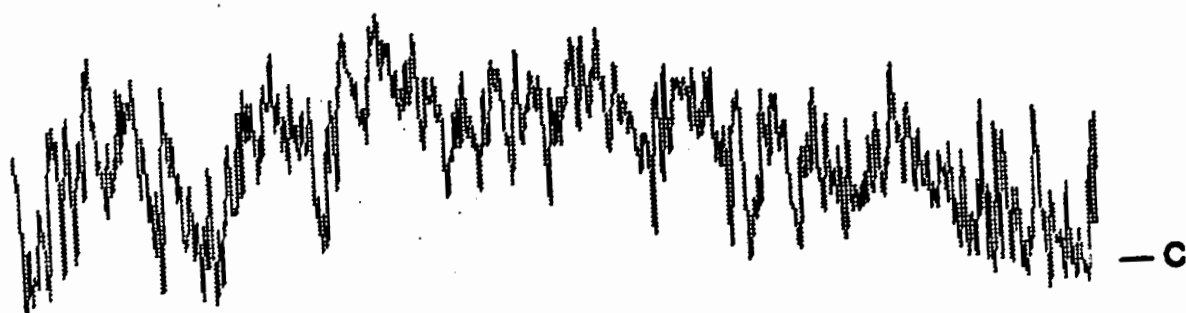
Tubule segment	No.	Drug or hormone	(mV)	Fo BEFORE	Fo AFTER	Channel response Increase - I Decrease - D No change - N
TAL	1	Bay K-8644	-10	0.000	0.000	N
	2	Chlorothiazide	0	0.000	0.000	N
			10	0.000	0.000	N
			20	0.000	0.000	N
			20	0.000	0.000	N
	3	PTH	0	0.000	0.000	N
	4	PTH	0	0.003	0.010	I
			10	0.001	0.002	I
			10	0.001	0.002	I
	5	PTH	0	0.000	0.000	N
			10	0.000	0.003	I
	6	PTH	0	0.000	0.019	I
	7	PTH	0	0.000	0.000	N
DCT	1	PTH	-20	0.000	0.320	I
			-10	0.000	0.090	I
			0	0.000	0.030	I
			10	0.000	0.010	I
			20	0.000	0.070	I
			30	0.000	0.280	I


Where Fo = fractional open time

**Figure 4.2.2.** Recordings demonstrating the response of the channel to Ca channel agonists and antagonists. **A**, the effects of the Ca channel blocker, nifedipene, and agonist, Bay K-8644 on a PST patch clamped at -20 mV. Channel activity previously abolished by 0.1 mM nifedipene was near maximal after exposure to the agonist Bay K-8644 (100  $\mu$ M). **B**, the open- and closed-time histograms before addition of drugs (top) and after addition of Bay K-8644 (below). All histograms could be described by two exponentials.

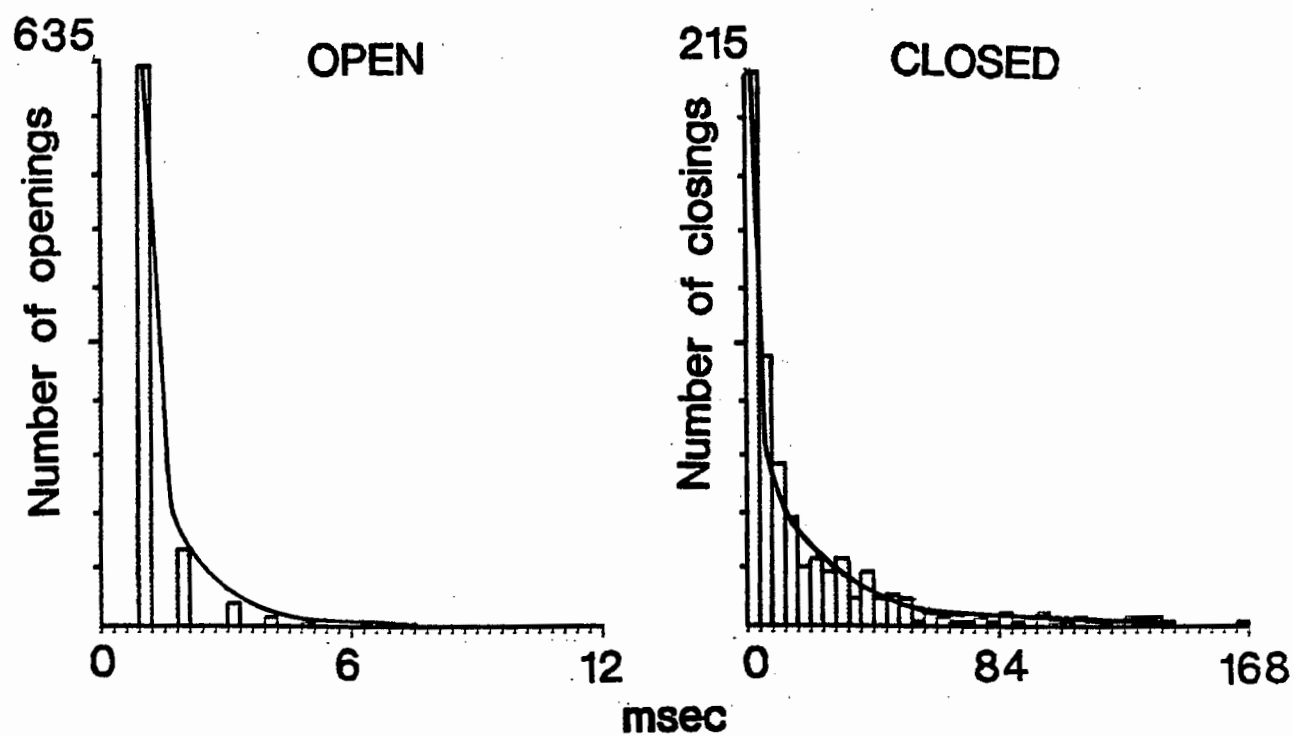
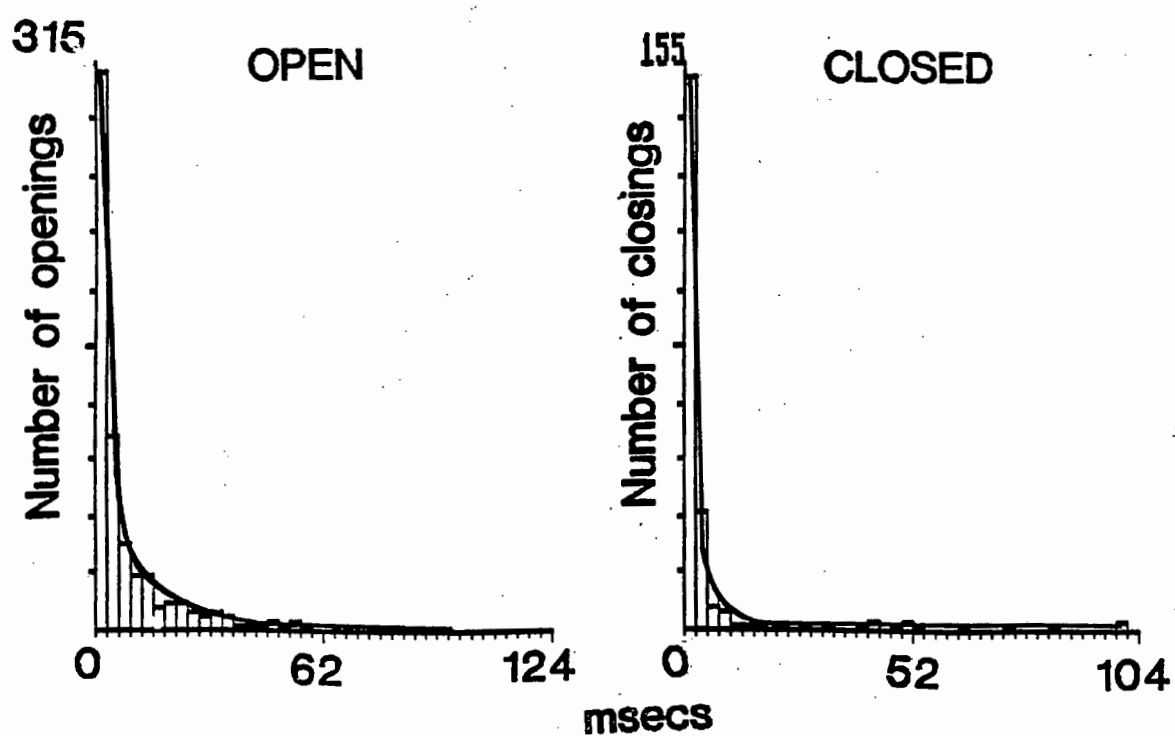
A

Control

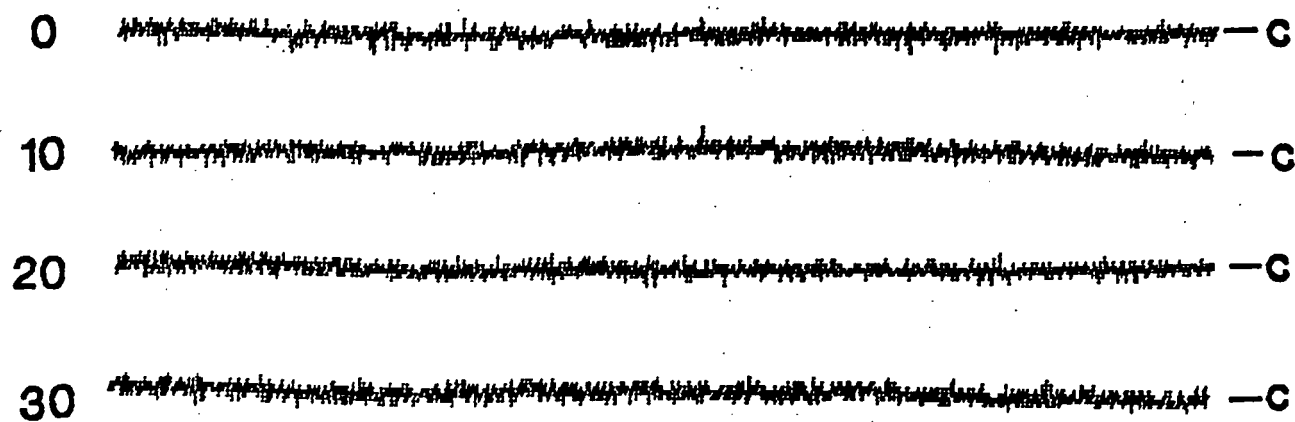
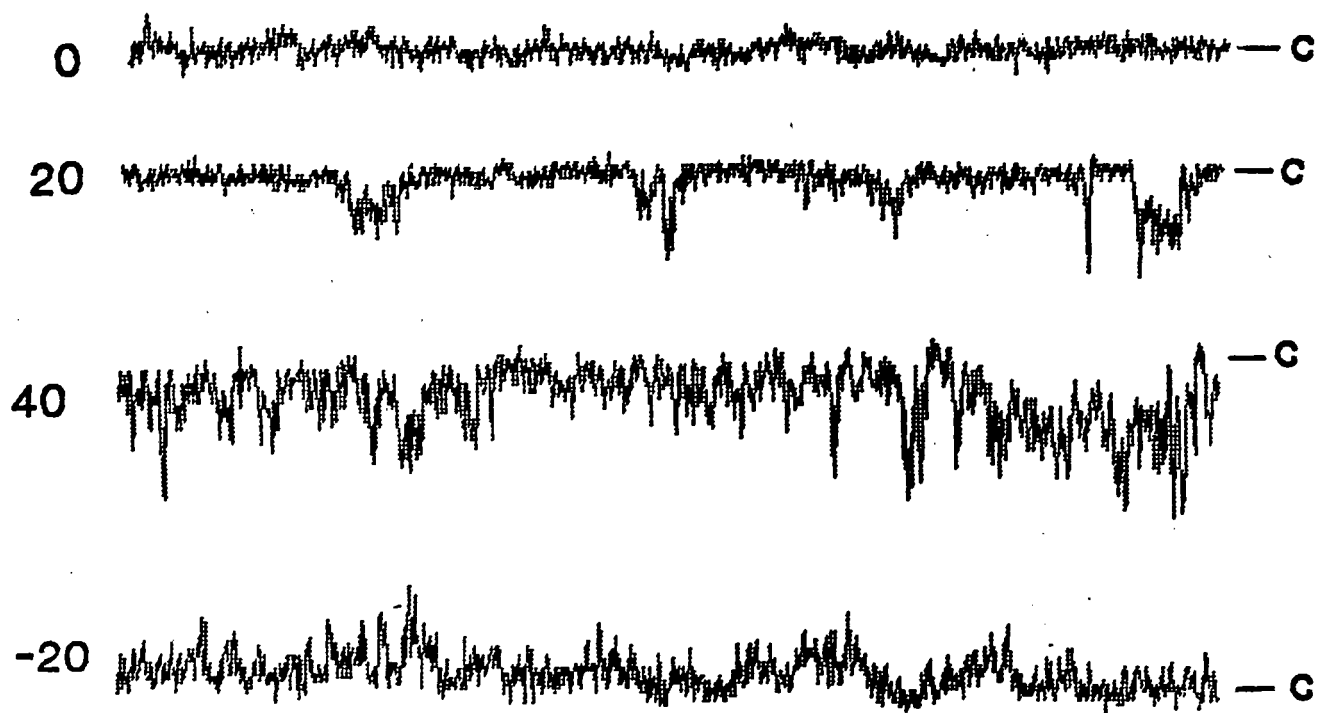
+ Nifedipene (100  $\mu$ M)+ Bay K-8644 (100  $\mu$ M)

1 pA   
0.2 sec



**B****Control****+Bay K-8644 (100  $\mu$ M)**

**Figure 4.2.3.** Channel recording from a DCT patch in the cell-attached configuration before and after the addition of PTH (100  $\mu$ M) to the bath. The patch, which was exposed to a number of different voltage clamp values contained no channel activity before the addition of PTH. Marked channel activity was observed about 5 minutes after the addition of PTH. The channel was active at all voltages applied to the patch and lasted until the seal broke down about 10 minutes later.

$V_p$  (mV)+ PTH (100  $\mu$ M)

1 pA  
0.2 sec

### 4.3. The quest for similar channels in human tubule segments

A search for similar channels was carried out with human tubule segments obtained from biopsy specimens. All patch recordings except one, were made on the basolateral membrane. It was not possible to tell which tubule segment was dissected, as only very short fragments could be isolated. Since, however, most of the tubule segments were relatively broad and frequently curved, and since the tubules under study were clearly not CCDs, or thin descending or ascending limbs, the recordings were presumably largely, if not exclusively from proximal tubules.

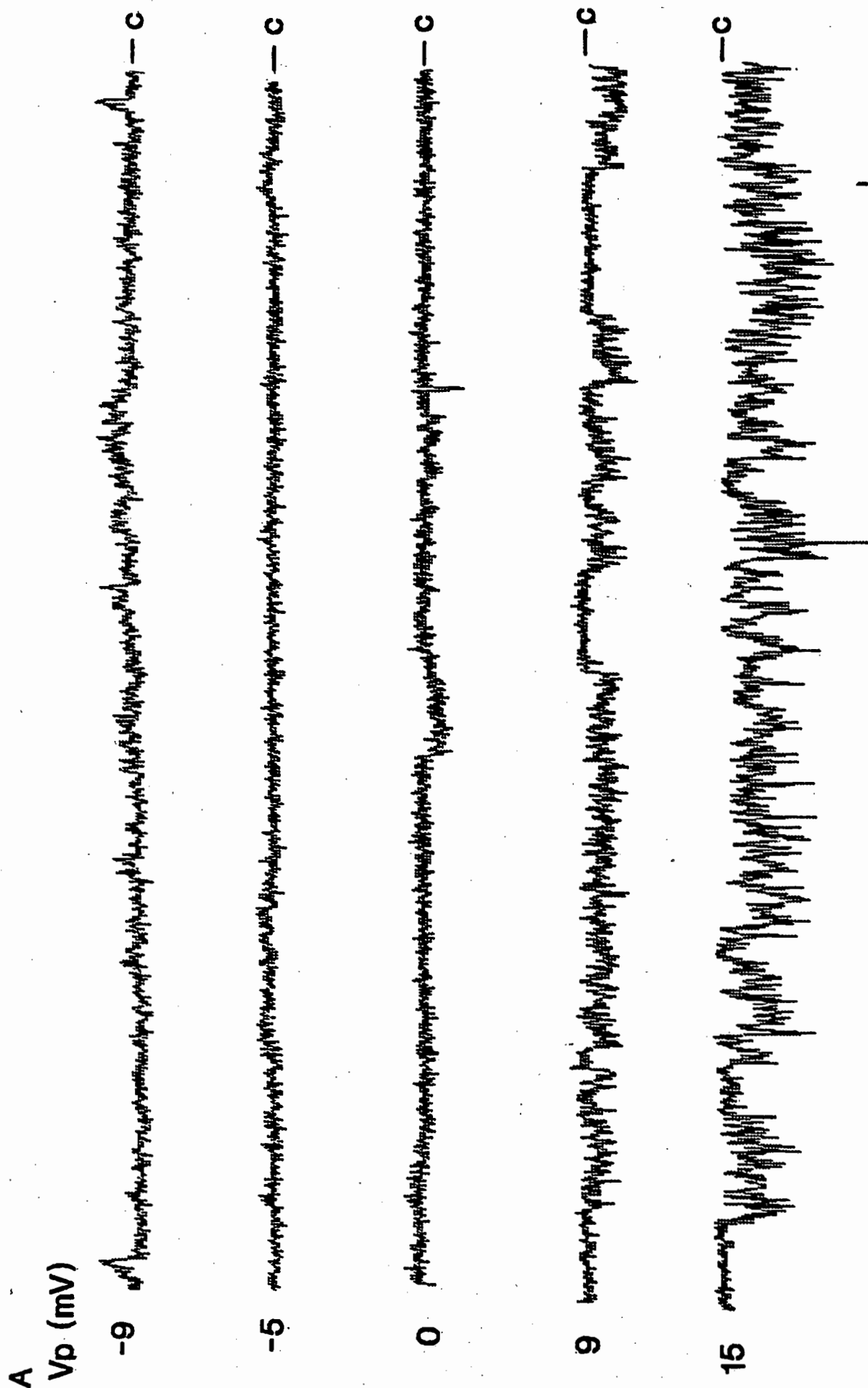
Fig. 4.3.1.A depicts a recording from an inside-out patch of the basolateral membrane of a human proximal tubule, held at a number of different clamp voltages. Qualitatively, the data were similar to the rabbit tubule data, in that the frequency of channel events as well as the mean open time was observed to increase as the voltage departed from the reversal potential (close to zero in every case); the three temporal patterns of channel behaviour seen in rabbit tubules were also a common feature of channel recordings here (the channel activity in the recording in Fig. 4.3.1. A shows predominantly "burst" activity, however.) The slope conductance of this channel as calculated by regression analysis of the current-voltage plot for "small squares" (Fig. 4.3.1.B) was 25 pS. The channel was also voltage-sensitive, the fractional open-time of the channel increasing with displacement of the clamp voltage from the reversal potential (Fig. 4.3.1.C). The open- and closed-time histograms for the recording in A at a voltage clamp of 9 mV are depicted in Fig. 4.3.1.D. Both histograms could be described by two exponentials. The rate constants were 1.53 and .278 for the open-time histogram, and .304 and .045 for the closed-time histogram. The mean open time was 3.5 ms and the mean closed time was 9.4 ms. The amplitude histogram (for all three modes of channel behaviour), as generated from the entire 9 mV recording in A (Fig. 4.3.1.E) revealed an exponential decay for the amplitudes. The mean unit current amplitudes (in the range of tenths of pico-amperes) of the "bursts" was significantly different ( $p < 0.05$ ) to those of "squares". The data obtained from human tubules are summarised in Tables 4.3.1, 2 and 3.

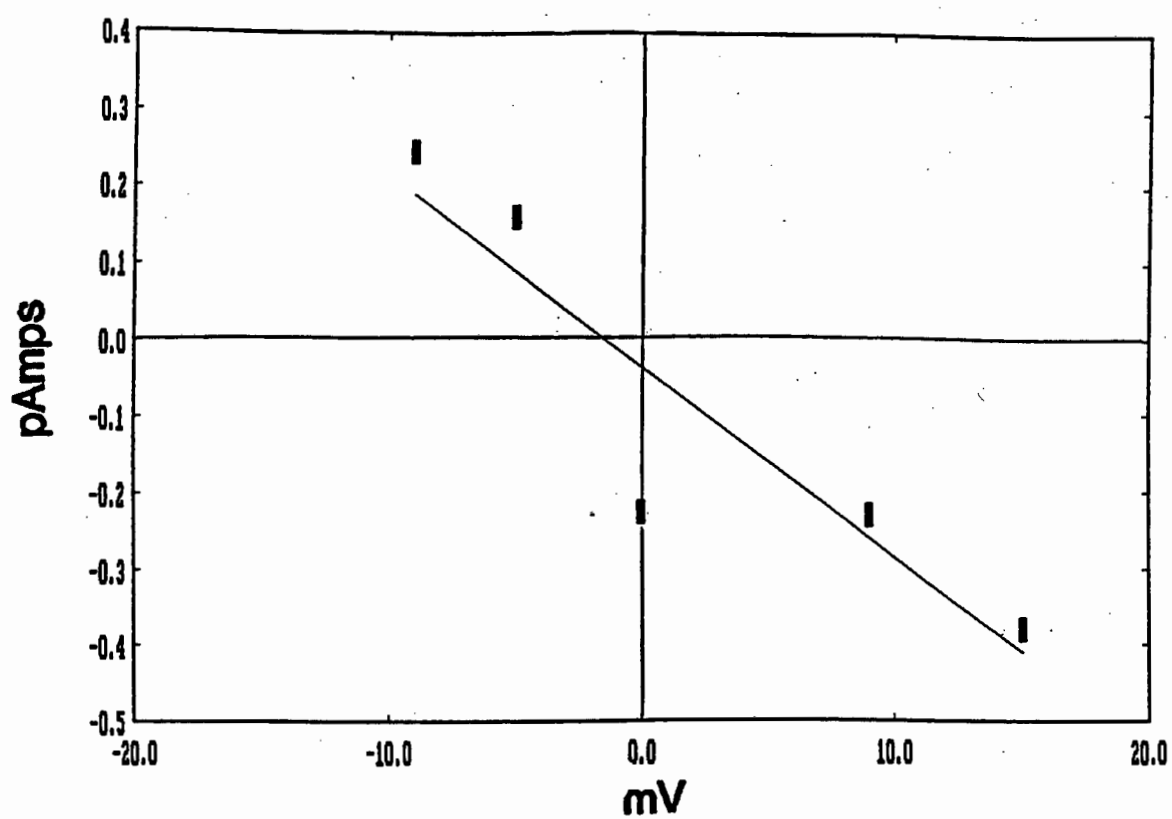
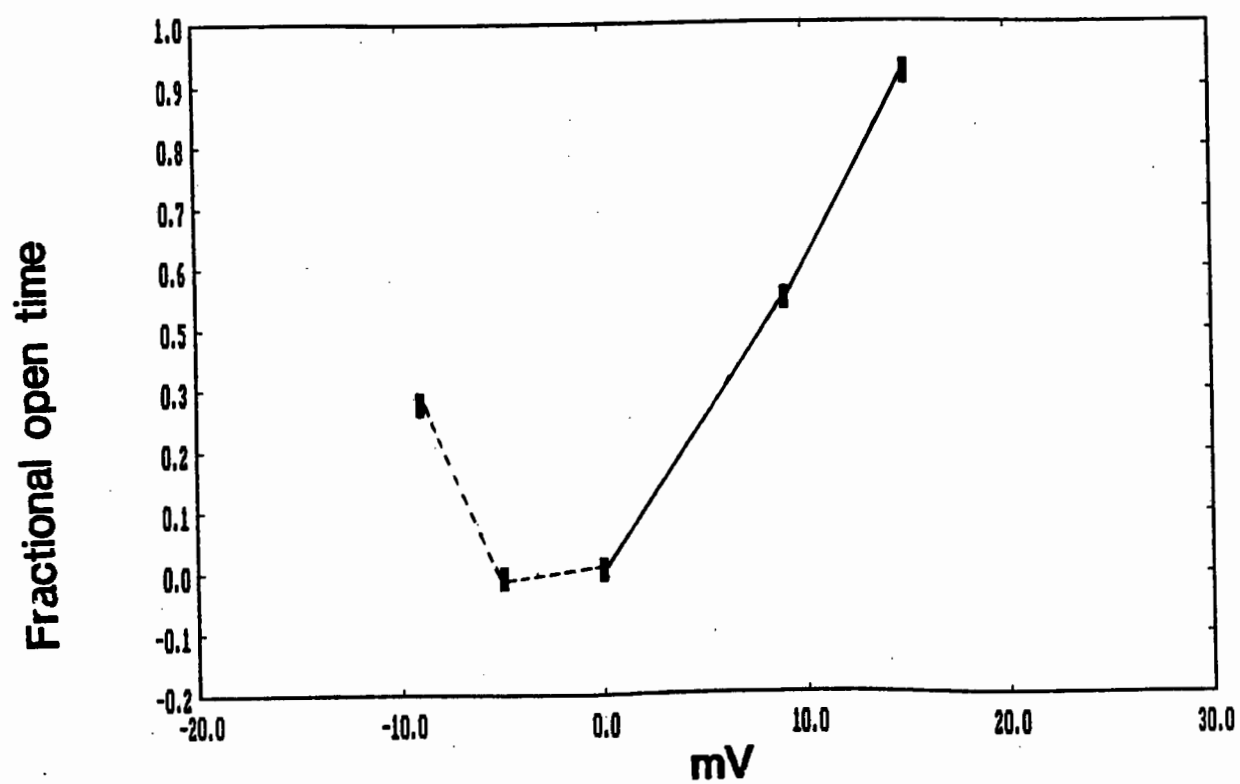
In as far as specimen availability allowed, the effects of the Ca

channel agonist, Bay K-8644 (n=1) and the Ca channel antagonist, nifedipene (n=2) were explored in a few experiments. The results are summarised in Table 4.3.3. At all voltages in which channel activity existed before drug addition, channel activity was completely abolished by the addition of both Bay K-8644 and nifedipene at concentrations of 100  $\mu$ M. Fig. 4.3.2 shows an example of a recording from the basolateral membrane of a proximal tubule held at a number of clamp potentials in both the cell-attached and inside-out configurations. The channel became noticeably more active in the inside-out mode, but activity was completely abolished by the addition of nifedipene (100  $\mu$ M). In another example of a recording in the cell-excised mode, also from the basolateral membrane of a proximal tubule (Fig. 4.3.3), the addition of Bay K-8644 (100  $\mu$ M) completely abolished channel activity previously observed at 10 mV. As this response was unanticipated, nifedipene (100  $\mu$ M) was then added to test for possible opposite effects of the drugs. The channel, however remained irreversibly blocked, even when held at a number of different voltage clamp levels.

In one case, a successful patch clamp experiment was performed on the apical membrane of a human tubule segment. The segment, which was convoluted and appeared to have a glomerulus attached to it, may have been a DCT. Patch recordings from this segment are shown in Fig. 4.3.4. The patch was held at a clamp voltage of 0 mV; the recordings reveal the existence of three distinct current levels, probably corresponding to three similar channels on the patch.

**Figure 4.3.1.** **A**, recordings from an inside-out patch of the basolateral membrane of a human proximal tubule, clamped at varying voltages. Channel activity was similar to data obtained from rabbit tubule apical membranes. The amplitude, frequency of channel events and the fractional open time increased as the clamp voltage departed from the reversal potential  $\pm(-5$  mV). **B**, current-voltage relationship for the recordings in **A**, as determined from analysis of "small squares". The slope conductance was 25 pS, and the reversal potential was -1.4 mV. **C**, plot of the fractional open time plotted against voltage. **D**, open- and closed-time histograms for the same patch in **A** clamped at 9 mV. Both histograms could be described by 2 exponentials. **E**, amplitude histogram for the same patch recording clamped at 9 mV ( $n=2559$ ). Most of the events were of small amplitude; the number of events fell exponentially at larger amplitudes. The threshold for detection of channel events was set at 0.25 pA.



**B****C**



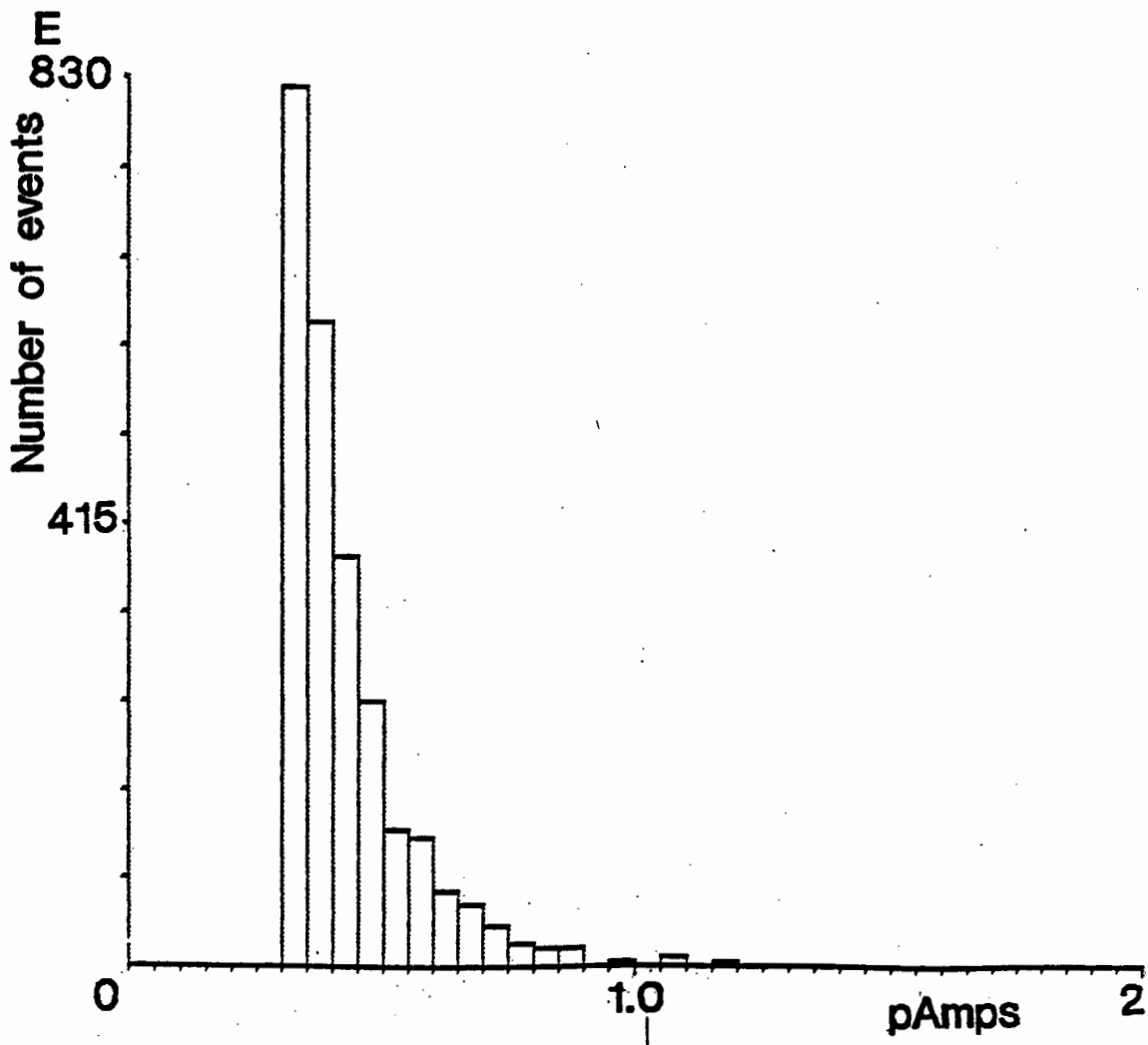
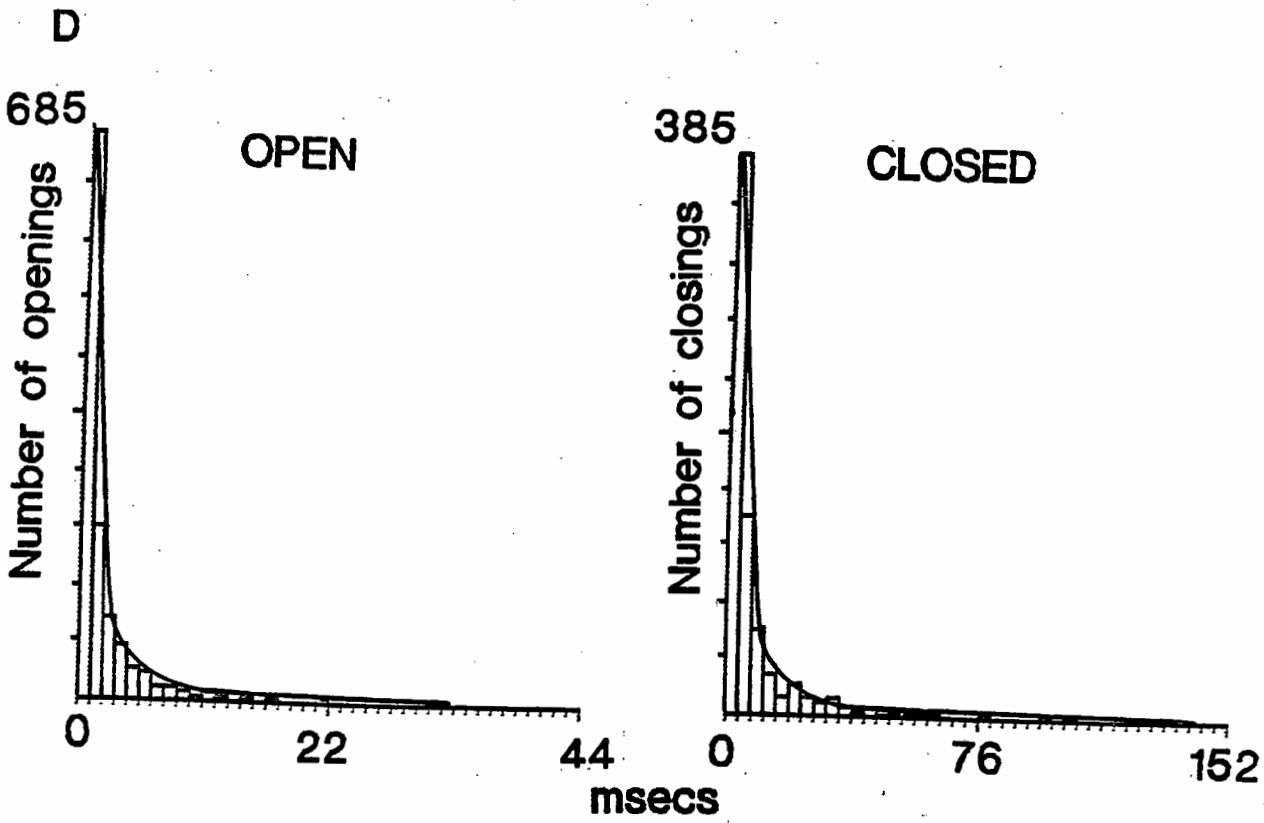
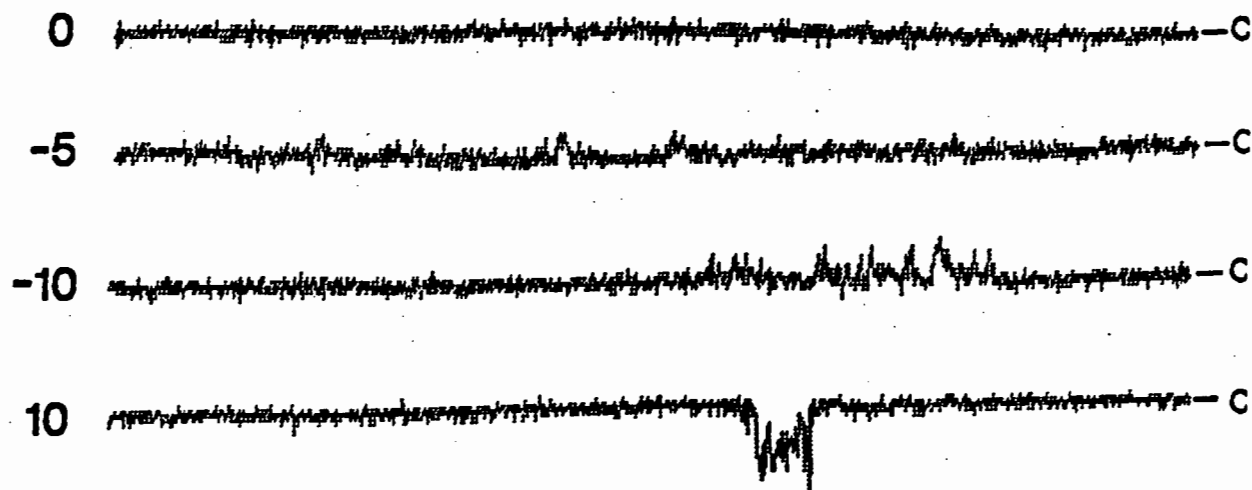


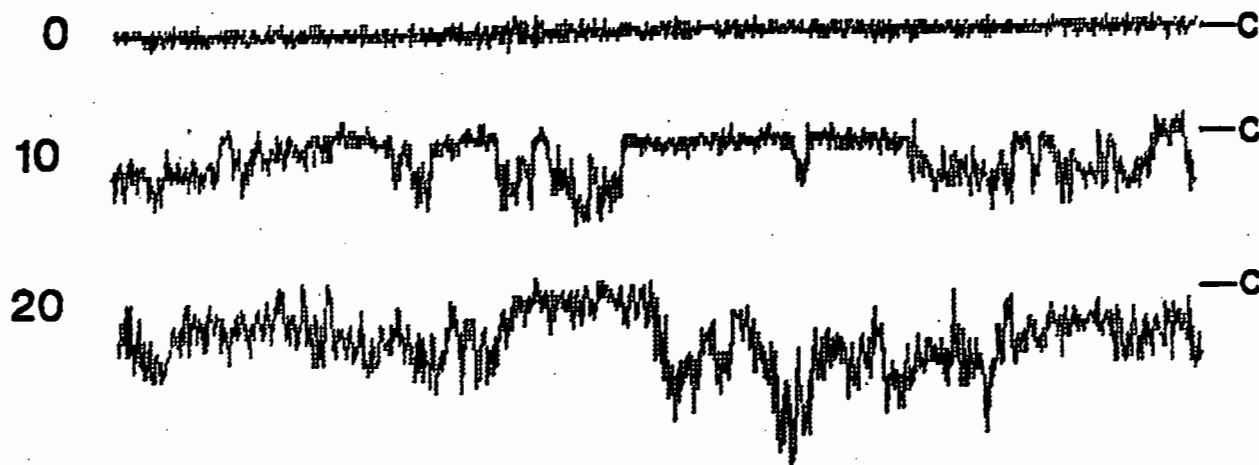
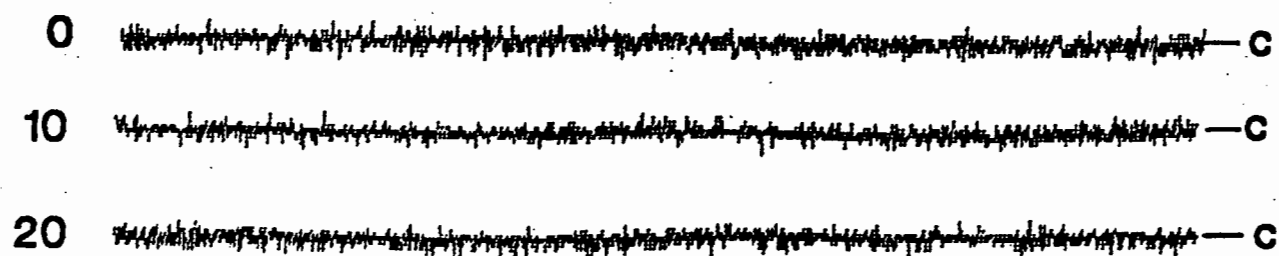
**Figure 4.3.2.** Channel recordings from the basolateral membrane of a human proximal tubule. The patch was clamped at a number of voltages both in the cell-attached mode and in the inside-out mode. When the patch was exposed to a bathing solution containing 100  $\mu$ M nifedipene, all channel activity was abolished.

Vp (mV)

CELL-ATTACHED



CELL-EXCISED

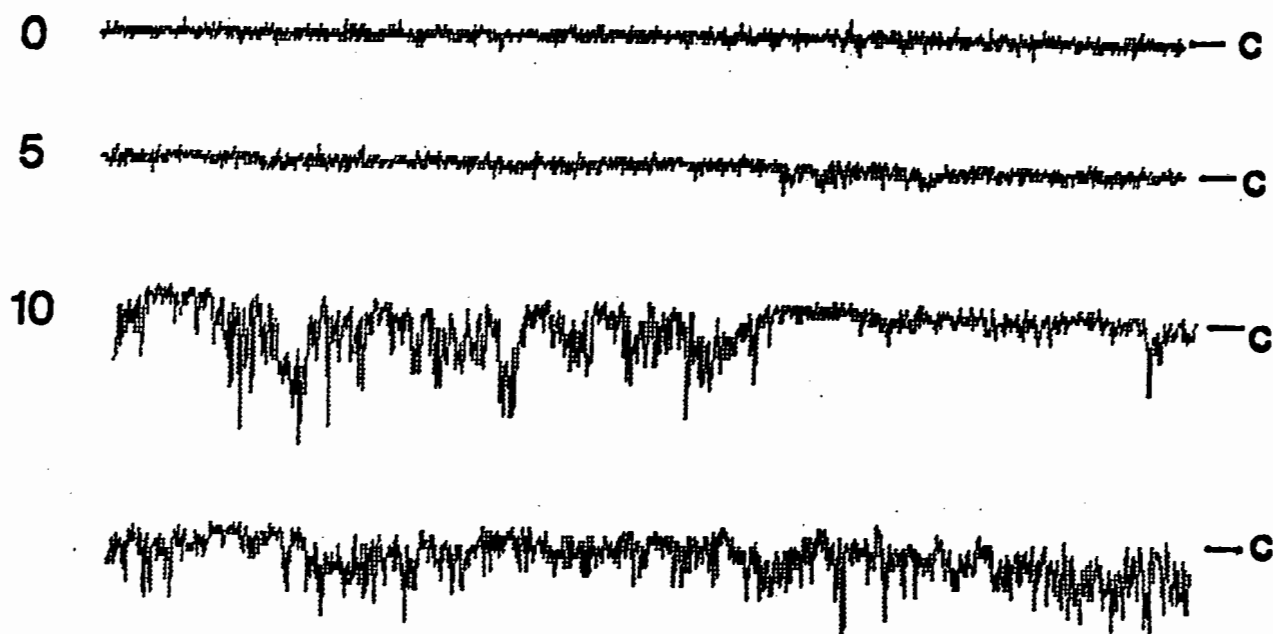
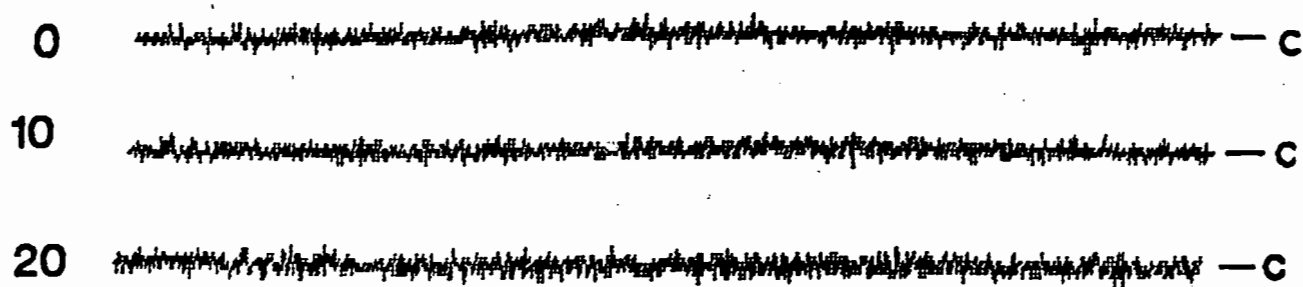
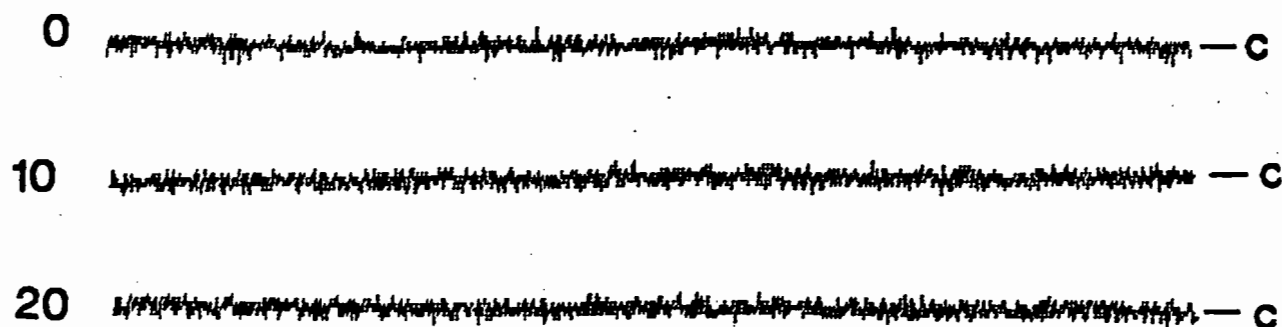
+ NIFEDIPENE (100  $\mu$ M)

1 pA  
0.2 sec

**Figure 4.3.3.** Channel recordings from the basolateral membrane of a human proximal tubule. The patch was clamped at a number of voltages in the inside-out configuration. Addition of Bay K-8644 (100  $\mu$ M) irreversibly blocked the channel. Addition of nifedipene thereafter had no further effect on channel activity.

Vp (mV)

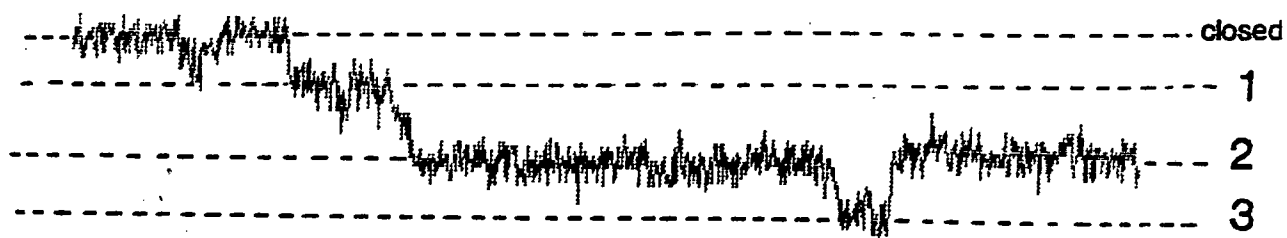
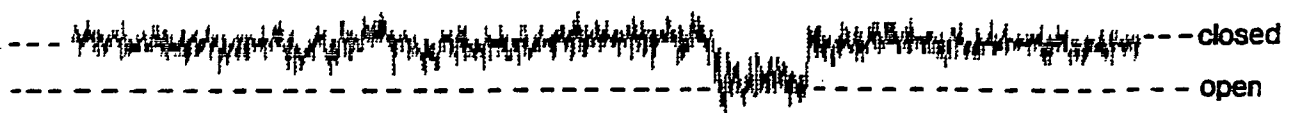
CELL-EXCISED

+BAY K-8644 (100  $\mu$ M)+ NIFEDIPENE (100  $\mu$ M)

1 pA

0.2 sec

**Figure 4.3.4.** Patch recordings from the apical membrane of a human tubule segment. All three traces are examples of the same recording made in the cell-excised mode, while the patch was held at a clamp voltage of 0 mV. Three distinct current levels denote the possible existence of three similar channels on the patch.



1 pA  
0.1 sec

**TABLE 4.3.1.** Comparison of mean unit amplitudes as determined for "burst analysis" and "square analysis" for human tubule segments, using the unpaired t-test.

Tubule	Voltage range	Mean unit amplitude (pA±s.d.)		df.	p
		Bursts	Squares		
PCT	-ve	.169±.013	.21±.042	9	s.
	+ve	-.19±.026	-.22±.018	24	s.

**TABLE 4.3.2.** Comparison of channel conductances as determined for "burst analysis" and "square analysis" for human tubule segments, using the unpaired t-test.

Tubule	No. patch records	No. voltage clamp records	Mean conductance (pS±s.d.)		p	Mean reversal PD (mV±s.d.)
			Burst	Squares		Squares
Proximal	21	8	22.6±17.7	27±7.6	n.s.	.25±1.1

**TABLE 4.3.3.** Human tubule response to agonists and antagonists

Tubule segment	No.	Drug	mV	Fractional open time BEFORE	Fractional open time AFTER	Channel response Increased activity I Decreased activity D No change N
Proximal	1	Bay K-8644	0	0	0	N
			10	.393	0	D
	2	Nifedipene	0	0	0	N
			10	-.35	0	D
			20	.385	0	D
			30	.07	0	D
	3	Nifedipene	0	0	0	N
			10	-.393	0	D



#### 4.4. Emergence of unexpected channel varieties in this study

The overall aim of this study was to locate Ca-permeable channels in the different tubule segments studied. During the investigation, however, channel events were recorded that did not conform to the characteristics thus far described. Some of these channels were discovered while experimenting with pipette or bath solutions of different ionic composition; others were discovered by chance while seeking Ca-permeable channels.

A summary of the other channel varieties found in this study is presented in Table 4.4.1. In the apical membrane of rabbit DCT, two high conductance channels were observed (79 and 108 pS; see Fig. 4.4.1.A). The pipette solution used in these experiments was a KCl Ringer solution. The reversal potentials were 5 mV and 4 mV respectively, suggesting non-selective channels. In the apical membrane of rabbit CCDs, two low conductance channels were observed. One of these channels was observed in the inside-out configuration with KCl Ringer in the bath, and  $\text{CaCl}_2$  in the pipette; the other was recorded in the cell-attached configuration while searching for Ca channels. The reversal potentials for these channels were 13.4 and 54 respectively. A similar low-conductance channel (5 pS) was observed in the basolateral membrane of a human proximal tubule (Fig. 4.4.2.). Fig. 4.4.1.A is an example of a recording from one of the non-selective high conductance channels in the inside-out patch of a DCT. The pipette solution, the composition of which is described in the methods, contained a high concentration of KCl (140 mM). The channel was "square" in profile and the current-voltage relationship (Fig. 4.4.1.D) revealed a slope conductance of 108 pS and a reversal potential of 4 mV. The squares were not interspersed with "bursts" or flickering. These values suggest a high- conductance non-selective channel in this segment.

Fig. 4.4.1.B is an example of a low conductance channel recorded from rabbit CCD in the cell-attached configuration, held at different clamp potentials. The I-V plot for this channel yielded a value for slope conductance of 4 pS and a reversal potential of 54 mV. These values suggest a low conductance K channel.

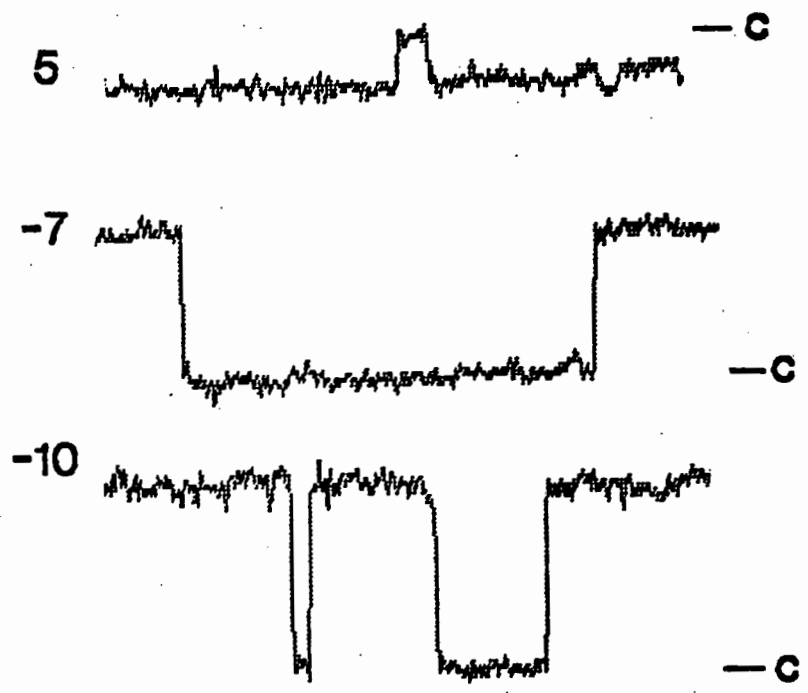
Fig. 4.4.1.C depicts a channel recording from the apical membrane of rabbit proximal tubule clamped at zero mV. The pipette contained KCl (143 mM). The channel event had a "square" shape and there were at least two channels on the patch. It was not possible, however to determine the conductance or selectivity of the channel as the patch did not last long enough to be exposed to more than one voltage.

Fig. 4.4.2 depicts a channel recording from the basolateral membrane of a human proximal tubule in the cell-attached configuration, held at different clamp potentials. The recording shows "square" current events and there were at least two channels on the patch. The conductance of the channel was 5 pS, and the reversal potential was 47.8 mV (the current-voltage relationship is not shown). It was interesting to note that at 15 mV clamp potential, a third channel became active. The identity of this channel was not explored, but the "bursts" of activity observed were similar in appearance to those described in chapter one of this section (and shown in Fig. 4.3.1).

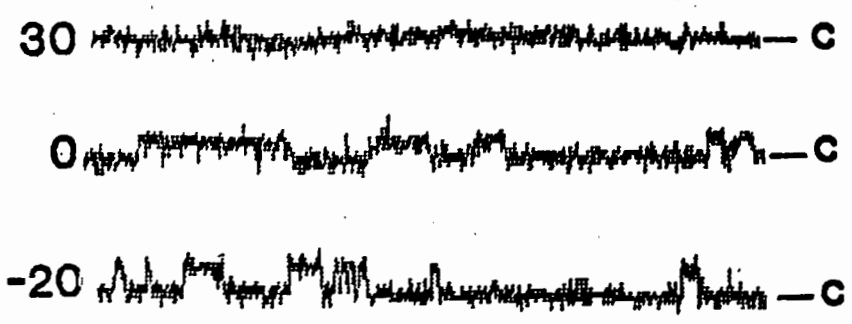


**Figure 4.4.1.** Other channel varieties detected during the investigation. **A**, a high conductance channel recorded from the apical membrane of a DCT patch with characteristically "square" openings. The channel activity was recorded in the inside-out mode and the pipette solution contained KCl (143 mM). The current-voltage relationship for this channel (D) yielded a slope conductance of 108 pS, and a reversal potential close to 4 mV. **B**, A low conductance K channel recorded in the cell-attached configuration from the apical membrane of a rabbit CCD. The patch pipette contained  $\text{CaCl}_2$  (70 mM) and the bath contained NaCl (140 mM). The current-voltage relationship for this channel (E), yielded a slope conductance of 4 pS, and a reversal potential of 54 mV. **C**, channel recording from the apical membrane of rabbit proximal tubule. The recording was made in the inside-out configuration and the pipette contained KCl (140 mM). The recording was made at 0 mV only and it was thus impossible to construct an I-V plot. It is clear however, that there was more than one channel on the patch. **D and E**, current voltage relationships for the recordings in A and B respectively.

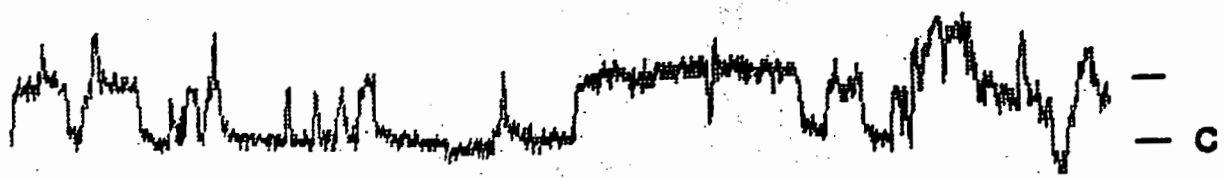
A



B

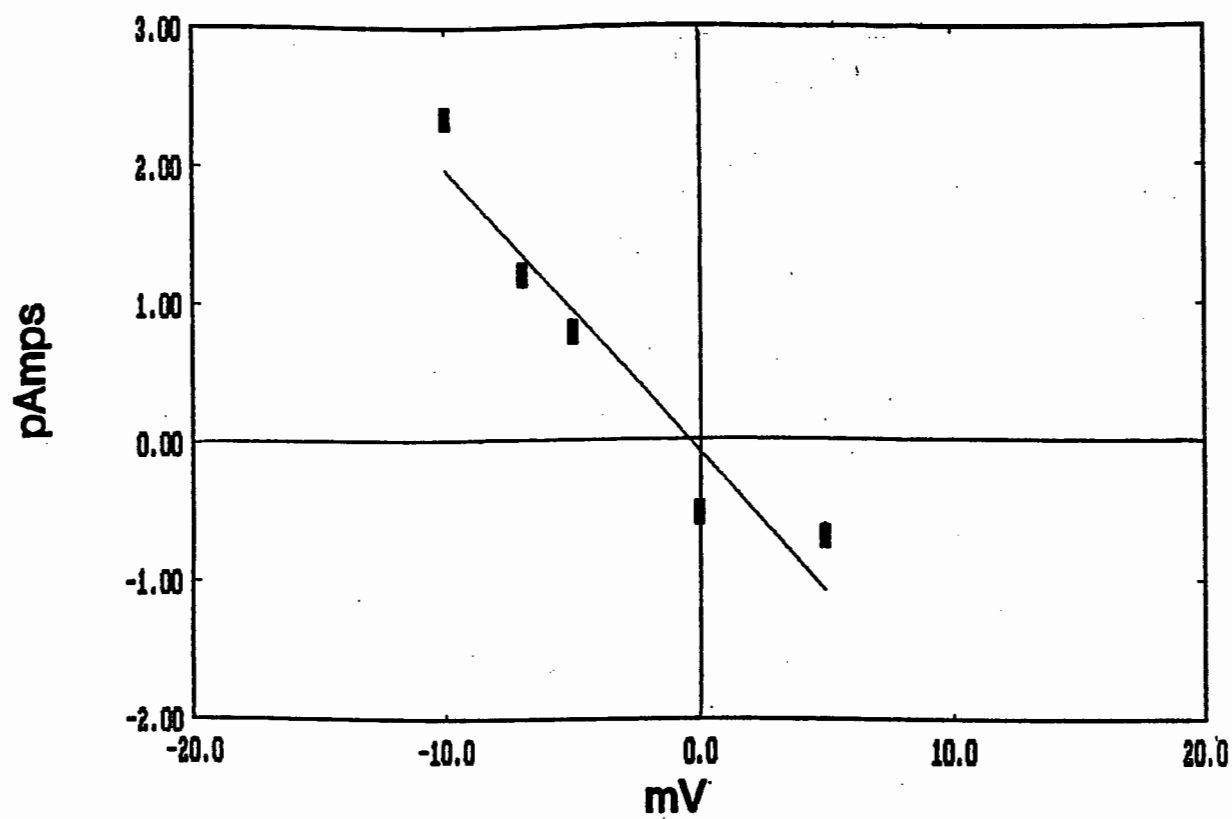


C



1 pA |  
0.2 sec

D



E

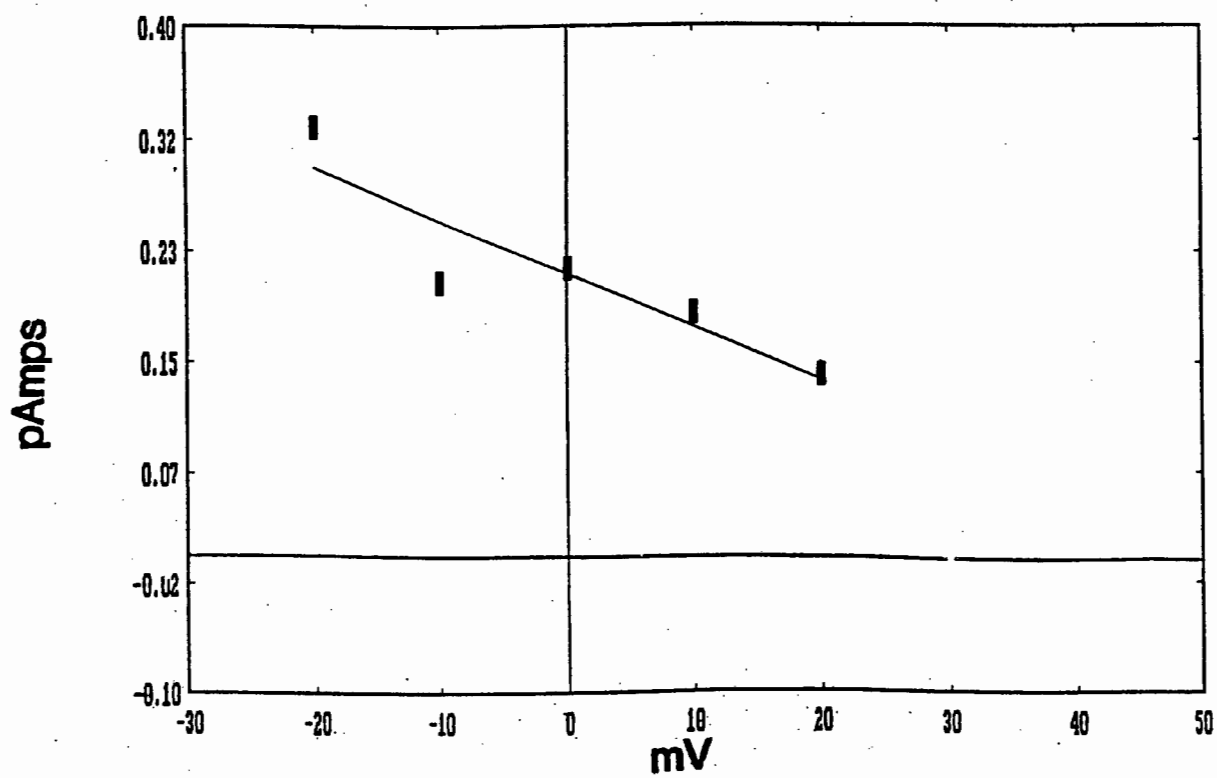
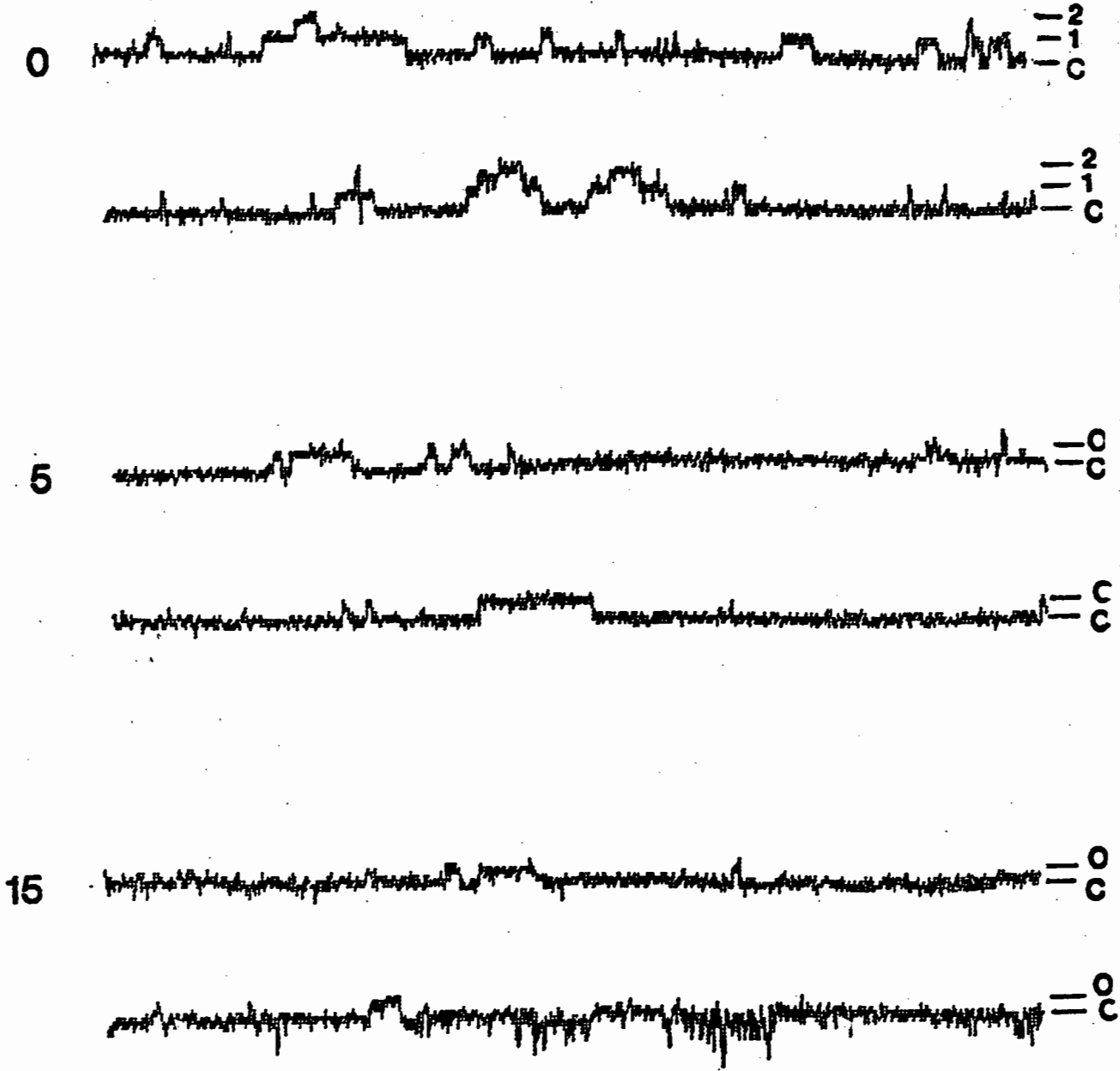


**Figure 4.4.2.** Channel recording from the basolateral membrane of a human proximal tubule. The recording was made in the cell-attached configuration. The pipette contained  $\text{CaCl}_2$  (70 mM) and the bath contained NaCl (140 mM). The channel had a slope conductance of 5 pS and a reversal potential of 47.8 mV (I-V relationship not shown). The channel was probably selective for K ions and there were at least two channels on this patch.

Vp (mV)

CELL-ATTACHED



1 pA |  
0.2 sec



**SECTION FIVE**

**DISCUSSION**

## SECTION FIVE

### DISCUSSION

#### 5.1. DISCUSSION OF METHODS

##### 5.1.1. Tissue preparation

About 10% of all rabbit kidneys dissected were diseased, and were thus very difficult to dissect. However, once tubule segments were successfully dissected out, the condition of the kidney did not appear to play any role in determining the success rate of seal formation. On average, the younger rabbits (of about 1 kg body weight) appeared to have healthier kidneys than the older ones, and so the younger specimens were generally used. In early experiments, a heating device consisting of an insulated wire filament, was included in the patch chamber to enable experiments to be performed at 37°C. However this setup was found to introduce much unwanted noise in the patch recordings, and was later abandoned. Thus, the majority of experiments were carried out at room temperature. Although it could be argued that such experiments do not represent true physiological conditions, experiments performed at room temperature have been common practice amongst a number of research groups (Marunaka and Eaton, 1990; Koeppen *et al*, 1984; Palmer and Frindt, 1988; Parent *et al*, 1988).

Identification of tubule segments was not always definitive at least in the case of the TALs and PSTs. The TALs and PSTs are not dissimilar in morphology, making it difficult to distinguish between the two, unless their origins and/or terminations are noted during dissection. The DCTs are very similar to the PCTs in morphology. The criterion used for the identification of a DCT, was that it should either be connected to a glomerulus at the point of connection to the TAL, or that the transition between the connecting tubule and CCD was clear, i.e, a clear transition between a convoluted segment and a segment having the morphology of a CCD (see Fig. 5.1.A and B).

The preferred choice of techniques used to expose the luminal membrane was the ripped tubule technique. The advantage of the technique was that it could be done in a relatively short time, allowing more time for actual experimentation. This was found to be important as most tubule segments did not appear to remain alive for longer than about two hours after dissection. The formation of long-lasting tight seals was virtually impossible on dead or degenerating tissue. A precaution that had to be taken when using this technique was that the broken patch electrodes be filled

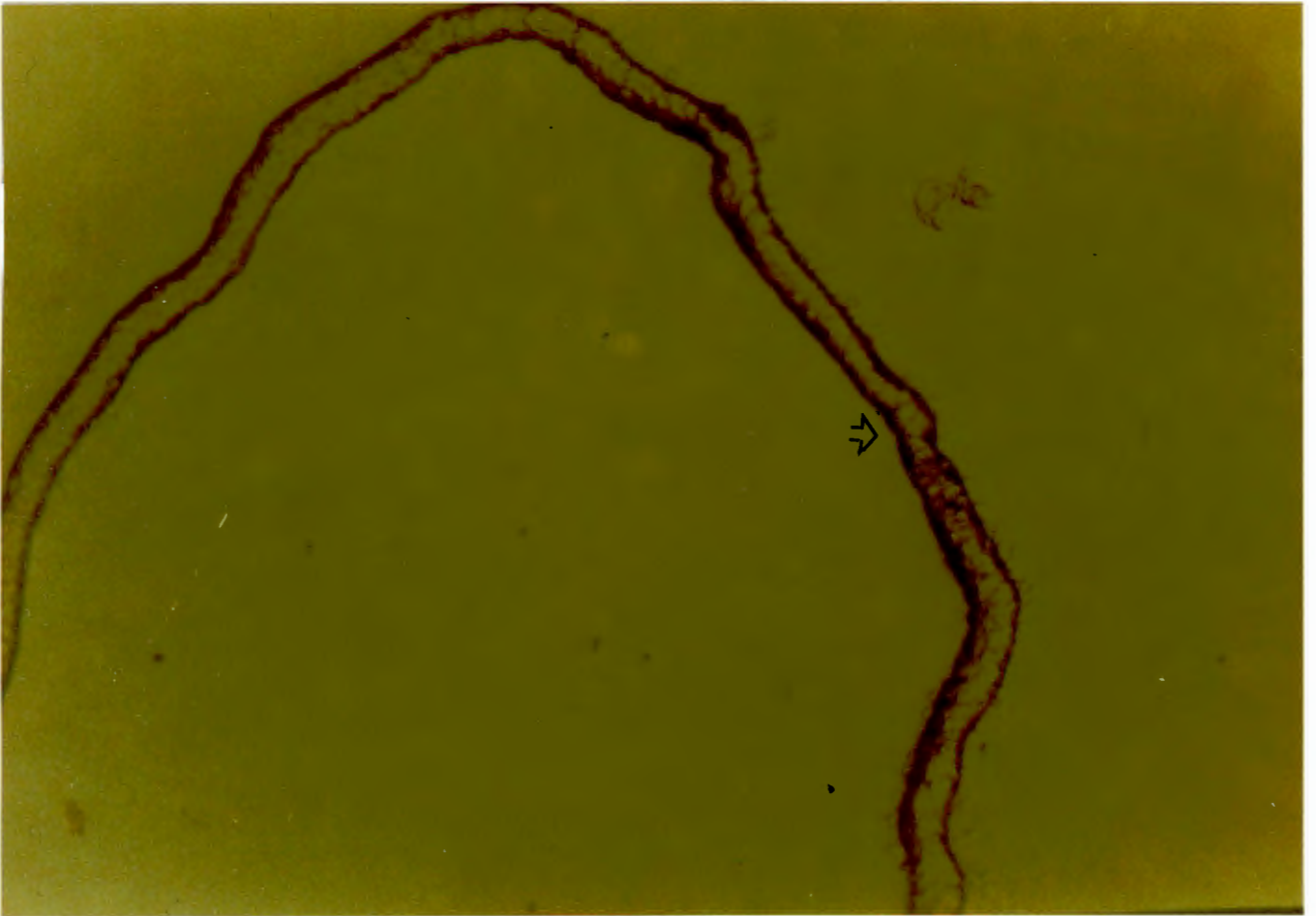


**Figure 5.1. A,** photograph of a DCT (magnification = 60 times). Note the transition between the connecting tubule and the CCD (shown by the arrow).

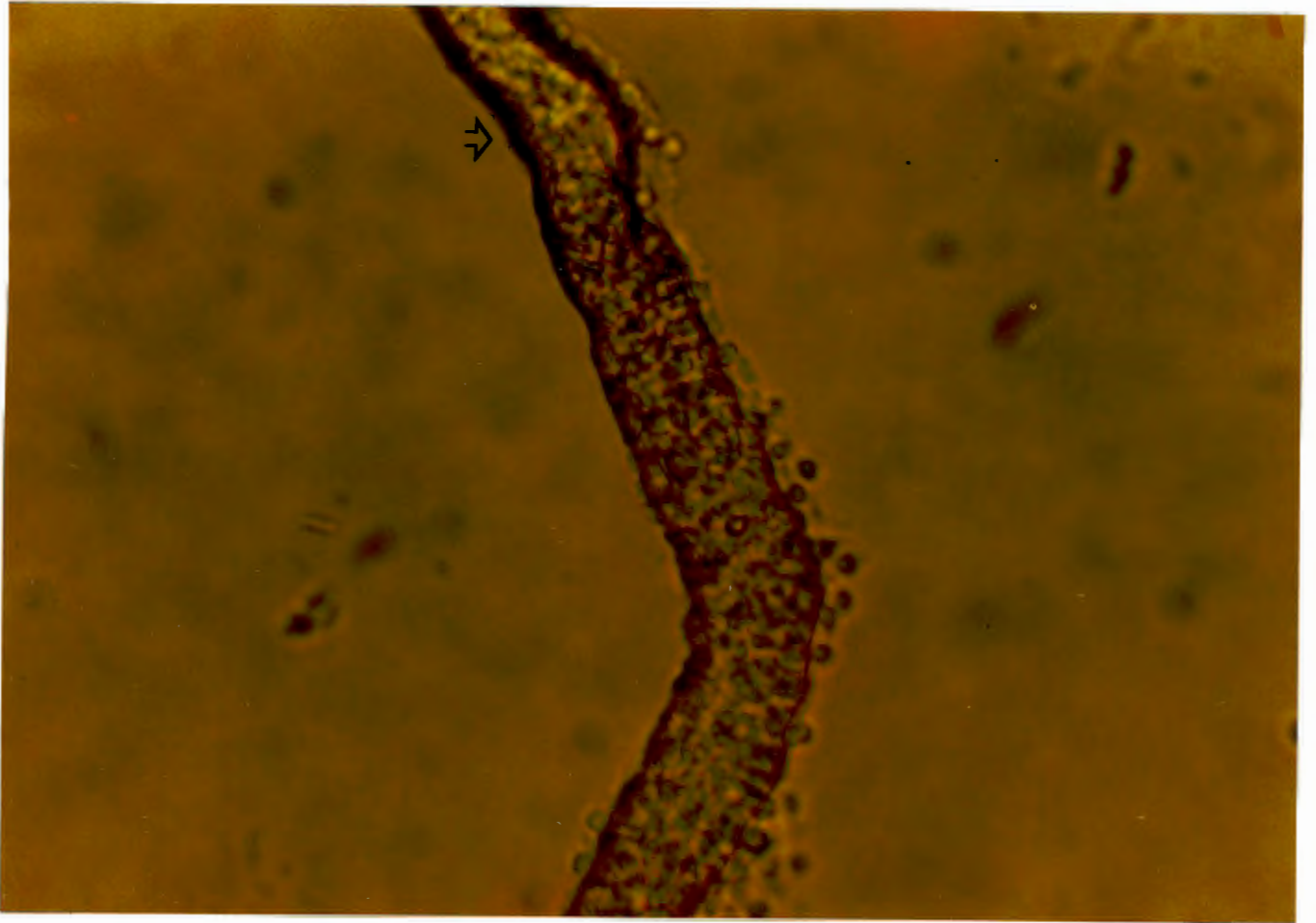


**Figure 5.1. B**, photograph of a small segment of the tubule in A in the region of the arrow (magnification = 150 times), showing more clearly the transition between connecting tubule and CCD.

with solution, prior to dissection. This was to prevent the tubules from being sucked into the broken pipettes by capillary action. Also, a frustrating aspect was that manipulation of the tubule segment with the patch electrodes usually resulted in the tubule breaking into a number of pieces, rather than being neatly torn open.

The isolated perfused tubule technique, on the other hand, was found to be technically laborious and time consuming. Also, a difficulty with this technique was that once an experiment was set up, the tubule orifice was nearly always orientated towards the bottom of the bath chamber. In this position, the patch electrode could not gain access to the lumen of the tubule. This problem was solved by placing a small piece of concave glass at the bottom of the dish (see photograph in Fig. 3.1. of the methods). The orifice of the holding pipette containing the tubule was then lowered to below the level of the glass, resulting in a reorientation of the tubule such that the orifice was accessible to the patch electrode. In both techniques, addition of collagenase (0.2g/l) to the perfusion fluid (in isolated perfused tubule experiments) or bathing fluid (in ripped tubule experiments) seemed to make no difference to the success rate of tight seal formation.

Human kidney biopsy samples were obtained on an irregular basis from the hospital. When these samples were placed in a dissecting dish, it was found that a number of tubule segments with no basement membrane, appeared, apparently spontaneously, in the bath, following minimal dissection. The photograph in Fig. 5.2. shows an example of such a segment as compared to a segment with the basement membrane intact. This feature was found to be extremely useful, as no further dissection was necessary on such tubules, and the basal membrane was thus directly accessed by the patch electrode. The reason for the absence of basement membrane on such segments was not discovered. They were, however, very friable, broke apart easily, and appeared to be tubular casts. All-in-all, they were reminiscent of the basement-membrane-free Malpighian tubules obtained by the "squeeze technique" (Nicolson et al, 1991), which are similarly patch-able on their basolateral aspect. It seems likely that the hypoxia attendant upon the half-hour delay between obtaining the biopsy sample in the hospital, and its arrival in the laboratory, plays some part in their production. Originally it was hoped that the apical membrane could be accessed, so that data

could be compared with rabbit tubule segments. Since the tubule segments were so short, however, this was extremely difficult using the available techniques, and thus only one experiment was successfully performed on the apical membrane. Another problem with segments dissected from biopsy samples was that it was almost impossible to make an accurate identification of the type of tubule segment under investigation.

However, since most segments had one or two slight convolutions, and since they were clearly not collecting ducts, it was assumed that the segments were probably from the proximal convoluted tubule.

### **5.1.2. Application of the patch clamp technique**

Attainment of a tight seal on the apical membrane of freshly dissected tubules was found to be a difficult and laborious procedure. Consequently the project remained exploratory in nature, i.e., the low success rate never allowed an in-depth investigation into any particular field or aspect of this research. Of the few tight seals that were formed, only a small percentage lasted long enough for recordings to be made, most lasting only a few seconds. The reason for this difficulty never became apparent. Some tubules appeared to be covered with a sticky mucous-like substance which attached in strands to the pipette tip when it was withdrawn. It is also possible that the microvilli on the apical surface of proximal segments provided an obstacle to seal formation, although Gogelein and Greger (1984) have suggested that this is not a reason for poor seal formation.

Many subtle variations in the fabrication of the patch pipettes were attempted to try to increase the success rate of seal formation. For example, some patch pipettes were constructed using borosilicate glassware; pipette tip diameters were varied; pipettes were firepolished for different time periods. All these variations made no difference on the success rate of seal formation, which remained exasperatingly low.

A source of irritation was the Ag/AgCl wire forming the electrode within the pipette. It was found that this had to be rechlorided before each experiment, as repeated insertion of the patch pipettes into the electrode holder scraped some of the AgCl off the wire. This resulted in a continually fluctuating pipette potential which was not conducive to seal formation. Another source of irritation was the sensitivity of the electrode tip to even the slightest vibrations. In spite of the baseplate being cushioned on squash balls, doors closing or brisk walking in the nearby passage were enough to cause considerable vibration of the pipette tip. If this occurred at a crucial moment, a seal in the process of forming might



be lost.

During an attempt at forming a tight seal, it was found that the longer the suction was applied, the greater was the chance of seal formation. Sometimes a maintained suction of up to 5 minutes was necessary for a gigaseal to form. Generally, data was not recorded from patches having seal resistances of below about 5 G $\Omega$ . A significant improvement in seal formation occurred when a positive pressure was applied through the patch pipette as the pipette was lowered onto the cell. This possibly kept the tip free of any debris on its path towards the cell.

Finally, since the aim of the project was simply to establish the existence of Ca-permeable channels, recordings were made primarily in the inside-out patch configuration. A few recordings were made in the cell-attached configuration, however the scope of the project did not include a comparative study of the two modes.

### 5.1.3. Solutions and drugs

The composition of the solution within the patch pipette was dictated not only by the need for a charge carrier capable of permeating Ca channels, but also by the need to block other channels that might exist on the apical membrane (Light *et al*, 1988). Initially, BaCl<sub>2</sub> was included in the pipette solution as Ba is both a charge carrier through Ca channels and, at positive insertion voltages, a K channel blocker (Miller 1987). Later, however, it was felt that a CaCl<sub>2</sub> pipette solution would be a more reliable indicator of Ca channel activity. Amiloride was also added to the patch electrode to block any Na channels on the patch. The bathing solution did not contain sulphates or phosphates. This was important as BaCl<sub>2</sub> precipitated with such compounds, completely blocking the pipette tip. The bath Ringer contained glucose, and Na acetate, and in later experiments, alanine (5 mM) was also added (Weinberg *et al*, 1990). These were added in a bid to maintain the tubule integrity for as long as possible. The depth of the bath solution was kept as low as possible, as this minimised the noise level of recordings. In some experiments, the Ringer was diluted with isosmotic mannitol to test for chloride permeability ("half NaCl Ringers"). The rationale behind the use of this solution was to create

a chloride gradient, so that any shift in the reversal potential of the experiment would indicate whether the channel was predominantly permeable to Ca ions or Cl ions.

The technique of exposing the patch to solutions of different ionic composition and solutions containing drugs started off as a virtually impossible endeavour before the "plastic sleeve" method and, later, the "hanging drop" technique were employed. Initially, the patch was moved through the air-water interface to the alternate solution. However, the length of time that the patch was exposed to the air nearly always resulted in the breakdown of the tight seal before the alternate solution was even reached. This problem was partially resolved by dividing the main bath solution into two parts with a strip of Sylgard (Dow-Corning). This lessened the distance between the two bath solutions, and thus the time exposed to air. However, this was still not adequate to ensure the survival of the tight seal. In order to avoid exposure of the patch to the air, a technique was attempted which involved aspirating the bath solution from the patch chamber while simultaneously refilling it with the alternate solution. In our experiments this technique was not found to be feasible as aspiration of the solution from the bath resulted in simultaneous suction of the tubules from the bath.

A significant breakthrough in this technology came with the advent of the "plastic sleeve" method which enabled a patch solution change to take place without exposure of the patch to air. The procedure followed was, in essence, similar to that devised by Quartararo and Barry (1987). The technique resulted in a greater number of successful solution changes, but still had a few distinct disadvantages. One of these was that the plastic sleeve was manipulated with a pair of forceps during recording. This introduced a sudden very large noise component which was often enough to cause seal breakdown. This problem was later rectified, however, by constructing a syringe attachment to the sleeve; the sleeve could then be remotely controlled simply by expelling or aspirating air through a second syringe. Another disadvantage with the technique was that the capillary action of the sleeve in the bath fluid drew enough fluid into the sleeve to entirely cover a large part of the electrode. This introduced a considerable noise component into the recordings; as a result, the analysis of such recordings was more difficult.

The final and most successful variation in the solution change technique was the "hanging drop" technique. The method encompassed a smooth transition from one bathing solution to the next, with minimal disruption of the patch. An initial setback in the use of this technique was that the tissue under investigation was often situated a distance away from the hanging drop. This meant that the pipette had to be extensively manipulated to line the patch directly beneath the drop. This manipulation often took a long time and was disruptive to the tight seal patch. The problem was solved simply by placing the tissue almost directly beneath the hanging drop. The pipette could then be lifted directly out of the solution and into the drop. Thus, for smooth recordings with a high signal-to-noise ratio, the best combination was to use a bathing solution at as low a level as possible, with the "hanging drop" apparatus to allow smooth solution changes.

In cases where parathyroid hormone was added to the bath, a difficulty was found in the choice of methods used to administer the hormone while the patch was in the cell-attached configuration. The idea of replacing the bath solution with one containing the hormone was rejected as the possibility of disrupting the cell-attached patch or losing the remaining tubule segments in the bath, seemed very high. The method finally adopted was therefore simply to expel a small drop of solution containing the hormone into the bath. The procedure was carried out under two assumptions: firstly that the hormone diffused rapidly and equally throughout the solution, and secondly that the process of administration of the drop containing the hormone was not sufficient to detach the patch from the cell, resulting in a cell-excised recording. Neither of these assumptions may have held true in reality.

#### **5.1.4. Data recording and storage**

We chose to sample our data recordings at a rate of 1 or 2 kHz. Computer and disc memory constraints allowed a maximum of ten or five minutes of recording for these sampling rates respectively to be stored on disc. Although there was the choice of using a higher sampling rate (4 kHz), this would only have allowed two and a half minutes of recording. Thus the sampling rate used most frequently was 1 kHz. This was dictated by the

need for long data recording periods. Finally, however, the use of the digital-audio tapedeck solved the problem of limited recording times, as up to three hours of uninterrupted data could be recorded by this machine.

A problem confronted when recording data was whether the chosen sampling rates (1 or sometimes 2 kHz) were sufficient to significantly distort the shape or amplitude of the signal, or exclude openings of very short duration. In order to determine these possible effects on the recordings, a square wave generator was connected to the recording apparatus. Signals in a range of frequencies from 40 to 400 Hz were then recorded and stored by the apparatus. Fig. 5.3. shows examples of these recordings at 40 Hz and at about 350 Hz respectively.

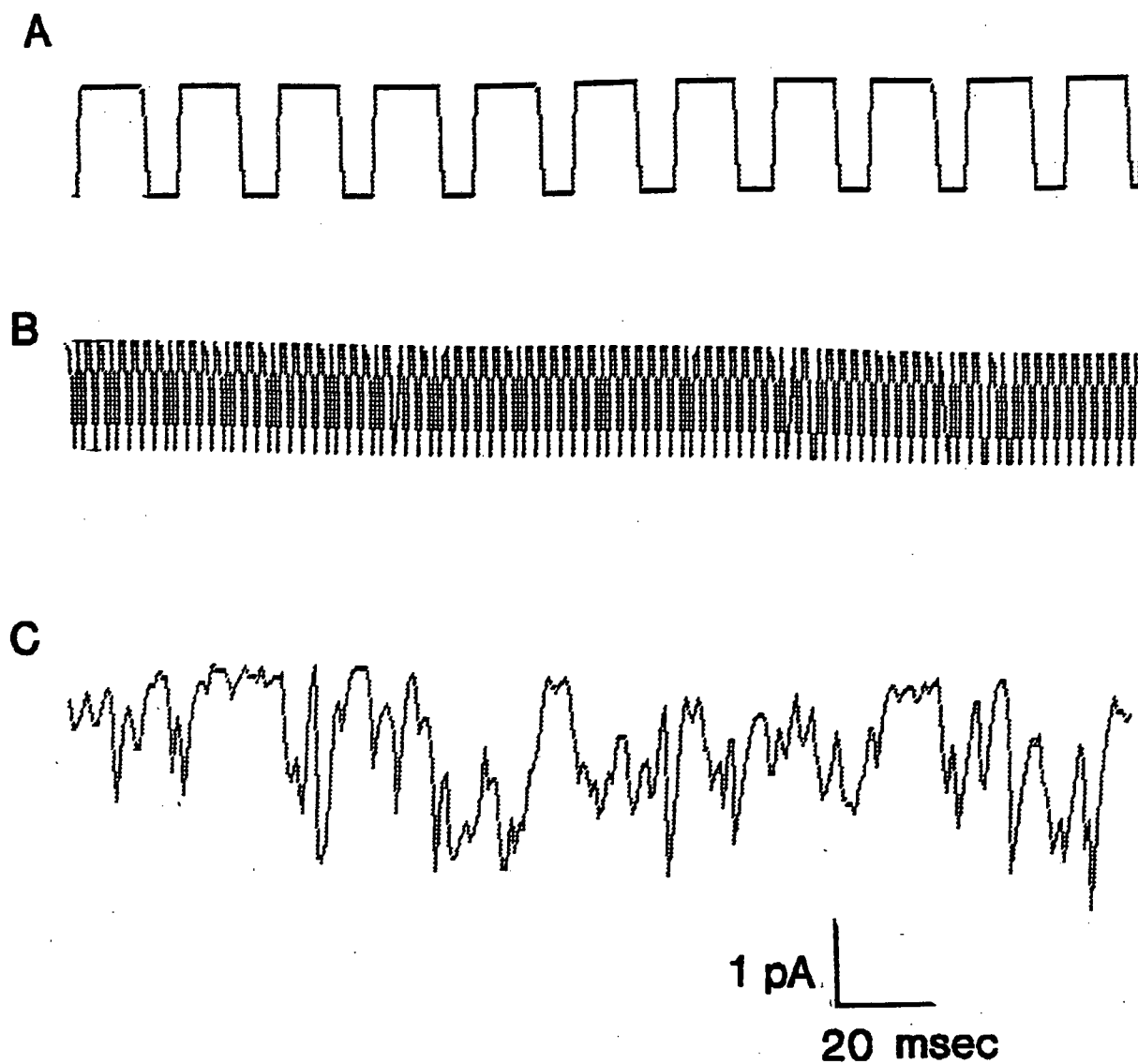


**Figure 5.3.** A, a square wave pulse recorded at a frequency of 40 Hz by the recording apparatus. B, the same square wave at a frequency of about 350 Hz. C, a typical "burst" event sampled from the recordings. The frequency of the events within the burst is clearly less than the 350 Hz signal in B.

In both recordings, the amplitude of the square pulse remained unchanged, i.e. the selected sampling rate did not attenuate the high frequency signal. Also shown (Fig. 5.3.C) is an example of a typical "burst" recording from an experiment sampled at 1 kHz. The frequency of events in this recording is clearly less than the frequency of the 350 Hz recording in B. On the basis of these experiments, it was felt that the sampling rate provided recordings that were sufficiently representative of the analog signal. In addition, McManus *et al* (1987) have suggested that the error introduced by sampling is only large when the sampling period exceeds the time constant for the open- and closed-time histograms. In their analysis, they found that decreasing the sampling period decreased the error: when the sampling period was less than 20% of the time constant of the open- and closed-time histograms, then the sampling error became small enough to introduce negligible error in the measured number of intervals. In accordance with this criterion, the mean open- and closed-time constants in this study were usually at least five times greater than the sampling interval, suggesting that this source of error was negligible. A question that also arose was whether the selected corner frequency of the filter (500 Hz) was high enough to include the majority of frequencies in our recordings; if the open time of events was very short, then the filter characteristics would preclude detecting these or would detect events at apparent amplitudes less than their true amplitude. However, typical "burst" recordings (as in Fig. 5.1.C.) showed that most events had frequencies that were well within the bandwidth of the filter settings, and were thus unlikely to be distorted. In addition, the mean open and mean closed times of our channel data were generally well within the bandwidth of the filter settings, suggesting that the majority of recorded data was not significantly distorted by filter settings. A digital filter was also available in the computer program. The features of this filter are described in the methods; however, this was rarely used.

Undoubtedly, events of very high frequency were either excluded or significantly distorted during recording. However, this is an unavoidable concomitant with current recording techniques, and of little relevance to the aim of this project, which was merely to establish the presence, or

otherwise, of Ca-permeable channels in tubular apical membranes.

A source of irritation during the recording procedure was that stepwise changes in pipette holding potential were often sufficient to irreparably damage the tight seal at the electrode tip. While this problem could be avoided by using the potentiometer control to induce gradual voltage changes, this was found to be a fairly laborious procedure. During the excitement of a good recording, it was much easier to press a switch to induce a voltage change than to adjust a dial.

Once the data was recorded, it was immediately stored on disc. Up to ten minutes of data could be stored on a 800 Kbyte disc. Machine constraints presented two shortcomings: the first was that a ten minute data recording took about 8 minutes to save to disc. This meant that valuable recordings occurring during these 8 minutes would be wasted. The second shortcoming was that one had a maximum of only ten minutes during which to perform all the necessary procedures required to characterise the channel on the patch. This was particularly frustrating during experiments in which the long term effects of hormones or drugs were being investigated. Towards the end of the project, the acquisition of a digital-audio tapedeck solved both of these problems, and allowed up to 3 hours of uninterrupted data recordings.

### **5.1.5. Data analysis**

The standard techniques used to analyse patch clamp data (described in Colquhoun and Sigworth, 1983) assume that the current through a single channel consists of rectangular pulses with flat tops and infinitely short transition times. A large percentage of data in this study did not have these characteristics. Consequently, although the techniques used here closely follow the strategy of Colquhoun and Sigworth (1983), additional methods were employed to attempt to quantify the more unique features of the data recorded in this study.

#### **5.1.5.1. Event amplitude**

Quantification of event amplitudes involved two separate techniques. The first was the simple measurement of "square" or "rectangular" current

pulses. Since these pulses generally varied in amplitude, where possible, the mean amplitude of the 20 smallest squares measured at each voltage was chosen to represent the mean unitary current amplitude for any given voltage clamp value. "Squares" of larger amplitude were not used in this measurement, as the aim was to get an estimate of single unit conductance for each trace; larger "squares" were assumed to be the sum of more than one subconductance state.

The second measure of current amplitude was achieved using the "burst analysis" procedure described in the methods. The technique is based on the assumption that there exist several favoured degrees of opening within each "burst". Thus if a "burst" of activity is compared to the rapid opening and closing of a door, then by analogy the assumption is that there is a higher probability of the door opening to certain "favoured" degrees than others, i.e., the absolute degree of each opening of the door in a number of successive openings is not a totally random process.

The "burst analysis" procedure was applied to only two bins at a time. This was done to minimise the effects of baseline drift on the peak amplitudes during "bursts". According to the assumption made (above), the histograms for the "burst analysis" were expected to display several discrete peaks, corresponding to favoured degrees of openings. The chi-squared test was used to test the significance of the observed frequency distribution of the peak amplitudes, against the theoretical frequency distribution expected for a purely random signal. The significance level thus gave an indication of the extent of "non-randomness" of the amplitudes of the "burst" recordings.

In most cases, "burst analysis" produced histograms with discrete peaks. These peaks were not always as clearly defined as might be expected from channel activity favouring discrete subconductance levels. However inasmuch as noise levels were often high, and taking into account the possible distorting effects of the sampling rate or filter settings, we distinguished between peaks, albeit "smeared" by noise. The difference between the peaks was then averaged, to produce an estimate for the mean unit amplitude as measured for "burst" activity.

Using the automated analysis procedure, the amplitude histograms of entire recordings at given levels of voltage clamp (up to 2 minutes) were also computed for some recordings. For analysis of a trace of this length,



the effects of noise, drift, and machine settings are amplified. The aim of doing this, however, was not to search for or measure discrete peaks on the amplitude histogram, but rather to observe a general pattern that might emerge (i.e., exponential decay or discrete amplitude peaks).

#### **5.1.5.2. Open- and closed-time histograms**

Although the measurement of open- and closed-time intervals was done automatically, the sections of analysed recording were validated visually using the cursor. The purpose of the validation was to check that the automated analysis procedure in fact yielded true measurements of all channel events. Sections of some recordings proved refractory to the automated analysis; these sections were deleted from the final analysis. Thus in many cases, the analysis was performed repeatedly for different segments of a single recording. Those segments containing a minimum of 1000 events were used for estimation of time constants and rate constants. The fractional open time was determined by calculating the mean of fractional open times measured for each segment in a voltage clamp recording.

The results of this analysis are not entirely accurate for several reasons. 1) The first problem concerns limited frequency resolution. The sampling rate chosen and the filter frequency setting probably resulted in very short openings being indistinguishable from random noise fluctuations about the baseline; similarly, measured openings were in some cases possibly too long, because some actually consisted of two or more openings separated by unresolved closures. 2) The second problem was that the threshold setting chosen was always a subjective estimate of single channel conductance. The threshold needs to be set high enough to avoid counting unusually large noise peaks as channel events, but low enough to catch as many true events as possible. In setting the threshold value, it was not always easy to find a compromise to meet both these needs. 3) Lastly, most of the recordings in this study contained openings at multiple levels of current amplitude. Although it was assumed - for the sake of simplicity - that these events corresponded to multiple conductance levels of a single channel, it is of course possible that some records depicted events emanating from more than one channel. Such

recordings are generally unsuitable for looking at distributions of open times and shut times, because if two channels are open, there is no way of telling when one of them closes, whether the one that closes is that which opened first or that which opened second.

Although these three factors were probably sufficient to induce significant error in the measurement of amplitudes and event durations, the analysis techniques used here were nevertheless performed on every one of the recordings as standard procedure to provide at least a crude estimate of conductance, mean open and closed times, rate constants, and the number of open and closed states of the channel (as judged by the number of exponentials in curve-fitting), all of which contribute to identifying the "signature" of the channel. In some cases the amplitude data were pooled to construct collective I-V plots for the data.

In addition to the standard techniques, alternative analysis procedures were also applied to certain parts of the data (see results) to test for the possible validity of diffusional or fractal models. These procedures involved generation of both phase space plots and log-log plots of the open- and closed-time distributions. Data samples of between 500 and 2000 channel events were used for these alternative analysis procedures. Korn and Horn (1988) have suggested, however, that such data sample sizes are probably too small to discriminate between fractal and Markov models.

#### **5.1.6. Computer programs for data recording and analysis.**

The software used in this laboratory for data recording and analysis followed closely the strategy of Sigworth (1983). The "PATCH" program used to record the data did not undergo many alterations during the course of the study; however the "ANALYSE" program was continually modified and changed to ensure that the analysis of data was as accurate as possible. Some routines, such as the "burst analysis" procedure, did not follow the standard strategies, and were developed to quantify those sections of recordings which were considered unique. A difficulty with the continual evolutionary process of the software development, was that the data had to be reanalysed every time an improvement was made to the program. This was time consuming and

soul destroying!

The "burst analysis" routine is unique in that it considers all events within a "burst" to be in the open state. In terms of parameter settings, the main differences between the "burst analysis" routine and conventional amplitude measuring routines are in the threshold settings and the baseline settings. In "burst analysis", the threshold value is set as low as possible within machine constraints. The smallest possible differences between events are thus included so as to reveal any underlying patterns of "burst" behaviour. The baseline setting does not need to correspond to the true baseline of the recording. This is because ultimately, for generation of the histograms, the amplitude differences between peaks, rather than their absolute amplitude is important.

The routines used to measure open- and closed-time intervals generally follow standard procedures. A small difference, however, is the "peaks" and "spikes" options in the list of parameters. These were included to obtain an accurate measure of "spike" amplitude and duration in the recordings. When analysing large sections of data for measurement of amplitudes and event durations, the "peaks" and "spikes" options were always chosen, as these gave the truest representation of channel event duration and amplitude in the recordings.

## 5.2. DISCUSSION OF RESULTS

### 5.2.1. The search for calcium channels in rabbit renal tubules

Although the patch clamp technique is more difficult to apply to cells from the living animal than to cells grown in tissue culture and enzymatically cleaned, channel activity in cultured cells may differ from that in their counterparts in the living animal (Merot *et al*, 1988). The former course was therefore pursued despite the very infrequent attainment of suitably "tight" and long-lasting giga-ohm seals. Indeed, obtaining recordings from our preparation was an extremely rare occurrence. Sometimes, experiments were performed on a daily basis for up to three weeks before a suitable recording was made (the maximum number of unsuccessful experiments in a row was seventeen). The largest number of recordings came from CCDs. This was because although tight seals were not easier to obtain in this segment, once obtained, they lasted longer on average than patches obtained from other segments, and so were more suitable for voltage clamp recordings. A possible reason for the higher incidence of long lasting seals in this segment is that the cells of this segment appear to be hardier and have a higher longevity outside their native environment than cells of other segments. The effects of drugs and hormones was not as fully investigated as had been hoped. This was due in part to the difficulty in obtaining long-lasting seals for recording, but was compounded by the technical difficulties associated with transferring the patch to alternate solutions. The results of these studies therefore remain preliminary.

Application of the patch clamp technique to human renal biopsy preparations was found to be considerably easier than on rabbit tubules. This was because seals were formed on the basolateral membrane of the human tubules, yielding about a 20% seal success rate. Indeed, in a few cases, tight seal formation was attempted on the apical membrane of human tubules, without success (except in one case only). The very modest number of drug additions (n=3) obtained in human kidney tubule experiments was a reflection of tissue availability rather than technical difficulties.

The "square" current events in Fig. 1.A. are an example of the longer duration "square" events which occurred relatively infrequently in our recordings. Most "squares" used in measurement of amplitudes had durations of between 5 and 50 ms. In some cases, it was difficult to discriminate between the longer duration "squares" and "bursts". For example, the portion of trace outlined and enlarged in Fig. 4.1.4.A might, at first glance, appear to be a single "square" event. However, subsequent "burst analysis" of this section of trace revealed three discrete peaks on the histogram corresponding to favoured degrees of opening (Fig. 4.1.4.B). These favoured degrees of opening are usually referred to as multiple conductance states. When the "burst analysis" procedure was applied to "square" events of long duration, only one discrete peak was visible on the amplitude histogram. Most of the "burst" histograms revealed separate, discrete peaks. Sometimes the peaks were not as clear-cut as those shown in the histogram in Fig. 4.1.4.B, and were "smeared" with noise. This was probably due to intrinsic noise within "burst" activity as well as the limited resolution of the recording apparatus. In addition the peaks on the "burst" amplitude histograms were not always evenly spaced apart, suggesting that favoured degrees of opening of the channel were not necessarily separated by some unit amplitude. Thus the mean of the differences between peak amplitudes was computed to determine mean unit conductance.

The amplitude differences between successive peaks within a "burst" (rather than the absolute amplitudes) were also computed in some cases, and displayed on a "jump" histogram (Fig. 4.1.4.C.). The histogram shows that large jumps in amplitude between successive peaks, are less frequent than small jumps; as the relationship is exponential, this is consistent with the magnitude of successive jumps being randomly determined.

#### **5.2.1.1. Are these real channel data?**

Many of the recordings, especially the "burst" recordings, displayed unusual characteristics, in that the channel events were not typically "rectangular" or "square" in shape. In classical terms, one of the distinguishing features of a channel is the "square" pattern of a current

recording. Is it possible, therefore, that the sections of channel activity defined as "bursts", are simply either noise recordings or noise resulting from seal breakdown, and not real channel data? It is believed that our recordings demonstrate real channel data, for the following reasons:

1) The "burst" histograms display discrete peaks in amplitude, usually evenly spaced apart. The number of data points in the bins corresponding to the amplitude peaks differ significantly ( $p < .001$  in most cases) from the average number of events per bin. These are not features expected in the analysis of random noise.

2) Many tight seals lasted for longer than ten minutes. "Bursts" in these recordings were preceded and followed by long periods of low-noise baseline, suggestive of a consistently tight seal. One of the features of seal breakdown is that the seal loses its "tightness" resulting in noisy leak currents, and fluctuating baselines.

3) "Bursts" often occurred superimposed upon, or closely preceded or followed by "square" channel events. This is not a pattern of events expected to occur during the random noise generated by seal breakdown.

4) The collective I-V plots demonstrate that the mean unit current amplitudes, as determined for "bursts" and "squares" (Figs. 4.1.2 and 4.1.5.A), are independent of voltage. The amplitude of noise, on the other hand, would be expected to vary with the voltage imposed on the patch.

5) Exposure of the patch to different drugs or parathyroid hormone (discussed in the next chapter) often resulted in block or activation of channel activity. A noise recording would not be expected to respond to the addition of drugs or hormones.

These five observations suggest that the channel activity observed is not simply a noise recording or an artifact resulting from seal breakdown.

#### **5.2.1.2. Multiple identical channels, multiple channel types, or multiple conductance states?**

The observation of three temporal patterns of activity led us to ask whether there was perhaps more than one channel type on the patch. To test for this possibility, the need arose to find means to quantify these different modes of activity. The development of the "burst analysis" procedure not only enabled us to quantify the amplitude profile of "bursts", but also provided us with a means of comparing "burst" activity with "square" channel activity. In practice, the results of these two analysis procedures could be compared by determining the mean unit current amplitudes and I-V relationships for both "squares" and "bursts". In this study, I-V plots were constructed for the entire data sample, as well as for individual recordings. It is interesting that the profile of the I-V plots determined for the entire data sample are very similar for both the "burst" data and the small "squares" data (Figs. 4.1.2 and 4.1.5.A). In both of these plots, the absolute mean unit current amplitude as determined for "bursts" or "squares" did not increase above and below the reversal potential. Thus the "bursts" and "squares" in these recordings not only share similar amplitude characteristics under conditions of varying voltage, but the mean unit amplitudes (shown in Table 4.1.3) for "bursts" were significantly different to and roughly half the amplitude of the mean unit amplitudes for "squares". This difference can also be seen by inspection of the collective graphs. A possible reason for this is the amplitude of the small "squares" was such that it would have been impossible to see "squares" half that amplitude in the prevailing noise level. These results support the argument that the three temporal patterns of activity are different manifestations of the same channel. Furthermore, since "squares", "bursts" and "spikes" occurred together consistently in nearly every recording, it is unlikely that they represent three different channel types. An interesting observation was that the mean unit amplitudes for the DCT were significantly higher than for the other segments, for both "squares" and "bursts". The possible functional significance of this is discussed later.

Collective I-V plots were also determined for the different tubule segments individually, and these exhibited similar profiles to the one

displayed in Fig. 4.1.2. An unexpected finding, as shown by the collective I-V plots, was that the (absolute) mean unit current amplitudes remained unchanged above and below the reversal potential in spite of varying patch voltages, i.e., were voltage-independent; it is unlikely that this observation is the result of recordings from a multichannel patch or from a patch containing multiple types of channels because unitary events in such cases would be expected to increase or decrease with varying levels of voltage clamp. The finding is best explained by recordings from a patch containing a single channel with multiple conductance states. In such a case, the individual conductive units comprising the different dimensions of the channel protein become saturated with the current flowing through the channel. Thus if the voltage applied to one side of the patch is increased, the current flowing through the individual conductive units remains the same; this necessitates the recruitment of a larger number of conductive units to allow a greater flow of current through the channel. When the applied potential exceeds the reversal potential for the channel, the direction of current flow through the conductive units simply reverses direction, while the amount of charge flowing through a single conductive unit per unit time remains the same. By analogy, the channel can be thought of as a multibarrelled pipe with a convex orifice on one side. If the pipe is held vertically, and an increasing quantity of sand is poured into the convex orifice, initially the sand will only flow through the central barrel. As the quantity of sand is increased, a greater number of barrels will be recruited to account for this increasing quantity. The amount of sand flowing through any individual barrel, however, remains independent of the quantity of sand poured into the mouth of the pipe, i.e., it reaches saturation.

The concept of multibarrelled channels was explored by Hunter and Giebisch (1987). These workers have provided evidence for the presence of four parallel, equally conductive subunits that make up a K channel in the distal tubule of *Amphiuma*. The difference between their model and the one here, however, is that the open probability of their channel was controlled by a main gate which acted either to occlude or expose the four subunits in unison. This was inferred by the presence of frequent closures from the fourth conductance state of the channel to the zero-current level. In addition, the amplitude of the current flowing through the



conductive units was voltage-dependent. The channel in this study was probably not controlled by a main gate, however, as closures from a some maximal conductance state to the zero-current level were rarely seen (as shown by the "jump" histogram). Sudden transitions between a number of conductance states often observed are more likely to result from the random and simultaneous recruitment or closure of a number of conductive units, dictated perhaps by the voltage across the membrane, the ionic gradient, or the availability of ions in the vicinity of the channel pore.

A third variation in current-voltage relationships was explored using total mean current (Fig. 4.1.5.B). This plot was determined for a relatively small data sample which represented patches exposed to a wide range of voltage values. The plot shows some interesting characteristics: the collective means of total mean current between -20 mV and 20 mV appear to be not dissimilar. However, as the voltage departs from these values, the total mean current is observed to increase for both positive and negative applied potentials. This phenomenon is seemingly in contradiction with the pattern observed for the I-V plots determined for "bursts" and small "squares"; however it can be explained by the fact that total mean current is not a reflection of the amount of current flowing through a single conductive unit; on the contrary, the total mean current most likely reflects the number of conductive units of the channel that are recruited, i.e., an increase in the applied voltage results in an increase in the number of conductive units recruited. This in turn would increase the total mean current through the channel.

Linear regression was not attempted on any of the three variants of collective I-V relationships, since the mean amplitudes in each case were not significantly dependent on voltage. The mean slope conductance as determined for the collective I-V data plots was therefore not calculated. The reversal potentials for these plots were consistently close to zero, far removed from the Nernst potential of any single ion species in this study. An interesting study would have been to observe the channel response to a number of voltage changes within the narrow range in which the unitary events reverse polarity (i.e., between -5 mV and 5 mV). It may be possible that there is a linear relationship between conductive unit amplitude and voltage in this range, i.e., with small enough voltages applied across the

patch, the conductive units may not yet be saturated. If this were the case, then an estimate of slope conductance, within this narrow voltage range, could be obtained from such data.

A further argument in favour of multiple conductance states was derived from the observation that the current amplitude often displayed sudden transitions between a number of different unitary levels. This is demonstrated in Fig. 4.1.6, which shows two channel events from the same patch occurring within a few seconds of each other. The second event rose abruptly to a level four times that of the unit amplitude of the first, before falling equally abruptly to zero. In terms of binomial probability theory, the probability of several identical channels opening or closing simultaneously is vanishingly small.

#### **5.2.1.3. Individual channel data:**

The recordings shown in Fig. 4.1.7.A are an example which demonstrates how "square", "burst", and "spike" activity may all occur on the same membrane patch. For every individual recording, clamped at a minimum of three voltages, the slope conductance was determined, as calculated by linear regression, for both "bursts" and small "squares". In many cases, however, (Fig. 4.1.7.B and C for example), the points on the I-V plots clearly did not show a simple linear relationship. Also, the data points were in many cases too few to determine whether or not a linear relationship existed. These factors, taken together with the evidence that the collective I-V plots for our data were non-linear, suggest that the linearity of the individual I-V data plots was, in fact, possibly illusory; the application of linear regression analysis was therefore possibly unwarranted. However, inasmuch as the length of data recordings usually did not allow exposure of the patch to a large number of voltages, linear regression was nevertheless applied to the current-voltage data in the face of doubt over the existence of linear relationships.

The mean conductances computed, - in individual I-V plots - for both "burst" and small "square" analysis in the different tubule segments (Table 4.1.3) show some interesting patterns. For both "burst" and "square" analysis, the mean conductance was similar for all segments except the DCT. For this segment, the mean conductance was significantly higher

than that of the other segments. In addition, the mean conductances as determined for "square analysis" were, in the case of each segment, except the PSTs and the TALs, significantly different to the conductances determined for "burst analysis". This regularity is surprising in view of the methodological difficulties described above. A further very interesting observation was that the pattern of mean conductances, as calculated by linear regression for the individual I-V data plots, could be reconciled with the mean unit current amplitudes: the unit amplitudes for the "squares analysis" were roughly twice the value of the unit amplitudes obtained for "burst analysis". Thus, in spite of sources of error in the methods used to compute these values, it is believed that they are nevertheless helpful in the interpretation of the results.

The reversal potentials for the individual I-V plots were, as in the case of the collective data plots, consistently close to zero (see Table 4.1.3). Such a value can be accounted for by the Goldman equation, and indicates that the channel is non-selective. Both the fractional open time (Fig. 4.1.7.D) and the mean open time increased with displacement of the clamp voltage from the reversal potential, suggesting that the channel in this study was a voltage-sensitive channel. The amplitude histogram shown in Fig. 4.1.7.E was computed for all three temporal patterns of channel activity in a two-minute segment of recording and is not to be confused with the "burst" amplitude histogram shown in Fig. 4.1.4.B. Because this amplitude histogram was computed for a relatively long time period, the effects of noise, baseline drift, and limited frequency resolution are likely to cause significant smearing of the histogram data. In spite of this, however, the histogram can be described by a random exponential decay curve. This profile has been considered to be suggestive of multiple conductance states (Cull-Candy and Usowicz, 1987). The open- and closed-time histograms shown in Fig. 4.1.7.E could both be described by two exponentials. Nearly all recordings yielded double exponentials for both open- and closed-time histograms. This suggests that the channel has two open states and two closed states.

In addition to the standard statistical procedures, alternative procedures were also applied in some cases to individual patch recordings. This was done to test the possible application of Liebovitch's fractal model and of Millhauser's unidimensional ion diffusion model to the

data (Liebovitch *et al*, 1987; Millhauser *et al*, 1988). To this end, log-log plots of the open- and closed-time histograms (Fig. 4.1.7.E), as well as phase space plots for successive channel amplitudes (Fig. 4.1.4.D.), and open times (Fig. 4.1.7.H.) were determined. The phase space plots, usually computed for 1000 - 2000 channel events, revealed no underlying pattern or strange attractor, suggesting that the data could not be described by the deterministic chaotic processes that underlie the fractal model. In all cases tested, the log-log plots could be well described by a linear relationship. Since Liebovitch has shown that such a linear relationship can be accounted for by the fractal model, the high correlations observed are in accord with Liebovitch's fractal model. Since these plots do not show a linear regime followed by a precipitous drop, however, these data cannot be accounted for by the diffusion model put forward by Millhauser *et al*, (1988), i.e., in theory, the ion channel protein in our study does not randomly sample a large number of different, but simply related, conformations during the gating period, as proposed by Millhauser. Although the log-log plots showed very good correlations, however, the standard error of the estimate for the fitting procedures was still greater than that measured for single or double exponential curves on the normal open- and closed- time histograms. The duration histograms are, in most cases, best described by double exponentials. Of the three models tested, therefore, the data are probably best described by simple Markov kinetics (Colquhoun, 1987). The data samples used for these alternative procedures, however, were probably too small to accurately determine which model is best suited to our data (see Korn and Horn, 1988).

### **5.2.2. The quest to further characterise the channel.**

Experiments were undertaken to test for the possible Cl permeability of the channel as well as its responses to different channel blockers and agonists. Most of these experiments were performed on CCD patches. This is because tight seals obtained on cells of this segment were more stable and lasted longer than on the other tubule segments; the strength and durability of the tight seal are important determinants for experiments such as these, which involve extensive manipulation of the membrane patch. Due to the technical difficulties involved in such experiments, the data are

few. The results are thus preliminary and further investigation is required.

#### **5.2.2.1. Solution changes**

The use of "half NaCl Ringer" in the bath to test for Cl permeability follows the protocol of Gogelein and Greger (1986). Initially, the observed reversal potential shifts were corrected for by measuring the diffusion potential arising across the membrane patch as a consequence of the differing ionic composition of the solutions on both sides. Subsequently, however, Gogelein (1990) has shown that this diffusion potential should not affect the reversal potential of the channels present in the membrane patch, the latter being determined solely by the clamp potential and the interelectrode liquid junction potential. The initial correction of the reversal potential was therefore erroneous and we recorrected to the observed reversal potential shifts.

In experiments using "half NaCl Ringer", the expected Nernst potential for Cl ions is about 18 mV; when Na thiocyanate or Na acetate is used in the bath, the expected Nernst potential for Cl is, in theory, infinitely positive, as these bath solutions contain no Cl ions. Of the CCD patches exposed to alternate solutions, the reversal potential shifted substantially towards the Nernst for Cl in five cases, suggesting significant Cl permeability of these channels. In two cases, the reversal potential shift was in the negative direction, suggesting a predominant Ca permeability (now less opposed by Na diffusion into the pipette), and in four cases, the reversal potential did not shift significantly either way, suggesting a non-specific ion permeability. The reversal potential shift on the PST patches could not be determined owing to excessive noise on the recordings. The DCT patch exposed to Na thiocyanate showed a substantial reversal potential shift in the negative direction, suggesting that this channel was predominantly permeable to Ca ions.

All of these experiments were performed using the plastic sleeve method. As discussed above (discussion of methods), this technique introduced a considerable noise component into the recordings. This made the interpretation of the data difficult in some cases (impossible in the case of the PSTs). Another possible source of error in these experiments was the estimated value of the reversal potential shifts which were

measured by constructing I-V plots before and after the solution change. Some of these plots were constructed using only three data points, the reversal potential of these plots being calculated by performing linear regression analysis of the data points. Since in reality, the I-V plots may not have had a linear relationship, and since the data points were too few to perform an accurate statistical analysis of the plots, the reversal potential shifts calculated were hardly accurate. However, since in most experiments, it was possible to qualitatively determine a rough estimate of the reversal potential before and after the solution change by observing where channel activity reversed direction on the trace, the errors in the quantitative analysis do not invalidate the qualitative interpretation of these data.

These data are thus consistent both with the presence of Cl channels in the CCD, and Ca-permeable non-selective channels in the CCD and DCT. As will be discussed later, Cl channels have been shown only to exist in cultured intercalated cells of the CCD (Light et al, 1990); it is therefore possible that patches containing Cl channels in this study were from these cells. In the Ca-permeable channels, it is likely that the current flow at positive clamp voltages reflected predominantly the trans-channel movement of Ba or Ca from the pipette into the bath (with some possible Cl movement), while that at negative clamp voltages reflected predominantly the movement of Na in the opposite direction (the concentration of K in the bath fluid being relatively negligible). More experiments of this nature are clearly needed, however, to characterise the relative ion permeabilities of the channel, not only in these segments, but in the other segments too.

#### **5.2.2.2. Experiments with Ca channel agonists and antagonists, and parathyroid hormone: the expected and the unexpected.**

In these experiments, the channel's fractional open time response was used as an indicator to test the effects of the drugs or parathyroid hormone. Pharmacological doses of the drugs and PTH were used in all cases, as it was hoped to elicit a maximal effect of these agents on channel activity. Most of the experiments were performed on CCD patches using the Ca channel agonist Bay K-8644, or the antagonist

nifedipene (see Table 4.2.3). However, the antagonists D600 and verapamil, and the diuretic hydrochlorothiazide were also used. Table 4.2.2 shows that most of the recordings that elicited no response after the addition of drugs had no channel activity to begin with. It is very possible therefore, that there were no channels on these patches. In one case, addition of Bay K-8644 produced an increase in channel activity, an expected result for a voltage-sensitive L-type Ca-permeable channel. In some cases, however, the unexpected occurred where agonists appeared to behave as antagonists and vice versa. These effects were seen on CCD patches where nifedipene ( $n=2$ ), verapamil ( $n=2$ ) and D600 ( $n=1$ ) increased channel activity, and Bay K-8644 ( $n=2$ ) decreased channel activity. This is not all that surprising, however, in view of the fact that there exist a number of reports already of dihydropyridine blockers acting as agonists and dihydropyridine agonists acting as antagonists (Miller and Fox, 1990). It is possible therefore that either the high concentrations of drugs or the prevailing voltage clamp conditions in this study brought about these opposite effects. It is also possible, however, that, since the recordings are of relatively short duration, these effects are illusory, and are simply the result of spontaneous fluctuations in fractional open time.

The effect of voltage clamp on the channel's response to an antagonist was clearly seen in the case of verapamil addition. Addition of this drug reduced the fractional open time at  $-20$  mV, but increased it at positive insertion voltages. Chlorothiazide was added to one CCD patch, and reduced fractional open time. The result might be considered to be unexpected, because this diuretic is known to increase Ca reabsorption, presumably via activation of Ca-permeable channels, and is believed to act primarily on the DCT, and not on the CCD. The data are insufficient, however, to draw any real conclusions about the chlorothiazide effects.

In the case of the PST, the response was as expected; Fig. 4.2.2 demonstrates how channel activity previously abolished by  $0.1$  mM nifedipene was near maximal after exposure to the agonist Bay K-8644: both the fractional open time and the mean open time increased considerably when compared with the control, while the mean closed time decreased after the addition of Bay K-8644. Addition of this drug, however, did not appear to effect the number of exponentials used to

describe the open- and closed-time histograms (Fig. 4.2.2.B), suggesting that the number of open and closed states of the channel did not change. In both the control and the Bay K-8644 recording, the channel behaviour manifested predominantly as "burst" behaviour, this "burst" behaviour being more pronounced in the presence of Bay K-8644. In support of these data is a report by Lacerda and Brown (1989) in which they observed that Bay K-8644 alters the "bursting" activity of cardiac Ca channels; its major effects were on "burst" duration, "burst" open time and "burst" closed time. Although in the experiments here, addition of Bay K-8644 did not alter the number of open or closed states, the mean open and mean closed times were markedly altered by the presence of the agonist. These results were expected, on the basis of the assumption that the activity was recorded from a Ca-permeable channel in this segment.

PTH was tested only on cell-attached patches from TALs and DCTs. This is because these segments are the site for the hypercalcaemic action of PTH (Friedman, 1988). The TALs were the most difficult segments to patch, and the DCTs were the hardest to dissect; this explains the paucity of data from these segments. Bay K-8644 and chlorothiazide were found to have no effect on TAL patches, but the patches tested showed no activity to begin with. PTH augments Ca absorption both in the TAL and the DCT (Rouse and Suki, 1990). Many hormones are known to activate second messengers in the cell which in turn enhance Ca entry by activating Ca channels (Peterson, 1990). On this assumption, recordings in these studies were made in the cell-attached configuration, with the addition of PTH to the bath solution. The PTH was made up from bovine parathyroid acetone powder. Since only a rough estimate of the concentration of PTH in this crude extract was available, the calculated concentration of PTH in the bath solution was only a rough approximation of the actual concentration. The pharmacological dose of 100  $\mu$ M cited was therefore only an approximate estimation. Of the TAL patches exposed to a solution containing PTH (n=5), three elicited an increase in fractional open time after exposure (see Table 4.2.3). In the example (non-continuous traces) shown in Fig. 4.2.3, DCT channel activity was observed only about five minutes after the addition of PTH. This activity was predominantly of the "burst" variety, and the fractional open



time revealed voltage-sensitivity (data not shown). Initially, the possibility was considered that channel activity was simply induced by patch excision, which might have occurred during the process of PTH addition to the bath. However, the fact that channel activity occurred only five minutes after PTH addition, and since there were no other major disruptions during the experiment, this possibility is unlikely. These results therefore suggest that PTH induces activation of existing, or recruitment of new, Ca-permeable channels in the apical membrane of the DCT, presumably via activation of a second messenger system in this segment. This notion is consistent with studies by Backskai and Friedman (1990) on the DCT, in which they show that a PTH-stimulated rise in intracellular Ca results from Ca entry through DHP-sensitive channels.

The traces shown in Figs. 4.2.2 and 4.2.3 are not continuous recordings. This is because during the process of exposing the patch to alternate solutions containing the drugs, a large noise component of fairly long duration was introduced into the recordings. However, although the traces shown are samples from the recording, they reflect the rest of the channel behaviour observed in the recording.

In this study, the fractional open time was the only parameter measured before and after drug or hormone addition. An interesting study would have been a closer examination and analysis of changes in the mode of channel behaviour before and after drug or hormone addition. Tsien *et al* (1985) have shown that DHPs do not alter the amplitude of unitary Ca events, but produce a striking change in the pattern of channel opening. They proposed that binding of drugs does not plug the pore, but instead favours one or more modes of gating. Pure agonist effects arise when mode 2 is specifically favoured, and pure antagonist effects result when mode 0 is preferentially stabilised; these extremes encompass a wide range of intermediate possibilities for partial agonist or antagonist effects. More recently, Lacerda and Brown (1989) have provided evidence to suggest that the kinetics within a mode, as well as the channel conductance, are altered by the addition of DHP agonists and antagonists to Ca channels in guinea-pig cardiac myocytes. Because of the insufficiency of our data, none of these effects were sought in this study.

### 5.2.3. The quest for similar channels in human tubule segments

The data obtained from the basolateral membrane of human tubule segments was comparable to the data obtained from the apical membrane of rabbit tubules: in raw data traces, three similar temporal patterns of activity ("squares", "bursts", and "spikes") were observed and often occurred together. The same analysis procedures described previously were therefore used in this study. The collective I-V plots for both the small "square" amplitudes and the "burst" amplitudes (as determined by "burst analysis") showed a non-linear profile similar to that observed for the rabbit data, suggesting that the measured unit current amplitudes were not dependent on voltage. The mean unit current amplitudes were, however, slightly smaller than for rabbit, at least in the case of the "squares". The example of an individual I-V plot as determined for "squares" appears to have a linear relationship. The profile of this plot is not the same as the I-V plot for rabbit data in Fig. 4.1.7.C; however in all cases the data points were too few to draw any conclusions concerning the differences in individual I-V plots. The channel was voltage-sensitive, the fractional open time and the mean open time increasing with departure of the clamp potential from the reversal potential. The open- and closed-time histograms could both be described by two exponentials, suggesting, as in the case of the majority of rabbit tubule data, that the channel possesses two open states and two closed states. The amplitude histogram computed for a recording of a patch clamped at 9 mV ( $n=2559$  events) could also be described by an exponential curve, suggesting subconductance states on the patch rather than a number of identical channels. The mean conductances computed for "burst" analysis were greater on average than those computed for rabbit "burst" data; however the mean conductance for "squares" was similar to rabbit tubule "squares" data. The reversal potential, as calculated by linear regression, was consistently close to zero, suggesting a non-selective channel, the permeability of which can be described by the Goldman equation. The alternative analysis procedures applied to the human data revealed no pattern on the phase space plots, while the log-log plot of the open- and closed-time histograms could be described by a linear relationship (data not shown). This is comparable with the rabbit tubule

data.

In a few cases in this study, Bay K-8644 and nifedipene were used to further characterise the channel. In all cases channel activity present on the membrane patch was completely abolished during exposure of the patch to either the agonist or antagonist. In the example shown in Fig. 4.3.2 the channel became more active in the excised mode - this may have been due to exposure to a higher Ca concentration in the bath - but was completely blocked by exposure to nifedipene. This result is consistent with a voltage-sensitive L-type Ca-permeable channel. The example in Fig. 4.3.3 shows how channel activity from a patch in the excised mode was completely abolished after exposure to the agonist Bay K-8644. The channel was then exposed to nifedipene to test whether this might have an opposite effect and activate the channel, but the channel remained irreversibly blocked, even when later exposed to a normal Ringer solution. This is an unexpected result for a L-type Ca-channel. Once again, the high pharmacological doses and prevailing voltage clamp conditions in this study might have had a profound effect on the channel's response to agonists and antagonists. No experiments were done to test the relative ion permeabilities of the channel. Although data were obtained from the apical membrane in one case, they were too few to adequately characterise the channel in this membrane.

The data reported here are consistent with a voltage-sensitive, non-selective, Ca-permeable channel, and are consistent with the data from the apical membrane of rabbit tubules. These results are surprising because they suggest that similar Ca-permeable non-selective channels exist both on the apical membrane and the basolateral membrane of mammalian renal tubules.

#### **5.2.4. Emergence of unexpected channel varieties in this study.**

Different channel types were not actively sought in this study, but emerged by chance, either while experimenting with different pipette and bath solutions, or while seeking Ca-permeable channels.

Two distinct varieties of channels were found: one variety (n=2) was found in the apical membrane of rabbit DCT using a KCl Ringer pipette solution. These channels were distinguished by a "square" current shape, a

high slope conductance as calculated by linear regression (Fig. 4.4.1.D), and a reversal potential close to zero. This suggests the existence of a non-selective channel in the membrane of this segment, with different characteristics to the Ca-permeable channel already described. The existence of such a channel has not yet been reported in the literature. The other type of channel was found in the apical membrane of rabbit CCDs ( $n=2$ ) and in the basolateral membrane of a human tubule segment ( $n=1$ ). This channel was found by chance while using bath and pipette solutions suitable for seeking Ca-permeable channels; it is described by a low slope conductance and "square" shaped channel events. In the cell-attached configuration, the measured reversal potentials were fairly close to the Nernst potential for K ions, assuming an approximate intracellular concentration of 100 mM for these ions. This suggests that these channels were predominantly permeable to K ions. Since in reality, however, the I-V relationships determined for this channel (for example, Fig. 4.4.1.E) may have shown rectification at higher voltages which were not tested, and since no means of determining the actual K gradient across the patch were available, it cannot be concluded that the channel was exclusively K-permeable. The low conductance channel observed in the inside-out mode with KCl Ringer in the bath had a reversal potential of only 13.4 mV. Since a high K gradient existed across the patch (the calculated Nernst potential for such a gradient is about 86 mV), this value probably reflects a predominantly non-selective channel with some K permeability.

An interesting observation was that in some cases, the "square" shape of these channel varieties occurred together with the typical "burst" behaviour that has been extensively characterised. An example of this is seen in Fig. 4.4.2: the traces suggest the existence of at least two identical low conductance K channels on the patch; however, at a clamp potential of 15 mV, the upward "square" channel event occurs together with a downward "burst" event. At a first glance, it may appear that this downward event in fact simply represents a closure to the baseline, and that there are three similar low-conductance channels on the patch. On closer examination, however, it can be observed that this downward activity exhibits current amplitudes which are greater than the "square" channel amplitudes on the same trace. This suggests the presence of two

types of channels on this patch, one of which is qualitatively similar to the Ca-permeable channel described in this study.

The low conductance channels described here are consistent with the low conductance K channel reported by Frindt and Palmer (1989) in the apical membrane of rat cortical collecting duct. In the case of the human tubule (Fig. 4.4.2), it was not known exactly which segment was patched, but if it was a proximal tubule, the presence of a low-conductance K channel in this segment is interesting in that such a channel has not yet been reported to exist in the proximal tubule of *mammalian* kidneys. Further studies are clearly needed to localise and characterise these other channel varieties in more detail both in rabbit and human tubule segments. A detailed investigation of these channels was not pursued, as their characterisation did not fall within the scope or aims of this thesis.

### 5.3. GENERAL DISCUSSION

#### 5.3.1. Some final comments on the methods

Throughout all stages of this project the more difficult course was pursued of applying the patch clamp technique to cells obtained from living tissue rather than cells grown in tissue culture and enzymatically cleaned. The consequence of this choice was the very infrequent attainment of suitably "tight" and long-lasting seals. Many different variations in the technique were attempted in order to enhance the rate of data collection. These included the use of different types of glassware in the fabrication of patch pipettes, the use of different solutions in the pipette and bath, and the addition of collagenase to the bath solution, to mention but a few. These permutations were to no avail, and it became the accepted practice to patch a large number of different tubule segments before gigaseals were attained on any one segment. Experimental progress was thus extremely slow, and very often data were not forthcoming for weeks at a time. For this reason, the investigation remained exploratory in nature. Also, since the aim of this study was simply to demonstrate the presence or otherwise of Ca-permeable channels in renal tubule apical membranes, the study was not confined to only one tubule segment. Experiments involving the exposure of patches to solutions of different ionic composition or solutions containing drugs were exceptionally laborious, because they involved the movement of the patch through the air-water interface to an alternate solution. The experiments reported here are thus very preliminary, and further investigation is required. The hanging drop technique which was finally employed, proved to be easier and more efficient than the others. Another breakthrough in the development of the technology was the acquisition of the digital audio tapedeck which enabled long periods of data to be stored. Much of the earlier data was lost, as the computer RAM memory wasn't available to store the still incoming channel events, during the 8 minutes it took to save the data previously stored in RAM to disc.

The data analysis procedures used in this study essentially followed standard procedures. How reliably could the multibehavioural channel activity observed in our study be quantified using these techniques? In the autoanalysis procedure, the setting of the parameters was subjective. This meant that a fractional change in, for example, the threshold setting, could reduce the number of measured channel events by as much as half of the original value. The parameters were therefore always chosen to include as many of the real events as possible, while excluding noise peaks. A means of analysing "burst" activity was developed by incorporating an additional "burst analysis" routine into the software. This provided a means of quantifying "burst" data, the nature of which did not conform to the standard definitions of "burst" behaviour. For a number of reasons discussed previously, the histograms, computed from even "validated" automated analysis of channel amplitudes and durations, could not be absolutely accurate. But this is a universal problem. It is felt therefore, that the histograms are accurate enough for the purposes of this study and provide a basic "fingerprint" of the channel. A list containing the measured variables of the entire data sample is presented in the appendix.

### **5.3.2. How do these data fit in with current evidence?**

The data recorded in this study could be qualitatively described by three temporal patterns of activity. "Squares" and "spikes" have been commonly observed in most published patch clamp data. However, "bursts", as presented and defined in this study (cf p.82), do not appear to have been widely documented previously. For reasons discussed earlier, it is highly improbable that this type of recording originates simply from noise or seal breakdown. Indeed there is to date some experimental evidence for this kind of activity, notably, in two separate studies on non-excitabile tissue: 1) Gardner *et al* (1989) have demonstrated the existence of a voltage-insensitive Ca-selective channel in T-lymphocytes. Channel openings were characterised by a bursting behaviour, i.e. periods of quiescence interspersed with periods of intense "bursts" of channel activity, exhibiting fluctuating amplitudes in a continuously open channel. Their traces also show the presence of "spikes" and "squares". These workers did not assign

a conductance value to their data, but described unitary current events as having an approximate amplitude of 0.7-0.8 pA at the resting membrane potential. 2) A relatively early patch clamp study by Koeppen *et al* (1984) on the apical membrane of rabbit cortical collecting duct revealed the presence of fairly large channel events which appeared to be the summation of several unitary events. These workers suggested that the various levels of current amplitude could be observed if a grid were superimposed on the record. After examination of 60 minutes of records in this way, they considered the idea that unitary currents of a few tenths of a pico-ampere were most likely the fundamental units of current and that the larger units were multiples of these units. The I-V relationship, constructed by plotting unitary events against the holding potential, was markedly non-linear (showing rectification at positive clamp voltages), had a reversal potential close to zero mV, and at negative holding potentials a slope conductance of 4 pS. They concluded that these channel events most likely reflected the activity of K channels in this tissue.

Both of these studies show very interesting similarities to the data here, not only in the qualitative features of channel behaviour, but also in some of the quantitative aspects, such as the values for unitary amplitude (in the range of tenths of pico-amperes for both studies) and the measured reversal potential in the second study (close to zero).

The reversal potential of the channel reported here was consistently close to zero, far removed from the Nernst potential of any single ion species in this study. Although sought for, apical Cl channels have not been detected on the luminal membranes of either the proximal tubule (Gogelein, 1990) or the thick ascending limb (Greger *et al*, 1990), suggesting that these cell membranes do not possess anion-selective channels. Transepithelial Cl movement in the distal nephron is also generally believed to occur via paracellular rather than transcellular routes (Schuster and Stoker, 1987). There is, however, some experimental evidence of a cAMP-activated Cl conductance in the collecting duct (Schuster, 1986; Gross *et al*, 1988), while apical Cl channels have been described in a variety of cultured cells of distal nephron origin. Thus Nelson *et al* (1984) have described a 400 pS Cl channel in A6 cells; Christine *et al* (1987), a 120 pS Cl-selective ion channel in cultured collecting duct



principal cells; Light *et al* (1990), a 303 pS Cl channel in cultured intercalated cells; and Marunaka and Eaton (1990), 3 pS and 8 pS Cl channels in A6 cells. In the basolateral membrane of rat thick ascending limbs, Greger *et al* (1990) have reported the existence of a 42 pS Cl channel.

In five of the nine CCD luminal patches, in which the bath fluid was replaced with isosmotic diluted Ringer, the reversal potential became more positive by 10 to 30 mV, consistent with a finite Cl permeability. This phenomenon was not explored further, but it appears that at least some of the channels in the CCD patches were not cation-selective. On the basis of existing evidence for the presence of Cl channels in the nephron, however, it can be argued that the majority of data in this study are representative of a Ba- and Ca-permeable, non-selective cation channel.

Several non-selective ion channels have been described in renal tissues. In the apical membrane of primary cultures of the rat inner medullary collecting duct, Light *et al* (1988) characterised a non-specific cation channel, inhibited by amiloride. In the brush border of cultured proximal tubular cells of the rat, Marom *et al* (1988) reported voltage-insensitive non-specific cation channels. Non-selective channels with a conductance of 50 pS have also been described in the basolateral membrane of the late proximal tubule of rabbit (Gogelein and Greger, 1986), in the basolateral membrane of the thick ascending limb of Henle's loop in the mouse (Teulon *et al*, 1987) with a conductance of 25 pS, as well as in the apical membrane of cultured cells from rabbit proximal convoluted tubule (Merot *et al*, 1988) with a conductance of 13 pS. In addition, Palmer and Frindt (1988) have reported in passing, a non-selective cation channel with a conductance of 23 pS in the apical membrane of rat cortical collecting tubule; no further details were given. None of these have been reported as occurring elsewhere in the nephron, as Ba-permeable, or as displaying the same variations in channel behaviour as the channel observed in this study. Nevertheless, it is possible that one or more of these non-selective channels are similar to the channel characterised here.

The channel explored here was Ba and Na permeable; manifested as "bursts", "squares", or "spikes"; possessed multiple subconductance states with a low unit slope conductance (as measured by the "burst" and "small

squares analysis"); was voltage-sensitive; responded in some cases to dihydropyridine agonists and antagonists, as well as to PTH; and displayed kinetics consistent with two open states and two closed states. Voltage-sensitive Ca channels have been described in a number of tissues other than renal, with characteristics not dissimilar to those found here. Thus some of these characteristics are: (1) in guinea-pig cardiac ventricular cells, Hess *et al* (1984) have proposed three modes (mode 1, mode 0, and mode 2) of channel gating to describe three patterns of observed channel behaviour. Although it is debatable whether these modes adequately describe the data recordings in this study, it is nevertheless interesting that three different modes of behaviour have been recognised to occur from one channel type. (2) Ca channel kinetics consistent with two open and two closed states have been reported as being necessary for describing recordings containing "burst" activity (Rojas *et al*, 1990). (3) Ca channel conductances, as recorded in a variety of cell types in various species, are usually small. For example, slope conductances of 5-15 pS have been described in cardiac cells (Reuter, 1983); of between 5 and 50 pS in hippocampal neurones (Jahr and Stevens, 1987), where the channels were permeable to Na and caesium, but not Ca at the lowest conductances. In non-excitabile tissue, a 24 pS Ca channel has been found in mouse pancreatic  $\beta$ -cells (Rorsman *et al*, 1988); two non-selective Ca channels of 18 pS and 5 pS have been demonstrated in human neutrophils (von Tscharner *et al*, 1986); and 3 and 13 pS Ca-selective channels have been described in human carcinoma cells (Mozhayeva, 1990). (4) Non-selective Ca-permeable channels have been demonstrated in non-excitabile tissue (von Tscharner *et al*, 1990; Penner *et al*, 1988); and in a number of cases, Ca channels are also Na-permeable (Jahr and Stevens, 1987; Liu *et al*, 1989; Reuter, 1983; Benham and Tsien, 1987). Indeed Kostyuk *et al* (1990) have suggested that any Ca channel can be modified to become Na-permeable under certain conditions. (5) Multiple conductance states of Ca permeating channels have been demonstrated in outside-out patches from primary cultures of hippocampal (Jahr and Stevens, 1987) and cerebellar (Cull-Candy and Usowicz, 1987) neurones, in T-lymphocytes (Gardner *et al*, 1989), in GH3 cells where at least five conductance states were observed (Kunze and Ritchie, 1990), as well as in planar lipid bilayers incorporating the Ca

release channel complex from skeletal sarcoplasmic reticulum (Liu *et al*, 1989). (6) It is widely accepted that the L-type voltage-sensitive Ca channel is sensitive to dihydropyridine agonists and antagonists in a number of tissue types (see Miller and Fox, 1990).

It is not felt that the channel in this study can be adequately described by the mean slope conductances that were calculated by measuring unitary current amplitude, for reasons discussed previously. Nevertheless, these values are interesting, and their meaning should not be dismissed, for several reasons: firstly, there is a striking similarity in these mean conductance values between the different tubule segments, with the exception of the DCT. Secondly, for all segments (including the DCT) there appears to be a definite relationship between the conductance values obtained for "bursts" and for "squares", suggesting that these different manifestations of behaviour are from the same channel type. Thirdly, the slope conductances as calculated for small "squares", are well within the range defined for L-type voltage-sensitive Ca channels. These have been reported to have a conductance of between 20 and 25 pS (in 100 mM Ba) for a number of excitable cell varieties (Miller and Fox, 1990). Voltage-sensitive Ca-permeable channels in non-excitable tissue types too have been shown to have conductance values within this range (von Tscharner *et al*, 1986; Rorsman *et al*, 1988).

An interesting feature of the channel in this study is the saturation of the unit current amplitude, shown by the collective I-V plots. Ruff *et al* (1986) have reported that current flow through the Ca channel is very complicated and non-ohmic due to saturation, and suggested that saturation probably results because the ions pass through the channel by binding to specific sites in the channel and moving in a "hop-scotch" fashion from one binding site to the next. Other channels have also been reported to show current saturation when the electrical driving force is increased; for example, Almers and McCleskey (1984) have shown that the potassium current in human muscle becomes saturated for large depolarisations of the cell membrane. We are not aware of any studies thus far that have reported total saturation of current flowing through a channel for both negative and positive holding potentials, similar to that observed in our study.

Some of the data in this study were obtained from cell-attached

patches. Since these data are few, however, a comparative study of the two patch configurations was not performed. An interesting phenomenon, however, occurred in those recordings from cell-attached patches which were later excised: channel activity observed in the cell-attached mode increased notably in the cell-excised mode. This phenomenon has also been observed in a patch containing a non-selective cation channel in the basolateral membrane of mouse thick ascending limb (Paulais and Teulon, 1989). A possible explanation for this phenomenon, suggested by these workers, is that the channel is gated by unphysiologically high Ca activities on the cytosolic side. It is possible that this channel is similar to the one found here. Another feature of cell-attached recordings was that the reversal potential values on the I-V relationships were nearly identical to those for recordings from cell-excised patches. In cortical collecting duct Na channels, Palmer and Frindt (1988) have suggested that this phenomenon is probably the result of a small cell potential ( $<5$  mV). In the recordings in this study, however, this observation is probably what would be expected for a non-selective channel, regardless of the intracellular potential.

The observation of similar channels on the basolateral membrane of human tubules is interesting, and was unexpected. Initially, experimentation on the apical membrane of human tubules was attempted in order to try and confirm the findings in this tissue type. However, owing to the relative ease with which the patch clamp technique could be applied to the basolateral membrane, the study was ultimately confined to this membrane. Most of the biopsy samples used were obtained from patients with various renal diseases. Some of these include systemic lupus erythematosus, mesengial capillary glomerulosclerosis, acute tubular necrosis, rapidly progressive glomerulonephritis, and mesangio-proliferative glomerulonephritis; it is therefore very possible that the data obtained from these samples are not a good indicator of channel activity in the normal human kidney. There has been no work to date on ion channels of any nature in the human kidney. However, it seems likely that the channels found on the basolateral membrane of human (proximal) tubules may also exist on the basolateral membrane of rabbit (proximal) tubules. Indeed there is evidence for the existence of a non-selective channel on the basolateral

membrane of rabbit late proximal tubule (Gogelein and Greger, 1986) as well as on the basolateral membrane of mouse thick ascending limb (Paulais and Teulon, 1989). The possible functional role of such channels in the basolateral membrane as well as in the apical membrane is discussed in some detail later.

The emergence of other channel varieties in this study was exciting and unexpected. Although these data are fragmentary, they are suggestive of two different types of channels: a non-selective channel with a high conductance in the apical membrane of rabbit DCT, and a low-conductance K channel in the apical membrane of rabbit cortical collecting duct and in the basolateral membrane of human (proximal) tubules. A high-conductance non-selective channel has not yet been reported to exist in either the apical or basolateral membrane of the DCT. On the other hand a low conductance K channel has been shown to exist in the apical membrane of rat cortical collecting duct (Frindt and Palmer, 1989). A most interesting observation was that channel activity from these other channel varieties sometimes occurred together with the "bursts" so typical of the Ca-permeable channel characterised in this study (Fig. 5.4 for example). The observation of these two clearly different channel varieties on a single patch is also a strong indication of the fact that the "burst" recordings were not simply artifacts due to seal breakdown.

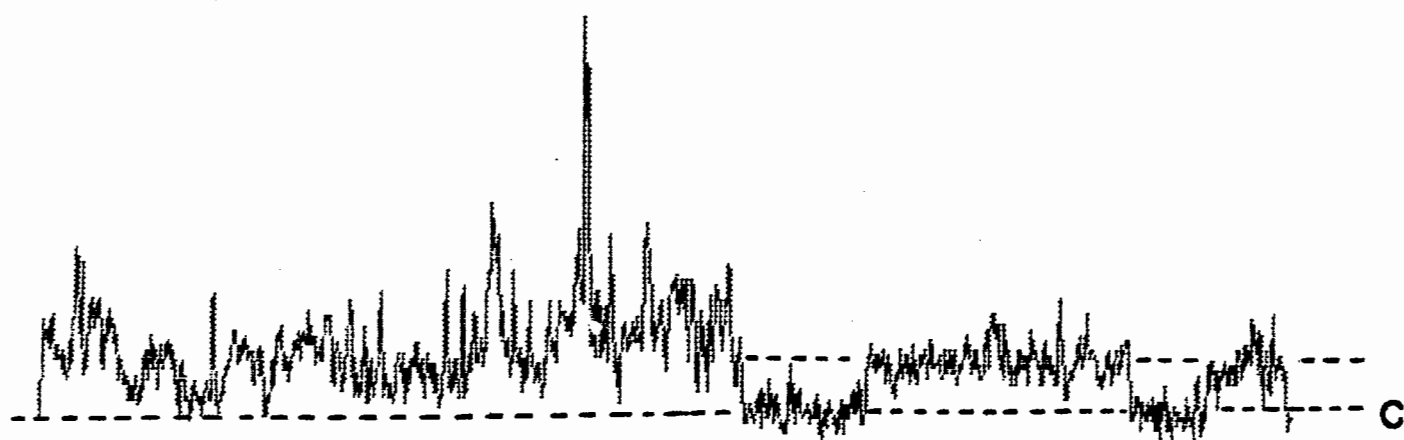


**Figure 5.4.** Example of a recording from a cell-excised patch in the apical membrane of a CCD. The bath solution contained KCl Ringers (KCl 140 mM), and the pipette solution,  $\text{CaCl}_2$  (70 mM). The trace shows an example of "bursts" and "spikes" superimposed on "square" channel events

### **5.3.3. Is there an adequate model to describe the structure and gating kinetics of the channel?**

It is well known that channels are structures formed by specialised proteins that span the cell membrane. In the past decade, much effort has been directed towards describing the structure of these channel proteins and developing kinetic models to explain their behaviour. Before attempting to assign a kinetic model to the channel observed in this study, it is important to first focus down to the microscopic level of the protein molecule comprising the ion channel, and to try to piece together some facts concerning the molecular details of the gating processes for ionic channels. Some early insight into the gating processes in Ca channels in frog muscle has been provided by Almers and McCleskey (1984). These workers showed that a non-selective current flowed through voltage-sensitive Ca channels in Ca-free solutions; however Ca channel blocking agents and micromolar Ca concentrations blocked the non-selective current. The findings were explained by postulating that ions flowed through the pore in a single-file fashion, and that the channel had ion binding sites that were highly selective for Ca ions. Their model of a Ca channel suggests that ions must overcome energy barriers to enter or leave the pore. The channel contains two binding sites, and the free energy of the ion-binding site combination is lowest when calcium is at the binding site. Consequently, when Ca is present, the channel binding sites will be occupied by Ca ions, and other cations will be excluded from the channel. Indeed, binding sites are evident in most voltage-sensitive cation channels because the amount of current flowing through a channel saturates with increasing ion concentration. Specific binding sites are thought to be located in or immediately outside the pore, so that an ion has to bind to the binding site before it can pass through the channel. Kostyuk *et al* (1989) have emphasised that, in the light of recent data, it is necessary to abandon the simplified idea about the selective filter of the Ca channel as a rigid structure not subjected to any dynamic changes during passage of ions through the ion channel. Passing ions interact with the channel wall and produce changes in it, thus affecting the gating mechanism.

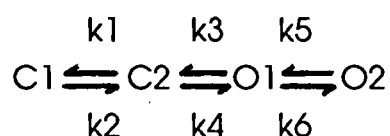
Some light has recently been thrown on the structure of channel proteins in a model provided by Liboff and McLeod (1988). They suggested that a channel is composed of three parts: there is a middle region containing, in the simplest configuration, a tubular channel that extends through the entire membrane thickness. There are also two specialised geometries at either end, extending away from the membrane into the cell interior. The two geometries serve as gating mechanisms, allowing influx of ions to the channel at one end and efflux from the channel at the other. In such a model there are two distinct energy areas; one at either end, connected to the gating mechanism, and another, lower energy region within the channel itself. They suggested that the energy distribution in this middle region enjoys "a periodicity reflecting the repeat order of the internal lattice due to the wraparound  $\alpha$ -helices that form the channel". It was suggested that these  $\alpha$ -helices act as building blocks, twisting together to form either a central cylindrical hole or one that is perhaps interwoven through the body of the protein. According to these workers, ions may therefore follow prescribed helical paths through the channel. Furthermore they developed a theory to suggest that one finds a set of quantised states for the conductivity, which can be derived from "cyclotron resonance" conditions. These workers claim that such a model serves to provide a relatively clean explanation for the multiple conductance states in many membrane channels.

The variety and number of ion channels that have subconductance states demonstrates the generality of the phenomenon. A criterion for recognising subconductance states has been proposed by Fox (1987): a channel substate should interconvert with the channel main state; thus direct transitions from one conductance level to another should be observed. It has been found, however, that openings to the substate also occur independently of openings to the main state (Hamill et al 1981; Trautmann, 1982; Takeda and Trautmann, 1984). The number of subconductance states has also been shown to be temperature-dependent (Chinn and Narahashi, 1989). Subconductance states are simply the result of subunit-type behaviour, and occur when channel conductance changes in increments of equal amplitude, as if one, then two or several identical subunits are being recruited. However, although,

the main state conductance of many channels has been shown to be an integer multiple of the lowest substate conductance, channels formed by subunit aggregation need not necessarily have equal substate conductances (Fox, 1988). Study of subconductance states may provide useful information about channel structure and permeation mechanisms. Although the channel in this study does not appear to have a main state conductance level, the data suggest that there are discrete subunit conductance states, which in some cases, appear to be identical. In addition, direct transitions from one conductance level to another are often observed. The channel protein here may thus consist of a multimeric structure of subunits, which lack a single overriding gating mechanism. This model is similar to a model proposed for the calcium release channel of sarcoplasmic reticulum (Liu *et al*, 1989) in which the opening of the central pore of the channel is regulated by separate coupled subgates, present within the channel complex.

What portion of this protein molecule controls the gating kinetics of the channel? In this study, the various agonists and antagonists opened or blocked the channel from the cytoplasmic side, and in some cases these effects were voltage-dependent; thus they probably bind to a site near the cytoplasmic opening of the pore. This suggests that the gating mechanism is at the cytoplasmic side, as is the case with many other cation channels (Jan and Jan, 1989), and supports recent views that the channel is asymmetrical with regards to its structure and gating properties. In the cases in which the channel was irreversibly blocked, it is possible that the drug became "trapped" in the channel as it closed.

Standard, as well as alternative statistical procedures have been applied to the patch clamp data in this study. From counting the number of exponential components in the observed open- and closed-time histograms, the channel could be described by at least two open and two closed states. In the simplest case, therefore, the kinetics of the channel might be described by the following scheme of channel gating:





where C1 and C2 denote the shut states, O1 and O2 denote the two open states, and  $k_1$ - $k_6$  are the rate constants for the reaction. According to this kinetic model, the channel protein is viewed in terms of discrete kinetic states that interconvert as a result of a conformational change. According to Markovian principles, upon which this model is based, the rates of transitions between states are time-independent and set to some mean value that is determined ultimately by random stretching and bending of the channel protein.

More recent views of channel kinetics (outlined by Pallota, 1991) suggest that these kinetic states probably correspond to many different conformational states, and that unless these conformational states directly affect channel opening and closing, the kinetic approach cannot detect them. It is therefore unlikely that the few discrete states in the above kinetic scheme are sufficient to account for the fact that protein molecules can adopt many conformations.

The observation of the irregular "burst" nature of the recordings, as well as considerations of protein dynamics prompted exploration of alternative fractal models (Liebovitch *et al*, 1987) and ion diffusional models (Millhauser, 1988). Essentially the fractal model assumes that the channel can exist in an infinite number of energy states, perhaps due to subtle differences in protein conformation. Consequently, transitions from one state to another would be governed by a continuum of rate constants, rather than a few discrete states. The diffusional model proposes that the channel can occupy many conformational states, but assumes that the number of required rate constants is small because these rate constants are all equal. Openings occur as the channel "diffuses" from the closed to the open state, with open lifetimes determined by the time it takes the channel to diffuse back to the closed states.

The predictions for these alternative theories were tested on the data by generating log-log plots of the open- and closed-time histograms, and phase space plots for consecutive channel amplitudes and open times. The absence of a "strange attractor" on the phase space plots suggests that the fractal model is not suitable for describing sequential channel

amplitudes or open times. Although the linearity of the log-log plots is a phenomenon that can be accounted for by the fractal model, the samples were too few to adequately test this model.

When modelling patch clamp data, the view usually taken is that the simplest kinetic scheme is the correct scheme; and the simplest kinetic scheme is interpreted to mean that with the fewest conformational states. The question remains as to whether these descriptions are realistic from a molecular point of view. Thus, although the data are best described by a two state Markovian model, and although the data samples used were not large enough to adequately test the predictions laid down by the fractal and diffusional models, the theories that these models put forward nevertheless provide an attractive explanation for some of the qualitative features of channel behaviour observed in this study, notably: 1) in many cases channel events do not appear to simply switch from a closed to an open state, but rather undergo a gradual transition between states, involving the opening (or closing) of many conductive units comprising the channel. It is easy to imagine that such a process is governed by a continuum of rate constants. 2) It is conceivable that the "burst" activity, when viewed at different time scales, has the property of self-similarity which underlies the fractal concept. 3) The "burst" phenomenon is also elegantly explained by an analogy encompassed by the diffusional model; the illustration is of an ion approaching an energy barrier, which when encountered causes a channel opening. When the particle is near the barrier, the probability of encounter is high, so that when one event occurs, it is very likely that several more will follow. When the particle is far from the barrier, the probability of encounter is low and a long quiescent period will follow.

Thus, although the successful application of these alternative analytical techniques to patch clamp data remains controversial, the concepts underlying fractal and diffusional models nevertheless provide an exciting alternative view of channel kinetics and behaviour.

#### 5.3.4. What is the functional role of these channels in the kidney?

As the observations were confined mostly to excised inside-out patches, we cannot comment on the channel's characteristics *in vivo*: as with other channel types, these might well be modulated by a number of intracellular factors. In general the data presented here are consistent with the presence of apical, voltage-sensitive, Ba- and Ca- permeable non-specific cation channels in all the tubule segments examined. This finding is in accord with earlier descriptions of Ca (and Na) reabsorption along the whole length of the mammalian nephron (Friedman, 1988).

It is of particular interest that the channel was found in the DCT with a mean unit current amplitude significantly higher than for the other segments. It is generally agreed that Ca reabsorption here occurs wholly by active transport. Its presence here is consistent with passive entry of Ca ions into the cell, and with subsequent exit to the peritubular fluid by active transport across the basolateral membrane. Also, since Ca movement in this segment is exclusively transcellular, it is conceivable that more efficient Ca conductive pathways are required to allow the passive movement of Ca across the apical membrane. This might explain why the mean unit current amplitude for this segment is higher than for the other segments.

The pipette solution in this study contained a hypo-osmotic solution (70 mM  $\text{CaCl}_2$  has an osmolality of approximately 150 mOsmoles). Such a solution would act as a negative hydrostatic pressure in the pipette. The possibility therefore exists that the channels in this study were stretch-sensitive; such channels might play a role in cell volume regulation.

The positive effects of PTH on the channel in the TAL and the DCT are consistent with the effects of PTH on these segments *in vivo*: PTH reduces the GFR, thereby decreasing the filtered load of Ca, and enhances tubular reabsorption of Ca resulting in decreased Ca excretion. These effects are confined to the cortical thick ascending limb and the DCT (Rouse and Suki, 1990). There is evidence to suggest that PTH leads to the activation of dihydropyridine-sensitive Ca-permeable channels in these segments (Bacskai and Friedman, 1990). This activation may be indirectly induced by intracellular second messengers.

The channel described here may also represent a key component in the maintenance of the parallelism between Ca and Na clearance in the kidney. This parallelism is borne out by the observation that changes in Ca excretion are closely paralleled by changes in Na excretion, even during various types of diuresis or variations in Na intake. Evidence points to the fact that Ca reabsorption parallels Na reabsorption in all segments with the possible exception of the proximal straight tubule and the distal tubule. It is thus conceivable that a Ca- and Na-permeable channel might exert some control in maintaining the parallelism between Ca and Na clearance; this control might be achieved if the channel is able to alter its Ca:Na selectivity ratio depending on the relative concentrations of the two ions, or other influencing factors, in the lumen. Fine control might also be achieved if the channel is able to recruit any number of conductive units to regulate the diffusion of ions across the membrane.

The functional significance of a Ca-permeable, non-selective channel in the basolateral membrane of human (or other mammals) proximal tubule is unclear. It is unlikely that the channel here is involved in transcellular Ca reabsorption, as the ionic gradient for Ca ions across the membrane would result in the movement of Ca back into the cell through such a channel. It is possible, however, that the channel might play a role in the modulation of Na or Ca reabsorptive flux through the epithelium. It might also play a role in cell volume regulation processes.

What are the clinical implications of such a Ca transporting channel in the kidney? Perhaps the most important disorder of renal Ca excretion is idiopathic hypercalciuria, in which a normal plasma Ca level is associated with a high urinary Ca output, and with increased incidence of calcium oxalate and calcium phosphate kidney stones (Bronner, 1989). The pathophysiology of this disorder is not fully understood. In some cases, there is evidence to suggest a primary defect in tubular Ca reabsorption, to which dietary factors such as high salt or protein intake may contribute. Indeed, Modlin (1967) has shown that renal stone formers have an abnormally high ratio of urinary Ca to Na; this finding is consistent with some anomaly of a Ca and Na-permeable channel. At present, thiazides are commonly used in the prevention of renal stone formation (Yindt *et al*, 1970; Gill and Rose, 1985; Finlayson, 1974). This diuretic is thought to act by increasing the luminal permeability to Ca in the distal nephron. It is

therefore possible that it alters transcellular Ca flow by exerting its effect on a Ca-permeable channel, and in this way, corrects hypercalciuria. In the light of this possibility, there may be other agents too that are effective in enhancing Ca reabsorption by acting on a Ca-permeable channel.

### **5.3.5. Where to from here?**

This study provides a platform upon which future studies can be built. Before considering future studies, however, it is important to first consider, in hindsight, what would have been done at the start of the project, if what is known now was known then.

Firstly, owing to the extreme difficulty in obtaining tight seals from the apical membrane of freshly dissected tubules, and the resultant slow rate in data collection, the study would have been confined to the basolateral membrane of human and possibly also rabbit tubules. Long lasting tight seals could be obtained more easily on this membrane than on the apical membrane. Secondly, experiments involving solution changes and drug additions would have been performed using the "hanging drop" technique. The advent of this technique in the study considerably reduced the number of "seal deaths" during transfer. It also enabled relatively noise-free recordings to be made in the alternate solution. Thirdly, initial experiments would not have been performed on isolated perfused tubules. Although this technique enables access of the lumen to a patch electrode, the ripped tubule technique was less laborious and more efficient. Finally, the final version of the data analysis program would have been used throughout the project. The continual modification of the program during the course of the project meant that data had to be reanalysed on a regular basis.

The characterisation of the channel in this study with Ca channel agonists and antagonists and solutions of different ionic composition is still at a fairly preliminary stage. This characterisation clearly needs to be taken further to clarify the channel's response to these drugs as well as to determine the relative ion permeabilities of the channel. A further challenge is a deeper investigation into the effects of PTH and diuretics (such as chlorothiazide) on single Ca-permeable channel activity in the

DCT and TAL. The data provided here are preliminary but suggestive of PTH-induced channel activity. Another useful future study would be the search for Ca-permeable channels on the apical membrane of human tubules. Although the properties of these channels in the apical membrane of rabbit tubules are most probably the same as in human tubules, it would nevertheless be interesting to confirm their presence here. Indeed, the single experiment performed on the apical membrane of a human tubule segment in this study, is suggestive of their presence here.

Finally, future studies will be required to determine the relative contribution of apical Ca-permeable channels to total Ca transport in the kidney. This will require the application of techniques such as the isolated perfused tubule technique and whole cell recording techniques to determine the macroscopic behaviour of the total population of these channels per cell and per tubule segment. A comparison of single channel data and whole cell data will then be useful in determining the number of these channels per cell and therefore the measure of their contribution to transcellular Ca movement.

Indeed, an ongoing Ca-45 flux study using isolated perfused tubules has recently been embarked on by us in this department and is providing additional evidence in support of the existence of a Ca-selective channel down the length of the nephron. These studies are making use of the isolated perfused technique to perfuse rabbit tubule segments with the isotope Ca-45. The concentration of Ca-45 that appears in the bath is then a measure of the Ca reabsorption across the tubular wall. Some of these preliminary data (unpublished) are shown in Fig. 5.4.

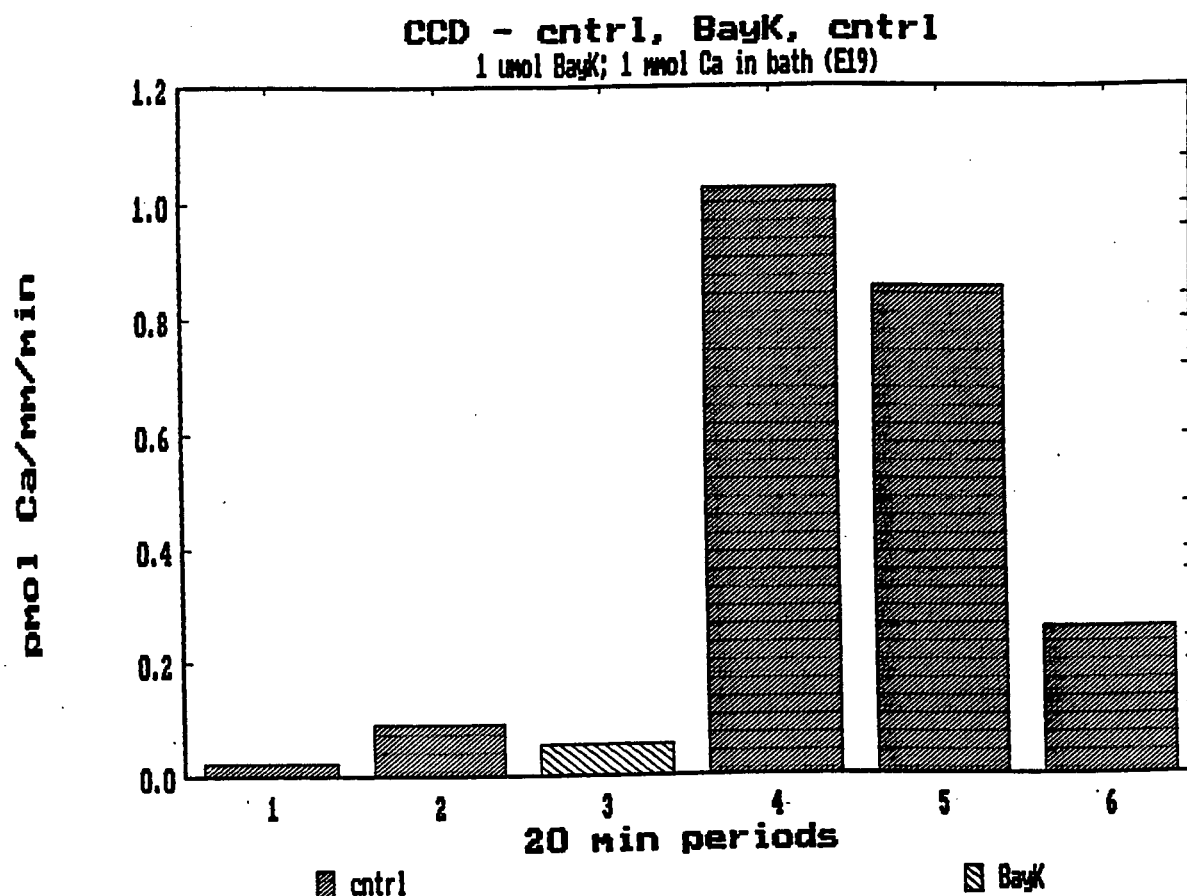


**Figure 5.4.** Bar graph depicting the profile of Ca reabsorption in a CCD before, during, and after addition of Bay K-8644. A similar profile has been observed for the PST and TAL (data not shown).

The addition of Bay K-8644 (1  $\mu$ M) to the perfusate appeared to increase the rate of Ca reabsorption; this increase was generally observed to occur several minutes after addition of the drug and was maintained for a considerable length of time after washout of the drug, before a decrease was observed.

The reason for this delayed effect of Bay K-8644 is not known. A possible explanation, however, is that it may take time for the Ca-ATPase in the basolateral membrane to be "switched on" following increased ( $\text{Ca}_i$ ) due to Bay K-8644-stimulated increase in Ca channel activity. There may thus be a certain measure of intracellular Ca pooling that takes place prior to extrusion. Thus far, these studies are providing additional evidence for the existence of a dihydropyridine-sensitive Ca-permeable

channel down the length of the nephron, and are also suggestive of a significant role of this channel in renal Ca transport.



**SECTION SIX**

**CONCLUSION**

## SECTION SIX

### CONCLUSION

In conclusion, the channel described in this study possesses the following basic characteristics:

- 1) The reversal potential of the channel is consistently close to zero, indicating that the channel is non-selective. A number of non-selective channels have been shown to exist in the kidney.
- 2) Many of the recordings show channel activity in the downward direction. This corresponds either to the movement of Ca or Ba out the pipette or the movement of Cl into the pipette. However, since Cl channels have been shown not to exist in certain parts of the nephron, this downward current most likely corresponds to a Ba or Ca flux through the channel. Channel activity in the upward direction most probably reflects the movement of Na ions into the pipette.
- 3) In a number of cases the channel responded to dihydropyridine agonists and antagonists, as well as to parathyroid hormone. Although these studies are preliminary, such sensitivity to these pharmacological agents is considered to be a hallmark of the L-type, voltage-sensitive Ca channels.
- 4) The channel exhibits multiple conductance states with unit current amplitudes in the range of tenths of picoamperes. Measurement of such unitary amplitudes enabled a subjective estimation of mean slope conductances. In spite of this subjectivity, these values are consistent with values for other voltage-sensitive Ca channels in both excitable and non-excitable tissue. Multiple conductance states have been shown to occur in Ca channels from a number of tissue types, including non-excitable tissue.

It is felt therefore that the present study provides evidence consistent with

the presence of apical, voltage-sensitive, Ba- and Ca-permeable, non-specific cation channels in all the rabbit tubule segments examined. This finding is presently being confirmed in studies measuring fluxes of Ca-45 tracer isotope from lumen to bath in isolated perfused rabbit tubules. The existence of such a channel is in accord with earlier descriptions of Ca reabsorption along the whole length of the nephron.

A similar channel was found in the basolateral membrane of human tubules. The basic "signature" of this channel was similar in nearly all respects to that of the channel found in the apical membrane of the rabbit tubules. Its functional significance, however, is not clear.

In the majority of cases the Ca-permeable channel described here has kinetics consistent with two open states and two closed states. Although alternative analysis techniques were applied to the data in some cases, the data samples were too small to accurately interpret the results of these analyses.

The nature of this study is exploratory. The prospects of future research in this field are thus exciting and should represent a challenge to any investigator interested in epithelial Ca channels.

Preliminary accounts of this work have been presented at the 31st International Congress of Physiological Sciences (Helsinki, 1989), and at the NATO Advanced Research Workshop on "Calcium Transport and Intracellular Calcium Homeostasis" (Lyon, 1990).

## **SECTION SEVEN**

### **REFERENCES**

## SECTION SEVEN

### REFERENCES

- Aldrich, R.W., and Yellen, G. (1983). Analysis of nonstationary kinetics. In "Single-Channel Recording" (B. Sakmann and E. Neher, eds.), pp 287-299. Plenum Press, New York.
- Almers, W., and McCleskey, E.W. (1984). The non-selective conductance in calcium channels of frog muscle: calcium selectivity in a single file pore. *Journal of Physiology (Lond)* 353, 585-608.
- Armstrong, C.M., and Matteson, D.R. (1985). Two distinct populations of calcium channels in a clonal line of pituitary cells. *Science* 227, 65-67.
- Ashcroft, F.M., Rorsman, P., and Trube, G. (1989). Single calcium channel activity in mouse pancreatic  $\beta$ -cells. In "Calcium Channels: Structure and Function". D. Wray, R. Norman, and P. Hess, eds.), pp 410-412, New York Academy of Sciences, New York.
- Backskai, B.J., and Friedman, P.A. (1990). Activation of latent Ca channels in renal epithelial cells by parathyroid hormone. *Nature* 347, 388-391.
- Beam, K.C., Knudson, C.M., and Powell, J.A. (1986). A lethal mutation in mice eliminates the slow calcium current in skeletal muscle cells. *Nature* 320, 168-170.
- Bean, B. (1989). More than a Ca channel. *Trends in Neurological Sciences* 12 No.4, 128-130.
- Bean, B.P. (1985). Two kinds of calcium channels in canine atrial cells. Differences in kinetics, selectivity and pharmacology. *Journal of General Physiology* 86, 1-30.
- Beck, L.H., and Goldberg, M. (1973). Effects of acetazolamide and parathyroidectomy on renal transport of Na, calcium, and phosphate. *American Journal of Physiology* 224, 1136-1142.
- Benham, C.D. and Tsien, R.W. (1987). A novel receptor-operated Ca-permeable channel activated by ATP in smooth muscle. *Nature* 328, 275-278.
- Bengele, H.H., Alexander, E.A., and Lechene, C.P. (1980). Calcium and Magnesium transport along the inner medullary collecting duct of the rat. *American Journal of Physiology* 239, F24-F29.
- Bindels, R.J.M., Timmermans, J.A.H., Bakens, R.J.J.M., Hartog, A., van Leeuwen, E., and van Os, C.H. (1990). Mechanisms and sites of transepithelial Ca transport in kidney cells. *NATO Advanced Research*

Workshop on "Calcium Transport and Intracellular Calcium Homeostasis."  
Lyon, France.

Bleich, M., Schlatter, E., and Greger R. (1990). The luminal K channel of the thick ascending limb of Henle's loop. *Pflügers Archives* 415, 449-460.

Bourdeau, J.E. (1986). Calcium transport across the pars recta of cortical segment 2 proximal tubules. *American Journal of Physiology* 251, F718-F724.

Bourdeau, J.E., and Burg, M.B. (1979). Voltage-dependence of calcium transport in the thick ascending limb of Henle's loop. *American Journal of Physiology* 236 (4), F357-F364.

Bourdeau, J.E., Hellstrom-Stein, R.J. (1982). Voltage-dependent calcium movement across the cortical collecting duct. *American Journal of Physiology* 242, F285-F292.

Bronner, F. (1989). Renal calcium transport: mechanisms and regulation - an overview. *American Journal of Physiology* 257 (Renal Fluid Electrolyte Physiol.26), F707-F711.

Bronner, F. (1990 a). Transcellular Calcium Transport. In "Intracellular Calcium Regulation". (F. Bronner, ed.) Wiley-Liss.

Bronner, F. (1990 b). Transepithelial calcium transport in gut and kidney. NATO Advanced Workshop on "Calcium Transport and Intracellular Calcium Homeostasis." Lyon, France.

Bronner, F. (1991). Calcium entry and calcium channels. Personal communication. In press.

Bronner, F., and Stein, W.D. (1988). CaBP facilitates intracellular diffusion for Ca pumping in distal convoluted tubule. *American Journal of Physiology* 255 (Renal Fluid Electrolyte Physiol.26), F558-F562.

Bronner, F., Pansu, D., and Stein, W.D. (1986). An analysis of intestinal calcium transport across the rat intestine. *American Journal of Physiology* 250 (Gastrointest. Liver Physiol.13), G561-G569.

Bruns, M.E.H., and Bruns, D.E. (1990). Calbindin-D9K localisation and gestational changes in the utero-placental unit: A model for a maternal-fetal calcium transport. NATO Advanced Research Workshop on "Calcium Transport and Intracellular Calcium Homeostasis." Lyon, France.

Burg, M., Grantham, J., Abramov, M., and Orloff, J. (1966). Preparation and study of fragments of single rabbit nephrons. *American Journal of Physiology* 210, 1293-1298.

Campbell, D. 1987 Chaos: Chto Delat? *Nuclear Physics* 2, 541-567.

Carbone, E., and Lux, H.D. (1984). A low voltage-activated calcium conductance in embryonic chick sensory neurons. *Biophysical Journal* 46, 413-418.

Cheung, W.Y. (1980). Calmodulin: An introduction. In "Calcium and Cell Function" (W.Y Cheung ed.) Vol.1, Academic Press.

Chinn, K., and Narahashi, T. (1989). Temperature-dependent subconducting states and kinetics of deltamethrin-modified sodium channels of neuroblastoma cells. *Pflugers Archives* 413, 571-579.

Christakos, S., Brunette, M.G., and Norman, A.W. (1981). Localisation of immunoreactive vitamin D-dependent calcium binding protein in chick nephron. *Endocrinology* 109(1), 322-324.

Christine, C.W., Laskowski, F.H., Gitter, A.H., Gross, P., and Fromter, E. (1987). Chloride-sensitive single ion channels in the apical membrane of cultured collecting duct principal cells. *Pflugers Archives* 468, R32.

Cohen, C.J., McCarthy, R.T., Barrett, P.Q., and Rasmussen, H. (1988). Ca channels in adrenal glomerulosa cells: K and angiotensin 2 increase T-type Ca channel current. *Proceeding of the National Academy of Sciences* 85, 2412-2416.

Colquhoun, D. (1987 a). Practical analysis of single channel recording. In "Microelectrode Techniques: the Plymouth Workshop Handbook." (P.T.A Gray, M.J Whitaker, N.B. Standen, eds.), pp 83-104. The Company of Biologists, Ltd., Cambridge.

Colquhoun, D. (1987 b). The interpretation of single channel recordings. In "Microelectrode Techniques: the Plymouth Handbook." (P.T.A Gray, M.J Whitaker, N.B. Standen, eds.), pp 105-135. The Company of Biologists, Ltd., Cambridge.

Colquhoun, D., and Hawkes, A.G. (1983). The principles of stochastic interpretation of ion channels mechanisms. In "Single-Channel Recording." (B. Sakmann and E. Neher, eds.), pp 135-176. Plenum Press, New York.

Colquhoun, D., and Sigworth, F.J. (1983). Fitting and statistical analysis of single channel records. In: "Single Channel Recording" (B. Sakmann and E. Neher, eds.), pp 135-175, Plenum Press, New York.

Condat, C.A., and Jackle, J. (1989). Closed-time distribution of ionic channels. *Biophysical Journal* 55, 915-925.

Corey, D.P., and Stevens, C.F. (1983). Science and technology of patch recording electrodes. In "Single-Channel Recording" (B. Sakmann and E. Neher, eds.), pp.53-68, Plenum press, New York.

Costanzo, L.S., and Weiner, I.M. (1974). On the hypocalciuric action of chlorothiazide. *Journal of Clinical Investigation*. 54, 628-637.

Costanzo, L.S., and Windhager, E.E. (1978). Calcium and sodium transport by the distal convoluted tubule of the rat. *American Journal of Physiology* 235(5), F492-F506.

Cota, G., and Stefani, E. (1985). Fast and slow Ca channels in twitch

muscle fibres of the frog. *Biophysical Journal* 47, 65a.

Cull-Candy, S.G., and Usowicz, M.M. (1987). Multiple-conductance channels activated by excitatory amino acids in cerebellar neurons. *Nature* 325, 525 - 528.

Demongeot, J., Jacob, C., and Cinquin, P. (1987). Periodicity and chaos in biological systems. New tools for the study of attractors. In "Chaos in Biological Systems" (H. Degan, A.V. Holden and L.F. Olsen, eds.), pp 255-265. Plenum Press, New York.

Doucet, A., and Katz, A.I., (1982). High affinity Ca-Mg ATPase along the rabbit nephron. *American Journal of Physiology* 242 (Renal Fluid Electrolyte Physiol.11), F346-F352.

Duarte, C.G., and Watson, J.F. (1967). Calcium reabsorption in proximal tubule of the dog nephron. *American Journal of Physiology* 212, 1355-1360.

Edwards, B.R., Baer, P.C., Sutton, R.A.L., and Dirks, J.H. 1973. Micropuncture study of diuretic effects on sodium and calcium reabsorption in the dog nephron. *Journal of Clinical Investigation* 52, 2418-2427.

Edwards, B.R., Sutton, R.A.L., and Dirks, J.H. (1971). Micropuncture study of calcium reabsorption in the dog kidney. *Clinical Research* 19, 807.

Edwards, B.R., Sutton, R.A.L., and Dirks, J.H. (1974). Effect of calcium infusion on renal tubular reabsorption in the dog. *American Journal of Physiology* 227, 13-18.

Fatt, P., and Katz, B. (1953). The electrical properties of crustacean muscle fibres. *Journal of Physiology* 120, 171-204.

Findlay, F., Ashcroft, M., Kelly, R.P. Rorsman, P., Peterson, O.H., and Trube, G. (1989). Calcium currents in insulin-secreting  $\beta$ -cells. In "Calcium Channels: Structure and Function". (D. Wray, R. Norman, and P. Hess, eds.) pp 403-409, New York Academy of Sciences, New York.

Finlayson, B. 1974. Renal lithiasis in review. *Urologic Clinics of North America* 1(2), 181-212.

Fleckenstein, A. (1988). Historical overview. The Ca channel of the heart. *Annals New York Academy of Sciences* 522, :1-16.

Fox, A.P., Nowycky, M.C., and Tsien, R.W. (1987). Kinetics and pharmacological properties distinguish three types of calcium currents in chick sensory neurons. *Journal of Physiology* 394, 149-172.

Fox, J.A. (1987). Ion channel subconductance states. *Journal of Membrane Biology* 97, 1-8.

Frick, A., Rumrich, G., Ullrich, K.J., Lassiter, W.E. (1965). Microperfusion study of calcium transport in the proximal tubule of the rat kidney. *Pflügers Archives* 286, 109-117.



Friedman, P.A. (1988 a). Basal and hormone-activated calcium absorption in mouse renal thick ascending limbs. *American Journal of Physiology* 254 (Renal Fluid Electrolyte Physiol.23), F62-F70.

Friedman, P.A. (1988 b). Renal calcium transport: sites and insights. *News in Physiological Sciences* 3, 17-21.

Frindt, G., and Palmer, L.G. (1987). Ca-activated K channels in apical membrane of mammalian CCT, and their role in K secretion. *American Journal of Physiology* 252 (Renal Fluid Electrolyte Physiol.21), F458-F467.

Frindt, G., and Palmer, L.G. (1989). Low conductance K channels in apical membrane of rat cortical collecting tubule. *American Journal of Physiology* 256 (Renal Fluid Electrolyte Physiol. 25), F143-F151.

Frindt, G., and Palmer, L.G. (1989). Low-conductance K channels in apical membrane of rat cortical collecting tubule. *American Journal of Physiology* 256 (Renal Fluid Electrolyte Physiol.25), F143-F151.

Gardner, P., Alcover, A., Kuno, M., Moingeon, P., Weyand, C.M., Goronzy, J., and Reinherz, E.L. (1989). Triggering of T-lymphocytes via either T3-Ti or T11 surface structures opens a voltage-insensitive plasma membrane calcium permeable channel. *Journal of Biological Chemistry* 264, 1068-1076.

Garnier, D., Rougier, O., Gargouil, M., and Coraboeuf, E. (1969) Analyse electrophysiologique du plateau des responses myocardiques mise en evidence d'un courant lent entrant en absence d'ions bivalents. *Pflugers Archives* 313, 312-342.

Gill, H.S., and Rose, G.A. 1985. Idiopathic hypercalciuria. *Urological Research* 13, 271- 275.

Gleick, J. (1987). *Chaos: making a new science*. New York: Viking.

Gogelein, H. (1988). Chloride channels in epithelia. *Biochemica et Biophysica Acta* 947, 521-547.

Gogelein, H. (1990). Ion channels in mammalian proximal renal tubules. *Renal Physiology and Biochemistry* 13, 8-25.

Gogelein, H., and Greger, R. (1984). Single channel recordings from basolateral and apical membranes of renal proximal tubules. *Pflugers Archives* 401, 424-426.

Gogelein, H., and Greger, R. (1986 a). A voltage-dependent ionic channel in the basolateral membrane of late proximal tubules of the rabbit kidney. *Pflugers Archives* 407 (suppl 2), S142-S148.

Gogelein, H., and Greger, R. (1986 b). Na-selective channels in the apical membrane of rabbit late proximal tubules (pars recta). *Pflugers Archives* 406, 198-203.

Gogelein, H., and Greger, R. (1987). Properties of single K channels in the basolateral membrane of rabbit proximal straight tubules. *Pflügers Archives* 410, 288-295.

Gogelein, H., and Greger, R. (1988). Patch clamp analysis of ionic channels in renal proximal tubules. *Nephrology* 1, 159-178.

Gogelein, H., and Pfannmüller, B. (1989). The nonselective cation channel in the basolateral membrane of rat exocrine pancreas. *Pflügers Archives* 413, 287-298.

Goldberger, A.L., and West, B.J. (1987). Chaos in Physiology: Health or disease. In "Chaos in Biological Systems" (H. Degani, A.V. Holden and L.F. Olsen, eds.), pp 1-4. Plenum Press, New York.

Goldberger, A.L., Rigney, D.R., and West, B.J. (1990). Chaos and fractals in human physiology. *Scientific American*, 35-41.

Goto, K., Kasuya, Y., Matsuki, N., Takuwa, Y., Kurihara, H., Ishikawa, T., Kimura, S., Yanagisawa, M., and Masaki, T. (1989). Endothelin activates the dihydropyridine-sensitive voltage-dependent Ca channel in vascular smooth muscle. *Proceedings of the National Academy of Sciences* 86, 3915-3918.

Gray, R.A. and Johnstone, D. (1986). Multiple types of calcium channels in acutely exposed neurones from the adult guinea pig hippocampus. *Journal of General Physiology* 88, 25a.

Greger, R., and Gogelein, H. (1985). Role of K conductive pathways in the nephron. *Kidney International* 31, 1055-1064.

Greger, R., Bleich, M., and Schlatter, B. (1990). Ion channels in the thick ascending limb of Henle's loop. *Renal Physiology and Biochemistry* 13, 37-50.

Grissmer, S., and Cahalan, M.D. (1989). Divalent ion trapping inside potassium channels of human T-lymphocytes. *Journal of General Physiology* 93, 609-630.

Gross, P., Minuth, W.W., Ketteler, M., and Fromter, E. (1988). Ionic conductances of cultured principal cell epithelium of renal collecting duct. *Pflügers Archives* 412, 434-441.

Guggino, S.E., Guggino, W.B., Green, N., and Sacktor, B. (1987 a). Blocking agents of Ca-activated K channels in cultured medullary thick ascending limb cells. *American Journal of Physiology* 252 (Cell Physiol.21), C128-C137.

Guggino, S.E., Guggino, W.B., Green, N., and Sacktor, B. (1987 b). Ca-activated K channels in cultured medullary thick ascending limb cells. *American Journal of Physiology* 252 (Cell Physiol. 21), C121-C127.

Gutnick, M.J., Lux, H.D., Swandulla D., and Zucker, H. (1989). Voltage-dependent and calcium-dependent inactivation of calcium channel current in identified snail neurones. *Journal of Physiology* 412, 197-220.

Hamill, O.P., Marty, A., Neher, E., Sakman, B., and Sigworth, F.J. (1981). Improved patch clamp techniques for high resolution current recording from cells and cell-free membrane patches. *Pflügers Archives* 391, 85-100.

Heizmann, C.W. (1990). Molecular and functional aspects of some cytosolic calcium-binding proteins. NATO Advanced Research Workshop on "Calcium Transport and Intracellular Calcium Homeostasis." Lyon, France.

Hess, P., Lansman, J.B., and Tsien, R.W. (1984). Different modes of Ca channel gating behaviour favoured by dihydropyridine Ca agonists and antagonists. *Nature* 311, 538-544.

Hunter, M., and Giebisch, G. (1987). Multi-barrelled K channels in renal tubules. *Nature* 327, 522-524.

Hunter, M., Kawahara, K., and Giebisch, G. (1986 a). Potassium channels along the nephron. *Federation Proceedings* 45, 2723-2726.

Hunter, M., Lopes, A.G., Boulpaep, E., and Giebisch, G. (1986 b). Regulation of single potassium ion channels from apical membrane of rabbit collecting tubule. *American Journal of Physiology* 251 (Renal Fluid Electrolyte Physiol. 20), F725-F733.

Imai, M. (1981). Effects of parathyroid hormone and N<sup>6</sup>, O<sup>2</sup> dibutyryl cyclic AMP on Ca transport across the rabbit distal nephron segments perfused in vitro. *Pflügers Archives* 390, 145-151.

Imai, M. (1981). Effects of parathyroid hormone and N<sup>6</sup>, O<sup>2</sup>-Dibutyryl Cyclisc AMP on Ca transport across the rabbit distal nephron segments perfused inj vitro. *Pflügers Archives* 390, 145-151.

Jahr, C.E. and Stevens, C.F. (1987). Glutamate activates multiple single channel conductances in hippocampal neurons. *Nature* 325, 522-525.

Jamison, R.L., Frey, N.R., and Lacy, F.B. (1974). Calcium reabsorption in the thin loop of Henle. *American Journal of Physiology* 227, 745-751.

Jan, L. Y. and Jan Y. N. (1989). Voltage-sensitive ion channels. *Cell* 56, 13-25.

Jensen, K.S., Holstein-Rathlov, N., Leysacc, P.P., Mosekilde, E., and Rasmussen, D.R. (1987). Chaos in a system of interacting nephrons. In "Chaos in Biological Systems" (H. Degan, A.V. Holden and L.F. Olsen, eds.), pp 23-32. Plenum Press, New York.

Kagan, Y.Y., and Knopoff, L. (1981). Stochastic synthesis of earthquake catalogs. *Journal of Geophysical Research* 86, 2853-2862.

Kass, R.S., and Arena, J.P. (1989). Influence of pH<sub>o</sub> on calcium channel block by Amlodipine, a charged dihydropyridine compound. *Journal of General Physiology* 93, 1109-1127.

Kawahara, K., Hunter, M., and Giebisch, G. (1987). Potassium channels in Necturus proximal tubule. *American Journal of Physiology* 253 (Renal Fluid Electrolyte Physiol. 22), F488-F494.

Klee, C.B. (1980). Calmodulins: Structure-function relationships. In "Calcium and Cell Function", (W. Cheung, ed.), Vol.1, Academic Press.

Koeppen, B.M., Beyenbach, K.W., and Helman, S.I. (1984). Single-channel currents in renal tubules. *American Journal of Physiology* 247 (Renal Fluid Electrolyte Physiol. 16), F380-F384.

Koeppen, B.M., Biagi, B.A., and Giebisch, G.H. (1983). Intracellular microelectrode characterization of the rabbit cortical collecting duct. *American Journal of Physiology* 244 (Renal Fluid Electrolyte Physiol. 13), F35-F47.

Kolb, H. (1990). Ion channels in Opossum kidney cells. *Renal Physiology and Biochemistry* 13, 26-36.

Korn, S.J., and Horn, R. 1988. Statistical discrimination of fractal and Markov models of single-channel gating. *Biophysical Journal* 54, 871-877.

Kostyuk, P., Akaike, N., Osipchuk, Y.U., Savchenko, A., Shuba, Y.A. (1990). Gating and permeation of different types of calcium channels. In "Calcium Channels: Structure and Function". (Dennis Wray, Robert Norman, and Peter Hess, eds.), pp 63-69, New York Academy of Sciences, New York.

Kostyuk, P.G., and Kristhal, O.A. 1977. Separation of sodium and calcium currents in the somatic membrane of mollusc neurons. *Journal of Physiology (London)*, 270, 545-568.

Kostyuk, P.G., Shuba, M.F., and Savchenko, A.N. (1987). Three types of calcium channels in the membrane of mouse sensory neurons. *Biological Membranes* 4, 366-373.

Kuno, M., and Gardner, P. (1987). Ion channels activated by inositol 1,4,5 triphosphate in plasma membrane of human T-lymphocytes. *Nature* 326, 301-304.

Kunze, D.L. and Ritchie, A.K. (1990). Multiple conductance levels of the dihydropyridine-sensitive calcium channel in GH3 cells. *Journal of Membrane Biology* 118(2), 171-178.

Lacerda, A.E., and Brown, A.M. (1989). Nonmodal gating of cardiac calcium channels as revealed by dihydropyridines. *Journal of General Physiology* 93, 1234-1273.

Lang, F., Friedrich, F., Paulmichl, M., Schobersberger, W., Jungwirth, A., Ritter, M., Steidl, M., Weiss, H., Woll, E., Tschernko, E., Paulmichl, R., and Hallbrucker, C. (1990). Ion channels in Mardin-Darby canine kidney cells. *Renal Physiology and Biochemistry* 13, 82-93.

Lassiter, W.E., Gottschalk, C.W., and Mylle, M. (1963). Micropuncture study

of tubular reabsorption of calcium in normal rodents. *American Journal of Physiology* 204, 771-775.

Lavenda, B.H. (1981). Brownian motion. *Scientific American*, 70-84.

Lawson, D.E.M. (1990). Vitamin D and calbindin gene transcription. NATO Advanced Research Workshop on "Calcium Transport and Intracellular Calcium Homeostasis." Lyon, France.

Lee, C.O., Taylor, A., and Windhager, E.E. (1980). Cytosolic calcium ion activity in epithelial cells of *Necturus* kidney. *Nature* 287, 859-861.

Lewis, M., and Rees, D.C. (1985). Fractal surfaces of proteins. *Science* 230, 1163-1165.

Liboff, A.R., and McLeod, R. (1988). Kinetics of channelised membrane ions in magnetic fields. *Bioelectromagnetics* 9, 39-51.

Liebovitch, L.S. (1988) Analysis of fractal ion channel gating kinetics: Kinetic rates, energy levels, and activation energies. *Mathematical Biosciences* 93, 97-115.

Liebovitch, L.S., and Sullivan, J.M. (1987). Fractal analysis of a voltage-dependent potassium channel from cultured mouse hippocampal neurons. *Biophysical Journal* 52, 979-988.

Liebovitch, L.S., and Toth, T.I. (1991). A model of ion channel kinetics using deterministic chaotic rather than stochastic processes. *Journal of Theoretical Biology* 148, 243-267.

Liebovitch, L.S., Fischbarg, J., and Kumiarek, J.P. (1986). Fractal model of ion channel kinetics. *Journal of General Physiology* 88, 34a-35a.

Liebovitch, L.S., Fischbarg, J., Koniarek, J.P., Todorova, I., and Wang, M. (1987). Fractal model of ion channel kinetics. *Biochim. Biophysics Acta* 896, 173-180.

Light, D.B., McCann, F.V., Keller, T.M., and Stanton, B.A. (1988). Amiloride-sensitive cation channel in apical membrane of inner medullary collecting duct. *American Journal of Physiology* 255 (Renal Fluid Electrolyte Physiol. 24), F278-F286.

Light, D.B., Schwiebert, E.M., Fejes-Toth, G., Fejes-Toth, A.N., Karlson, K.H., McCann, F.V., and Stanton, B.A. (1990). Chloride channels in the apical membrane of cortical collecting duct cells. *American Journal of Physiology* 258 (Renal Fluid Electrolyte Physiol. 27), F273-F280.

Lipscombe, D.L., and Tsien, R.W. (1987). Noradrenaline inhibits N-type Ca channels in frog sympathetic neurons. *Journal of Physiology* 390, 84P.

Liu, Q., Lai, F.A., Rousseau, E., Jones, R.V. and Meissner, G. (1989). Multiple conductance states of the purified calcium release channel complex from skeletal sarcoplasmic reticulum. *Biophysical Journal* 55, 415-424.

Loirand, G., Mirroneau, C., Mirroneau, J., and Pacaud, P. (1989). Two types of calcium currents in single smooth muscle cells from rat portal vein. *Journal of General Physiology* 412, 333-349.

Lovejoy, S. (1982). Area-perimeter relation for rain and cloud areas. *Science* 216, 185-187.

Madison, D., Fox, A.P., and Tsien, R.W. (1987). Adenosine reduces an inactivating component of calcium current in hippocampal CA3 neurons. *Biophysical Journal* 51, 30a.

Mandelbrot, B.B. (1983). *The fractal geometry of nature*. W.H. Freeman and Co. publishers, San Francisco.

Marom, S., Dagan, D., Winaver, J., Palti, Y. (1989). Brush-border membrane cation conducting channels from rat kidney proximal tubules. *American Journal of Physiology* 257 (Renal Fluid Electrolyte Physiol.26), F328-F335.

Marunaka, Y., and Eaton, D.C. (1990). Chloride channels in the apical membrane of a distal nephron A6 cell line. *American Journal of Physiology* 258 (Cell Physiol. 27), C352-C368.

Marunaka, Y., and Eaton, D.C. (1990). Chloride channels in the apical membrane of a distal nephron A6 cell line. *American Journal of Physiology* 258 (Cell Physiol. 27), C352-C368.

McManus, O.B., Blatz, A.L., and Magleby, K.L. (1987). Sampling, log binning, fitting, and plotting durations of open and shut intervals from single channels, and the effects of noise. *Pflugers Archives* 410, 530-553.

McRobie, A., and Thompson, M. (1990). Chaos, catastrophes and engineering. *New Scientist* 9, 41-45.

Merot, J., Gachot, B., Le Maout, S., Tauc, M., and Poujeol, P. (1988). Patch clamp study on primary culture of isolated proximal convoluted tubules. *Pflugers Archives* 413, 51-61.

Mikami, A., Imoto, K. Tanabe T., Niidome T., Mori Y., Takeshima H., Narumiya S. and Numa S. (1989). Primary structure and functional expression of the cardiac dihydropyridine-sensitive calcium channel. *Nature* 340(6230),230-233.

Miller, R.J. (1987). Multiple calcium channels and neuronal function. *Science* 235, 46-52.

Miller, R.J., and Fox, A.P. (1990). Voltage-sensitive calcium channels. In "Intracellular Calcium Regulation". ( F. Bronner, ed.), pp 97-138, Wiley-Liss.

Millhauser, G.L. Salpeter, E.E., and Oswald, R. (1988a). Rate amplitude correlation from single channel records. *Biophysical Journal* 54, 1165-1168.

Millhauser, G.L., Salpeter, E.E., and Oswald R.E. (1988b). Diffusion models of ion channel gating and the origin of power-law distributions from single channel recording. *Proceedings of the National Academy of Sciences* 85,

1503-1507.

Modlin, M. (1967). The aetiology of the renal stone: a new concept arising from studies on a stone free population. *Annals of the Royal College of Surgeons, England* 40, 155.

Mozhayeva, G.N., Naumov, A.P., Kuryshv, Y.A. (1990). Inositol 1,4,5-triphosphate activates two types of Ca-permeable channels in human carcinoma cells. *FEBS* 277, 233-234.

Nakazawa, K., Saito, H., and Matsuki, N. (1988). Fast and slow inactivating components of Ca channel current and their sensitivities to nicardipine in isolated smooth cells from rat vas deferens. *Pflugers Archives* 411, 289-295.

Neher, E., and Sakmann, B. (1976). Single channel currents recorded from membrane of denervated frog muscle fibres. *Nature* 260, 799-802.

Nelson, D.J., Tang, J.M., and Palmer, L.G. (1984). Single channel recordings of apical membrane Cl conductance in A6 epithelial cells. *Journal of Membrane Physiology* 80, 81-89.

Nemere, I. (1990). Intestinal calcium transport: Lysosomes and microtubule-associated calbindin-D28K. NATO Advanced Research Workshop on "Calcium Transport and Intracellular Homeostasis." Lyon, France.

Ng, R.C.K., Rouse, D., and Suki, W.N. (1984). Calcium transport in the rabbit superficial proximal convoluted tubule. *Journal of Clinical Investigation* 74, 834-842.

Nicolson, S., Isaacson, L.C., and Gemeke, D. (1991). A new method of preparing the basal membrane of renal tubules for patch clamp, using beetle malpighian tubules. *Pflugers Archives* 417, 654-656.

Nilius, B., Hess, P., Lansman, J.B., and Tsien, R.W. (1985). A novel type of cardiac calcium channel in ventricular cells. *Nature* 316, 443-446.

Nowycky, M.C., Fox, A.P., and Tsien, R.W. (1985). Three types of neuronal calcium channel with different calcium agonist sensitivity. *Nature* 316, 440-443.

Olivera, B.M., Gray, W.R., Zeikus, S.R., McIntosh, J.M., Victoria de Santos, J.R., and Cruz. (1985). Peptide neurotoxins from fish-hunting cone snails. *Science* 230, 1338-1343.

Pallota, B.S. (1991). Single ion channel's view of classical receptor theory. *FASEB Journal* 5, 2035-2043.

Palmer, L.G. (1986). Patch-clamp technique in renal physiology. *American Journal of Physiology* 250 (Renal Fluid Electrolyte Physiol.19), F379-F385.

Palmer, L.G., and Frindt, G. (1986). Amiloride-sensitive Na channels from the apical membrane of the rat cortical collecting tubule. *Proceedings of the National Academy of Sciences* 83, 2767-2770.

Palmer, L.G., and Frindt, G. (1988). Conductance and gating of epithelial Na channels from rat cortical collecting tubule. *Journal of General Physiology* 92, 121-138.

Palmer, L.G., and Sackin, H. (1988). Regulation of renal ion channels. *FASEB Journal* 2, 3061-3065.

Pang, P.K., Wang, R., Wu, L.Y. Karpinski, E., Shan, J., and Benishin, C.J. (1990). Control of calcium channels in neuroblastoma cells. *Experimental Gerontology* 25, 247-253.

Pansini, A.R., and Christakos, S. (1984). Vitamin D-dependent calcium-binding protein in rat kidney. *Journal of Biological Chemistry* 259 (15), 9735-9741.

Parent, L., Cardinal, J., and Sauve, R. (1988). Single-channel analysis of a K channel at basolateral membrane of rabbit proximal convoluted tubule. *American Journal of Physiology* 254 (Renal Fluid Electrolyte Physiol.23), F105-F113.

Penner, R., Mathews, G., and Neher, E. (1988). Regulation of calcium influx by second messengers in rat mast cells. *Nature* 334, 499-504.

Peterson, O.H. (1990). Regulation of calcium entry in cells that do not fire action potentials. In "Intracellular Calcium Regulation". (F. Bronner, ed.), pp 77-96, Wiley-Liss.

Peterson, O.H., and Maruyama, Y. (1983). What is the mechanism of the calcium influx to pancreatic acinar cells evoked by secretagogues? *Pflugers Archives* 396, 82-84.

Peterson, O.H., and Peterson, C.C.H. (1986). The patch-clamp technique: Recording ionic currents through single pores in the cell membrane. *News in Physiological Sciences* 1, 5-8.

Pualais, M., and Teulon, J. (1989). A cation channel in the thick ascending limb of Henle's loop of the mouse kidney: inhibition by adenine nucleotides. *Journal of Physiology* 413, 315-327.

Quartararo, N., and Barry, T.N. (1987). A simple technique for transferring excised patches of membrane to different solutions for single channel measurements. *Pflugers Archives* 410, 677-678.

Ramachandran, C., and Brunette, M.G. (1989). The renal Na/Ca exchange system is located exclusively in the distal tubule. *Biochemical Journal* 257, 259-264.

Reeves, J.P., Ahrens, D.C., Cheon, J., and Durkin, J.T. (1990). Sodium-calcium exchange in the heart. NATO Advanced Research Workshop on "Calcium Transport and Intracellular Calcium Homeostasis." Lyon, France.

Regan, L.J. (1987). Calcium channels in freshly dissociated rat cerebellar Purkinje cells. *Biophysical Journal* 51, 223.



Reuter, H. (1983). Calcium channel modulation by neurotransmitters, enzymes and drugs. *Nature* 301, 569-574.

Reuter, H., and Scholz, H. (1977). A study of the ion selectivity and the kinetic properties of the calcium dependent slow inward current in mammalian cardiac muscle. *Journal of Physiology (London)* 264, 17-47.

Rocha, A.S., Migaldi, J.B., Kokko, J.B. (1977). Calcium and phosphate transport in isolated segments of rabbit Henle's loop. *Journal of Clinical Investigation* 59, 975-983.

Rojas, E., Hidalgo, J., Carrol P.B., Li M and Atwater I. A new class of calcium channels activated by glucose in human pancreatic beta-cells. *FEBS Letters* 261(2),265-270.

Rorsman, P. (1988). Two types of calcium current with different sensitivities to organic Ca channel antagonists in guinea pig pancreatic alpha 2 cells. *Journal of General Physiology* 91, 243-254.

Rouse, D., and Suki, W.N. (1990). Renal control of extracellular calcium. *Kidney International* 38, 700-708.

Rouse, D., Ng, R.C.K., and Suki, W.N. (1980). Calcium transport in the pars recta and thin descending limb of Henle of the rabbit, perfused in vitro. *Journal of Clinical Investigation* 65, 37-42.

Rouse, D., Ng, R.C.K., and Suki, W.N. (1980). Calcium transport in the pars recta and thin descending limb of Henle of rabbit, perfused in vitro. *Journal of Clinical Investigation* 65, 37-42.

Ruff, R.L. (1986). Ionic channels, 1. The biophysical basis for ion passage and channel gating. *Muscle and Nerve* 9, 675-699.

Sackin, H. (1987). Stretch-activated potassium channels in renal proximal tubule. *American Journal of Physiology* 253 (Renal Fluid Electrolyte Physiol.22), F1253-F1262.

Sackin, H., and Palmer, L.G. (1987). Basolateral potassium channels in renal proximal tubule. *American Journal of Physiology* 253 (Renal Fluid Electrolyte Physiol.22), F476-F487.

Sakmann, B., and Neher, E. (1983). Geometric parameters of pipettes and membrane patches. In "Single-Channel Recording" (B. Sakmann and E. Neher, eds), pp. 37-52, Plenum Press, New York.

Sanguinetti, M.S., Krafte, D.S., and Kass, R.S. (1986). Voltage-dependent modulation of Ca current by Bay K-8644. *Journal of General Physiology* 88, 369-392.

Saunders, J.C.J. (1987). The patch clamp technique: setting up. BSc(HONS) thesis. Department of Physiology, Medical School. University of Cape Town.

Savitzky, A., and Golay, M.J.E. (1964). Smoothing and differentiation of data by simplified least squares procedures. *Analytical Chemistry* 36 (8), 1627-1639.

Schaffer, W.M. (1987). Chaos in ecology and epidemiology. In "Chaos in Biological Systems" (H. Degan, A.V. Holden and L.F. Olsen, eds.) pp 233-248. Plenum Press, New York.

Schramm, M. and Towart, R. (1985). Modulation of calcium channel function by drugs. *Life Sciences* 37, 1843-1860.

Schuster, V.L. (1986). Cyclic adenosine monophosphate-stimulated anion transport in rabbit cortical collecting duct. *Journal of Clinical Investigation* 78, 1621-1630.

Schuster, V.L. and Stoker, J.B. (1987). Chloride transport by the rat cortical and outer medullary collecting duct. *American Journal of Physiology* 253, F203-F212

Schreiner, W., Kramer, M., Krischer, S., and Langsam, Y. (1985). Non-linear least-squares fitting. *PC Tech Journal*, 170-190.

Shareghi, G.A., and Agus, Z.S. (1982). Phosphate transport in the light segment of the rabbit cortical collecting tubule. *American Journal of Physiology* 242, F379-F384.

Sigworth, F.J. (1983). An example of analysis. In "Single Channel Recording" (B. Sakmann and E. Neher, eds.), pp 301-321. Plenum Press, New York.

Sutton, R.A.L., and Dirks, J.H. (1975). The renal excretion of calcium: a review of micropuncture data. *Canadian Journal of Physiology and Pharmacology* 53, 979-988.

Takeda, K.B. and Trautman, A. (1984). A patch-clamp study of the partial agonist actions of tubocurarine on rat myotubes. *Journal of Physiology (London)* 349, 353-374.

Takens, F. (1981). Detecting strange attractors in turbulence. In "Lecture Notes in Mathematics" (D. Rand and L. Young), pp 366-81. Springer, New York.

Taniguchi, J., Yoshitomi, K., and Imai, M. (1989). K channel currents in basolateral membrane of distal convoluted tubule of rabbit kidney. *American Journal of Physiology* 256 (Renal Fluid Electrolyte Physiol. 25), F246-F254.

Taylor, A.N., McIntosh, J.E., and Bourdeau, J.E. (1982). Immunocytochemical localisation of vitamin D-dependent calcium binding protein in renal tubules of rabbit, rat, and chick. *Kidney International* 21, 765-773.

Tedeschi, A., Miadonna, A., Lorini, M., Aràquati, M., and Zanussi, C. (1990). Receptor operated but not voltage-operated, calcium channels are involved in basophil leucocyte activation and histamine release.

International Archives of Allergy and Applied Immunology 90 (1), 109-111.

Teulon, J., Paulais, M. and Bouthier, M. (1987). A calcium-activated cation-selective channel in the basolateral membrane of the cortical thick ascending limb of Henle's loop of the mouse. *Biochimica et Biophysica Acta* 905, 125-132

Thomasset, M., Parkes, C.O., and Cuisinier-Gleizes, P. (1982). Rat calcium-binding proteins: Distribution, development, and vitamin D dependence. *American Journal of Physiology* 243 (Endocrinol. Metab.6), E483-E488.

Trautman, A. (1982). Curare can open and block ionic channels associated with cholinergic receptors. *Nature* 298, 272-275.

Trautwein, W., and Pelzer, D. (1988). Kinetics and  $\beta$ -adrenergic modulation of cardiac calcium channels. In "The Calcium Channel: Structure, Function, and Implication". (Moradi M, Nayler W, Kazda S, Schramm M, eds.), pp 39-53 Springer-Verlag.

Tsien, R.W. (1983). Calcium channels in excitable membranes. *Annual Review of Physiology* 45, 341-358.

Tsien, R.W., Bean, B.P., Hess, P., Lansman, J.P., Nilius, B., and Nowycky, M.C. (1986). Mechanisms of calcium channel modulation by  $\beta$ -adrenergic agonists and dihydropyridine Ca channel agonists. *Journal of Molecular and Cell Cardiology* 18, 691-710.

Tsien, R.W., Hess, P., Lansman, J.B., and Lee K.S. (1985). Current views of cardiac calcium channels and their response to calcium antagonists and agonists. In "Cardiac Electrophysiology and Arrhythmias", pp 19-21.

Ullrich, K.J., Rumrich, G., and Kloss, S. (1976). Active calcium reabsorption in the proximal tubule of the rat kidney. *Pflügers Archives* 364, 223-228.

Vassilev, P.M. (1990). A simple hanging-drop patch-clamp technique for studying single-channel activities in excised membrane patches. *Pflügers Archives* 415, 497-500.

Verma, A.K., Filoteo, A.G., Stanford, A.G., Stanford, D.R., Wieben, E.D., Penniston, J.T., Strehler, E.E., Fischer, R., Heim, R., Vogel, G., Mathews, S., Strehler-Page, M.A., James, P., Vorher, T., Krebs, J., Carafoli, E. (1988). Complete primary structure of a human plasma membrane Ca-pump. *Journal of Biological Chemistry* 263, 14152-14159.

Vincenzi, F.F., and Hinds, T.R. (1980). Calmodulin and plasma membrane calcium transport. In "Calcium and Cell Function"; edited by W.Y. Cheung. Vol. 1. Academic press.

Vogel, G., and Stoeckert, I. (1967). Die Bedeutung des Natriums für den renal-tubularen Calcium Transport bei *Rana ridibunda*. *Pflügers Archives* 298, 23-30.

Von Tscharner, V., Prod'homme, B., Baggiolini, M., and Reuter, H. (1986). Ion channels in human neutrophils activated by a rise in free cytosolic

calcium concentration. *Nature* 324, 369-372.

Walser, M. (1961). Calcium clearance as a function of sodium clearance in the dog. *American Journal of Physiology* 200, 1099-1104.

Walser, M. (1961). Calcium-sodium dependence in renal transport. In "Renal Pharmacology", pp 21-41, Appleton-Century-Crofts, New York.

Walser, M., and Trounce, J.R. (1961). The effect of diuresis and diuretics upon the renal tubular transport of alkaline earth cations. *Biochemistry and Pharmacology* 8, 157.

Walsh, K.B., Begenesich, T.B., and Kass, R.S. (1989).  $\beta$ -adrenergic modulation of cardiac ion channels. *Journal of General Physiology* 93, 841-854.

Walters, J.R.F. (1990). The activity of the basolateral membrane Ca-pump and intestinal Ca-transport. NATO Advanced Workshop on "Calcium Transport and Intracellular Calcium Homeostasis." Lyon, France.

Wasserman, R.H., Fullmer, C.S., Chandra, S., Morrison, G., Cai, Q., and Tapper, D.N. (1990). The calbindins: Their discovery, distribution, properties and possible functions. NATO Advanced Research Workshop on "Calcium Transport and Intracellular Calcium Homeostasis." Lyon, France.

Weinberg, J.M., Venkatachalam, M.A., Garzo-Quintero, R., Roser, M.M., and Davis, J.A. (1990). Structural requirements for protection by small amino acids against hypoxic injury in kidney proximal tubules. *FASEB Journal* 4, 3347-3354.

Worley, J.F., and Kotlikoff, M.I. (1990). Dihydropyridine-sensitive single calcium channels in airway smooth muscle cells. *American Journal of Physiology* 259, L468-L480.

Yaari, Y., Hamon, B., and Lux, H.B. (1987). Development of two types of calcium channels in cultured mammalian hippocampal neurons. *Science* 23, 680-682.

Yabu, H., Yoshino, M., Someya, T., and Totsuka, M. (1989). Two types of Ca channels in mammalian intestinal smooth muscle cells. In "Calcium Channels: Structure and Function". (D. Wray, R. Norman, and P. Hess, eds.), pp 124-126. New York Academy of Sciences, New York.

Yindt, E.R., Guay, G.F., and Garcia, D.A. (1970). The use of thiazides in the prevention of renal calculi. *Canadian Medical Association Journal* 102, 614-624.

Yoshino, M., Someya, T., Nishio, A., and Yabu, H. (1988). Whole-cell and unitary calcium currents in mammalian intestinal smooth muscle cells: evidence for the existence of two types of Ca channels. *Pflügers Archives* 411, 229-231.

Zschauer, A., van Breeman, C., Buhler, F.R., and Nelson, M.T. (1988).  
Calcium channels in thrombin-activated human platelet membrane.  
Nature 334, 703-705.

## ***Appendix***

A) CCD spreadsheet data

B) TAL spreadsheet data

C) DCT spreadsheet data

D) PST spreadsheet data

E) HUMAN tubule spreadsheet data

KEY TO TABLE HEADINGS (LEFT TO RIGHT):

1) Patch no.

2) Code no.

3) Bath

4) Pipet

5) Clamp (mV)

6) Burst (pA)

7) Square (pA)

8) (regression)

9) #OT (fractional open time)

10) Mean OT (msec)

11) Mean CT (msec)

12) Oexp1 (open-time histogram exponential 1)

13) Oexp2 (open-time histogram exponential 2)

14) Cexp1 (closed-time histogram exponential 1)

15) Cexp2 (closed-time histogram exponential 2)







7	Coats	Ref	Inst	Clamp	Inst	sqares	ref	alt	MediOT	MediCT	Dep1	Dep2	Dep	Dep3
No				RV	PA	PA			press	press				
12	CD4	Ringer	BaCl2	-10	0.16	0.32	0.265	0.011	1.2	128.3	2.43	0.532	0.301	0.008
		Inside-out		1.5E-39	reversal probe			1.5E-39						
				10	-0.163	-0.33	-0.255	0.148	12.2	89	0.143		0.117	0.007
		NaCl/2		-10	0.184	0.447	0.365	0.042	1.2	31.9	1.14		0.143	0.026
				1.5E-39	0.153	0.35	0.29	0.03	1.2	41.1	2.21		0.182	0.022
				10	-0.16	-0.35	-0.27	0.44	18	26.8	0.043		0.232	0.03
				20	-0.161	-0.37	-0.31	0.055	1.2	24.2	1.61		0.126	0.026
13	CD6	Ringer	BaCl2	-5	reversal probe									
		Inside-out		1.5E-39	-0.2	-0.5	-0.29	0.304	RP REMAINS		0.119		0.099	0.073
				5	-0.19	-0.405	0.335	0.016	UNCHANGED		0.081			
									ENDN-					
		acetate		-5	0.185	0.315	0.315	0.045	SELECTIVE		0.178			
				1.5E-39		-0.295	-0.295		CHANNEL					
				5		-0.32	-0.32	0.025						
				10	-0.162	-0.411	-0.33	0.004						
		NaCl/2		10	-0.231	-0.38	-0.355	1.5E-39						
				20	-0.174	-0.42	-0.395	0.046						
14	CD7	Ringer	BaCl2	-10	0.135	0.32	0.32	0.006	1	164.7	2.77			
		Inside-out		1.5E-39	reversal probe									
				10	-0.16	-0.34	-0.31	0.011	1	99.6			0.45	0.01
		acetate		1.5E-39	0.174	0.45	0.45	REVPOSF						
				10	0.174	0.403	0.32	APLESCL						
				20	0.143	0.336	0.27							
				30	-0.152	-0.38	-0.345							
								ALSO DOWN						
		NaCl/2		1.5E-39	0.17	0.37	0.29	APLES CA						
				10	0.178	0.375	0.375							
				20	0.139	0.313	0.29							
				30	-0.185	-0.35	-0.35							
15	CD8	Ringer	BaCl2	-10										
		Inside-out		1.5E-39		-0.16		0.006	1.1	222.1	1.86		0.081	0.002
				10	-0.224	-0.19		0.012	1.2	109.8	1.42		0.123	0.004

7	NodeNo	Ref	Clamp	Surf	square	Ref	Alt	MeasCT	MeasCT	Dem1	Dem2	Dem	Cent
No.			rv	pa	pa			mvsec	mvsec				
			20		-0.15		0.016	1	75.1	2.79		0.095	0.008
							0.016	1	64.7	2.6			
		NaCl/2	-10		0.175		0.022	1.1	57.8	1.67		0.423	0.016
			1.5E-39		0.18		0.016	1.1	71.8	2.42		0.035	0.008
			10	0.106	0.19		0.011	1	91.3	3.33		0.089	0.008
			20		0.171								
			30										
			40		-0.2		0.021	1.1	57	1.84		0.054	0.013
			-10	0.169	0.246	0.195	0.01	1.6	125.4	0.925		0.052	0.005
			1.5E-39	-0.116	-0.2	-0.02	0.001						
			10		-0.23	-0.185	0.001	1.2	281.7	4.44	0.55	0.027	0.002
			20	-0.182	-0.34	0.23	0.06	2.2	47.3	0.325		0.104	0.012
		NaCl/2	1.5E-39	0.189	0.35	0.28	0.09	3.1	41.9	0.659	0.112	0.146	0.017
			10	0.171	0.34	0.215	0.02	2	106.5	1.387	0.119	0.154	0.007
			20	0.13	0.25	0.225	0.01	1.5	168.2			0.072	0.004
			30		0.2	0.185							
			40	-0.29	0.227	-0.22	1.5E-39	1	213			0.005	
			-10	0.179	0.37	0.315	0.378	3.8	9.3	0.348		0.198	0.056
			-5	0.18	0.495	0.35	0.272	4	14.9	0.731	0.167	0.182	0.047
			1.5E-39	-0.128									
			5	-0.158	-0.41	-0.34	0.072	2.4	39.1	1.44	0.38	0.094	0.011
			10	-0.192	-0.51	-0.38	0.105	2.5	27.3	0.608		0.176	0.019
		NaCl/2	-10	0.166	0.725	0.455	0.235	3.4	15.8	1.308	0.249	0.252	0.044
			1.5E-39	0.191	0.608	0.42	0.221	5.2	15	0.484	0.111	0.362	0.021
			10	0.162	0.38	0.34	0.024	3.2	146.3	0.576		0.092	0.005
			20	0.168	0.44	0.36	0.04	3.4	102.2	0.65	0.069	0.055	0.003
			30	0.161	0.43	0.315	0.059	2.7	55.8	6.787	0.444	0.19	0.023
			-20	0.28	0.429	0.395	0.381	2.7	8	0.88	0.184	0.618	0.114
			-10	0.15	0.3	0.3	0.04	1.7	56.7	0.715		0.149	0.008
			1.5E-39		reversal probe		1.5E-39	1.5E-39					
			10	-0.15	-0.365	-0.275	0.147	2.7	23.5	0.608	0.063	0.177	0.023
			-20	0.2			0.189	1.4	8	1.507	0.413	0.202	0.067
			-10	0.22			0.052	1.3	26.1	1.2	0.19	0.734	0.034









[illegible]







[illegible]





[illegible]



[illegible]

D)

PSTCodeNo	Bath	Pipet	Clamp	burst	small	#OT	MeanO	MeanCO	exp1O	exp2C	exp1C	exp2C
No.			mV	pA	squars	squares	msec	msec				
1	CA1	cellat	CaCl2	0	-0.2	-0.22	0.00	1.3	299			
2	CA2	cellat	BaCl2	100	too short and noisy to analyse							
3	DOGa		BaCl2	0	too little to analyse							
4	FR1	cell	-aBaCl2	0	-0.1	-0.192	0.00	2.3	738	too few channels		
5	FRI1	Ringer	BaCl2	-30	0.183	0.35	0.29	0.12	3.9	36.6		0.18 0.00
				-20	0.162	0.33	0.26	0.02	2.6	*****0.55	0.14	0.13 0.00
				-10	0.146	0.25	0.225	0.04	3.7	96.6	6.84	0.36 0.29 0.00
				0	rev pd							
				10	-0.14	-0.2	-0.23	0.07	2.7	43.1	0.47	0.08 0.14 0.00
6	FRI2	cell	-aBaCl2h	0	cant analyse;tooshort and scrappy							
7	Mon-scellat	BaCl2		-5	reversal potential							
	"			0	-0.12	-0.2	-0.21	0	2	3310		
	"			10	-0.15	-0.3	-0.31	0.12	6.3	62.9	0.28	0.04 0.10 0.01
	"			20	-0.17	-0.3	-0.32	0.01	3.4	432	0.29	0.01
	"			30	-0.18	-0.4	-0.35	0.34	8.6	26	0.27	0.04 0.12 0.02
8	P4	Ringer	BaCl2	-5	0.18	0.36	0.363	0.16	3.7	29.9	1.21	0.10 0.27 0.01
		inside-o		0	-0.15	-0.7	-0.78	0.02	2	*****0.30		0.08 0.01
				2	too scrappy all too scrappy							
				5								
9	P5	Ringer	BaCl2	-5	0.178	0.61	0.61	0.56	34.2	34.6	0.08	0.08 0.00
				0	-0.15	-0.3	-0.31	0.09	1.3	32.7	0.38	0.25 0.02
		C		5	-0.18	-0.4	-0.325	0.15	2.85	29	1.5	0.3 0.43 0.05
10	P6	Ringer	BaCl2	-15	0.175	0.46	0.46	0.44	3.9	8.8	0.93	0.14 0.69 0.09
				-5	0.16	0.38	0.3	0.11	2.4	33.8	2.31	0.41 0.20 0.02
		B		0		-0.1	-0.18	0.05	1.1	24.5	0.24	0.19 0.02
				5	-0.18	-0.3	-0.25	0.09	3.4	44.1	1.10	0.13 0.15 0.01
11	P7	Ringer	BaCl2	-10	0.205	0.36	0.25	0.24	1.8	20.1	4.78	0.45 0.16 0.02
		cell-excised		0	-0.18	-0.2	-0.24	0.09	8.7	*****0.33	0.01	0.05 0.00
				10	-0.18	-0.7	-0.24	0.03	1.8	82.6	3.28	0.56 0.10 0.00
12	P8	Ringer	BaCl2	0	-0.16	-0.9	-0.475	0.10	33.6	*****		
13	Prox5Ringer	BaCl2		0	Nodeterminable baseline;cant analyse							
				0	Dont know voltages							
				6								
				14								
14	Prox1-11	NaCl		-10	0.208	0.41	0.31	0.71	20.1	11	0.07	0.03 0.08
				100	0	0.206	0.34	0.265	0.66	18.3	13.4	0.14 0.02 0.10 0.01
		CaCl2		6	cant measure							
				20	20	-0.21	-0.4	-0.3	0.45	10.7	19.8	0.18 0.03 0.01 0.08
				30	-0.13	-0.3	-0.26	0.10	3.5	49.3	2.85	0.24 0.11 0.01
				40	-0.13	-0.3	-0.28	0.35	7	21	2.86	0.24 0.10 0.01
	try2			20								
15	PS1	Ringer	BaCl2	-15		0.34	0.275	0.02	3.4	159		



PSTCode	NoBath	Pipet	Clamp	burst	small	#OT	Mean	Mean	COexp1	exp2	Cexp1	Cexp2
No.		mV	pA	squars	squares		msec	msec				
		-5							5		0.41	0.01
		0	0.183									
		10		-0.6	-0.29	0.01						
		-10		0.35	0.26	0.00	1.5	*****				
		0		-0.3	-0.285	0.00	1	162				
		10		-0.4	-0.265	0.00	1.9	278				
16	PS2	20	-0.20	-0.4	-0.325	0.01	2	146	3.74	0.39	0.08	0.00
		-10										
		0										
		10										
17	PS2A Ringer	-10	0.169	0.51	0.516	0.86			too much drift			
		0	-0.19	-0.4	-0.385	0.21	11.6	58.8	0.10		0.05	0.00
		10	-0.17	-0.3	-0.275	0.07			too much drift			
18	PS3 Ringer	-10		0.31	0.315							
		0										
		10	-0.13	-0.4	-0.32	0.25	9.3	35.4	0.22		0.18	0.01
	acetate	20										
		20										
		25										
		30										
19	PS4 Ringer	-5										
		0										
		5										
	acetate	20										
	"	25										
20	PS5 Ringer	-10	0.153	0.36	0.275	0.11	2.5	27.5	5.53	0.35	0.06	
	cell-excised	0										
shift	n pos tive dir	10	-0.16	-0.2	-0.22	0.05	2.1	56.5	0.62		0.01	0.06
cl channel?												
	NaCl/2	0	0.186	0.47	0.475	0.51	5.9	8.1	0.50	0.1		
21	PSTAy cellat	0										
		5										
		15										
22	PSTBy cellat	-10										
		0	-0.2									
		10										
		20										
	excised	-10	0.175									
		0										
23	PSTCxc cellat	-10										
		0										
		10										
		20										
	excised	-10										
		-10	0.1									
		0										
		0										
		10										
		20	-0.15									

NICE SQUARES FOR THESIS

much noise for square measure

hardly any activity

should maybe look at #0 befor and atfter

PSTCode	NoBath	Pipet	Clamp	burst	small	#OT	MeanO	MeanC	Oexp1	Oexp2	Cexp1	Cexp2	
No.			mV	pA	squar	squares	msec	msec					
	Nifedipin		-20										
	BayK		-20										
25	PST1	cellatBaCl2											
26	PST2	"											
27	PST3	"											
28	PSTCA		16	cant	analyse								
	PSTCA1		20										
29	PSTCA	cellatBaCl2	16	cant	analyse'too much noise								
	PSTCA	"	16										
	PSTCA	"	20										
	PSTCA	"	25										
30	S1	cellatBaCl2	0	-0.19	-0.3	-0.24	0.08	15	*****	0.32	0.01	0.02	0.00
31	T-series	BaCl2	-6		0.17	0.175							
	A		0	-0.15	-0.2	-0.205	0.01	2.7	*****	0.26		0.11	0.00
	cell-exc6		-0.15	-0.3	-0.245	0.28	7.9	34.8	0.50	0.08	0.10	0.01	
			20	-0.19	-0.5	-0.33	0.56	17.3	20.2	0.24	0.03	0.14	0.03
			40	-0.18	-0.6	-0.42	0.80	39.2	10.0	0.59	0.06	0.10	
32	TH1	CA BaCl2	0	No	decent	baseline	to	analyse					
33	TH2a	BaCl2	0	Too	short;	NICE	SQUARES	FOR	THESIS				
34	TH3	cellatBaCl2	0	Almost	no	activity							
35	TU1	"BaCl2	0										
	TU2	"BaCl2	?										
36	TRY	";K=140	0	NICE	SQUARES	FOR	THESIS						
37	J1Try	cellatBaCl2	0	Cant	analyse								
38	TRY3a	"BaCl2	0	Cant	analyse								
39	JCATry3			No	channels								



Item No.	Code	Subj.	Pref.	Dura mV	Int. sec	Slope mV/sec	Lat. sec	Diff. sec	Muscle mass	Medial Dias	Deep Dias	Cas Dias	Cas Card
7	HUMAN	Finger	CoCl <sub>2</sub>	1E-39	-0.25								
8	HUMAN	Finger	CoCl <sub>2</sub>	1E-39	-0.15								
				5	-0.22								
9	HUMAN	Finger	CoCl <sub>2</sub>	-5	0.134 reversal note	0.23	0.21	0.053	1.8	46.1	0.77	0.05	0.07
			PCT	1E-39		-0.225	-0.225	0.002	1	672.2			
			proximal	5		-0.25	-0.23	0.114	2.2	27.5	0.62	0.06	0.13
			good trace	15	-0.181								0.02
10	HUMAN	Finger	CoCl <sub>2</sub>	-5		0.2	0.2	0.004	1	222.4			
			PCT	1E-39		REV PD							
				5		-0.15	-0.15	0.018	5.1	279.1			
11	HUMAN	Finger	CoCl <sub>2</sub>	-5		0.2	0.2	down 0.01					
			PCT	1E-39		-0.125	-0.125	0.006	1	345.7			
				5		-0.193	-0.193	0.004	1	107.9	3.11		0.15
				10		-0.21	-0.21	0.015	1.7	52.8	4.63	0.39	0.17
				15									0.01
12	HUMAN	Finger	CoCl <sub>2</sub>	-5	0.192	0.203	0.175	0.027	2.2	109.7	0.8		0.06
			cell-exposed	1E-39		-0.165	-0.165	0.002	1.1	719.5			0.06
				5	-0.236	-0.204	-0.204	0.009	1.6	234.3	0.91	0.15	0.14
13	HUMAN	Finger	CoCl <sub>2</sub>	1E-39		-0.293	-0.25	diff and up					
			PCT										
14	HUMAN	Finger	CoCl <sub>2</sub>	1E-39		0.15	0.15						
			PCT	5		0.15	0.15	0.002	1	544.1 handy on			
				10		0.2	0.2	0.005	1.3	301.7			
15	HUMAN	Finger	CoCl <sub>2</sub>	1E-39		-0.275	-0.185	too much dr					
			PST										
16	HUMAN	Finger	CoCl <sub>2</sub>	-10		0.24	0.24	0.044	11.7	344.9	0.29	0.02	0.04
			cell-altered	-5		0.15	0.15	0.036	1.3	70.3	0.42		0.17

[illegible]

[illegible]

F) Overall mean current amplitude data for "bursts" and "squares".

G) Standard error of the estimates for fitting functions of the log-log plots, single exponentials, and double exponentials of the open- and closed-time histograms.

Collective unit amplitudes for bursts (pA)

μV	-30	-20	-10	-5	0	5	10	20	30	40
SA	0.185	0.166	0.172	0.18	0.132	-0.19	-0.197	-0.164	-0.178	-0.28
	0.172	0.226	0.184	0.166	0.153	-0.159	-0.145	-0.199	-0.196	-0.186
	0.175	0.163	0.182	0.192	-0.162	0	-0.168	-0.169	-0.167	
	0.21	0.202	0	0.192	-0.151	-0.186	-0.15	-0.201	-0.183	-0.233
	0.183	0.175	0	0	0.143	-0.174	-0.189	-0.177	-0.133	0.06647
		0.195	0.15	0.18	0	-0.18	-0.187	-0.16	-0.185	
	0.185	0.28	0.173	0.178	-0.02	-0.184	-0.181	-0.182		
	0.01498	0.169	0.162	0.16	0	-0.154	-0.163	-0.203	-0.1737	
		0.162	0.135	0.177	-0.116	-0.161	-0.16	-0.19	0.02205	
		0.225	0.16	0.179	-0.128	-0.187	-0.224	-0.205		
		0.22	0.135	0.2	-0.184	-0.16	-0.192	-0.154		
		0.191	0.169		0.14	-0.191	-0.15	-0.232		
			0.179	0.164	-0.171		-0.175	-0.17		
		0.19783	0.15	0.05557	0.155	-0.1605	-0.171	-0.214		
		0.0353	0.162		-0.163	0.05006	-0.165	-0.202		
			0.151		-0.179		-0.183	-0.15		
			0.151		-0.154		-0.17	-0.193		
			0.18		-0.177		-0.191	-0.184		
			0.191		-0.165		-0.17	-0.18		
			0.146		-0.151		-0.145			
			0.205		-0.185		-0.153	-0.1857		
			0.208		-0.127		-0.183	0.02164		
			0.169		0		-0.177			
			0.153		-0.12		-0.138			
			0.175		-0.152		-0.164			
			0.1		-0.156		-0.143			
			0.183		-0.186		-0.187			
			0.191		-0.168		-0.199			
			0.155		0.206		-0.187			
			0.19		0.183		-0.19			
					-0.195					
			0.15537		0		-0.1732			
			0.0478		0.186		0.01997			
					-0.2					





Collective unit current amplitudes for squares

dy	-30	-20	-10	-5	0	5	10	20	30
0.455	0.27	0.255	0.35	0.23	-0.335	-0.27	-0.37	-0.34	
0.275	0.265	0.25	0.26	0.23	-0.195	-0.29	-0.355	-0.28	
0.365	0.35	0.385	0.25	-0.275	-0.33	-0.595	-0.35	-0.46	
0.29	0.31	0	0.33	-0.29	-0.25	-0.37	-0.33	-0.35	
	0.26	0.37	0	0.38	-0.325	-0.345	-0.265	-0.26	
0.34625	0.395	0.33	0.363	0	-0.25	-0.41	-0.15		
0.0825	0.35	0.275	0.61	0	-0.245	-0.19	0.23	-0.338	
	0.26	0.315	0.3	-0.29	-0.4	-0.33	-0.3	0.07823	
	0.405	0.3	0.175	-0.16	-0.31	-0.255	-0.21		
	0.38	0.23	0.35	-0.02	-0.255	-0.31	-0.405		
		0.285	0.31	-0.3	-0.585	-0.19	-0.34		
	0.3245	0.353	0.5	0.18	-0.33	-0.185	-0.32		
0.058569		0.26	0.275	0.25		-0.38	-0.3		
		0.25	0.25	-0.21	-0.3175	-0.275	-0.325		
		0.255		0.25	0.101074	-0.205	-0.33		
		0.25	0.308786	-0.24		-0.6	-0.395		
		0.31	0.140832	-0.277		-0.318			
		0.26		-0.29		-0.25	-0.28219		
		0.516		-0.25		-0.6	0.151118		
		0.315		-0.275		-0.208			
		0.275		-0.32		-0.405			
		0.425		-0.21		-0.216			
		0.26		-0.22		-0.23			
		0.215		-0.192		-0.31			
				0		-0.24			
	0.289125			-0.21		-0.29			
	0.092261			-0.78		-0.265			
				-0.31		-0.275			
				-0.18		-0.32			
				-0.24		-0.22			
				-0.475		-0.425			
				0.265		-0.42			
				-0.285		-0.55			
				-0.385		-0.325			
				-0.24		-0.38			



G)

No	S.E. for bn-bn		S.E. for ends		S.E. for done	
	dots		exponentials		exponentials	
	OPEN	CLOSED	OPEN	CLOSED	OPEN	CLOSED
1	69.6	10.3	11.2	13.9	1.8	4
2	192.8	96.9	5.1	5.2		1.9
3	290.7	117.2	6.7	10.6	1.5	3
4	84.3	4.8	8.4	9.2	8.2	2.4
5	120.3	32.2	2.3	5.1		1.9
6	14.8	26.5	7.1	5.2	2	1.9
7		147.7	9.7	16.8	1.7	5.6
8	5.6	17	3.5	6.3		2
9	35.7	49.7	8.2	7.6	4.5	1.4
10	8.4	21.9	14.6	15.2	3.5	5.6
11	125	5.1	2.1	9.3		4.4
12	135.5	73.8	8.2	7.5	2.9	4.3
13	5.6	17.9	6.4	7.5	3.2	2.8
14	21	21.9	1.2	4.4		4.4
15	144	2.6	1	5.4	1.9	2.2
16	23.3	36.1	5.8	2.7	2.1	3.9
17	201.5	12.1	3.7	14.3	1.5	3
18	6.5	45.8	5.9		1.1	
19	41	35.9	3.7	1	2.5	
20	9.9	28.3	6			4.5

Collective I-V plots for the "burst" and "small squares" data for the different tubule segments.

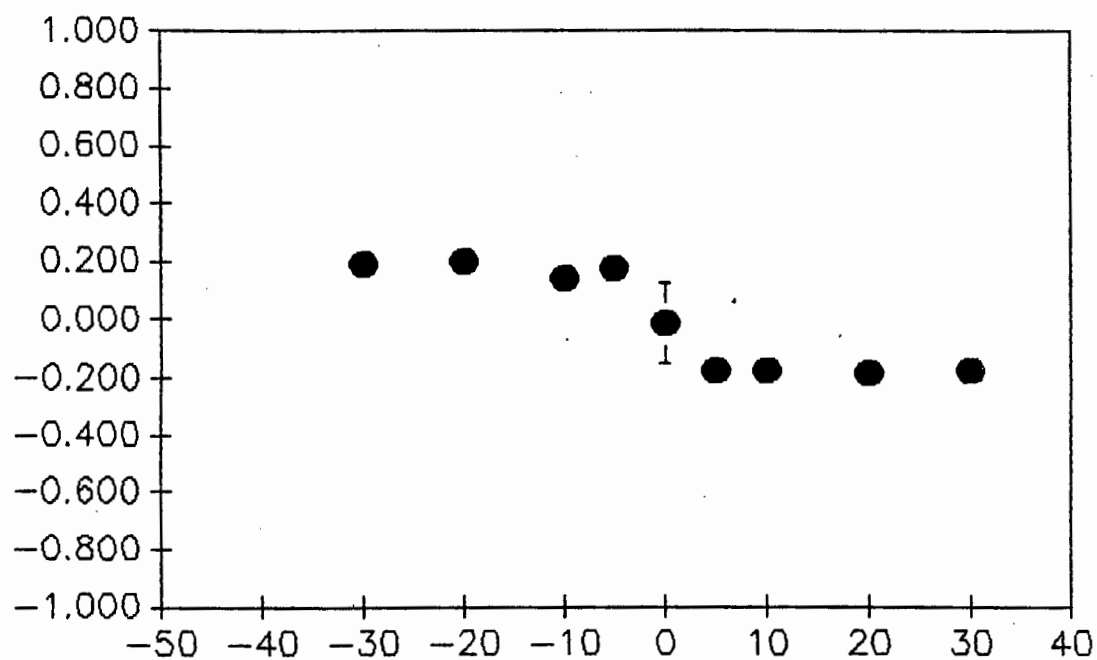


**Figure 1.** Collective I-V plot for "bursts" from the CCD data sample

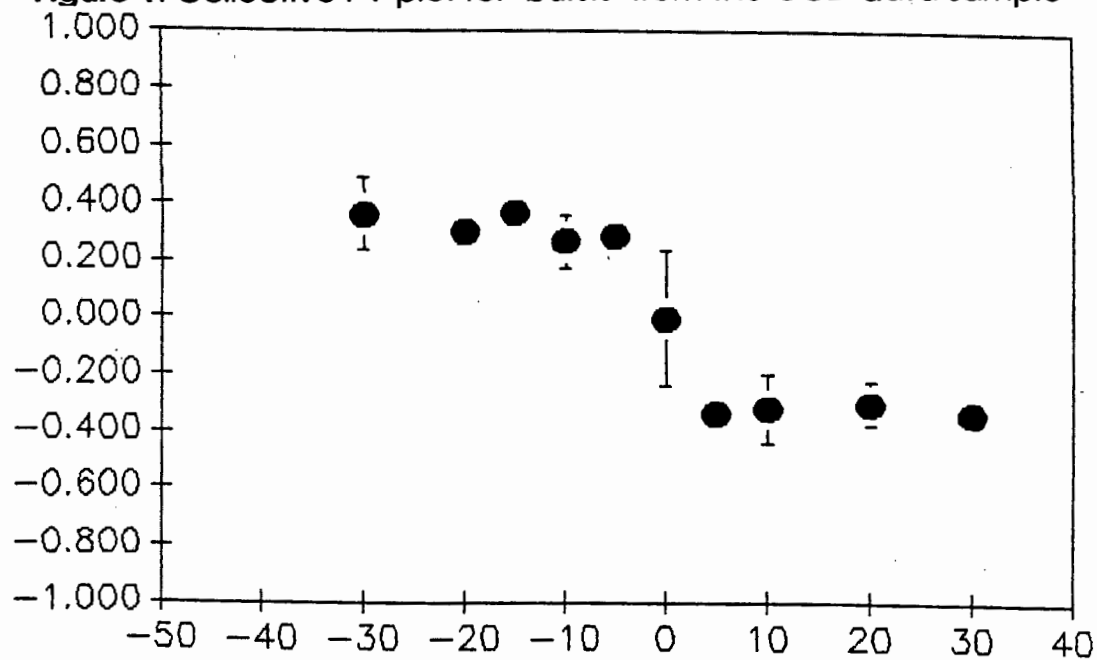


**Figure 2.** Collective I-V plot for "squares" from the CCD sample.

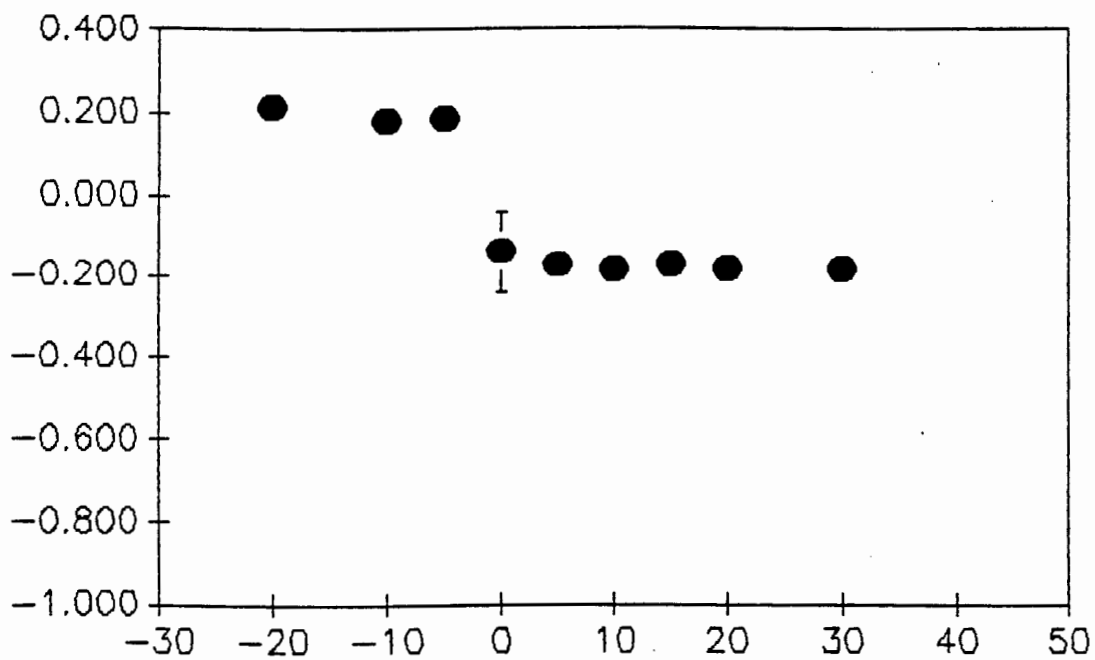


**Figure 3.** Collective I-V plot for "bursts" from the DCT data sample.

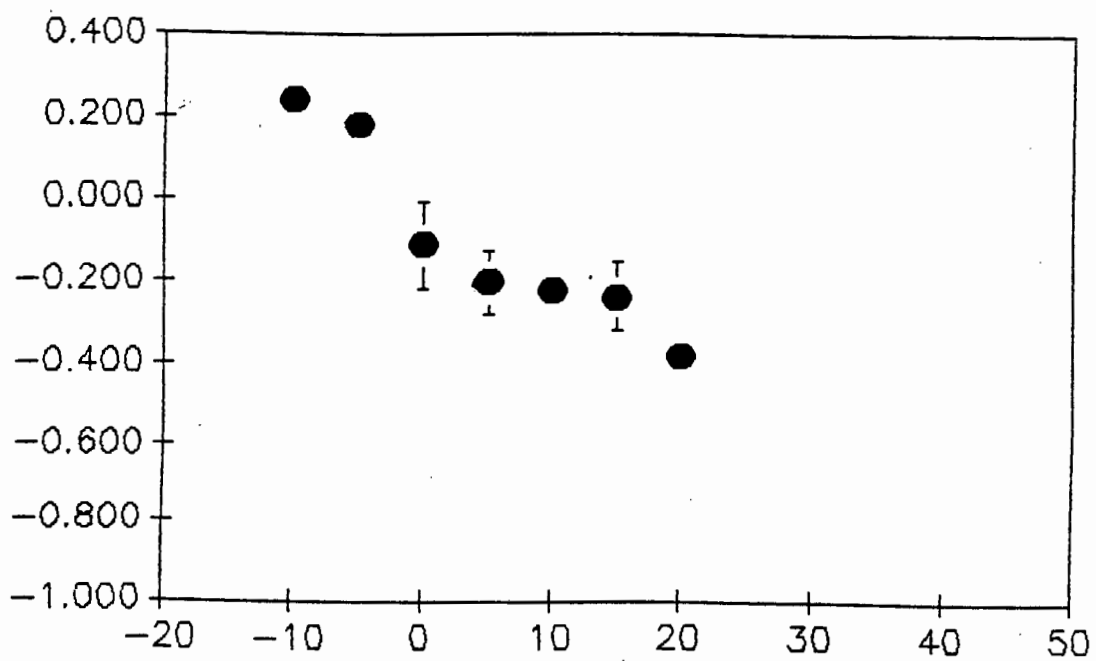


**Figure 4.** Collective I-V plot for "squares" from the human tubule data sample.

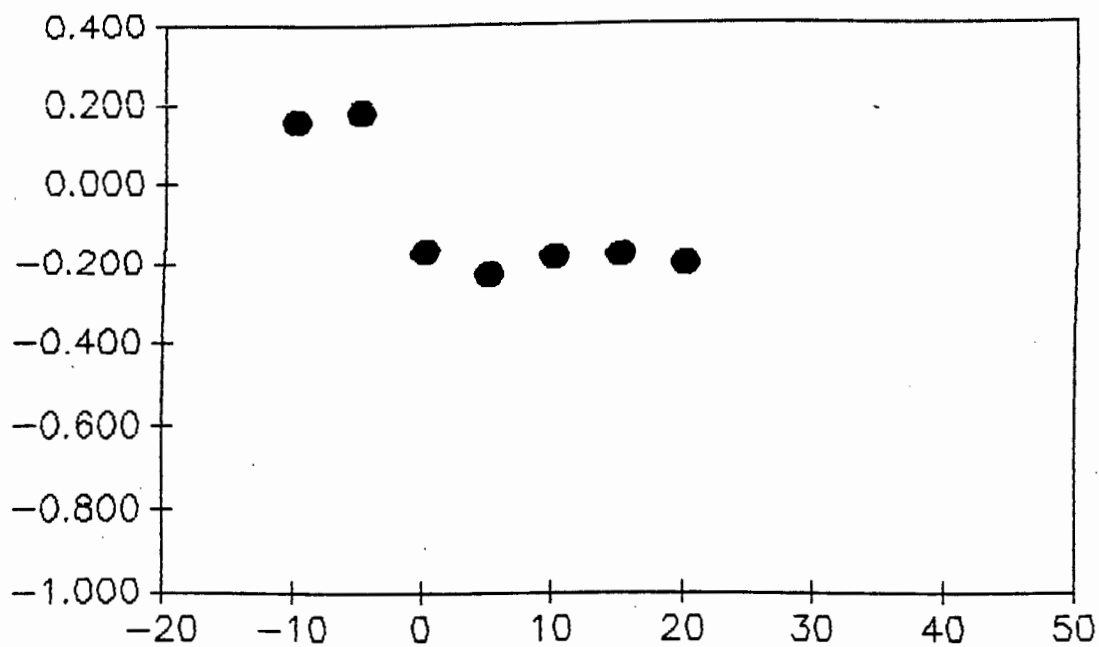


**Figure 5.** Collective I-V plot for "bursts" from the human tubule data sample.

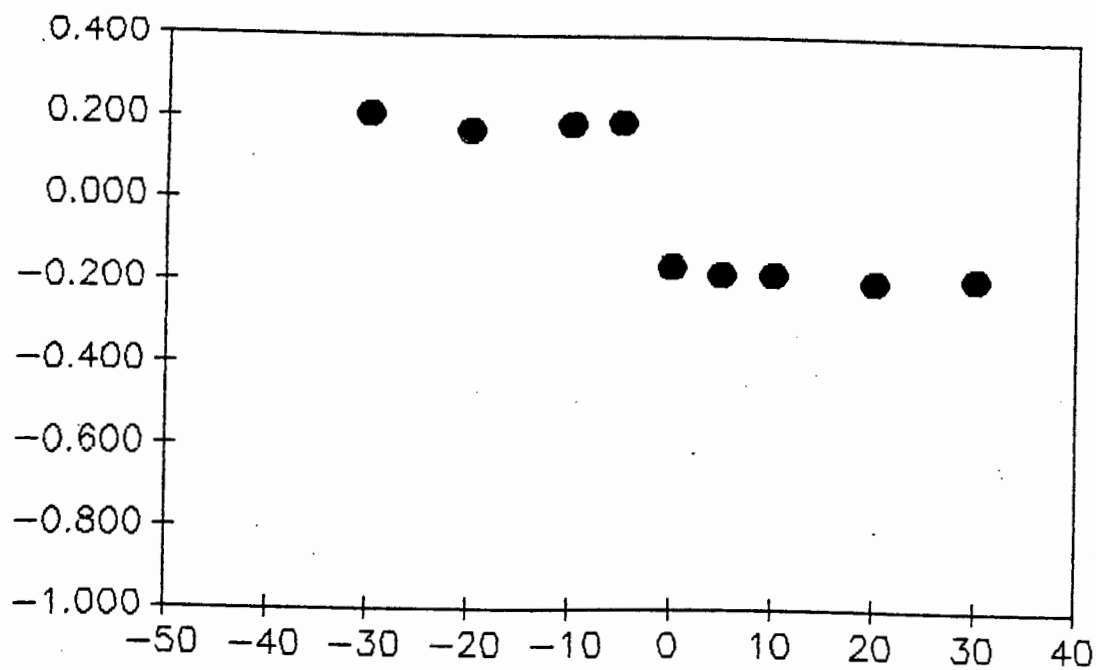


**Figure 6.** Collective I-V plot for "bursts" from the TAL data sample.

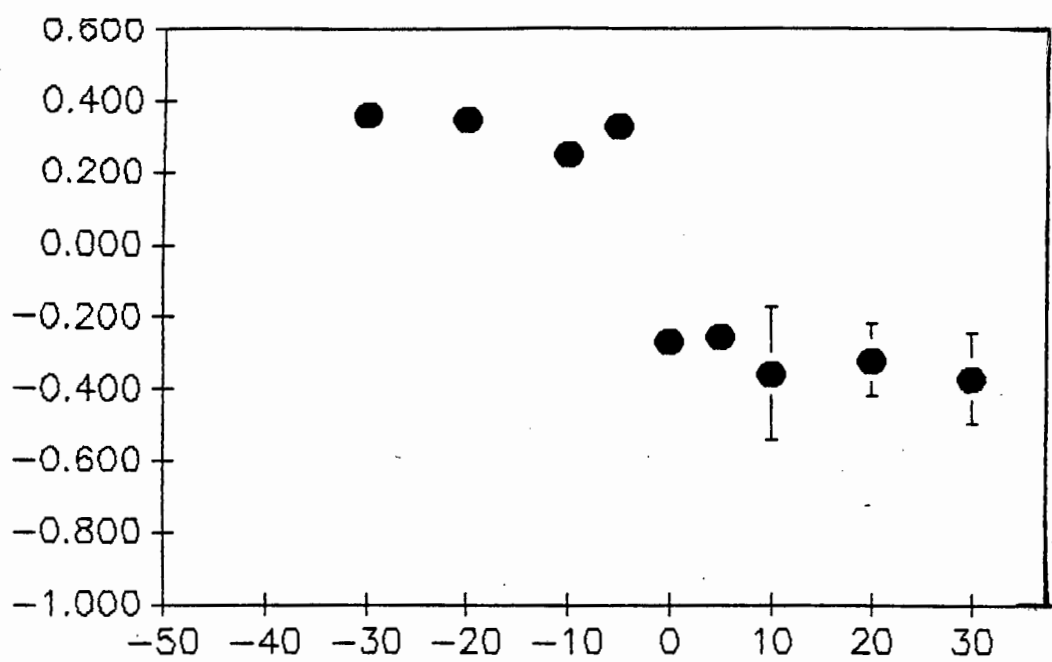


Figure 7. Collective I-V plot for "squares" from the TAL data sample.

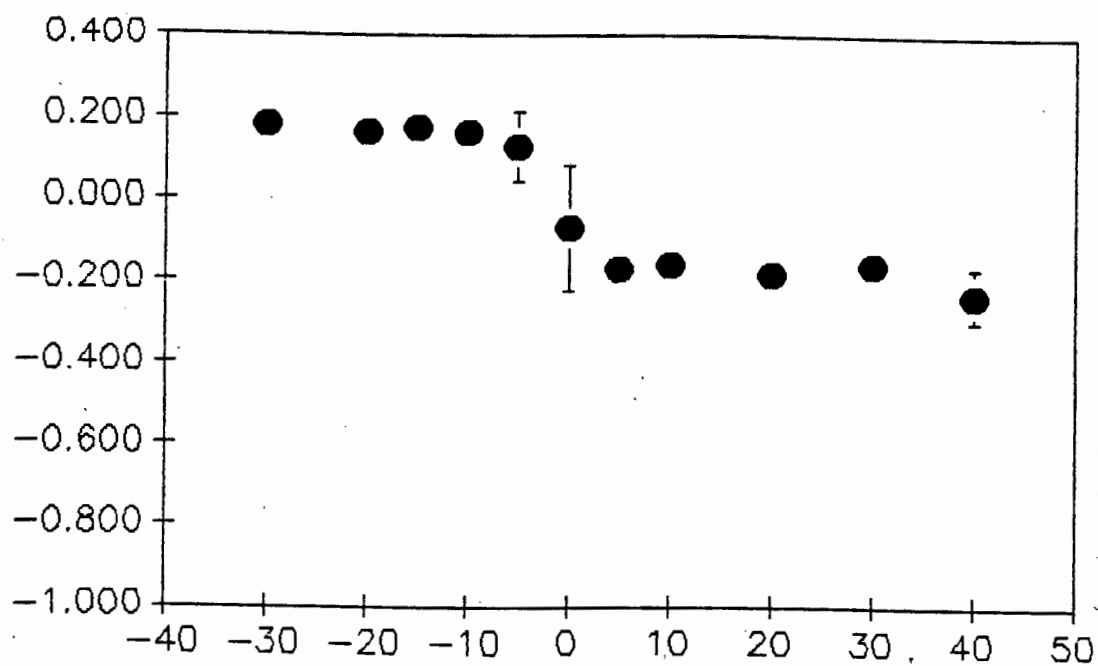
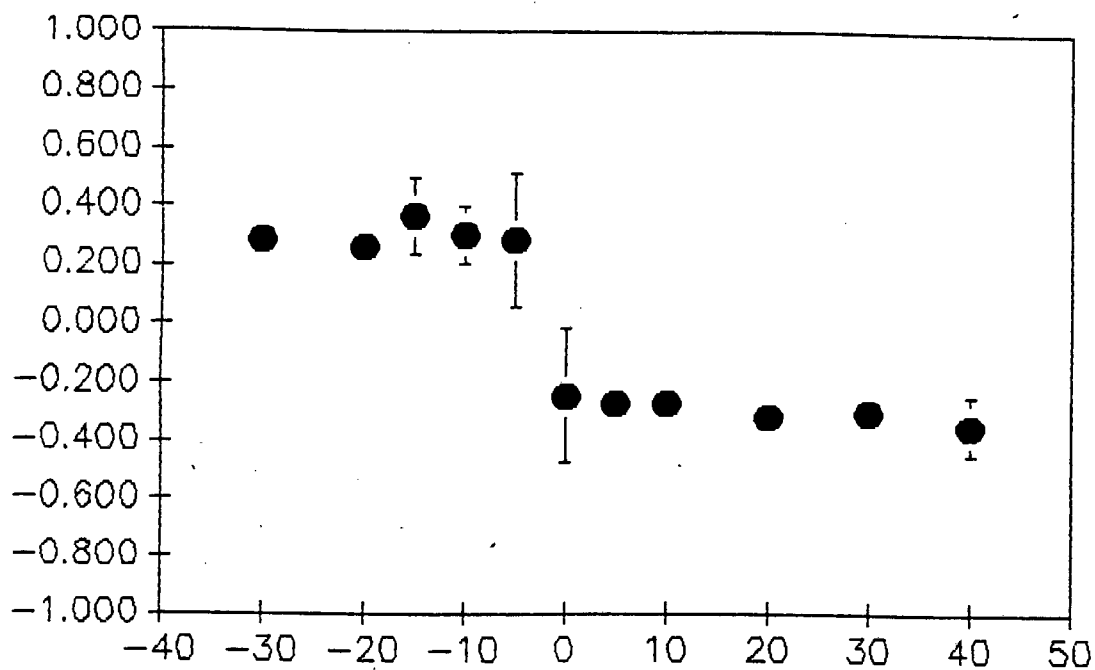
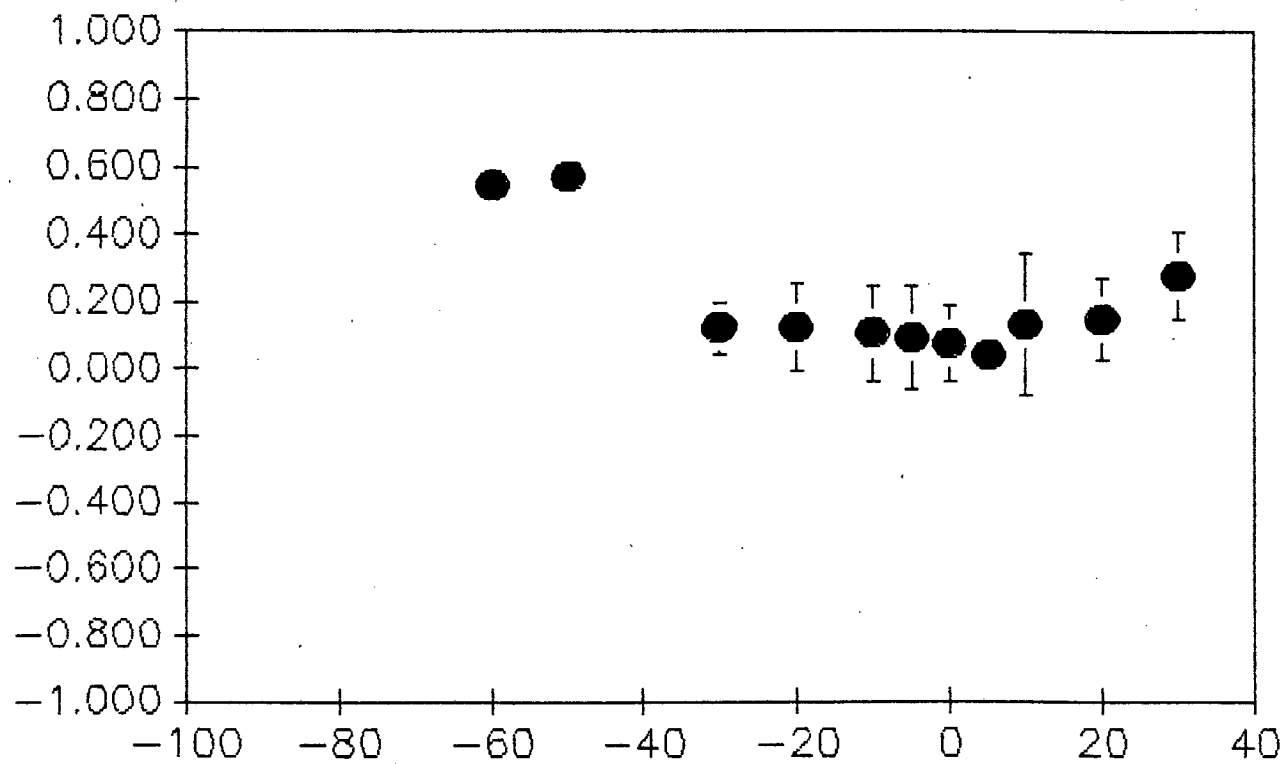


Figure 8. Collective I-V plot for "bursts" from the PST data sample.





**Figure 9.** Collective I-V plot for 'squares' from the PST data sample.



**Figure 10.** Collective plot of fractional open time for the entire data sample.